HIGH FREQUENCY TRANSFORMER, DESIGN AND MODELLING USING FINITE ELEMENT TECHNIQUE

BY

ADIL H. MUHAMMED, MPhil

A THESIS IS SUBMITTED FOR THE DEGREE OF DOCTOR OF PHILOSOPHY IN THE FACULITY OF ENGINEERING

THE UNIVERSITY OF NEWCASTLE UPON TYNE
2000

ABSTRACT

The field of high power density power supplies has received much attention in recent years. The area of the most concern is to increase the switching frequency so as to achieve a reduction in the power supply size. Such concern in high frequency power conversion units has led to many resonant structures (quasi, multi,and pseudo). In all resonant types, the power transfer from the source to the load is controlled by varying the ratio of operating to resonant frequencies. Every effort has been made to reduce the switching losses using zero voltage and/or zero current techniques.

In contrast, little attention has been given to the area of the design of the magnetic components at high frequency operation. It is usually accepted that the weak point in further high frequency power supply design is in the magnetic devices (transformer and inductor). No accurate model of the transformer taking into account the high frequency range has been performed yet. It is well known that as the frequency increases so the transformer model becomes more complicated, due to the complexity of the transformer element distribution, and the nature of frequency dependence of some of these elements. Indeed, work of this kind can take many directions, and the attempt here is to introduce a number of mathematics, analytical, numerical, and practical directions to model the transformer. The main factors affecting the high frequency performance are the eddy current losses, leakage flux and the effects due to the transformer elements, where the transformer is part of the resonant converter.

Two dimensional transformer finite element modelling is used to examine different cases, including open and short circuit conditions. The frequency dependency of the winding resistance and leakage inductance is fully explained. The practical design of the transformer and testing is used to valididate the simulation results. These results are supported by the results obtained from the mathematical formulation. Special attention is given to reducing both copper losses and leakage in the windings.

Three dimensional modelling of the high frequency transformer and the solution using a program solving the full set of Maxwell's equations is the original part of the present work. Frequency response characteristics are found and compared to that obtained from the test. Curves of these characteristics are used to predict a simplified transformer equivalent circuit. This circuit is used with the simulation of a full bridge

series resonant converter, where all units (. switches, control, isolation, feedback, and transformer) are represented by an equivalent circuit. The power supply operation and its behaviour in respect to the change with frequency of each of the transformer elements are examined. Two cases are considered through the simulation, when the operating frequency is above and when it is below the resonant tank frequency. The simulated results are validated by building a practical power supply.

In addition, the numerical solution of modelling the transformer by an equivalent network is also introduced. The highest possible number of elements (R,L, and C) are used, where all the elements are found using 2D FEM solution of both magnetostatic and electrostatic fields. This network is solved using the trapezoidal rule of integration and electric network theory. The examination of the influences of the distribution capacitances on the internal winding frequency response characteristic is carefully examined.

The last work in the present research is focussed on finding a general model of an exact transformer equivalent circuit to cover the wide frequency range. The thesis is completed with a conclusion.

ACKNOWLEDGEMENT

I would like to express my deepest thanks to Professor AG Jack, my supervisor for his support in all aspects of the work, and for being a constant source of encouragement throughout the most difficult times. I would like to thank him for pains undertaken during the final stage of writing.

I would also like to thank Dr. B. Mecrow for his contribution and help in the early stages of the work. As with most projects of this kind, a great many academic and technical people are owed a great deal of thanks.

I would like to express my special thanks to all my colleagues in the UG lab, Chris, Simon, Steve, Oystien, Ken, Phil, Jim, Hassan, Bernhard, Wander, and Christian, for their friendship and mutual encouragement.

I am also thankful to my parents, brothers and sisters who have undergone all the pains in my long absence.

Last but not least, my thanks to my wife Safiya who has never failed to offer help and support at all times, and my son Ala'a, and daughter Shaima'a.

SYMBOLS, PREFIXES, AND ABBREVIATION

H	magnetic field intensity	Am^{-1}
J	current density	Am^{-2}
A	vector potential	wb m^{-1}
B	magnetic flux density	T
D	electric flux density	Cm^{-2}
E	electric field intensity	Vm^{-1}
a	area	m^2
ℓ	length	m
C	capacitance	F
L	inductance	H
f	frequency	Hz
R	resistance	Ω
Z	impedance	Ω
Y	admittance	Ω^{-1}
I	current	A
V	voltage	V

Prefixes

g	ground
m	magnetising
d	distribution
r	resonant
oc	open secondary winding
sc	short secondary winding
p	primary winding
s	secondary winding
h	history (previous time)

Abbreviation

FEM	finite element method
EC	equivalent circuit
FFT	fast fourier transformer
HF	high frequency

CONTENTS

CHAPTER ONE

1.1 : INTRODUCTION

Since the introduction of the first practical power MOSFET in the 1970's, they have undergone major performance improvements, and are now widely accepted and used in power electronic equipment. They combine many features that make them suitable for a wide range of applications, including, light weight, high switching speed, low losses, and high power density. One of the areas where they are used is in power supply units. There are many basic topologies commonly used to implement a switching power supply. Each topology has unique properties which make it best suited for a particular application, such as high or low output power, voltage etc. Essentially, the size of the power supply unit is inversely proportional to the switching frequency, therefore most of the research nowadays is concerned with the high frequency range and Megahertz in particular. Higher switching frequencies made possible by power MOSFET transistors, new topologies and PWM (pulse width modulation) integrated circuits (which pack more control and supervisory features in a small volume), have contributed to making modern power supplies smaller. Power supplies have a very wide range of application including TV, PC, power system, X-ray, etc., and a reduction in power supply size has a significant effect on the cost of the overall system.

The development of high frequency power supplies encompasses circuit analysis, control theory and magnetic circuit design. It is generally accepted that the weak point in further increases in switching frequency comes mainly from the magnetic devices. Unfortunately, these magnetic devices (transformers and inductors) are unavoidable.

Transformers are present in most circuits serving many purposes, such as isolation, step up and down. Practically, there is no upper limit to their power handling capability, if proper design is achieved, but it is also one of the most difficult devices to model accurately as the operating frequency goes higher. An accurate model of the transformer with proper account of the effects of high frequency is essential to further design progress. When such a model is achieved, it should be possible to establish the important characteristics of the

magnetic structure and thereby assist in the drive for higher frequency. The model must be capable of predicting the effect of eddy currents in all transformer parts taking into account the frequency dependence of leakage and loss elements, and include capacitive effects between turns and between windings and earth.

There are many types of transformer categorised according to their operating frequency and power, such as power, wide band, pulse, etc. The power transformer usually operates over a narrow frequency band (i.e. the line frequency). A typical application for power transformers is in distribution systems for electric utilities. Power transformers are designed mostly to operate near the maximum allowable flux density under steady state conditions, near the highest possible voltage per turn and at the highest current density consistent with the cooling mechanism. Transformer operation above these limits will be destructive.

A pulse transformer is a transformer that operates in high frequency circuits providing isolation and low power signal amplification. Typical applications include communication equipments and feedback circuits.

Since the input to a power supply transformers is high frequency, high power, these transformers combine the features of power and pulse transformers and are termed wide band power transformers.

Among the first considerations in wide band transformer design is the efficiency. The high efficiency that is achieved in low frequency transformers cannot be compared with those in a high frequency transformer (wide band). The transformer losses are strongly related to frequency. These losses contribute to the economics of the system in which they operate. The heat due to transformer losses need to be considered as part of the equipment in which they are installed. It is crucial then to reduce these losses to an acceptable limit, since all switches, the transformer, and the control circuits are very close to each other in the power supply unit. Reducing the losses so as to reach higher efficiency is currently the subject of much attention. There are two losses mainly contributing to the total transformer losses, the core loss (which represents the no load loss), and the winding or copper loss (which represents the load loss). The core loss i.e. the power dissipated in the core consists of

eddy current and hysteresis losses. Hysteresis loss is consumed in the continuous reversal of the magnetic field due to the changing direction of the magnetising current. This loss is easier to control through the design stage than the eddy current loss. Eddy current loss is caused by circulating currents in the body of the core. This current is produced due to the induced voltage when the magnetic flux is changing. In principle, the induced voltage per turn in the core is the same as at in the secondary winding. The direction of this current is normal to the magnetic flux direction that produced it. At low frequency, the eddy currents can be reduced by laminating the core in the direction of the induced voltage. As frequency rises the required laminations become impracticable, and resort is made to Ferrites which naturally have low eddy currents by virtue of the granular structure. The core loss, which is determined by the core materials and the design is a function of the amplitude and frequency of the applied voltage. Core manufacturers have gradually improved core material properties, including the Ferrites which are widely used at present. The ideal transformer core material would have an infinite magnetising permeability and zero loss. In addition, the core material would have infinite saturation flux density, unfortunately current materials fall for short of this ideal.

Winding loss and leakage component calculations still represent a great challenge for a high frequency transformer designer. They are related to each other in the sense that any reduction in one tends to be at the expense of the second. Reducing the leakage magnetic fields is vital to avoid interference with other circuits within the power supply unit. Unfortunately, reducing the leakage also results in an increase in the distributed winding capacitance.

Many computational techniques have been applied to improve the analysis of transformer performance which have been aided by rapid developments in digital computers. One of the techniques which has been applied successfully to predict transformer performance at low and audio frequencies is the finite element method. This method provides a numerical solution of the electromagnetic field in each part of the transformer. The calculation results can be used to predict performance at the design stage. They also have a tutorial value in

providing a clear overall picture of the various aspects of the performance which are not easy to obtain by conventional methods.

1.2 : LITERATURE REVIEW

The major thrust of this thesis is to design, model, and analyse high frequency power transformers. To achieve economy in the design stage, and high operational performance of the transformer, it is vital to model the transformer accurately. The main factors that disturb transformer operation at high frequency, are winding eddy current losses, leakage, and the increasing influence of capacitance. The combination of distributed inductance and capacitance produces many natural frequencies which are troublesome if the transformer is used in a resonant converter.

When the frequency of the excited waveform is increased, current is not distributed uniformly through the conductor but in a skin around its periphery. This gives rise to the eddy current losses in the winding, i.e. as skin effect in a particular conductor, and as proximity effect with respect to currents in all other conductors. The proximity losses are minimised if the sub conductors are far apart, but the down side is an increase in leakage flux.

The problem of reducing the leakage flux while keeping the winding losses within acceptable limits has received considerable attention. In 1966, Dowell [1], derived an analytical formulation to predict the frequency dependence of winding resistance and leakage inductance. The relation was limited to the window area of the core (i.e. the core is not included). It only includes the effect of high frequency on the inductance and resistance, capacitance effects are not included. Different winding arrangements were calculated and discussed from a physics point of view. Another mathematical formulation to solve the skin effect problem in a conductor was given by Silvester [2] in 1967. A two dimensional model was used for this purpose. A resistive-capacitive network was used to avoid solving the full field equations. This was followed by another publication [3], using a resistive-inductive network to solve both skin and proximity effect losses. The procedure

of solution was the same i.e. by subdivision of the conductor into individual sub conductors, each of which was represented by a network branch. The methods were applied to the single conductor, but it becomes hopelessly complex when the system has many conductors.

Transformer models using equivalent R,L and C network have long been a common method of analysis particularly for fast transients. Fergestad [4] presented a different type of numerical method to calculate the transient voltage distributions, but still based on networks. The approach was to divide the winding into a number of sections to be solved numerically. Kasturi [5], introduced a method of solving the winding equivalent network through a companion network. Each element in the network was replaced by its equivalent which is derived using a trapezoidal rule of integration. As a result, the network is transferred at each time step to an entirely resistive system that can be easily solved. Many other papers have been published to model the transient characteristics for instance [6,7,8] are a selection.

Once capacitance effects come into operation at high frequency, the prediction of transformer frequency response is far simpler than its time (i.e. transient) response. This is because a transient excites all frequency modes. Therefore, the determination of transformer frequency response characteristics have received attention as the only reasonable method to model the high frequency transformer. In 1977, Degeneff [9], used the familiar equivalent winding network to calculate terminal and internal impedances and to predict the resonant and anti resonant frequencies. Many papers have also paid the same attention to the transformer frequency response [9,10,11,12]. Certainly, measurement can be used but it is difficult to predict the internal winding response, even with a capacitively coupled probe, damage to the winding insulation is unavoidable.

The enormous difficulty of modelling a high frequency power transformer is well recognised. Continued growth in computer science and technology has made it possible to contemplate increasingly accurate transformer models.

The rapid development of the finite element method since the 1970's has provided an improved method for the solution of transformer electromagnetic fields. The power of the

finite element method is well recognised, and its application to electromagnetic field problems has expanded dramatically since it was first drawn to the attention of electromagnetic analysts by Zienkiewicz [13]. The method has been applied with success to 2D low frequency eddy currents [14,15,16,17], and medium frequency [18,19] problems. Three dimensional applications have also been discussed extensively [13,20,21,22,23,24,25].

The finite element method can be used within an equivalent winding network model to predict the network elements. At the same time, attempts using the electromagnetic field equations directly has grown dramatically. In 1979, Perry [26] examined the variation of current density in a one dimensional reduction of a multilayer coil. The work was based on finding a relation of power dissipation with respect to the thickness and number of layers. On the same grounds, Beland [27] computed the eddy current losses in different shapes of conductors under the assumption that the induced currents flow on paths parallel to the sides. The frequency response of the impedance in multiconductor systems using 2D FEM was also introduced by Weiss [28]. The impedance was predicted from the calculation of loss density and stored magnetic energy. Many numerical methods have been used for eddy current field computations and magnetic device modelling. Konrad [17] presented a survey of such methods.

Some have given direct attention to the capacitance distribution through the winding. Chowdhuri [29] presented a method in 1987 to calculate the equivalent of the winding series capacitances. Laplace transforms were used to predict the input impedance response. In 1988, Vaessen [10], presented a method to model a high frequency transformer using the principle of two port networks aided with the measurement of admittance and transfer functions. Vandelac [30], presented eddy current losses (skin and proximity) using a field approach. The work provides an insight into minimising copper losses at high frequency including interleaving the winding. Proximity effects have also been studied widely by many [2,31,32]. An approach to calculate high frequency conductor resistance was presented by Goldberg [33] in 1989. In this work a layer of winding composed of discrete wires is converted into an equivalent continuous sheet. Further simplification was

achieved by assuming that each layer has a finite thickness and infinite length, and so the problem is reduced to one dimension. A detailed transformer model which includes winding losses was given by Wilcox [34] in 1989. The model was derived from the calculation of self and mutual impedances aided by test. A model derived from classical transformer theory was also presented in 1991 by Wilcox [35]. The procedure consists of decomposing the transformer into sections, and each section is represented by a network. The voltages and currents of each section are arranged in matrix form. The model can not be used to design a transformer, but it allows better a understanding of the transient phenomena.

The first confirmation of interaction between a resonant converter and a transformer was given by Wint [36] in 1991. A low frequency oscillation of the input and output of the power supply transformer was noticed and solved mathematically using an equivalent model. In 1993, Woivre [37] presented analytical and numerical models (FEM) to model the transformer and to calculate the frequency response characteristics. Fourier transforms were used to compute the over voltage transient effect. Morched [38] introduced a model to simulate the behaviour of a multiwinding transformer, over a wide frequency range. Another numerical solution to the winding of the high frequency transformer was presented by Leon et. al [39]. Ahmad et al [40] provided in 1994 a general transformer model to predict the high frequency behaviour. The capacitances within the model were computed using 2D electrostatic FEM, and magnetostatics to predict the winding resistance and leakage inductance. Frequency response characteristics were studied covering a frequency range of 0 to 1MHz. The core eddy current losses and hysteresis have received equal attention. Ahmed [41] and Basak [42] solved the core loss using 2D FEM in 1994. The confirmation of the need to use the core conductivity as a function of frequency was recognised in their work. Hysteresis losses in high frequency power transformers were also under attention, see for instance, Leon [43] in 1995. Lotfi [19], presented a method as well to calculate the frequency dependent resistance in a rectangular conductor. The solution is based on the ellipse formulation from the fact that the shape of

current in the conductor cross section is equivalent to an ellipse. The method was compared to the FEM result and applied at the power supply switching frequency.

All the methods discussed so far have limitations as well as lack of generalisation and so cannot used to model high frequency transformers. The attempt toward further frequency range with a full transformer model is hardly found. Therefore, the attention is given currently to model the whole transformer regardless of the design differences. High frequency effects are taken into account correctly. The model is solved using the full field equations by finite element technique.

1.3 : THESIS STRUCTURE

In the present work, an attempt is made to introduce a number of numerical and analytical methods supported by practical and mathematical processes. The aim is to examine the main factors that affect the performance of high frequency transformers used in power supply units. These factors are, winding losses, leakage, winding capacitances, core loss and their variation with transformer design, particularly with reference to use in resonant power supplies. A practical transformer has been designed and built as detailed in Chapter two, and a power amplifier is used to test the transformer impedance characteristics. Another concern of chapter two is the operation of the transformer in a full bridge series resonant converter. Particular attention is paid to consideration of an adequate way to simulate the transformer within the power supply unit. Practical aspects of building the power supply are also discussed in detail. The current and voltage waveform at the input and output transformer terminals provide a basis for justification of the simulation. In fact, the actual power supply can be used for the test purposes, since the series resonant converter can safely handle a short circuit, but the resonant tank elements could be coincident with the transformer elements which results in curves which differ from the transformer alone. The design procedure was used to examine a large number of cases to examine both the leakage and losses in the winding using a two dimensional finite element model as detailed in Chapter three. In this chapter, attention is paid to the frequency dependence of the winding resistance and leakage inductance. Since a two dimensional model is used for the magnetic field, capacitive effects cannot be represented placing a limit on the calculation below the frequency at which such effects appear. Winding arrangements such as the number of layers and turns are examined. The frequency dependence of these elements are also introduced analytically and compared with finite element and practical results.

The electromagnetic equations given by Maxwell are usually approximated at power line frequency by neglecting the displacement effects. This approximation may not be valid as the frequency goes into the Megahertz zone, where capacitance effects become

increasingly important. The magnetic and electric fields are coupled and three dimensional analysis is required. That is covered in Chapter four, where a numerical formulation involving the full set of Maxwell's equations is derived and then solved using a three dimensional finite element model. A simple model is used first for validating the results with just primary and secondary windings and no core (i.e. an air core transformer) and compared with practical results. The whole transformer model is then used to predict the actual open and short circuits impedances. Later in this Chapter, attention is given to the derivation of a simplified transformer equivalent circuit. The elements of this circuit are found directly from the resonant frequencies of both impedances curves. Indeed, most of these elements can be predicted directly from the finite element model calculations. There is however considerable difficulty in predicting the capacitance due to its complicated distribution in the actual transformer. Usually the capacitance effects are considered as frequency independent and can be solved electrostatically. This procedure can reduce the model to two dimensions but will never model all of the transformer elements accurately, because magnetic and electric fields are coupled to each other.

Chapter five, pays particular attention to capacitance effects within the transformer winding. The transformer winding is modelled by an "accurate" equivalent circuit which has series / parallel branches to represent the distributed nature of the field. The elements of this circuit (R,L, and C) are found by solving the 2DFE model magnetostaticaly and electrostaticaly individually. The full circuit is solved for transient problems numerically using the trapezoidal rule of integration. The combined effects of capacitance and inductance are viewed through the frequency response of the input impedance.

In Chapter six, full details of the power supply simulation is given, and the aim is to examine the effects of the transformer elements on the performance of the power supply. Each part of the power supply including switches (MOSFET), control, feedback isolation, and transformer is implemented using its equivalent representation, taking into account the high frequency effect of the switches. Two cases have been considered one above and the other below the resonant frequency. The simulated results are validated practically using the measurements described in Chapter two.

The high frequency response of wide band transformers is usually analysed by means of equivalent circuits. Although any circuit is not an exact representation of an actual transformer, it can be a convenient way of approximation. The representation of a transformer by an improved equivalent circuit is the subject of Chapter seven. The thesis is completed with conclusions.

CHAPTER TWO

PRACTICAL VALIDATION OF THE HF TRANSFORMER SIMULATION AND TEST

2.1: INTRODUCTION.

The size of a switched mode power supply unit is reduced by increasing switching frequency or by improving efficiency. Increasing the switching frequency leads to a large reduction in the magnetic components size (transformer and output filter), while increasing efficiency leads to less overall losses and hence to a smaller heat sink in the power supply unit. The transistor switching losses in the conventional pulse width modulation (PWM) limits the working frequency for the power supply (500khz - 1Mz). In PWM, the current waveform is driven mainly square in shape which increases switching losses on both turn-on and turn-off. These losses are mainly due to the overlap of falling current and rising voltage at transistor turn-off, or rising current and falling voltage at turn-on, plus the losses due to the rectifier reverse recovery. Using dissipative (RC) or nondissipative (LC) snubber circuits to reduce transistor switching losses is not a practical solution at higher frequencies. This is because the switching losses are not reduced if a dissipative snubber circuit is to be used, all that happens is that the losses shift from the transistor (MOSFET) to the resistance of the snubber circuit. In that case a larger heat sink is required for both the resistance and transistor. A nondissipative snubber circuit, on the other hand is troublesome at high frequency, because it acts as a resonant circuit around the transistor and stores energy that the transistor cannot handle. Resonant converters offer the advantage of overcoming these problem and hence reducing the switching losses. In these converters, the current waveform can be sinusoidal (or quasi sinusoidal) instead of square which minimises higher frequency harmonics and reduces noise. Also the transistor can turn-on and off at zero current or

zero voltage to eliminate the switching losses, and give low di/dt or dv/dt stresses with a good transient response.

Many resonant converters topologies have been proposed, which are used for different purposes, and these depend on their applications. Most of the topologies are mainly concerned about losses, power density etc., but a few are concerned with the transformer elements in particular the distributed capacitance. The transformer element values are very sensitive at higher frequencies approaching megahertz. Their value is important, first because the transformer elements are resonant elements and have to be accounted for in the resonant tank, and second because ways must be found to reduce the effect of these elements to get low EMI and reduction in stress.

The topology selected in this chapter is aimed to introduce a power supply that can be used to provide results which validate the simulation carried out in later chapters. The simulation results are used to examine the effect of each of the transformer elements within the normal operation of the power supply. This topology is a full bridge clamped mode series resonant converter, that is well documented in many papers [44, 45]. Later parts of this chapter concern tests on the actual transformer.

2.2: PRINCIPLES OF RESONANCE.

Resonance phenomena are very important physical effects in any circuit having RLC elements. During resonance, the circuit is purely resistive and maximum power can be delivered to the load if its value matches the load value. The circuit with RLC elements can have series, parallel, or a combination of series-parallel resonance. In this section, a brief introduction to the principle of resonance is given to establish terms but of course this is well known theory.

Fig.(2.1), shows a typical RLC circuit modelled in both the time and frequency domains, together with the magnitude and phase of the circuit impedance. The resonant condition occurs when the source voltage and current are in phase. This means, the

circuit impedance is a purely real number, which leads to the conclusion that the imaginary part of the circuit impedance is equal to zero. Hence, during resonance the circuit is equivalent to a single resistance. In order to satisfy this condition, the following applies;

$$Z(j\omega) = R + j(X_L - X_C) \quad \Omega$$

$$Z(j\omega)\Big|_{\omega=\omega_o} = R \qquad \Omega \text{ and,}$$

$$j(X_L - X_C) = 0 \Rightarrow f_o = \frac{1}{2\pi\sqrt{LC}} \quad (\text{Hz})$$

where f_o (Hz) is the resonance frequency, and $X_L = \omega L$, $X_C = \frac{1}{\omega C}$ Ω.

From these relations, three cases can be observed. First, when $f > f_o$ (source frequency larger than resonance frequency) i.e. above resonance, $X_L > X_C$, θ (the impedance phase angle) is positive. Hence the circuit is predominantly inductive. Second, when $f < f_o$ i.e. below resonance, $X_L < X_C$, θ is negative. The circuit is predominantly capacitive. finally, when $f = f_o$ (at resonance), $X_L = X_C$, θ is zero, and the circuit is purely resistive.

The circuit impedance curve shows that when the source frequency is zero (dc), X_C is ∞ (open circuit), and the impedance magnitude will be ∞ . When the source frequency tends to ∞, X_L is ∞, and the impedance magnitude will be at ∞ again. The only condition that the impedance magnitude is minimum is where the source (current or voltage) frequency is equal to the resonant frequency. The opposite conclusion can be made for the case of a parallel resonant circuit. At resonant frequency, the circuit impedance will reach its highest magnitude which equals the resistance value. If the resistance is removed (circuit with L and C only), the impedance magnitude could reach an infinite value (open circuit), but this case is not practical since there is an internal resistance accompanied with the inductor.

The resonant frequency has the same relation in both series and parallel RLC circuit, but the behaviour in these two cases is completely different. However, both series and parallel resonance could be present in the same circuit, as is the case with filters or the high frequency transformer discussed in the following chapters.

2.3: CONVERTER DESIGN.

Generally, the design of any type of converter is based on the numerical calculation of the dc voltage conversion ratio characteristics [46,47,48,49]. The dc voltage conversion ratio curves are obtained by solving differential equations for different modes of operation. These modes follow the switching pulses arrangement for the ON-OFF states of the switches. The characteristics are plotted as a function of normalised conversion frequency, which is the ratio of switching to resonant frequencies for simplicity of the calculations and generality of the results. All the currents and voltages can be normalised with respect to the resonant characteristic impedance ($\sqrt{L_r / C_r}$), and the transformer turns ratio.

However, the procedure of the full design is not illustrated in this chapter, the present power supply dc characteristics above and below the resonant frequency have already been given [45]. In the converter shown in Fig.(2.2), there are a few points of interest which deserve more attention. The first is the series diodes (Ds2&Ds4). In some circuits that require reverse voltage across the transistor, a blocking diode could be placed in series with the source or the drain terminals of the transistor (MOSFET). In a resonant circuit, the reverse voltage rises very quickly on cessation of forward current. The antiparallel diode within the MOSFET is not fast enough and a blocking diode is required. The blocking diode will prevent forward current from flowing through the transistor body diode, and the fast reverse recovery diode (D1-D4) carries the required forward current. The diodes (Ds2&Ds4) are then used to avoid conduction of the internal diode of the MOSFET.

The load in a series resonant converter is resistive in the transformer secondary side reflected to the primary by the turns ratio squared, and in series with the resonating LC elements. In the series resonant converter, the output inductor is omitted. This converter is used for high voltage application as it requires no output inductor. An output inductor for high output voltage would have to support large voltage across itself and would be bulky. Hence this converter can be used for either high or low output dc voltages. The

series loaded circuit can safely survive an output short circuit as the reflected load impedance is in series with the resonating Lr and Cr elements. This impedance is small compared to the characteristic impedance of the resonant tank elements (Lr and Cr).

2.4: POWER TRANSFORMER DESIGN.

Most switching power supplies transformers use Ferrite cores [33,46,50]. In general, Ferrites are ceramic ferromagnetic materials having a crystalline structure consisting of mixtures of iron oxide with either manganese or zinc oxide. Each Ferrite manufacturer processes different mixes of oxides for specific purposes. Ferrite cores are manufactured in a wide variety of shapes, EC, ETD, EF, U, RM,E, and many others shapes. With each of the shapes, there is a recommendation from the manufacturer to be used in an application which depends on the transformer power density. For instance, an E-core has been recommended to be used for a power of 500 Watt and over by Philips [51]. There are also many grade materials forming these shapes, 3C series, D series, S series, and many others. Each of these grade materials has a different material permeability and resistivity to fit the required application [18,41].

The performance of the power supply Ferrite core transformer is determined by the factors specified below :

- Geometry of the core and winding.
- The allowable temperature rise.
- The operating frequency.
- The minimum and maximum input voltage.
- The area occupied by the winding with respect to the window area.
- Peak value of the flux density in the core.

The size of the transformer is determined by the maximum volt-second product applied to the primary winding and the current flowing through the primary and secondary windings. The maximum volt-second product determines the maximum flux density

leading to core sectional area and primary turns selection. As the operating frequency increases, the volt-second product decreases, it is then possible to reduce the number of the primary turns or select a core with smaller area. The minimum number of primary turns is limited by the required turns ratio, beyond this any decrease in volt seconds due to frequency increase is achieved by a reduction in the core area. There is a limited frequency range for any core, because as the frequency increases the core and copper losses increase which leads to a reduction in the transformer efficiency. Operating the transformer above certain frequency no longer results in a size reduction, since a larger core is required to handle the losses.

The first step of material selection is the core loss defined by a curve of loss (usually in milliwatts or kilowatts per cubic centimetre or meter) versus peak flux density at different frequencies which is supplied by the manufacturers. From Faraday's law, which is used to calculate the number of primary turns, the larger the flux density, the lower the primary turns and the larger the allowable wire size, and the larger the output power. The limitation on higher flux density is the core loss, and hence increased core temperature rise. In this case the core loss is not the only limitation, the core may also go into saturation. The primary then cannot support the applied voltage, drawing large magnetising current and destroying the power transistor. The peak flux density has to be chosen so that the total core and copper losses result in an acceptably low temperature rise over ambient (i.e. room temperature). In order to avoid this method of choosing the peak flux density during the design, another way is desirable. The design for this work follows [52], and is built on selecting the core temperature rise rather than peak flux density at the operating frequency. This is a much safer way. The finite element analysis can be used for this purpose using magnetostatic and either two or three dimensional models. The finite element results can give the best selection of the flux density at which the leakage is minimum. These results can be compared with the practical results using a search coil around the core [42,53].

An E-shaped core with material grade 3F3 was used to design the transformer at 1MHz operating frequency, with the core dimensions as given in Fig.(2.3). The choice is made

that the maximum temperature rise due to the total loss (core and winding) will 40 C°. It is also assumed as a starting point that half the temperature rise occurs in the core due to iron loss and half in the winding due to $I^2 R$ and eddy loss. The core thermal resistance is equal to 14.8 C°/watt. The maximum transformer loss is then 1.35 watt. In order to use this value of loss in the manufacturer's loss curve given by Philips [51], the total loss has to be given per unit volume, which is the effective core volume, and that is equal to 1.35 / 17.6 = 76.8 mWatt / cm^3. From the loss curve at 1MHz, it is found that the maximum flux density is 16 mtesla (peak).

Important relations to examine the design limitation (winding loss or hysteresis loss) have been mentioned [52]. These two relations are :

$$\text{core size} = \frac{11.1\,(P_{in})^{1.12}}{K\,\Delta B\,f}\ cm^4 \qquad (1) \qquad \text{winding loss}$$

$$\text{core size} = \left(\frac{P_{in} * 10^4}{120\,K\,2\,f}\right)^{1.58} * \left(K_h\,f + K_e\,f^2\right)^{0.66}\ cm^4 \qquad (2) \qquad \text{core loss}$$

where; $P_{in} = P_o / \eta$ input power

K factor equal to 0.165 for full bridge

f operating frequency

K_h hysteresis coefficient = 4E-5

K_e eddy current coefficient = 4E-10

According to the same reference, if the core size calculated by relation (1) is smaller than that using relation (2), the design is limited by winding loss and not iron loss. At an output power of 500watt, the peak to peak flux density is 32mtesla and at 1MHz frequency, the first equation results in 2.8 cm^4, and the second equation in 3.66 cm^4. These results indicate that according to the design specifications, the smallest core required should be in the range between 2.8 - 3.66 cm^4. Therefore the core that is selected is E42, where the area product is its window area (A_w=1.78 cm^2) times the effective cross section area ($A_{eff.}$=1.82 cm^2), and that gives 3.2 cm^4.

2.4-1: PRIMARY TURNS.

Primary turns are calculated directly using Faraday's law [52,53]. The minimum primary turns to support a minimum of 150V input voltage at 1MHz frequency is :

$$N_p = \frac{V_{in} * 10^4}{2f \Delta B A_{eff.}} = 14 \text{ turns}$$

2.4-2: SECONDARY TURNS

In order to calculate the number of secondary turns to support 250V output voltage, the turns ratio has to be calculated and is given by :

$$n = \frac{N_p}{N_s} = \frac{\left(V_p - V_{MOSFET}\right) * \text{duty cycle}}{V_O - V_{DIODE}}$$

where V_{MOSFET}, V_{DIODE} are the voltage drops on the transistor and the output rectifier respectively [50,54], given a primary voltage duty cycle of 0.9, the turns ratio then is 0.52, and the secondary number of turns is 26.

2.4-3: PRIMARY- SECONDARY WIRING SPECIFICATION.

The selection of the wire size is usually found from the current density. The allowable current density is nearly the same in all the winding. A large increase in any single winding current density over other windings in the transformer leads to a hot spot in the coil. Wire tables give a current density usually in Ampere per unit area which provides a very rough guide to heating limits based upon typical (conservatively estimated) cooling. The cross section area of the wire required can then be estimated directly from the current density. The maximum primary current at minimum dc voltage of 150V and maximum input power of 625 Watt is :

$$I_{p\ max} = \frac{P_{in\ max}}{V_{in\ min}} = 4.1 \text{ Amp.}$$

The current density is the ratio of the current to the cross sectional area of the wire. Using insulated copper wire of 450 A/cm^2 leads to the size of the wire required, which is 0.009 cm^2 . The number of fine wires is selected according to the skin depth. At 1MHz (0.0066cm) the number is 64 of wire gauge 35 with the following specification; copper diameter 0.007cm, copper area 0.4E-4 cm^2 , insulator diameter 0.009 cm, and insulator area 0.7E-7 cm^2 .

The secondary current can be estimated directly from the turns ratio, giving 2.2 Ampere. Following the same procedure, the cross section area of the wire required to carry this current is 0.0048 cm^2 . Using the same wire gauge the number of fine wires is 32.

2.4-4: TEMPERATURE RISE.

It is important to check the validity of the temperature rise assumption which is 40 C^o as assumed earlier. The temperature rise can be found from the total losses (core and winding) and the thermal resistance (14.8 C^o / W) of the selected core. The thermal resistance comes from the manufacturers data for the core and is an experimentally determined figure using normal winding volume and fill factors. The core loss has been found earlier equal to 1.35W. The winding loss can be estimated from the primary current (4.1 Amp.), mean length of the turn (from the data sheet 9.3 cm), primary number of turns (14), and the resistance of the selected wire (wire specification 0.00032 Ω/cm , which gives a winding loss of 1.22W (assuming that eddy losses in the winding are insignificant). The total loss is then 2.57W, and the temperature rise is (2.57 * 14.8) equal 38C^o .

Since the estimated value of the temperature rise is less than that which has been assumed, the design is accepted. If this value is bigger than 40C^o , a larger core needs to be selected and the same design procedure repeated.

2.5: CONTROL TECHNIQUE.

In resonant converters, i.e. series, parallel, or series-parallel [45,48,55,56], the switching losses are reduced due to zero current or zero voltage techniques which need to be maintained for a wide range of load current and line voltage. The control circuit has the duty of maintaining any change and reflecting that as a change in the switching pulse width. There are two types of control technique namely fixed and variable frequency. The variable frequency control technique [52], uses frequency modulation to control the output voltage. The method uses the slope of the circuit impedance curve to control the output. The control circuit changes the frequency to move either toward or away from resonance, and thereby controls the energy transferred to the resonant circuit and to the load accordingly. In general, this technique suffers from a number of limitations. First, MOSFETs with a small transition time are required to maintain control at high frequency, second as the frequency approaches resonance, peak currents and voltages go higher stressing the resonant components which are designed to operate at a single frequency, and also the filter components which are usually designed at the lowest frequency. Practically this is not an easy task with respect to the frequency variation of this control circuit. Therefore it is desirable to keep the switching frequency constant [45,55].

Constant frequency control uses the conventional pulse width modulation (PWM) principle [57,58], to change the output. There are three kinds of constant frequency control strategy, direct duty cycle, voltage forward, and current mode. In all three types, the output voltage has to be compared with a fixed reference to give an error voltage which is used by the control circuit to modify the on-time. The total pulse frequency on and off is kept constant.

The constant frequency technique is the one currently used to control most power supplies. Dedicated integrated circuits are available for this task for instance UC3825A.

2.6: PRINCIPLE OF OPERATION.

The clamped mode series resonant converter as shown in Fig.(2.2), is a series resonant converter that can be regulated at a constant frequency by controlling the duty cycle ratio. Clamped means that the voltage across the tank (i.e. the resonant circuit) is held at zero for a period of the switching cycle until one of the MOSFET's in the opposite leg is triggered.

The duty cycle can be used as the control parameter while the switching frequency is constant. Constant frequency operation is realised by triggering the four MOSFETs in a time sequence so as to produce a quasi square voltage, which is applied across the resonant tank. Fig.(2.4) shows the theoretical bases of the switching pulses, tank voltage, resonant capacitor's voltage (Vcr), and the resonant inductor current (Ir). The four switching pulses are arranged as shown in this figure, where each of the two switches (i.e. MOSFET's) in one leg are delayed 180° with respect to the switches of the opposite leg [45].

At the start of the new switching cycle, T3 and T4 (Fig. 2.2) are conducting, while T1 and T2 are off. The resonant inductor (Lr) current starts to circulate and charge the resonant capacitor (Cr). When T3 is turned off, the current still circulates in the inductor through D1 and the capacitor voltage reaches a maximum. T1 is now turned on, forcing the resonant inductor current to change its polarity, and causing the capacitor to be discharged. The voltage is clamped to zero until T4 is turned off. When T2 is on the resonant capacitor charges to negative polarity and reaches maximum voltage when T1 is turned off. The inductor current circulates through D3 and T2 to discharge the resonant capacitor, and the process is repeated.

Two important points have to be considered. First, the resonant inductor current does not reverse until one of the switches in a leg is turned off. Considering the switching sequences of the four MOSFETs during the period that T1 is ON, T4 is ON for a short period shown in the Fig.(2.4), and during this period the current circulates through the tank only. When T4 is turned OFF, T2 will turn ON, therefore, the current polarity

remains the same until T1 in the first leg turns OFF, so the two leg switches turn OFF with no switching loss. Second the associated anti parallel diode is conducting before its switch is turned ON to force a zero voltage switching at transistor turn ON.

Further detail of the circuit operation can be found in publications on this type of converter [45,50].

2.7: PRACTICAL CONSIDERATION OF THE POWER SUPPLY.

Any power supply prototype consists of different stages such as, the input dc supply, switching circuit, isolation, control circuit, and output circuit as shown in the block diagram in Fig.(2.5). Each of these stages has its own problems. In addition to the specific considerations that will be explained shortly, it is clear that in a high power, high switching speed converter electromagnetic interference i.e. noise is going to be a problem. The following points help to reduce noise. Practical experience shows that they are necessary.

1- The control circuit has to be well spaced from the power circuit to reduce the interference.

2- The resistors that are used as peripheral components around the control circuit need to be of non-inductive type.

3- Twisted fine wires need to be used to connect parts of control circuit and the supply switching pulses should be kept as short as possible.

4- The resistors and capacitors have to be placed with as short leads as possible.

2.7-1: INPUT STAGE.

The dc input stage consists of a bridge rectifier and filter which convert the main ac voltage to dc. The rectifier circuit consists of an input transformer, full bridge diodes and an output capacitor. The input bridge diode circuits used in the present power supply are dual package SKKD2608 diode modules.

A capacitor input filter is used to reduce ripple and provide the required dc supply. The value of this capacitor needs to be accounted for in the design. If the value of this capacitor is too small, the result is a large ripple and lower minimum input voltage. If the capacitor value is larger than necessary, the recharging current is narrow and large in amplitude which increases EMI and gives higher losses. The energy required from the capacitor to provide the power supply is given by:

$$w = \frac{P_{in}}{f} \quad \text{Joules (Watt-second)}$$

Which is the input power over the line frequency of 50 Hz. The input capacitor value is :

$$C_{in} = \frac{w}{V^2_{peak} - V^2_{min}}$$

The input capacitor used in the power supply is an electrolytic of value 470μF (450V).

As a simple approach, the capacitor value can be found by using 1μF for every volt, with a little extra as tolerance.

2.7-2: POWER STAGE.

The power stage consists of four MOSFETs and the resonant tank. The selection of the MOSFET type depends on the rating of the input current and the maximum input voltage. The current can be found from the design specification of minimum input voltage, efficiency, output power and the duty cycle, resulting in 4.4Amp. following the

specification given earlier. The selection of at least a 5A MOSFET gives some margin. The MOSFETs currently used are IRF730 rated 400V and 5.5A.

The size of the heat sink used for the MOSFET can be estimated from the drain to source ON resistance. The temperature rise in the device (MOSFET) due to the loss in this resistance is one of the design specifications. This resistance is a function of temperature (increasing as the temperature increases), and is supplied in the manufacturer's data sheet. The value of this resistance for IRF730 is 1Ω at $25C^o$ and at the design value of $60C^o$ (i.e. a temperature rise of $35\ C^o$) its value is 1.3Ω . The power dissipated during the switching ON time then is the product of current squared, resistance and 0.45 (the On time), giving 11.3 Watt. The thermal resistance of the heat sink required at the specified temperature rise is (35/11.3) $3.1C^o$ /W . The heat sink used is $5\ C^o$ /W slotted ABL with a dimension of 33mm height and surface of 50mm*50mm.

The present power supply is aimed to operate below resonant frequency. The capacitor used in the resonant tank is 1.1nF (poly). The measured leakage inductance of the transformer is $4.1\mu H$ and this could be used as the inductor of the resonant tank if the frequency is high enough. However at practical frequency this inductance is not large enough to force zero voltage switching and to handle the power of the tank, so a series inductor is required. The design procedure for the inductor is similar to that used for the transformer, where here a small toroid ferrite core is used. However, the design procedure used to build this inductor is based on the inductor design step given by Evans [59].

2.7-3: ISOLATION STAGE.

Isolation circuits are vital for any power supply. There are three circuits with their features and functions as follows:

1- Isolation between the power input and output lines.

2- To provide a virtual ground for the top MOSFETs of the converter bridge.

3- Isolation between the output dc power and the control circuitry.

The first point relates to the HF power transformer that was discussed earlier. The second relates to the top MOSFET's whose sources are not ground referenced. The input switching signal is formed with respect to the ground of the power circuit rather than the emitter of the switch, and hence a dc isolation is needed. Basically, there are three ways that can be used to provide dc isolation between the gates of the power devices switches and the control circuit, a pulse transformer, DC-DC chopper circuit, or an optoisolator [50,52]. A pulse transformer can only sustain a limited duration pulse, and its output also swings from negative to positive. Furthermore, its leakage inductance has to be very small to achieve acceptable bandwidth. The chopper circuit also has bandwidth limitations and is therefore only really suitable for low frequency applications. The opto-coupler requires a separate dc supply for isolating the ground between its input and output (specifically an NMA series dc-dc converter). The optically coupled gate 6N137 used requires an additional stage at the output to regulate the switching current as shown in Fig.(2.6).

The third point relates to the isolation of the output voltage feedback to the error amplifier before entering the control circuit. The output voltage is first reduced using a voltage divider, and the result is used with an adjustable voltage regulator to drive the optoisolator.

2.8: CONVERTER OPERATION AND TEST.

The practical circuit is shown in Fig.(2.7). The power supply currently used is operating below the resonant frequency, where the ratio of switching to resonant frequencies is designed to be 0.8. This ratio is used to achieve better performance as recommended [45]. The frequency ratio can be adjusted by varying the number of turns of the series

inductor. Of course this ratio is not expected to be exactly 0.8, since that depends on how sensitive the instrument is that is used to measure the inductor.

Fig.(2.8a), shows measurements of the resonant capacitor voltage and resonant tank voltage. It can be noticed from this figure that zero voltage switching is clearly seen. The capacitor voltage and resonant tank voltage are rising from the point that both are almost zero. When the air gap of the core is changed or the frequency ratio goes higher (for instance 0.88), zero voltage switching is not guaranteed, and then external capacitors across the switches are required as shown in Fig.(2.8b). In this figure, zero voltage switching does not occur, and so the devices are switched on while the capacitor voltage is just starting to discharge. Therefore, external capacitors are required across each of the devices to force zero voltage switching or resonate this capacitor with an additional inductor in series with the transformer primary winding Fig.(2.9) shows the resonant inductor current. The measured waveforms may be compared with the simulations which are shown in Fig. (2.10-2.11). Good agreement is clearly seen. The detail of the simulation procedure for this type of converter is given in chapter six.

2.9: TESTING THE HF TRANSFORMER

The high frequency measurements are not different in principle to that at low frequency. The methods that were used for low frequency can be used with high frequency but care needs to be exercised. There are many methods that are used to measure the HF transformer elements (capacitance and inductance), including impedance, resonance and a bridge: Using a bridge circuit such as an Owen bridge [60] can yield the measurements of the coil resistance and inductance, but the impedance method is easy to use and it needs an ammeter and voltmeter only. The inductance here means any leakage, magnetising or self inductance, but the procedure of the test will decide which of these dominate the measurement. The leakage inductance could be approximately found for instance by shorting the secondary winding and measuring the primary inductance, and resistance. It is not possible however to split the values between windings. A similar

method can be used for magnetising impedance using an open circuit connection. The capacitances in different parts of the transformer can be found using these inductances (measured at low frequency) and the resonant frequencies (series and parallel). If measurement of capacitance is required directly rather than by calculation, it can be done using a capacitance bridge but the results are prone to error. Even given accurate measurement, the problem with capacitance determination still exists, because its distribution (i.e. between turns and between turns and earth) is important and there is no way to separate the components.

Transformer element measurement has been discussed in many publications [34,46,60,61,62]. Researchers have usually used an indirect way to estimate the element values such as via transfer functions (short circuit impedance and voltage gain)[63,64], together with fitting procedures.

In the present work, open and short circuit impedances are measured and used to model the transformer. Using these impedances, all the resonances experienced by the transformer can be viewed. During the measurements a variable frequency signal from a function generator is amplified and applied to the primary winding of the transformer. It is more safe to apply the signal to the high voltage terminals of the transformer and then refer the impedance to the winding required by the turns ratio of the transformer. The frequency response of this impedance is obtained from the ratio of input voltage to current or directly using an impedance analyser. A class AB amplifier, as detailed in Ref.[54], is used to amplify the signal of the function generator. The parameters of the amplifier have been improved by using high speed, high power transistors and capacitors to handle a bandwidth of 3 MHz. The amplifier can drive a voltage of 80V and a current of 1.2 A at the highest frequency. Depending on which of the impedances is to be measured, the secondary winding is open or short circuited. The most critical point in the test is when the measurement approaches the series resonant frequency of the transformer. The circuit can deliver a maximum current enough to fuse the transistor if care is not taken. In order to avoid repetition, the practical results will postponed to a later chapter so as to compare with these found using numerical methods.

2.10 : SUMMARY.

This chapter is concerned with two topics, the practical implementation of a high frequency power supply, and transformer testing. The power supply is built to provide the ground for justifying the simulation results that will be carried out in a later chapter. The converter used is a clamped mode series resonant converter, that clamps the voltage to zero until one of the switches in a converter leg is turned off. This converter uses a constant frequency control technique, which controls the duty cycle while keeping the switching pulse frequency constant. The reason for selecting this type of resonant converter is to serve the requirement of testing a high voltage transformer (since it is a high voltage converter), as well as a clear insight into the interaction between this resonant converter and its transformer.

A ratio of 0.8 of the switching frequency to the resonant frequency is used. When the switching frequency more closely approaches the resonant frequency, very high current flows through the tank causing unacceptable stress to the tank elements and increasing losses accordingly. Simulation has been used to study the effect of the internal transformer elements on the converter performance.

This kind of resonant converter can survive short circuit without damage, because during a short circuit, the load is reflected to the primary as a very low impedance connecting the LC resonant elements in series. Parallel resonant converters on the other hand reflect the short circuit impedance across the resonant capacitor, destroying resonance and sharply increasing switching losses.

It may seem advantageous to use the resonant converter to test the transformer, but this converter experiences deficiency during open circuits. Here, the reflected load impedance between the tank elements is high and hence very small current flow through the tank and primary winding (i.e. no or small transformer input current), and in addition :-

1- Many changes need to be made at each frequency required. The changes include, control circuit, drive, resonant tank elements, and the peripheral components of the PWM chip.

2- The resonant tank elements are in series with the transformer and could lead to an impedance measurement error, because the tank elements are part of the transformer internal (parasitic) elements.

For these reasons a linear power amplifier has been used to test the transformer.

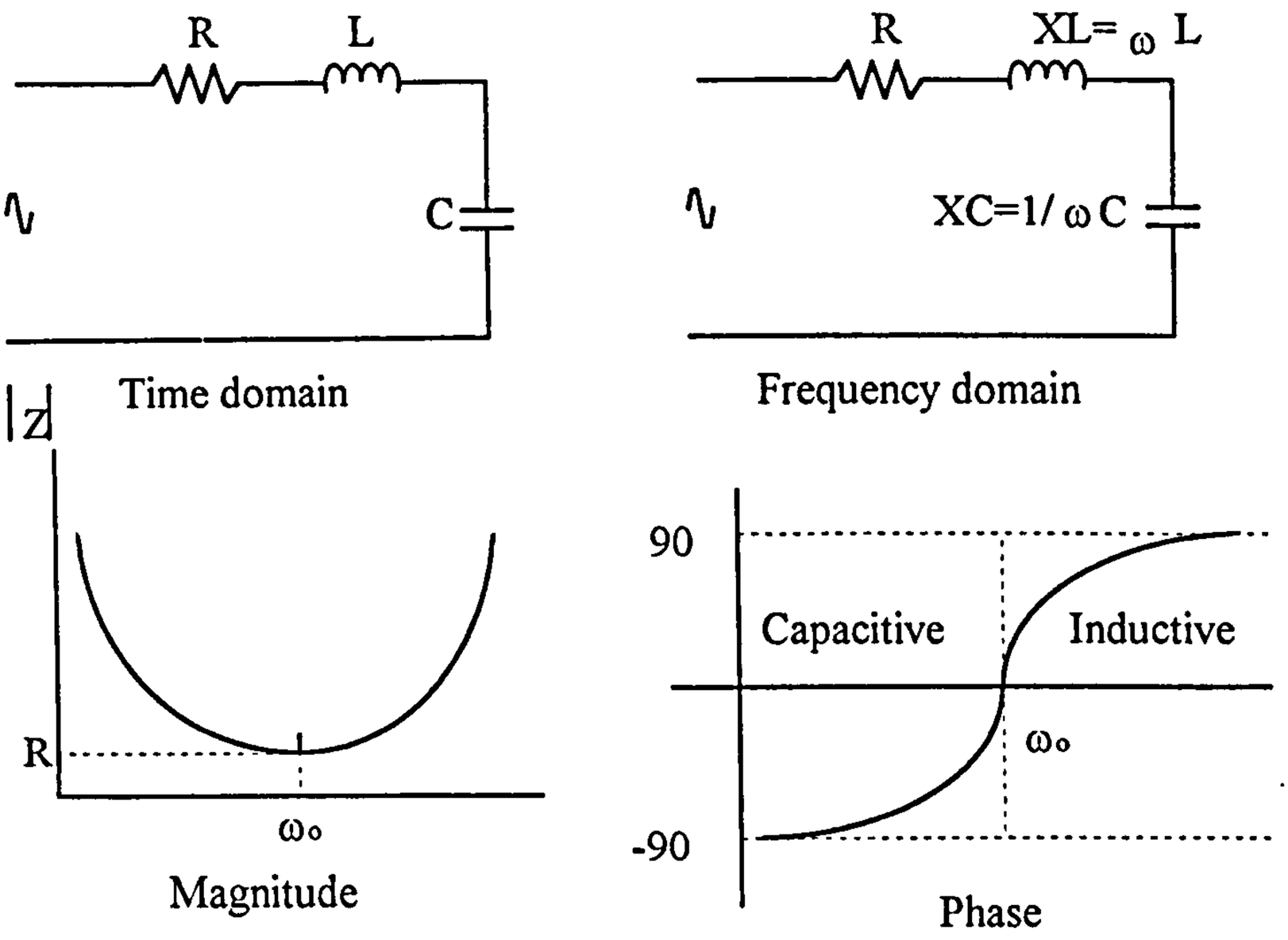

Fig.(2.1) Series resonance in an RLC circuit

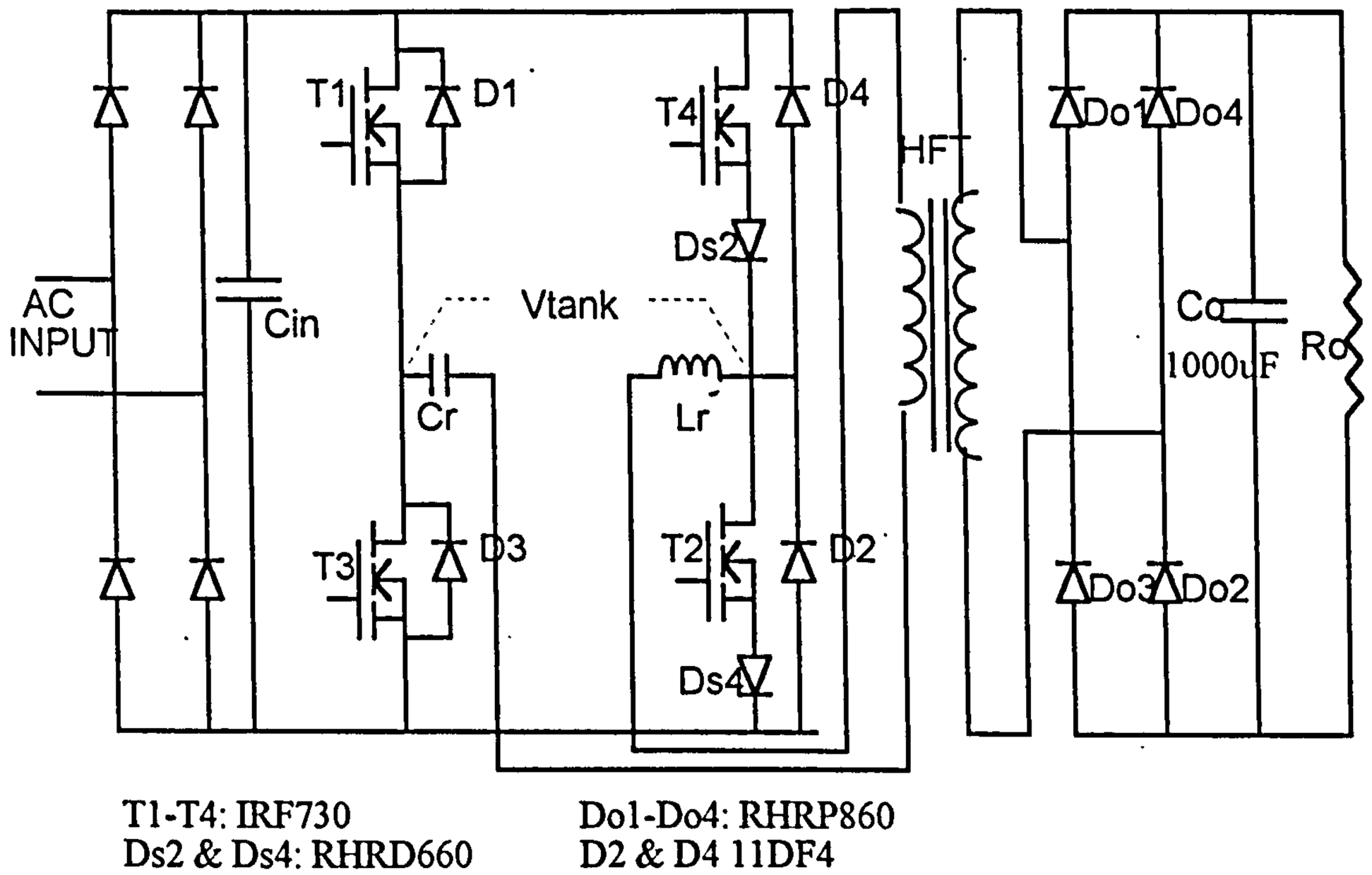

T1-T4: IRF730 Do1-Do4: RHRP860
Ds2 & Ds4: RHRD660 D2 & D4 11DF4

Fig.(2.2) Clamped mode series resonant converter

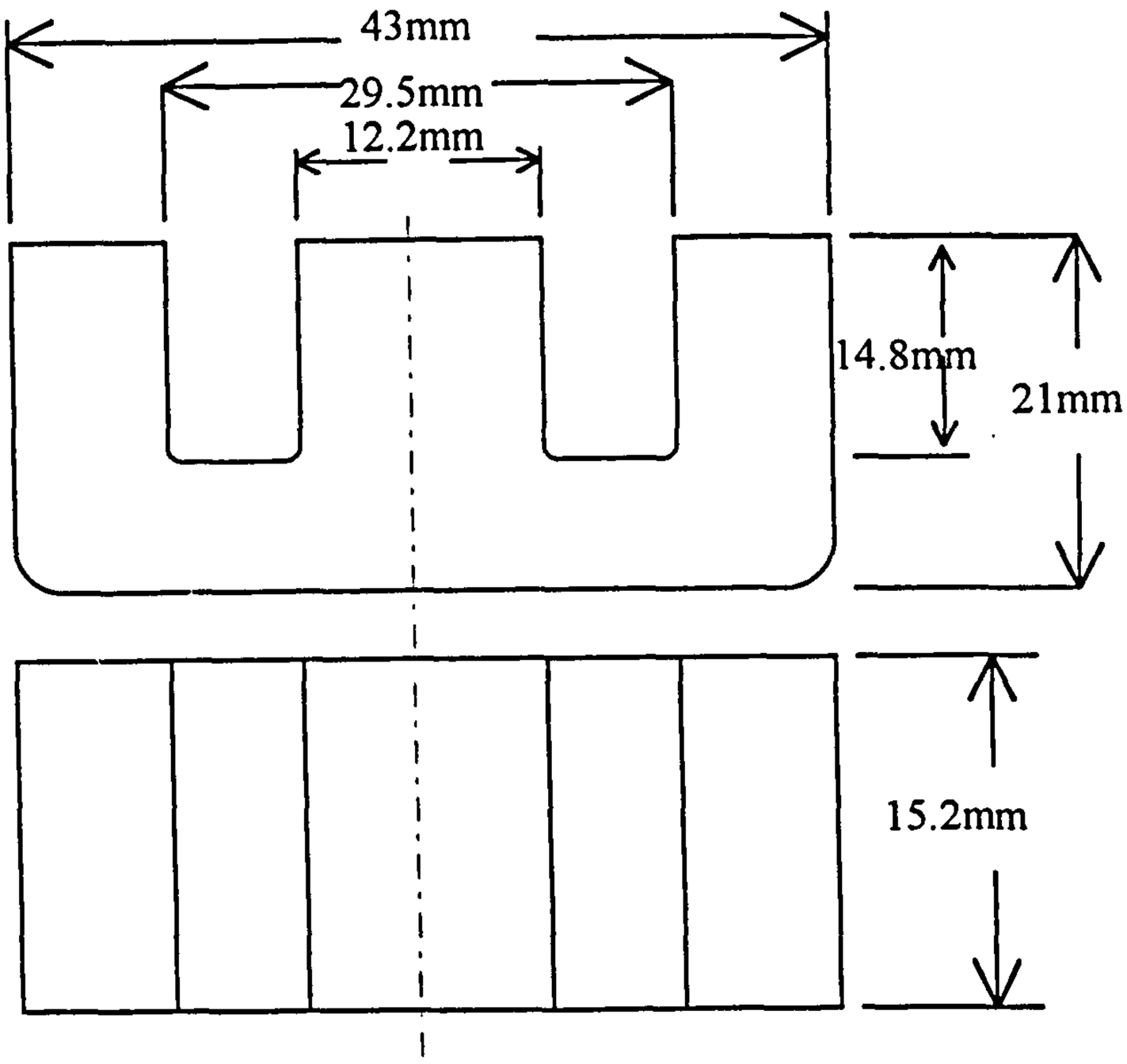

Fig.(2.3) : E-42 core dimensions

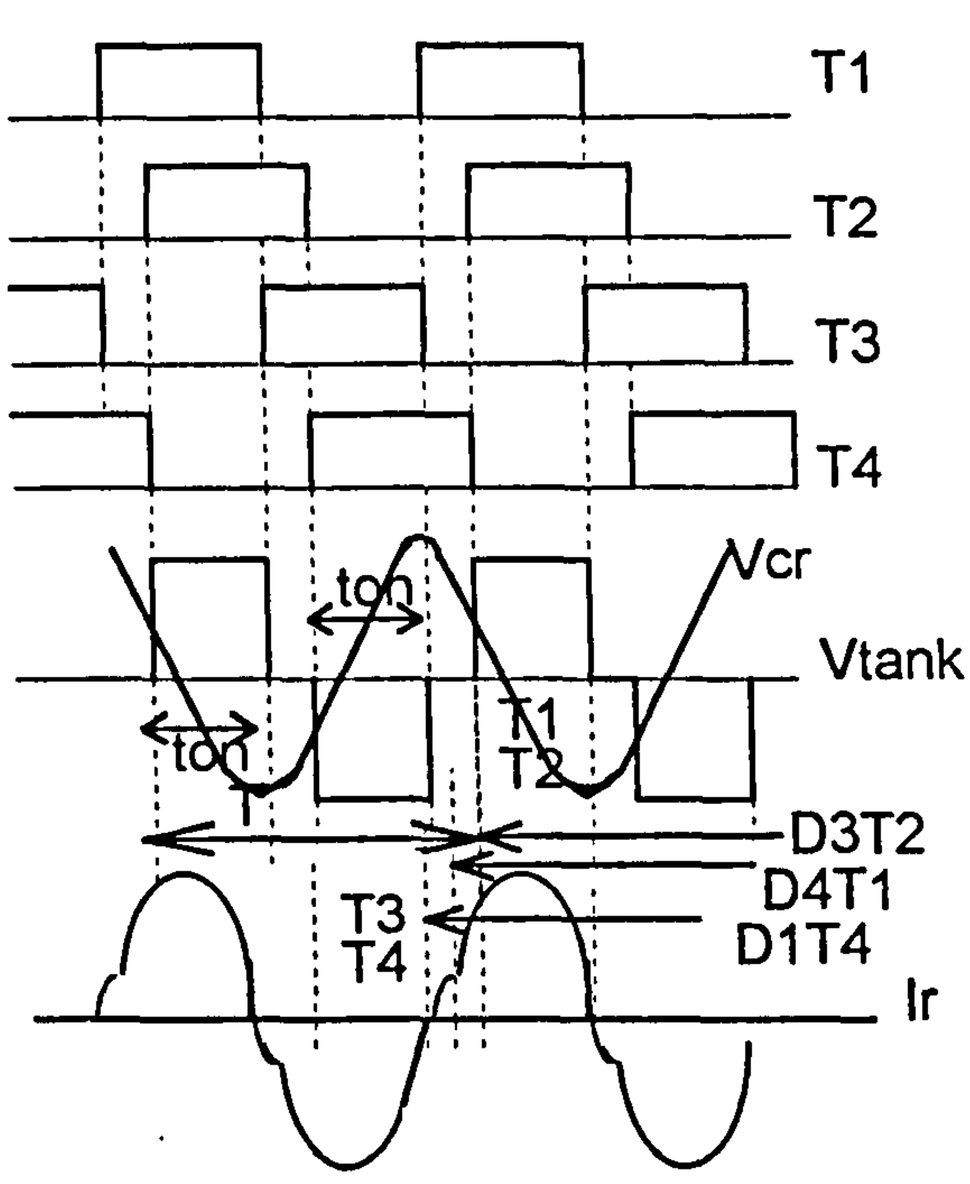

Fig.(2.4) : The theoretical bases of switching pulses

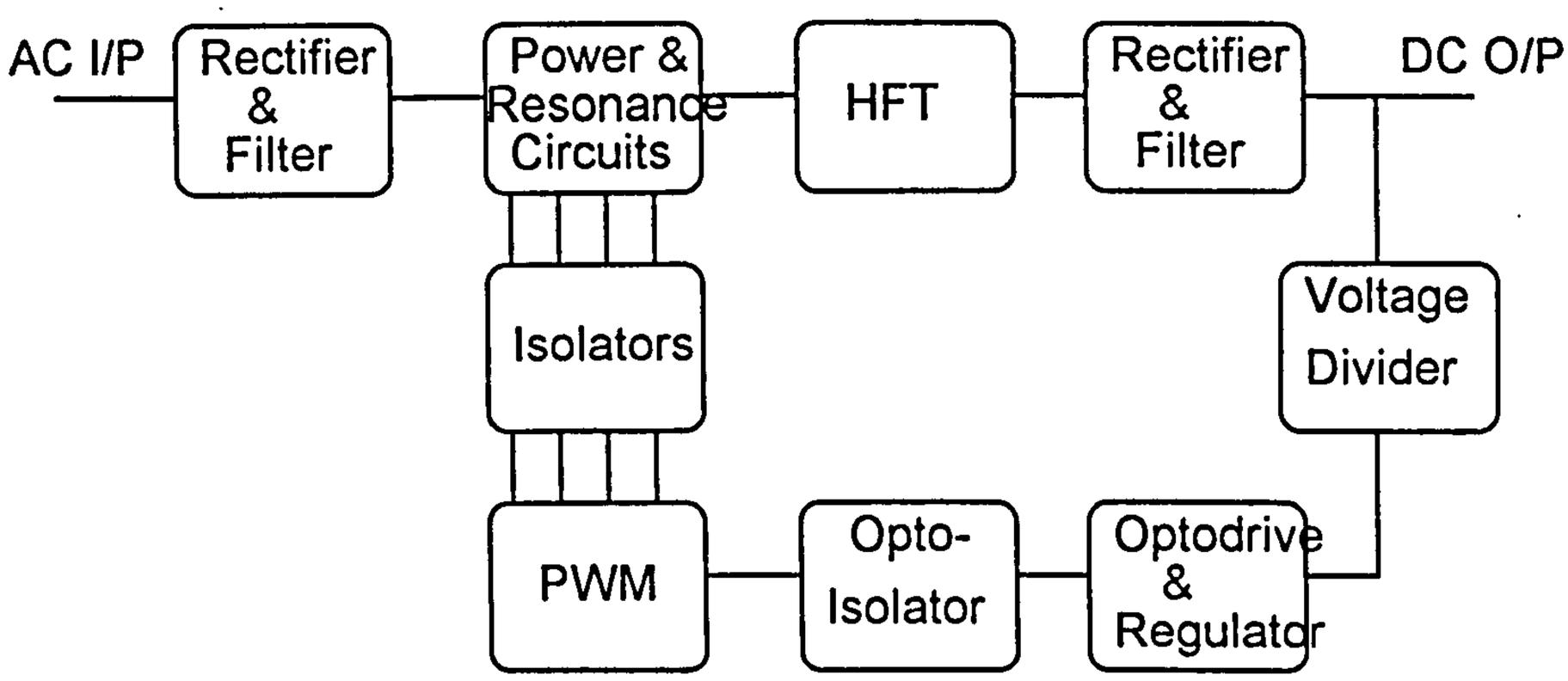

Fig. (2.5) : Block diagram of the power supply main stages

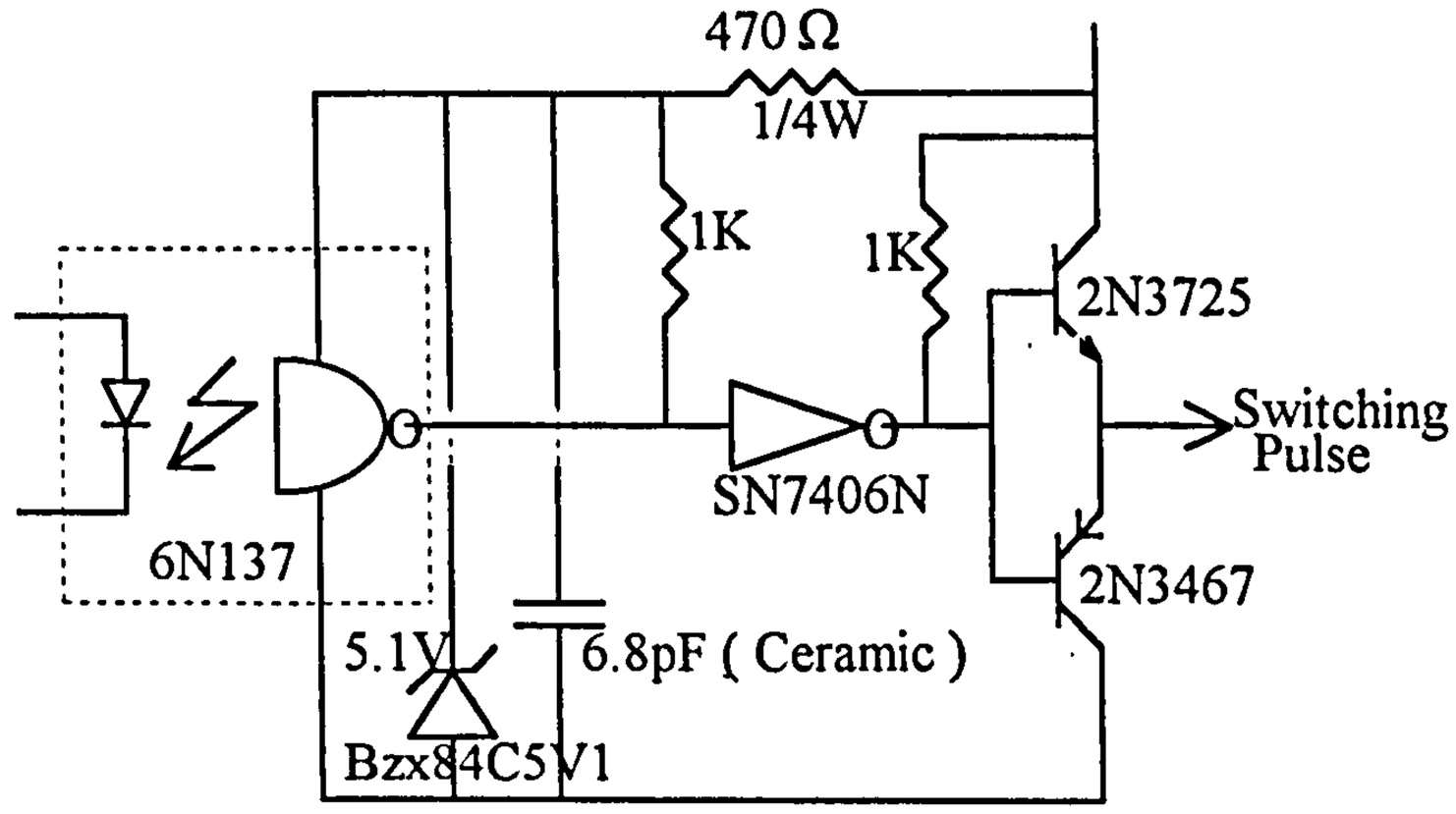

Fig.(2.6) Opto-coupler drive circuit

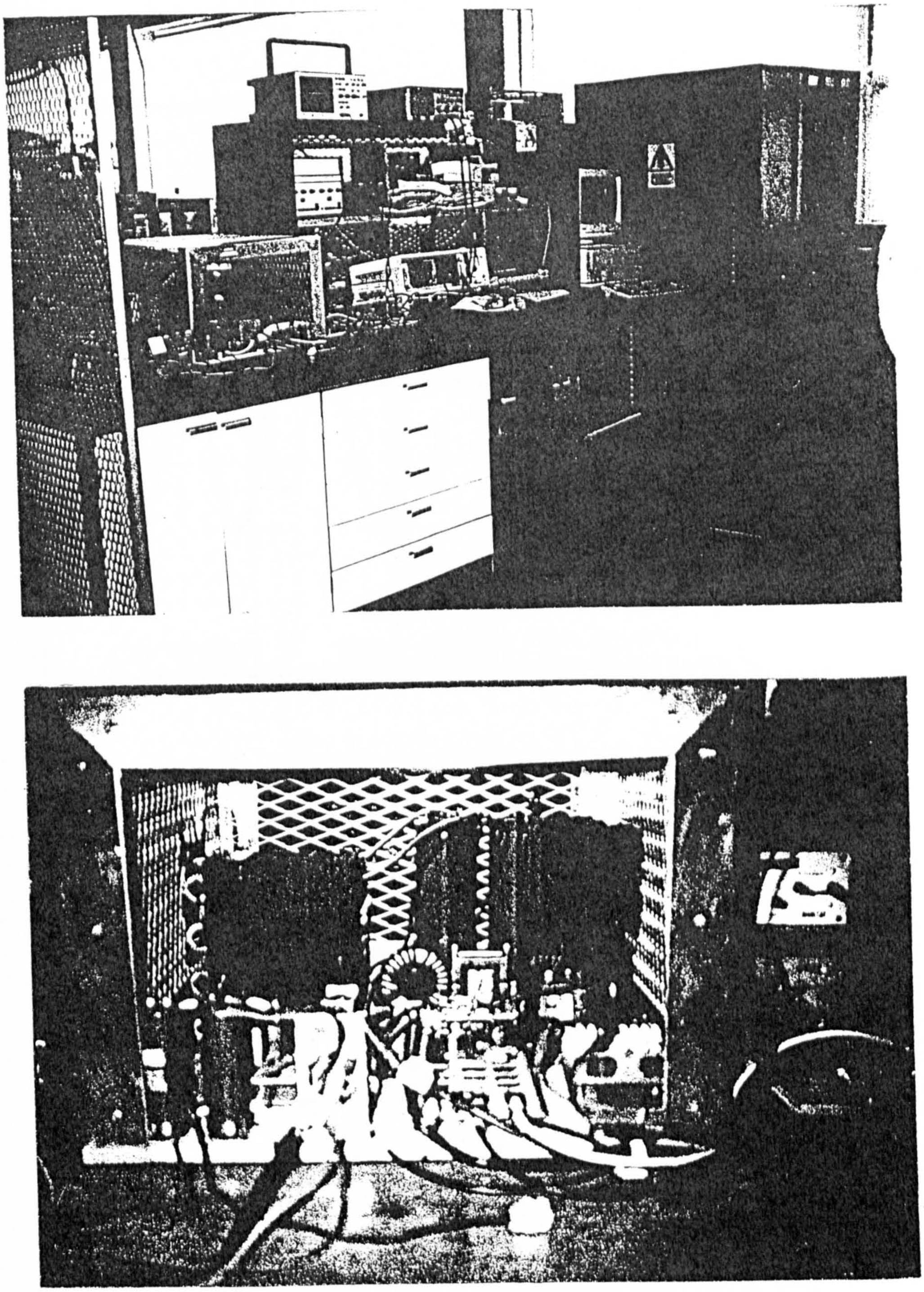

Fig.(2.7) Photographs of practical power supply

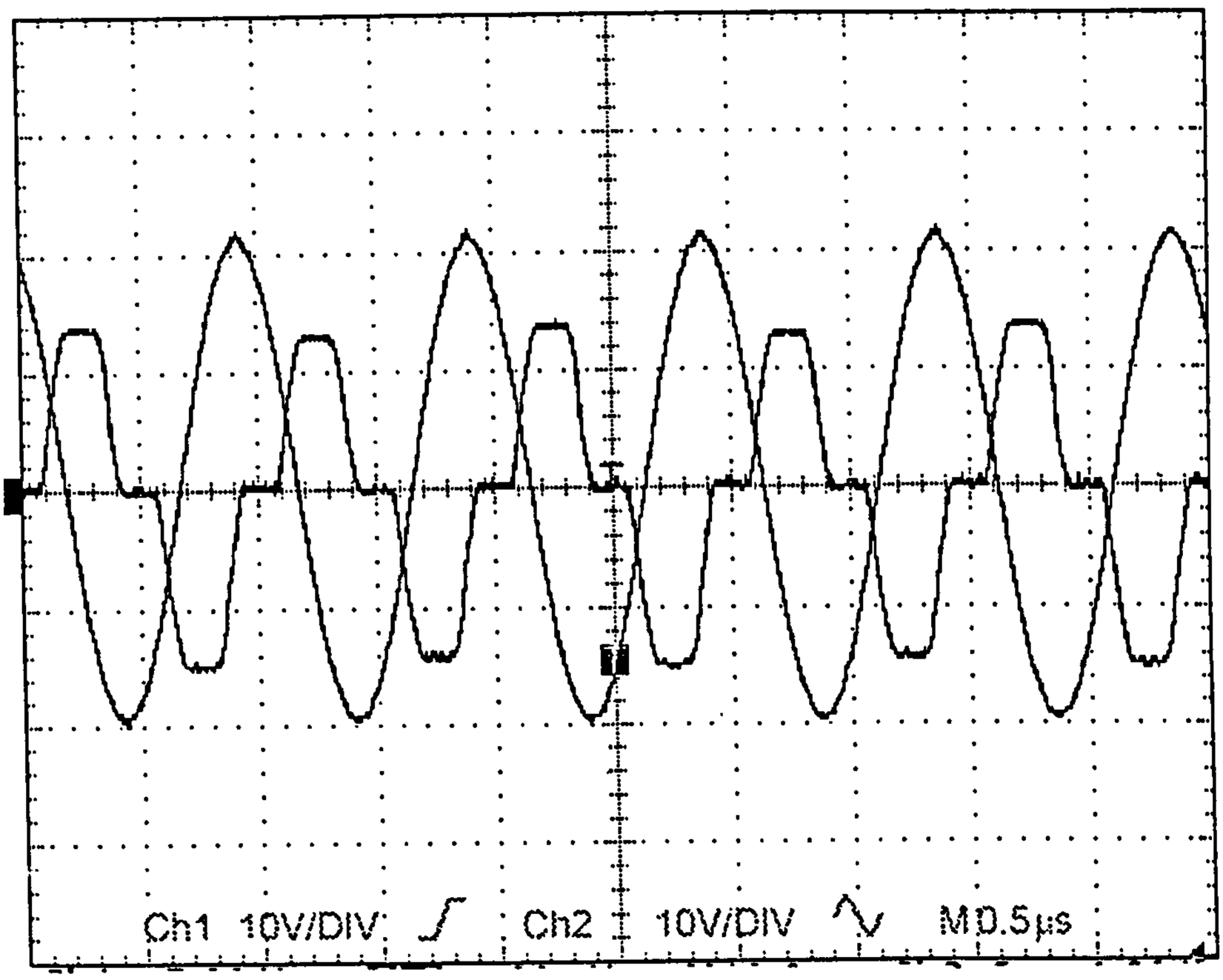

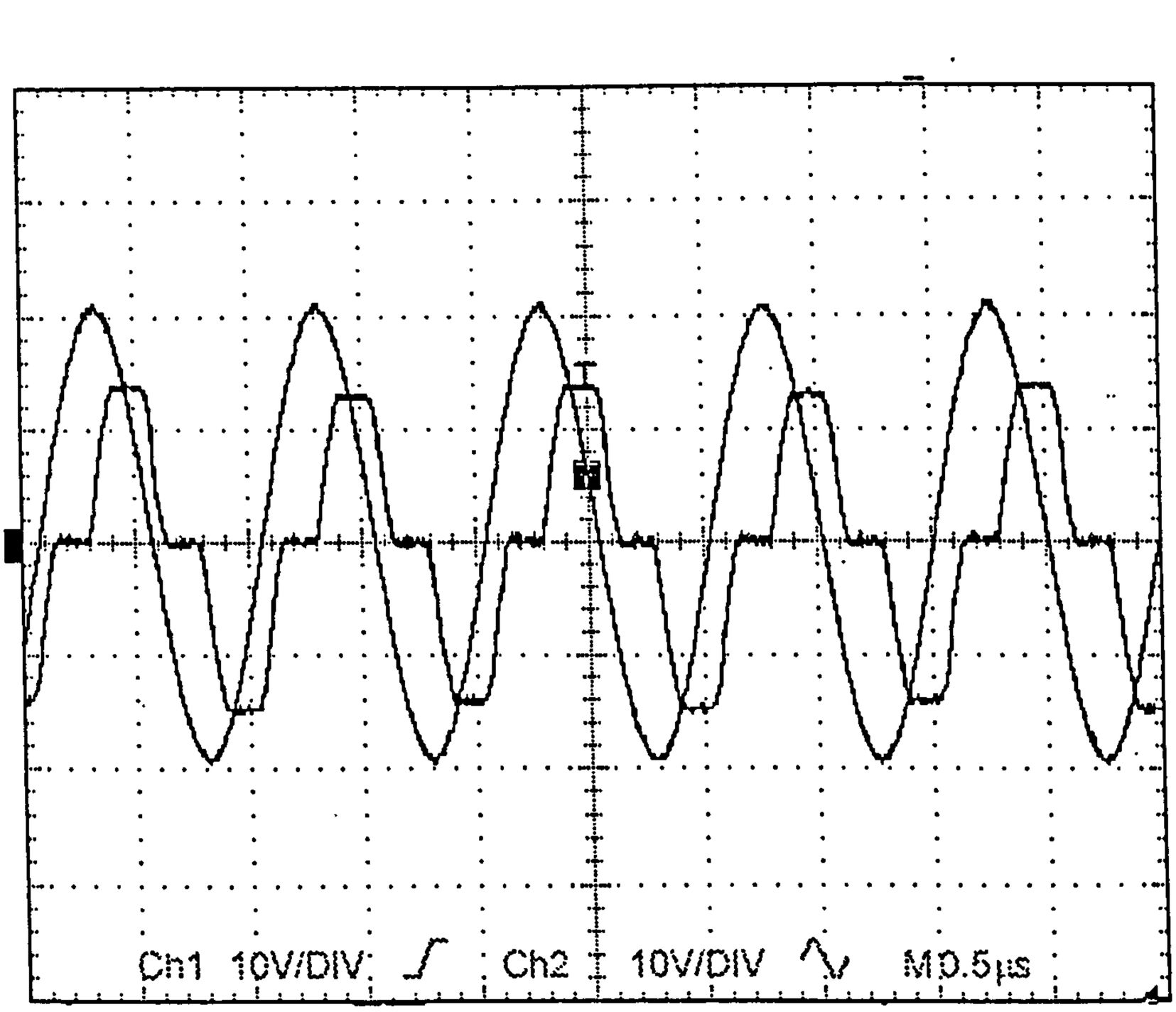

Fig.(2.8) : Resonant capacitor(Ch2) and tank voltages (Ch1)measured at 0.8 frequency ratio, (a) : Normal operation, (b) : Core air gap changed

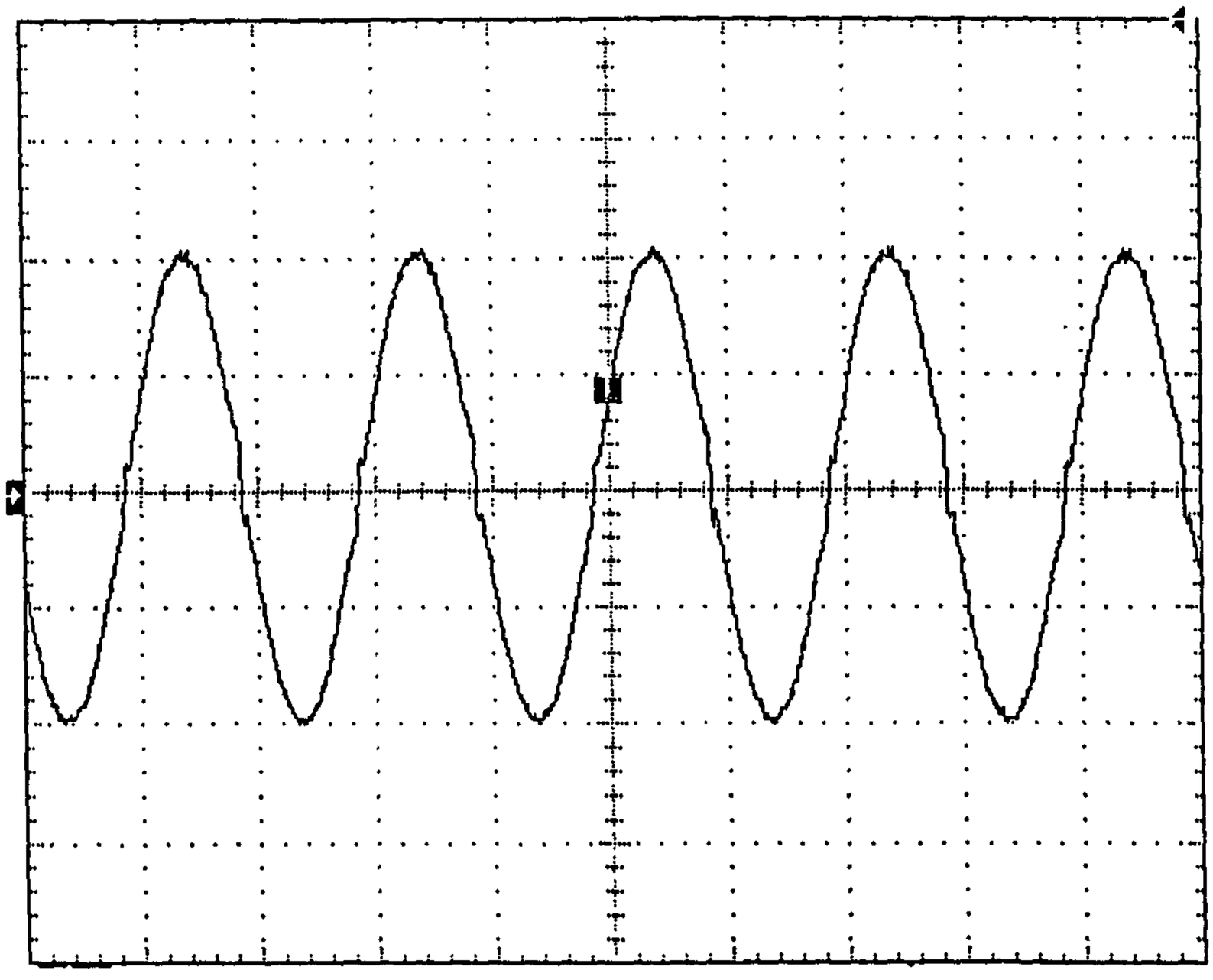

Fig. (2.9) ; Resonant inductor current measured at 0.8 resonant frequency
(1A/Div, 0.5 μs)

(a)

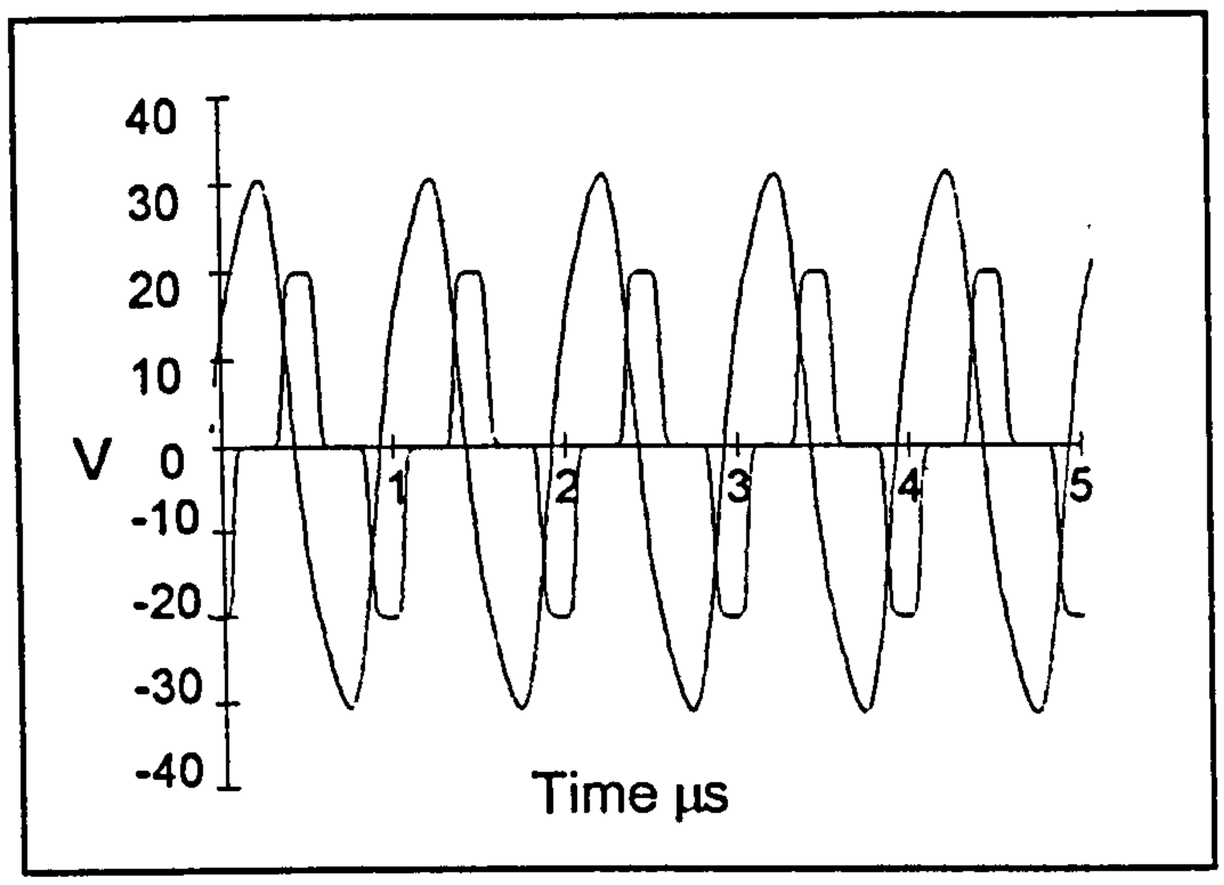

(b)

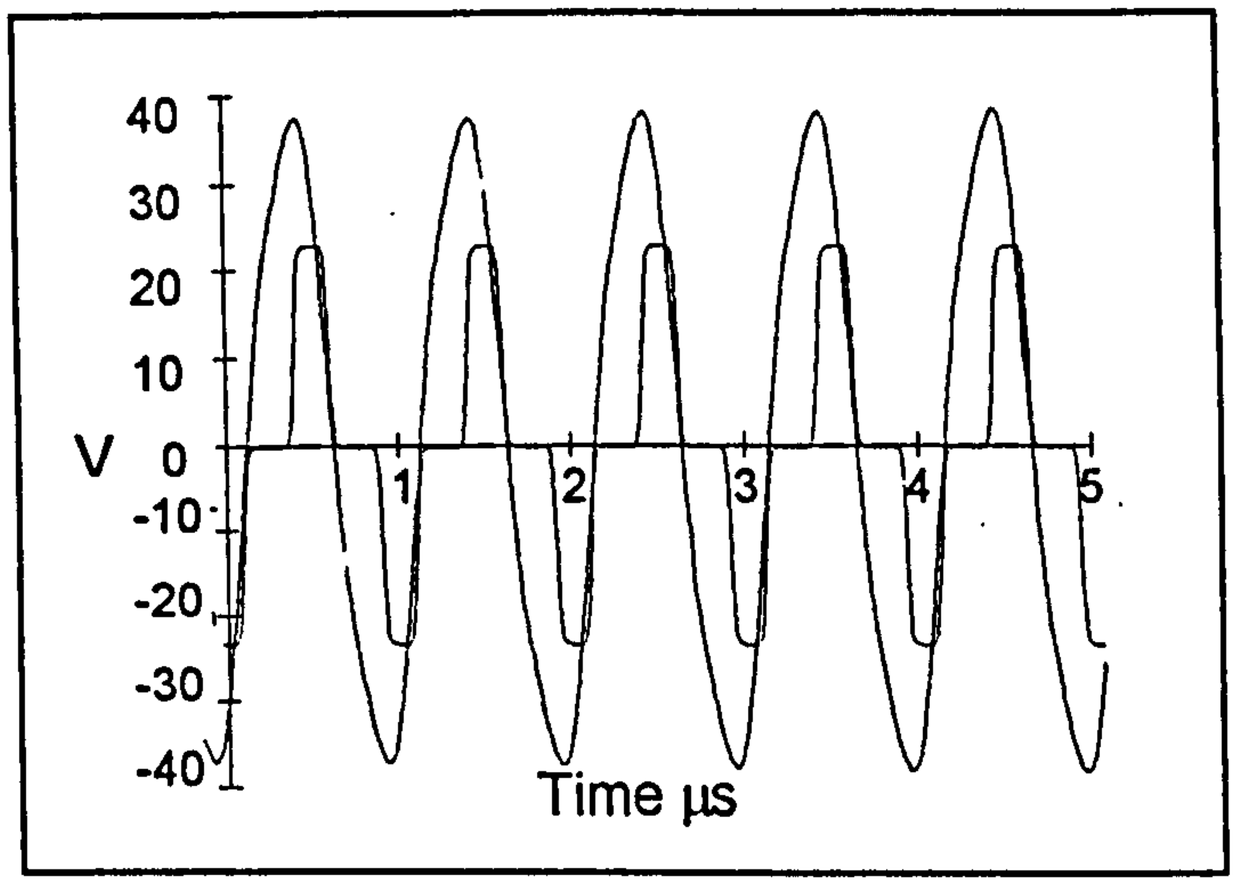

Fig. (2.10) : Simulated waveforms of resonant capacitor and tank voltages. (a) at frequency ratio 0.8, (b) : at resonant ratio of 0.88.

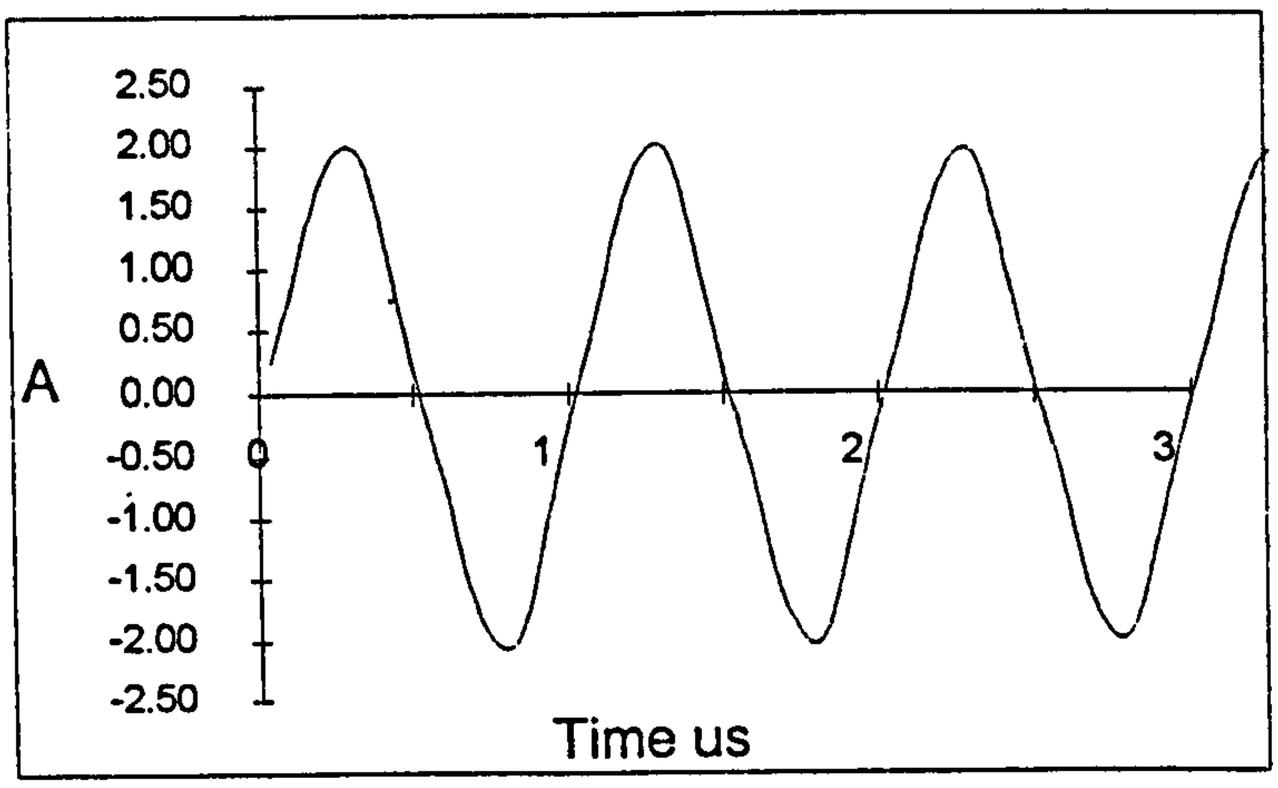

(a)

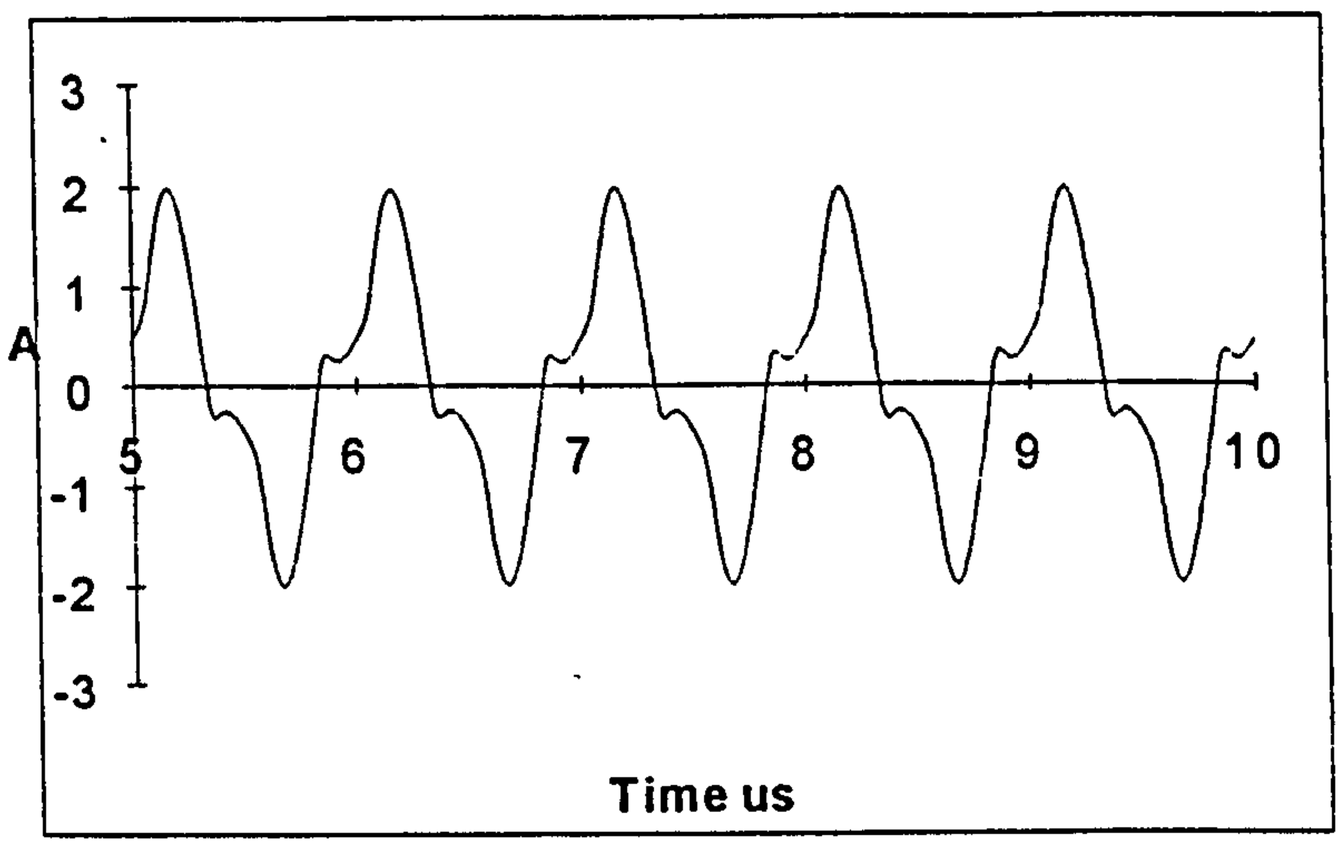

(b)

Fig.(2.11): Simulated waveforms:(a) Resonant Inductor current at frequency ratio 0.8

(b) Resonant Inductor current at frequency ratio 0.88

CHAPTER THREE

EFFECT OF EDDY CURRENTS IN TRANSFORMER WINDINGS BY 2-DIMENSIONAL FINITE ELEMENET METHOD

3.1: INTRODUCTION

Voltage is induced in a conductor when it links time varying magnetic field. The faster the change in flux, the more voltage is induced. If the conductor size is significant and / or the magnetic field is rapidly changing, voltage induced in various parts of the conductors can cause an internal current loop called eddy currents.

The eddy currents represent an advantage in some systems and disadvantage in others. In application such as transformers, the existence of these currents affects the performance of the transformer and cause losses. Away must found to minimise these effects. In some electroheat applications, they represent the source of heat due to the energy dissipated through the ohmic losses.

In our case, the existence of these currents in transformer needs to minimise for the following reasons:

1- They cause undesired ohmic loss in the windings both due to skin and proximity effects
2- They cause extra loss in the core and reduced its effective permeability
3- They cause stray loss in structural and containment components.

Thus, the study of the behaviour of these currents is very important in the search to reduce losses and thereby design a higher efficiency transformer.

As the frequency is increased and the power transformer size is reduced, eddy currents become one of the major limiting factors. The winding ac resistance and leakage inductance are strongly related to eddy current effects.

In order to analyse the eddy currents, Maxwell's equations are used. These equations describe completely the magnetic and electric fields. The form of these equations can be either differential or integral [23]. The best way to formulate these equations is in terms of potentials.

This chapter will consider eddy currents effects in some detail using one of the most powerful numerical methods which is the finite element method (FEM). This method is based on an approximate solution of Maxwell's equations [15,16,32,65] using the method of weighted residuals.

A closed form mathematical approach is available from the work done by Dowel [1], which is adopted by some researchers as a quick and simple method [19,30]. Greater accuracy is only possible using numerical methods and this is the subject of the work described here.

3.2 : 2-DIMENSION FINITE ELEMENT METHOD.

By its very nature a transformer is a three dimensional device. Both magnetic and electric fields are involved and they act in a sense normal to each other making the solution three dimensional and time varying. Three dimensional solutions [21] are expensive and time consuming, and it would be very useful to reduce analysis to two dimensions. Since the magnetic field is the main source of eddy current generation, the solution can be approximately reduced from three to two dimensions. What is being ignored is the displacement current which effectively in an ac sense "bleeds" charge between conductors and to ground. At low frequency ignoring this current is acceptable.

At high frequency the approximation becomes troublesome. This two dimensional analysis does include the effects of eddy currents, but will not be used to calculate all the parameters of the equivalent circuit model.

The beauty of the FEM comes from its flexibility. It is not restricted in any way by the irregular geometry or inhomogeniety of the field area to be solved. The main procedures of the FEM solution is :

1- Break up the geometry of the problem into a small elements.

2-Apply a different (approximate) equation to each element. For instant, the magnetic vector potential (A) which is the unknown is represented by a linear variation in each element.

3- Taken together the elemental equations form the overall system equations ,which become a matrix of simultaneous equations. The best solution methods for the size of the problem considered here appear to be semi-iterative methods such as Incomplete Cholesky Conjugate Gradients (ICCG) [66].

The finite element formulation that has been adopted using the magnetic vector potential is given in appendix A.1.

4- Post-processing of the results in order to obtain parameters of interest and to show the results in graphical form.

The main equation to be solved in the 2-dimensional program is :

$$\nabla \times \left(\frac{1}{\mu} \nabla \times A_z \right) = -\sigma \left(\frac{\partial A_z}{\partial t} + \nabla V_z \right) \qquad \text{---------- (3.1)}$$

During the solution, this equation is considered to have a sinusoidal source variation, which means a simple transference of the eddy current term into the frequency domain.

$$\frac{\partial A_z}{\partial t} = j\omega . A_z \qquad \text{----------} \quad (3.2)$$

In most power supplies, the current waveforms are not sinusoidal. Although, modelling this wave shape is possible, it greatly adds to computation time. Therefore, attention has been restricted to the fundamental component only.

3.2.1 : TWO DIMENSIONAL FE TRANSFORMER MESH MODEL.

Apart from the assumptions which have already mentioned, further simplifications have been introduced in order to make the problem numerically tractable:

1- The magnetic vector potential(A), and the source current density (J) have values in the z-axis only, which are constant in that direction.

2- The problem is treated as linear, where a single value of permeability and conductivity are applied. Hence, the hysteresis, saturation and temperature effects [41,43] are approximated or neglected.

3- The displacement currents [65] are absent,i.e.:

$$\frac{\partial D}{\partial t} = 0 \qquad \text{----------} \quad (3.3)$$

Fig. (3.1a) shows the mesh model of the transformer. Valid solutions must also satisfy the condition that the length of each element side has to be shorter than the skin depth. This condition is important to avoid excessive error. The well known skin depth relation is :

$$\delta = \sqrt{\frac{2}{\omega \sigma \mu}} \qquad \text{----------} \quad (3.4)$$

The conductors in the model are considered as having a square cross section with an area equal to that of a round wire. This approach has been considered by many researchers [1,30] to make the problem more manageable from a meshing viewpoint.

The answers for A and V (the net voltage at the end of the conductors) are effectively per unit of length in the direction of the turn. This can lead to a simple idea to obtain better accuracy, by noticing that the depth of the E-core viewed from the front is larger than that viewed from the sides. In that case the area available for the magnetic path is different in each side. Therefore two models are used one for each side as shown in Fig. (3.1b). The total winding impedance is the total of the impedance of the two models.

$$Z = \frac{2N}{I}\left(l_1 * \sum \nabla V + l_2 * \sum \nabla V\right) \quad \text{----------(3.5)}$$

Where l_1 and l_2 are the length from the front and side section of the core, and N is the number of turns. The calculation due to these two models improve the result by 2% at 1KHz and by 8% at 1MHz in comparison with that of using one model when compared with measurements.

3.2.2 : SERIES WINDINGS REPRESENTATION.

In the solution of the FE equations, the source that is used to drive equation (3.1) is either voltage or current. The term ∇V represents the voltage appearing at the ends of conductor expressed per unit length of the conductor. If the voltage is not given, for instance when the winding is connected to an impedance, an extra equation is required to solve the extended circuit. For example, when the impedance is a short circuit, the summation of ∇V is equal to zero, but its value for each individual conductor is not. The extra equation required is :

$$V = l * \sum_N \nabla V \quad \text{----------(3.6)}$$

where N is the number of turns, V is the voltage across the winding, and ∇V is the voltage between turns sections, where each turn is formed from two separate sections. This equation gives the flexibility required to link extended circuit with the FE analysis. A simple case is a capacitor connected across the terminals as carried out in reference [67], or by adding an external circuit as seen in the Fig. (3.2). When this figure is considered , equation (3.6) can be rewritten as :

$$V + I Z = - \ell \times \sum_{N} \nabla V \qquad \text{----------(3.7)}$$

The equation that represents the induced current in the winding is :

$$I = \iint_{s} J\,ds = -\iint j\omega\sigma A\,dxdy - \iint \sigma \nabla V dxdy \qquad \text{----------(3.8)}$$

Where ds is the conductor cross section area. This equation can be rearranged In order to include the series winding equation as :

$$-\iint \sigma \nabla V dxdy = I + j\omega \sum_{conductors} \iint \sigma A\,dxdy \qquad \text{----------(3.9)}$$

Equations (3.1), (3.6), and (3.9) can be formed into a matrix that is used to solve for A and ∇V. The use of the magnetic vector potential to calculate the winding inductance and resistance is given in appendix A.2.

In order to help to validate these equations, the transformer described in chapter two has been modelled but with very simple primary and secondary windings of only 4 turns each (each turn cross section area is the same as the true transformer)

The table below shows the results for the short circuit condition. Two conclusions can be drawn from the table. First, that the input voltage is equal to the summation of the voltage at the end of conductors in the primary winding, while their net value is equal to zero in the secondary as required. Secondly, the voltages across all conductors are relatively the same due to the absence of any capacitive effect. The small change in the

value of the secondary voltage can be explained due to the difference in leakage flux linked by each turn.

The high frequency losses in the winding will depend on the depth of the conductor relative to its skin depth and also on the position of the conductor relative to its neighbours (proximity effect). This very slight difference in induced voltage per turn at this low frequency (1KHz) will become larger as the frequency is raised.

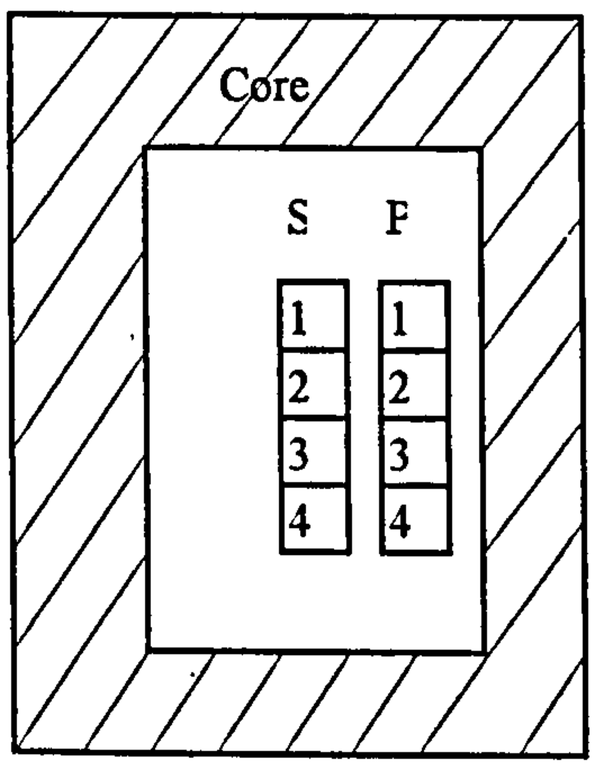

cond. No.	voltage / meter
	primary winding
1	-1.18635E+01 +j 8.11783E-01
2	-1.18635E+01 +j -8.11604E-01
3	-1.18635E+01 +j -8.11605E-01
4	-1.18635E+01 +j 8.11426E-01
	secondary winding
1	3.66716E-01 +j 2.23612E-01
2	-3.67713E-01 +j -2.25624E-01
3	-3.65717E-01 +j -2.24668E-01
4	3.66714E-01 +j 2.26679E-01

3.3 : EDDY CURRENT LOSSES IN TRANSFORMER WINDINGS AND CIRCUIT CONDUCTORS.

As switching frequency is increased, optimisation of the power transformer becomes a major concern. Eddy current losses and variation of inductance with frequency can greatly affect the transformer performance. The change in inductance with frequency becomes significant in size as compared to the total circuit inductance.

It will be useful to define some general principals and resulting phenomenon at the outset. It will also help to relate the effects to the terms often used to describe them. If an inductor is suitably manufactured from fine wire, its resistance and inductance will not vary with frequency. In practice, there will always be a frequency at which these eddy current effects start to become significant, and the current is forced into a surface layer by its own magnetic field. The resistance will clearly rise and hence the term " ac resistance " is coined. At the same time, as the resistance rises, the inductance falls because the area of the flux path is reduced by the width of the conductor. If the inductor has an iron core, the laminated or sintered core will also be affected by eddy currents, and its reluctance will rise which will also tend to reduce the coil's self and leakage inductance.

Yet a further effect is that any conducting components nearby will increasingly have opposing eddy currents induced in them, which will again appear as reduced coil inductance and increased coil resistance. The term ac inductance is often used to point to the fact that the effective inductance (self and mutual) reduces as the frequency rises.

More confusingly the term " parasitic inductance " is also used. The implication is that as frequency rises the " parasitic inductance " increases, and that therefore one could view the parasitic inductance as being negative in character.

Proximity is the effect whereby current is forced to flow in the edge of a conductor by the proximity to current in nearby conductors. It will have the same effect as

straightforward skin effect. In many transformer windings, proximity will be a larger effect than simple skin effect [2,31,52,68].

A numerical technique that includes all of the important effects and is in good agreement with the practical results is therefore essential.

In this section, different physical aspects of the winding arrangement are discussed. The aim is to understand the underlying principle and thereby lower leakage components and eddy current losses.

3.3.1: COPPER LOSSES IN THE CIRCUIT WIRING.

It is well known in eddy current analysis that extreme care must be taken in modelling correctly the rapid decay in field that occurs at conductor boundaries [28,52,69]. This problem will be troublesome as the frequency gets higher and losses are increased accordingly.

The main two effects that dominate the copper losses are the skin and proximity effects. The procedure of numerical solutions will start by considering one conductor only, and the principles deduced can be extended to include all the turns in the winding.

3.3.1.1: SKIN EFFECT.

Fig. (3.4) shows a copper conductor consisting of 64 (parallel , untwisted) fine wires forming the " go " half of a turn of the winding. The return half is not modelled due to the symmetry of the turn around the core.

In the top flux plot in Fig.(3.4), the conductor is carrying current at 1 KHz. At this frequency the skin depth is 2mm. This is much greater than the depth of bundle of wires which is 0.48 mm. The magnetic field varies across the conductor causing differential voltage in each wire, but the eddy currents which result are insufficient to redistribute the field.

When the frequency is increased to the level where the skin depth is much smaller than the wire thickness, the current inside the conductor will be non uniformly distributed as seen in Fig. (3.5). The bottom flux distribution of Fig.(3.4) is with a frequency of 1MHz. The skin depth is now 0.063mm, and the eddy currents redistribute the flux, so that every turn links the same flux. These currents are in the same direction as the main current at the conductor surface and oppose it further in. Hence, the current density falls exponentially within the conductor. The actual area of the conductor that carries current is reduced as the frequency increases, and so the ac resistance will be greater than its value at dc or low frequency and the loss increases accordingly.

In order to reduce this skin effect, the wire has to be divided into many fine wires and twisted, so that each of the fine wires occupies equally every position in the bundle. The main issue here is to see how fine the wire has to be. Many researchers [30,33,59] have used the common approximation that the current is evenly distributed across a skin depth (see sketch below). In this case the actual curve of the current density is replace by an equivalent rectangular distribution as shown in the diagram, which of course is much easier to apply. In fact this approximation is only valid provided that the conductor is far greater than the skin depth. Extending the argument to suggest that conductors should be no more than one skin depth deep in fact does not make best use of material.

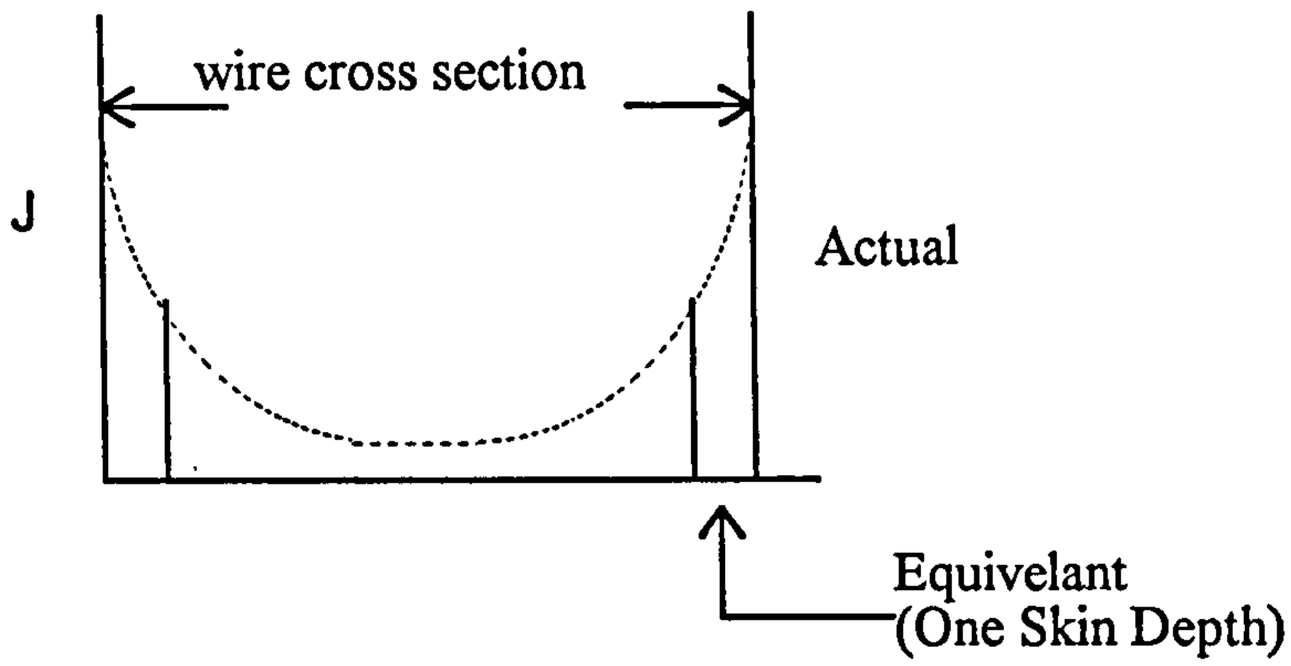

The finite element technique has been used to estimate an "optimum" value of wire size providing the best compromise between number of wires (and hence cost) and ac resistance. Different wires sizes with respect to the penetration depth relation have been modelled. The results show that a good ac to dc resistance ratio is achieved when the wire thickness is 1.2 times the skin depth.

In order to give additional support for this value, a method is derived for calculating the variation of the conductor resistance for a single square conductor against frequency. The resulting resistance value for a sinusoidal variation, for a single conductor is given by :

$$\frac{R_{ac}}{R_{dc}} = \mathrm{Re}\left[\sqrt{\frac{j\omega\mu}{\rho}} * b \coth\left(\sqrt{\frac{j\omega\mu}{\rho}} * b \right) \right]$$

Where the dc resistance is $\frac{\rho \ell}{b^2}$, and b is the side length. A full derivation of this equation is given in ref.[1] and discussed in ref.[52]. The resistance ratio is shown graphically in Fig.(3.17)as compared with that in ref.[1], which shows how its value is increased as the thickness to skin depth ratio gets higher. As can be seen, the ratio takes a sharp rise for the curve around $b/\delta = 1.2$. The accuracy of the finite element result provides validation for the method and helps justify its use for more complex problems.

3.3.1.2 : EQUIVALENT CIRCUIT MODEL OF THE WIRE.

It is often useful to form an equivalent circuit model. This approach is probably easier for a circuit designer to deal with.

In the finite element modelling, if the wire is placed in free space it will set up an infinitely extending magnetic field. To restrict computation the wire is encased in a bounded area to enclose the magnetic field at a reasonable distance. However, its size is still arbitrary, but it is a matter of numerical convenience to satisfy the requirements of the finite element solution. In practice there will always be a return wire(s) and the boundary conditions imply their existence.

Returning once more to the 64 stranded wires shown in Fig.(3.4), an equivalent circuit can be produced for these fine wires as shown in Fig. (3.3a). If these wires are modelled in one equivalent circuit, three elements can be clearly recognised. One of these elements is the resistance associated with the loss in each of the wires. The second element is the assembly of inductances associated with the operation of all wires acting together, this is termed the "external inductance" [3,46] and is given in the symbol Lext in Fig.(3.3a). The other inductance is associated with flux which lies between each parallel wire and reflects the fact that there is flux produced by each wire, which does not couple with other wires. It would be logical to describe the fine wire elements by an inductance matrix made of self and mutual terms, and the effect of proximity would demand the same for a resistance matrix [39]. However, The size of these matrices would be 64*64, which by any standards is large and cumbersome. In order to keep the computations as simple as possible, a single fine wire is considered. In this case the equivalent circuit can be reduced to the model shown in Fig. (3.3b). It should be noted that point "1" represents the outer surface of the conductor, while "2" is at the centre. In order to calculate the terms (elements) in the model, the impedance of the wire is calculated using finite elements at two different frequencies and the results are as given below.

frequency (kHz)	Z/m	R/m (Ω/m)	L/m ($\mu H/m$)
1.0	0.06 + j 0.0021	0.06	0.33
1000.0	0.16 + j 1.99	0.16	0.31

The inductance values above describe the total of two components (self inductance). One comes from the energy storage in the external magnetic field, and the other accounts for the magnetic energy distributed throughout the wire. At very high frequencies, the flux is effectively excluded from the wire and the effective inductance falls towards the external inductance. From the energy calculations ($\frac{1}{2} L I^2$), the internal inductances at these two frequencies are 34 nH/m and 13.7 nH/m while the external inductances are 0.316 μH/m and 0.31 μH/m respectively. These three components:- internal inductance, external inductance and resistance are the elements of the equivalent circuit of one wire.

The relevance of the skin depth can be seen clearly by applying a sine wave signal to the circuit of Fig.(3.3a). The values of the elements are the same as those calculated above. When the frequency of the voltage wave form is 1 KHz the current distribution will be uniform as seen in Fig.(3.6), because the internal reactance is relatively small compared to R (the resistive component). In the high frequency case, the current flow will be greatest at the surface and fall exponentially toward the centre of the conductor, due to the high value of reactance in comparision with resistive component.

3.3.1.3: PROXIMITY EFFECTS.

So far only one conductor has been considered, where the self induced eddy currents are called the skin effect eddy currents. Another important eddy current effect is the proximity effect [31,33,52]. This effect exist due to the flux linking surrounding conductors, which cause a circulating current in adjacent conductors as shown in the Fig.

(3.7). Flux is not going to be radially uniform when two adjacent conductors carrying the same current are considered. As the frequency is increased, current will concentrate on the outer surfaces of the conductors. The field will be additive on the outside and cancel in the middle. If the bundle of fine wires are in parallel and untwisted, the current will end up flowing in the outer wires, and the situation would be identical to having a solid conductor. For this case the current distributions in different wires within the conductor bundle including face, middle and far end at low and high frequencies respectively are given in Fig.(3.8 a,b). The effect of the eddy and proximity effects in the middle area which are opposing the main current in the surface is clearly shown in the figure.

As the space between the conductors is reduced, more field cancellation occurs. The losses will then be higher and the leakage inductance reduced. If each wire was very far from its neighbour, the proximity effect would be negligible but the leakage inductance would be high. This is clearly not a reasonable solution, the obvious solution is to twist the conductor bundle. This has the effect of forcing every wire to carry the same current, and hence reducing losses but also to minimise leakage inductance.

3.4 : SHORT & OPEN CIRCUIT ANALYSIS

The aim of the analysis is to make an attempt to minimise the copper [30] and eddy losses [28,70]. These losses depend on the total current carried by transformer windings. There are three current components forming this current, they are, load, magnetising, and capacitive currents. This analysis neglects the capacitive effects for the reasons already stated, and they are in general small in comparison to the leakage and copper loss. But their effects can not neglected for frequencies greater then 1MHz [71].

The load and magnetising currents can almost be separated by open and short circuit analysis. Since a Ferrite core of high permeability is used, the magnetising current will be small in comparison to the load current. It may be quite appreciable if the core has an air gap, and transformers used in power supplies need an air gap for two reasons, first to provide the required magnetising current to maintain zero voltage switching at light load [49], and second to avoid saturation caused by dc flux components in the transformer.

Finite Element analysis is used to consider the effects due to the two current components, and the transformer analysed is as before.

3.4.1 : SHORT CIRCUIT ANALYSIS

This analysis enables the determination of the copper loss and leakage flux components caused by the load current. In this analysis a rated current of 5Ampere is applied to the primary side, while the secondary terminals are short circuited. The equivalent circuit for this two dimensional model is shown in Fig.(3.9a). The values of the total ac resistance and leakage reactance for both windings are calculated and referred to the side on which the voltage is supplied.

$$R = R_p + \left(\frac{N_s}{N_p}\right)^2 R_s \qquad \text{----------(3.10)}$$

$$X_l = X_p + \left(\frac{N_s}{N_p}\right)^2 X_s \qquad \text{----------(3.11)}$$

On short circuit, the flux is low in the core and the magnetising current is negligible. The values of the circuit elements can be difficult to determine separately and accurately by test because of the domination of the inductor reactance. In the finite element analysis the values can be determined from the loss and the stored energy directly.

The field distributions during a short circuit in the secondary winding at different frequencies are shown in Fig.(3.10). As the frequency is increased, the flux tends to concentrate in the space between the windings. This change of field distribution reflects losses due to the proximity effect and also changes in the leakage inductance. The calculated impedance is the sum of the two finite element models (front and side elevations) as shown in Fig.(3.11) (Please refer to fig.(2.3) and ref.[51] for transformer overall dimensions). The total short circuit impedance in the primary side is given in Fig.(3.12) along with measured data and it can be seem that the agreement is reasonable. The curve shows that the calculation is viable up to 1 MHz, but above that capacitive effects cannot be neglected, the calculated impedance therefore only rises whilst the measured impedance turns over as capacitance starts to dominate. The total winding resistance and leakage inductance are given in Fig. (3.13a and b) respectively.

The most important factor that effects the leakage inductance is the gap between the windings, i.e. inductance increases as the gap increases. The effect of the gap on the loss is the opposite, i.e. falling with increasing gap as proximity effects reduce. The effect of winding separation is clearly seen in Fig.(3.14).

3.4.2 : OPEN CIRCUIT ANALYSIS

Traditionally, this test will establish magnetising characteristics, core loss and winding coupling (i.e. effective turns ratio). The assumption has been made for the core test that the permeability will be a single value, this means that the elements of the open circuit test to do with saturation, and harmonic production [6,43,72] are beyond the scope of the study. It is the case however that proximity effects are changed by the presence of the main field and effective winding resistances will not be the same on open circuit as they are on short circuit. An example of this effect is that even though the

current in the secondary winding is zero, there can still be eddy currents within it which sum to zero.

It should be noted that whilst ferrite cores exhibit a bulk conductivity which is around 10^6 smaller than lamination steel, it still becomes important at high frequency. This effect can be modelled and the results show that it is not a negligible effect. The results of both primary resistance and self inductance are shown in Fig.(3.15) respectively, and in this case the magnetising inductance falls as core eddy currents occur at about 1MHz.

3.5 : CORE PROPERTIES

The core used in this analysis is Ferrite E42 [51], the dimensions and all relevant data are given in chapter two. Fixed values of relative permeability and conductivity are used during the finite element modelling. These values are $\mu = 2200$ and $\sigma = 2(\Omega.m)^{-1}$, for permeability and conductivity respectively (taken to be the best match to the Ferrite manufacturers data).

In general, there are two types of losses in the core, eddy current and hysteresis losses. The finite element modelling showed that the largest effect was eddy current rather than hysteresis loss.

The core properties have virtually no effect on the transformer parameters during the short circuit, because flux in the core is small and hence the eddy currents in the core are negligible as compared to those in the winding. The short circuit test's main use is to examine the eddy current loss in the winding and the subsequent effect on the leakage inductance and winding resistance rather than effects in the core. The opposite state can be expected during the open circuit case, where the eddy current in and leakage of the winding are very small and can be neglected in comparison to the properties of the core.

Essentially, the open circuit and short circuit modelling (with conditions chosen to avoid saturation) give relatively good results as shown previously in Fig.(3.13a,b) and Fig.(3.15). The small difference between calculation and measurement values can probably be explained by the assumptions employed, for instance the single real value of the permeability.

In order to examine the effect of the core properties on the transformer parameters, high and low values of the permeability and conductivity are considered as shown in Fig.(3.16). This figure indicates (not surprisingly) that the self inductance is more sensitive to the value of permeability, while any change in the core conductivity results in a greater change in the winding resistance due to the loss effects of the eddy currents induced in the core. As the permeability is reduced, the frequency at which the self inductance curve falls is reduced. This frequency represents the maximum frequency that the core could realistically be used with such a value of permeability. This is in addition to the more obvious reduction in inductance with reducing permeability. The frequency at which the self inductance falls away shows the point at which skin effect starts to dominate.

Laminated steels require unpractically thin laminations to operate at very high frequencies. Ferrite have a very low bulk conductivity which allows high frequency operation, but it is easy to see from the results that skin depth eventually sets in the region of 1MHz. Extreme operating frequency will demand a reduction in conductivity, or acceptance of a reduction in permeability. It would also be possible to laminate the Ferrite.

3.6 : WINDINGS LAYERS AT HIGH FREQUENCY

In this section, the effect that occurs due to increases in the number of layers is considered (a layer here is taken to mean in its conventional transformer parlance, i.e. a

winding is made up from successive layers of helically wound coils). Again, the simulation is carried out with a wire thickness of 1.2 times the skin depth. The main concern is to find the value of the ac component of the resistance and inductance. Firstly, this gives an immediate feeling as to the limiting factors that restrict the design, and secondly the study can lead to a reduction in the losses and the leakage inductance, which are the main factors in minimising noise due to electromagnetic interference [53].

As the frequency is increased, the field in the gap between the windings is not effected, since it depends only on the dimensions. But inside the conductor, the current density falls exponentially with increasing depth into the conductor. When the flux within the conductor is reduced, the leakage inductance is also reduced. But this is not a good way to reduce the leakage inductance, since the penalty will be increased eddy current loss.

The problem of reducing the leakage inductance and keeping the eddy losses within reasonable limits has received great attention from many researchers [1,19,30,52]. Dowell solved the problem mathematically and the equations he used are fully detailed [1]. The principle works well but the main drawbacks are that the geometrical distribution of leakage field is assumed to be purely across the transformer window, and each layer of the winding is coalesced into a current sheet with simple assumptions made on current distribution within the sheet [30].

In this work, the calculations are done using FE analysis, where all the turns of the windings are included, and the core is fully modelled. The elements are chosen to be no larger than one third of a skin depth at the highest frequency. The primary and secondary windings are arranged in layers in the same way as the true transformer. The model allows variation in the number of layers to be considered, and the FE results from this are presented.

The dc components can be found either by solving the problem at zero frequency, where the equation to be solved is the magnetostatic form of Maxwell's equation (i.e. the eddy

current term in equation (3.1) made equal to zero), or using the closed form equations discussed in chapter five and given by Dowel [1].

There are two ways of calculating the ac components of the winding resistance and leakage inductance. The first is the simplest and involves a short circuit calculation, this gives a good approximation of the combination of the leakage in the primary winding and the leakage in the secondary reflected to the primary by the turns ratio. During a short circuit, the shunt inductance and resistance due to the magnetising flux and loss in the core are small and can be neglected. That means, during the short circuit, it appears that the impedance seen at the terminal is the primary and secondary leakage branches in series. The second method involves exciting a section of the winding, in this case each layer in turn and calculating the resulting flux linkage in the excited and all the other nonexcited section (layers). This procedure has to be repeated for each layer so as to build a matrix (detailed in chapter five). This matrix can then be used to determine the effective impedance resulting from any connection.

In the Dowell analytical solution, the leakage impedance calculation is done by dividing the primary winding into layered portions from the inside of the winding outwards. Each of the portions consists of two layers. There are two principles clearly explained in his work:

1- The leakage impedance of a particular layer needs to consider the effect of all of the other layers in the winding on the considered layer.

2- The leakage flux in each layer depends on the current in that layer and the total current between the layer and an adjacent point of zero mmf.

Hence, each portion of the winding is considered separately, and the primary leakage impedance is the sum of the leakage impedance of the portions. The analytical results are given in Dowel's work as a graph showing the different layers in the primary winding portions. It is clearly recognised that to include the secondary winding, the leakage

impedance of the portion forming part of the secondary has to be divided by the turns squared to refer it to the primary, which has two principal problems:

1- In the Dowell model, the flux in the gaps between the conductors is considered independent of frequency. In fact the leakage flux as it is expelled from the conductors tends to fringe around the conductors and make the leakage field non-uniform. This fringing involves the space around the windings.

2- There is a possibility of proximity effect between the primary and secondary layers, and consequently for a good solution both primary and secondary need to be modelled together.

Here, the ac to dc ratios of the leakage inductance and resistance are found using FE with the layers of the primary considered first. Each layer consists of 14 turns, therefore; two layers means 28 turns and so on, a half layer means 7 turns placed in the middle of the window. In consideration of primary layers only, it is easy to compare the results with Dowell's analytical solution. Fig.(3.17) shows, the comparison between analytical and FE, where a reasonably close agreement is seen. The vertical scales are the ac to dc inductance and resistance ratios respectively. The horizontal scale is effectively frequency (or rather the root of the frequency), but it is presented in terms of the ratio of the conductor size to the skin depth.

The figure shows that an increase in the number of layer apparently shows an increase in the ac resistance as compared to the dc, and a reduction in the inductance per turn for ac as compared to dc. It should be remembered that these results are taken against conductor thickness as a ratio of skin depth. Taking results for a fixed dimension of conductor and simply upping the layers actually puts more copper into the transformer window. When the fields become skin limited there is less space available for leakage flux and the inductance per turn falls. The conductors are close together and hence proximity is increased causing an increase in the ac resistance. Normally a choice for more layers implies a thinner layer and hence design changes in layers are not simple

verticals on these graphs. The point is however that the graphs allow any design to be analysed within the transformer window because of the way they have been normalised.

If the secondary is now added it is possible to use Dowell's work by reflecting the leakage impedance values obtained across the turns ratio. The finite element results are obtained directly using stored energy and loss as before. The two results are compared in Fig.(3.18), and the results show that the inductance per turn is reduced, and the loss resistance is increased by almost 30% as the conductor thickness to skin depth ratio varies from 1 to 10. The existence of the secondary layers add more loss which is reflected to the primary by the turns ratio. The case is not the same with the leakage components. The leakage flux depends on the space between layers and that of the rest of the window, and since the window space is part of the solution, the leakage components do not show much effect by altering the secondary layers.

3.6.1: LAYERS TOPOLOGY

In order to illustrate the effect of increasing the number of layers on the leakage and losses, the diagram below may be considered [30,52].

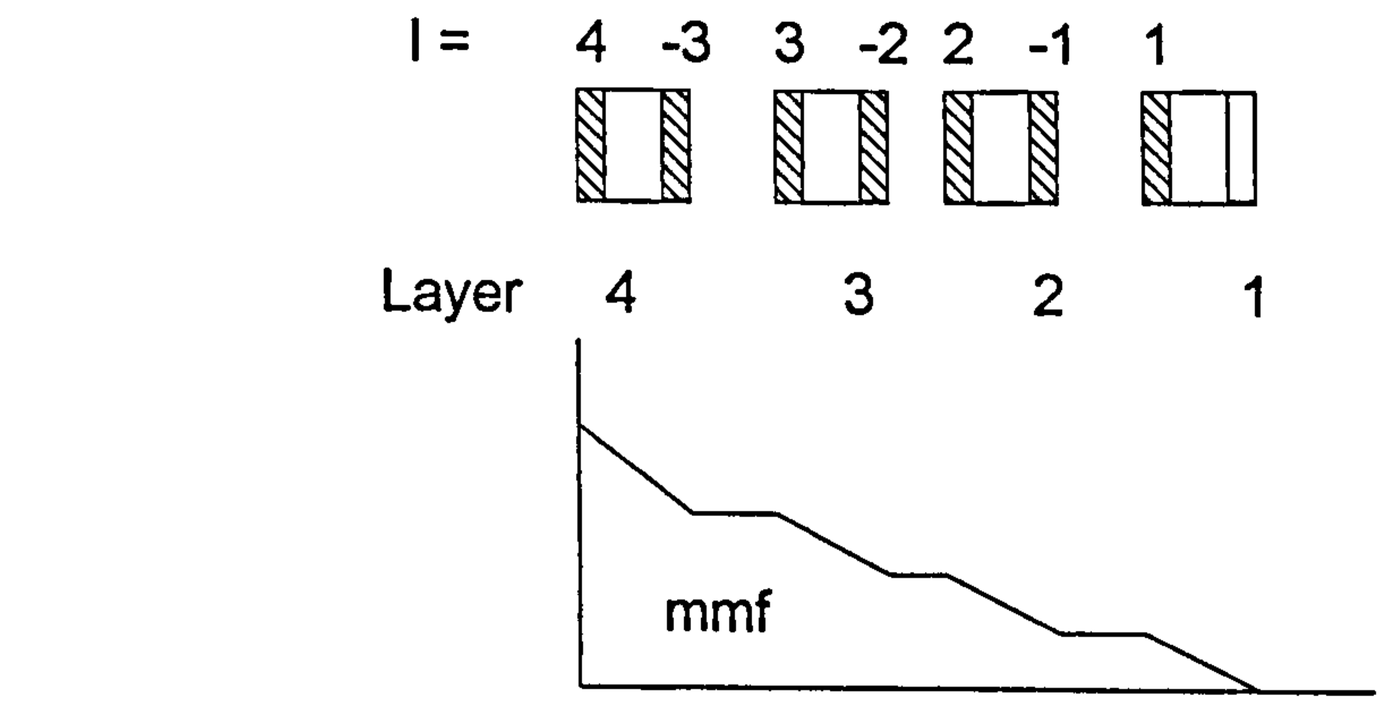

Assume a current of one ampere flows through four layers, each with two turns. The skin depth is 1.2 times the conductor thickness. The current in layer one causes a

magnetic field to exist in the gap between layer one and two. The opposite surface of the next layer has a nearly equal and opposite current induced in it by this flux. The net current in layer two has to be one ampere as has been assumed, and so a 2 amp current flows in the far surface of layer two, and so on for the rest of layers as shown in the above diagram. The mmf curve rises with layer responding to net current. The current density squared determines the loss density, the two surface currents in layer two alone cause losses of $(2)^2+(-1)^2=5$ times that in layer one. The same can be applied to the rest of the layers, where the losses are 13 times in layer three and 25 times in layer four with respect to layer one. The average resistance in all four layers is 25 +13 + 5 + 1 / 4 = 11 times that in layer one. Since the ac resistance in layer one is (for generality the whole area is 100%, and the area considered is 12%) 100 / 12 = 8.33 with respect to the dc across the whole conductor area, and it has two surfaces, the ac resistance is therefore equal to 4.167. That means the ac to dc ratio would be 4.167:1(the ratio of average ac to dc resistance is 11 * 4.167 = 45.8). In order to confirm the obtained result, the graph in Fig.(3.18) shows that four layers with depth ratio of 1.2 gives an ac to dc resistance of about 4 (average ac to dc ratio is 11 * 4= 44). If the penetration is larger than the conductor thickness, the mmf will not be zero at the middle of the conductor and the current cancellation will be complete. In this case the value of ac would be the same as the dc, and the current is distributed uniformly within the area of the conductor. The ratio of the ac to dc resistance is then equal to one .

Another consideration in the value of ac to dc ratios of leakage inductance and resistance can be observed. One of the main concerns using the graph is the number of fine wires that are used for a certain operational frequency. Consider for example, a single wire which forms one turn of a ten turns layer, with a wire gauge of area 0.033 cm^2 , and a transformer designed to operate at 1MHz, (where the depth of penetration is 0.066mm). This means that the conductor thickness is much greater than the depth of penetration. The ratio of conductor thickness to skin depth (say K) is 27.5. Referring this value of K to a single layer on the graph of fig.(3.18), it shows that there is a large difference

between ac and dc resistance as expected. In this case the system will not be able to handle the high losses. If this conductor is divided into four conductors each with 1/4 the original diameter, the number of conductors is then 40 with two layers, each with 20 conductors, K will be equal to 6.75 with respect to the original wire. The ac to dc ratio is still high and needs to be reduced. Again by dividing each of the four section of conductor into six, there are 60 wires placed in 2.5 layers, 25 wires per layer, each with diameter 0.075mm, and K is less and so on. Therefore, dividing the original conductor into many fine conductors is a very important way to reduce losses. This information can be obtained by deriving a graph of the type shown in Fig.(3.18) at the design frequency and number of primary and secondary layers. Further detail can be obtained from publications [1,30,52].

3.7 : ANALYSIS VALIDITY AT 1 MHz

In order to give the required validity to the FE analysis at 1 MHz, example 6.2 in reference [31] is considered. In this example an inductance needs to be built at a required value of 28 μH at 1MHz. The inner diameter of the toroidal core is 28mm, and the outer diameter is 40mm. The core material is Nickel-Zinc Ferrite with resistivity equal to $5\times10^{4}\ \Omega.\mathrm{m}$. The procedure that the author used to design this inductor is the same as that used by Dowell [1], where the conductor is considered to have a square section area to make the mathematical calculations more manageable. Using the reference equations, some calculations need to be prepared. The height of the core (H_c) equal 5.1mm, the inner and outer diameters are $D_i = 28mm$ $D_o = 40mm$, and the number of turns and strands are 77 and 16 respectively (as shown in the diagram below). The author predicted from the calculation that the optimum ac resistance for the winding length of 1.9m is 0.41 Ω, and the measured value is 0.48 Ω.

Finite Element analysis is used for the above specifications. The field distribution is shown in Fig.(3.19), at 1 MHz. From the loss relation the ac resistance is 0.456 Ω. The

finite element analysis has resulted in a value close to the practical result. The reasons behind the difference between the measured and calculated values may possibly be due to the neglect of conductor curvature, and secondly, the equation is mainly derived assuming infinite permeability and zero conductivity for the core. Using FE, it is possible to model circular wires and the core is more exactly and accurately modelled. This example shows the capability of the finite element analysis to solve any problem, and to be the first choice in comparison with other numerical methods.

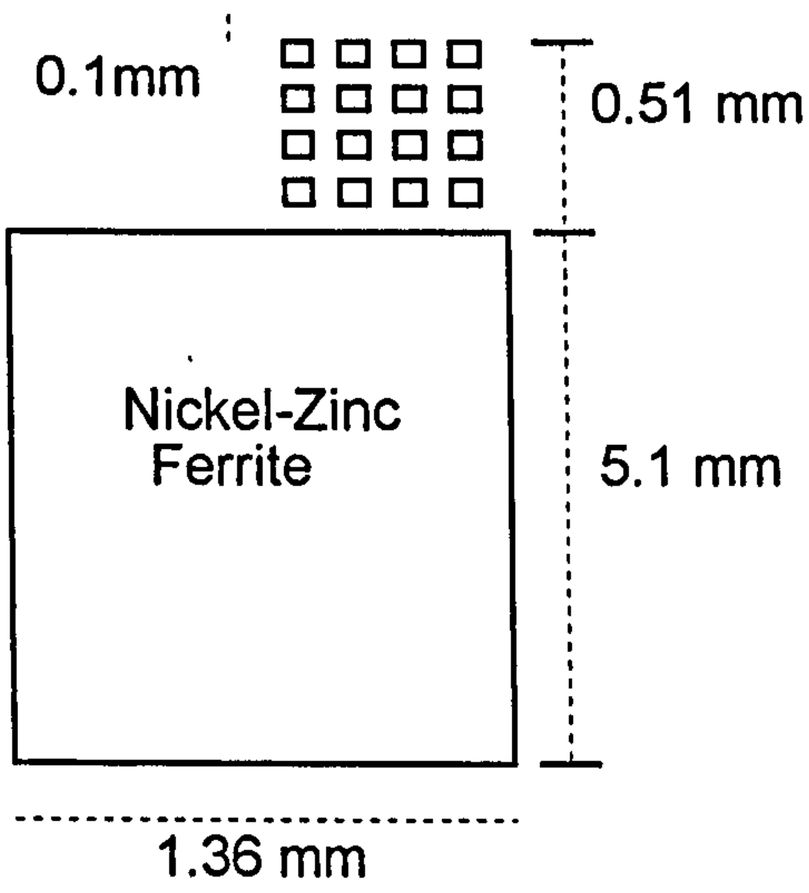

3.8 : SUMMARY

The ac component of magnetic field that exists between the primary and secondary windings is the main reason for proximity effects. This field is shown to be concentrated in the gap between the windings as the frequency goes up. This causes an induced current that is circulating within each conductor, adding to the conductor current in one surface of the conductor and opposing or cancelling current in the other. Effects like these together with the effects due to the self induced currents (i.e. skin effects) can be removed or at least reduced to acceptable level by using either twisted fine wires, or reducing the operating magnetic field strength. The field strength can be reduced by using a wider window area to accommodate the number of turns in less layers. Reducing

this field has another advantage as well, that is to make the transformer work with less saturation.

Another way to reduce the effective number of layers is by splitting the winding into small sections by interleaving. In this case each section of the primary winding faces one section of the secondary winding. If ampere-turn balance is achieved in each layer, full cancellation occurs for the field outside the conductors. Because of the reduced field in such an arrangement, the leakage inductance is reduced as required.

Also, the study in this chapter has shown that the winding resistance is a function of core conductivity, while the self inductance is a function of core permeability. So, by choosing a core material with a very high permeability and very low conductivity, the losses and leakage can be reduced greatly.

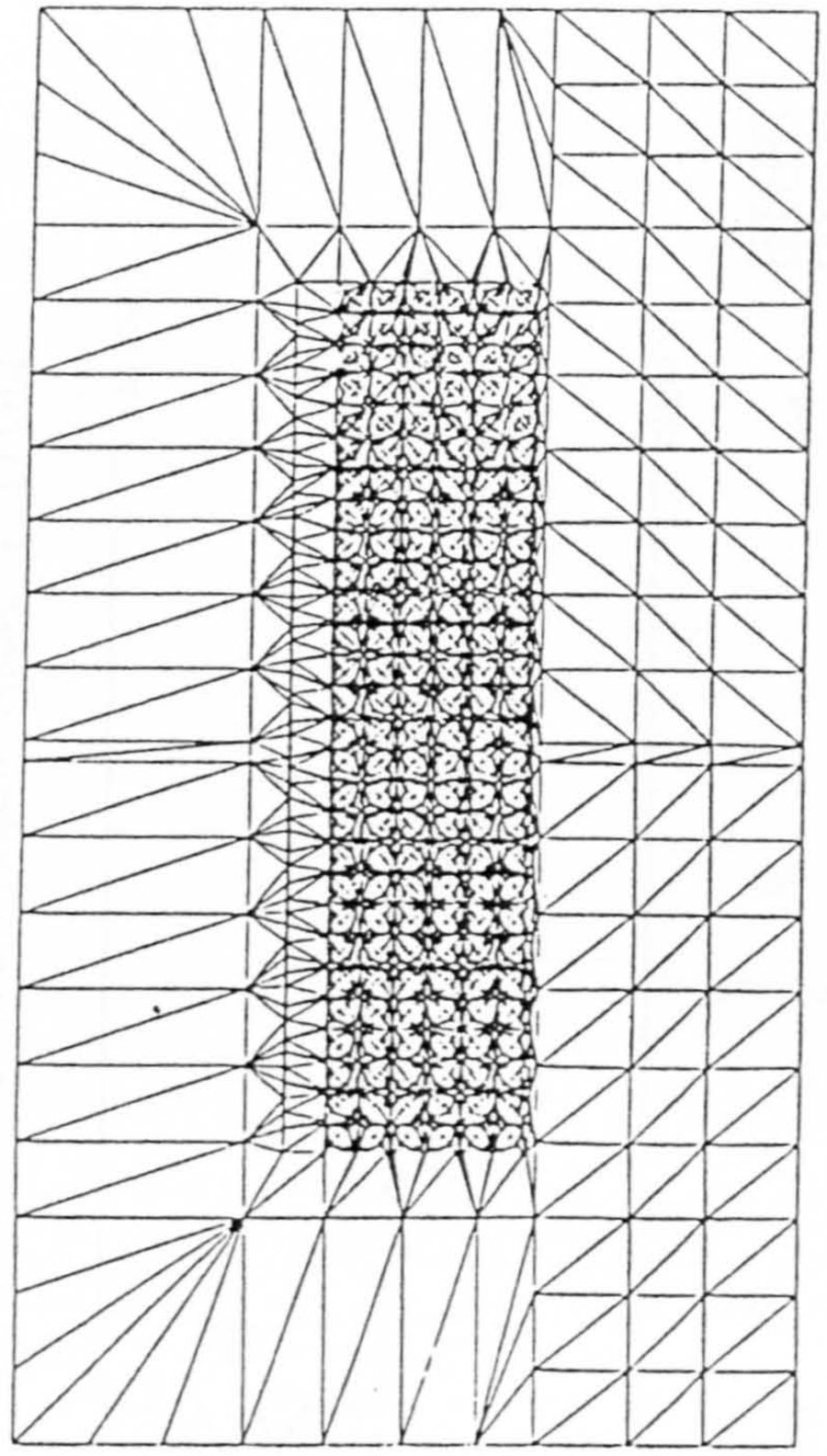

FIG. (3·1 B) : 2–Dimensional transformer mesh model

viewed from the side

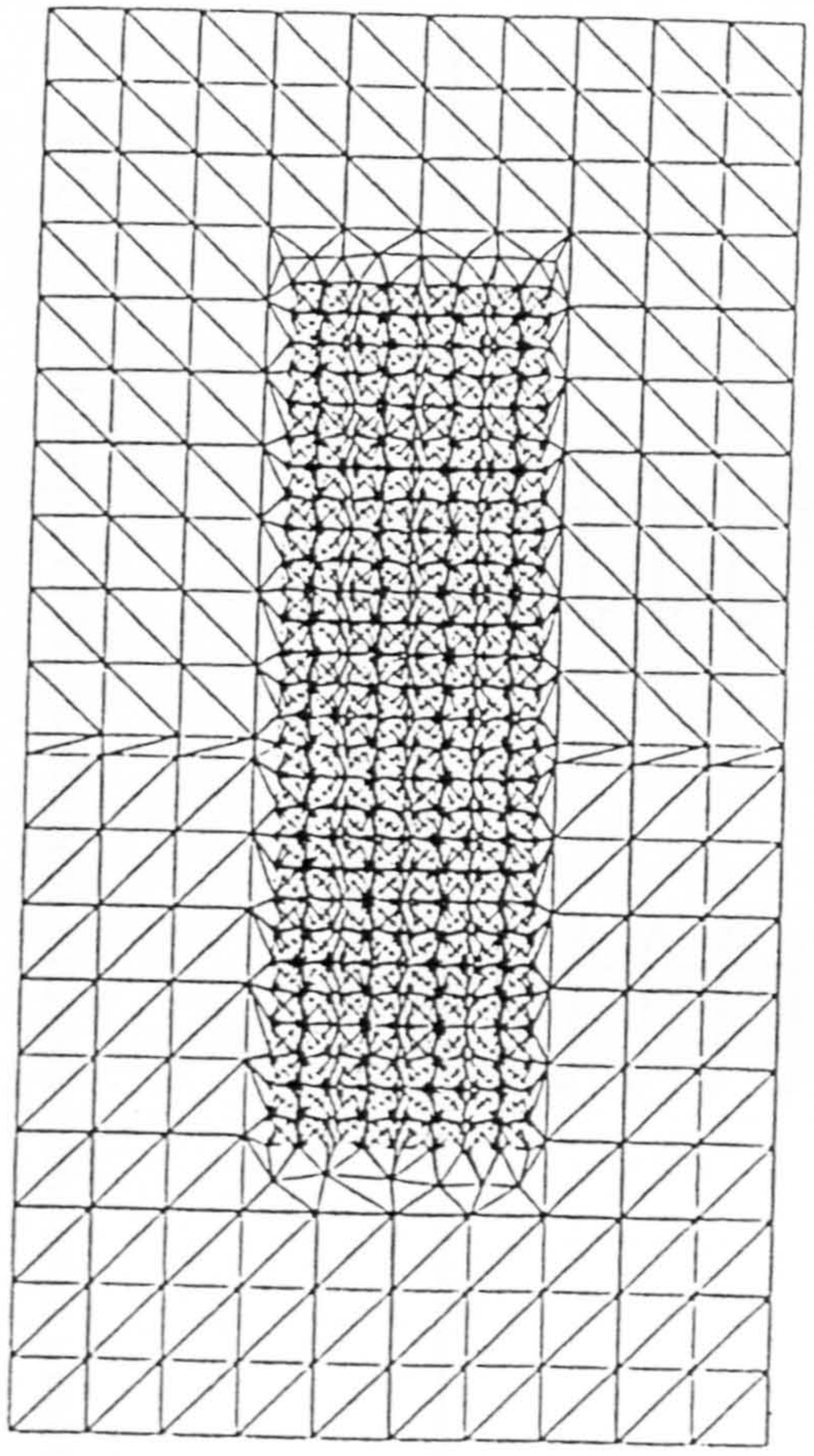

FIG. (3·1 A) : 2–Dimensional transformer mesh model

viewed from the front

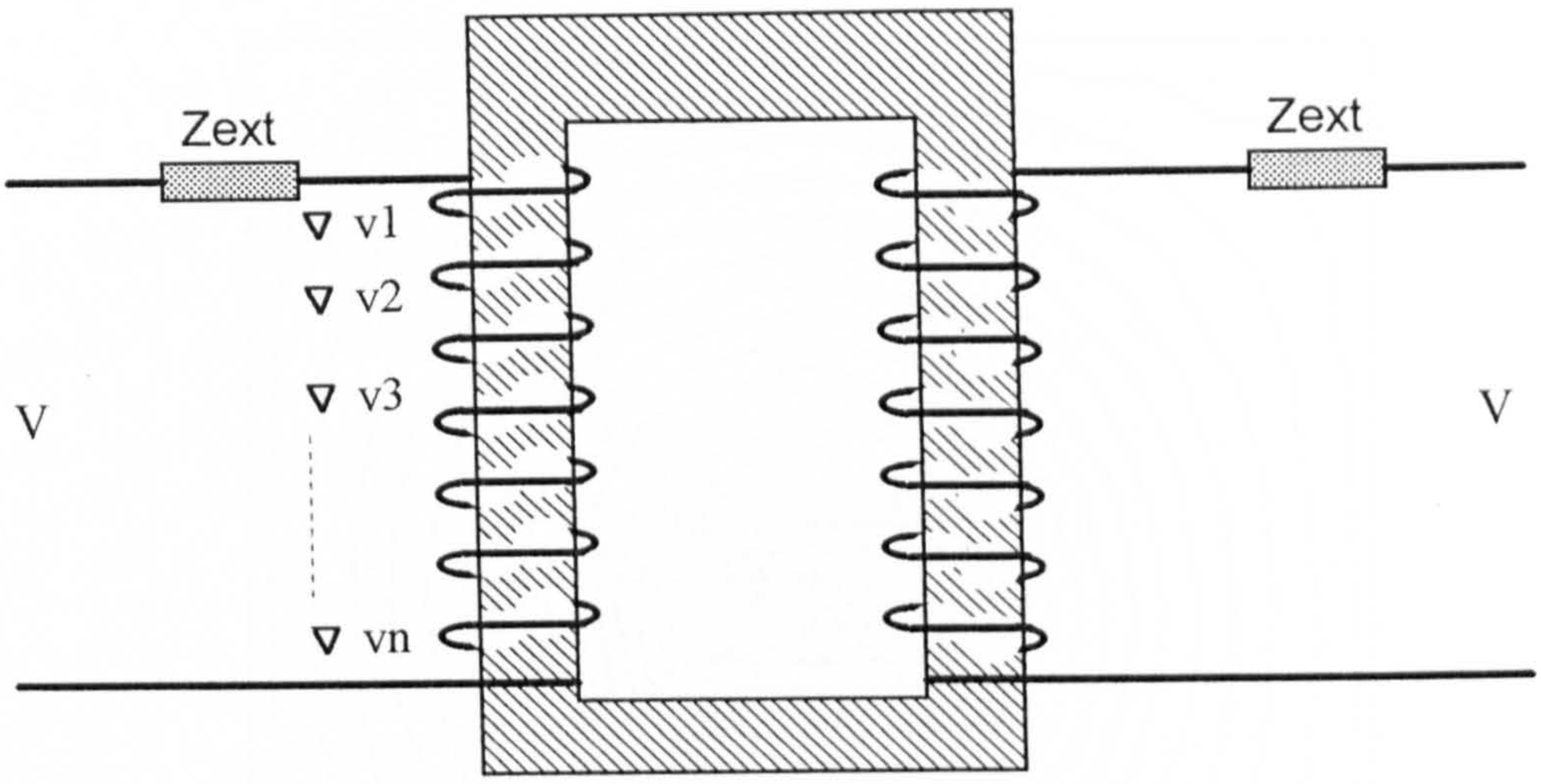

FIG.(3.2) : Principle of Finite Element Analysis with series winding

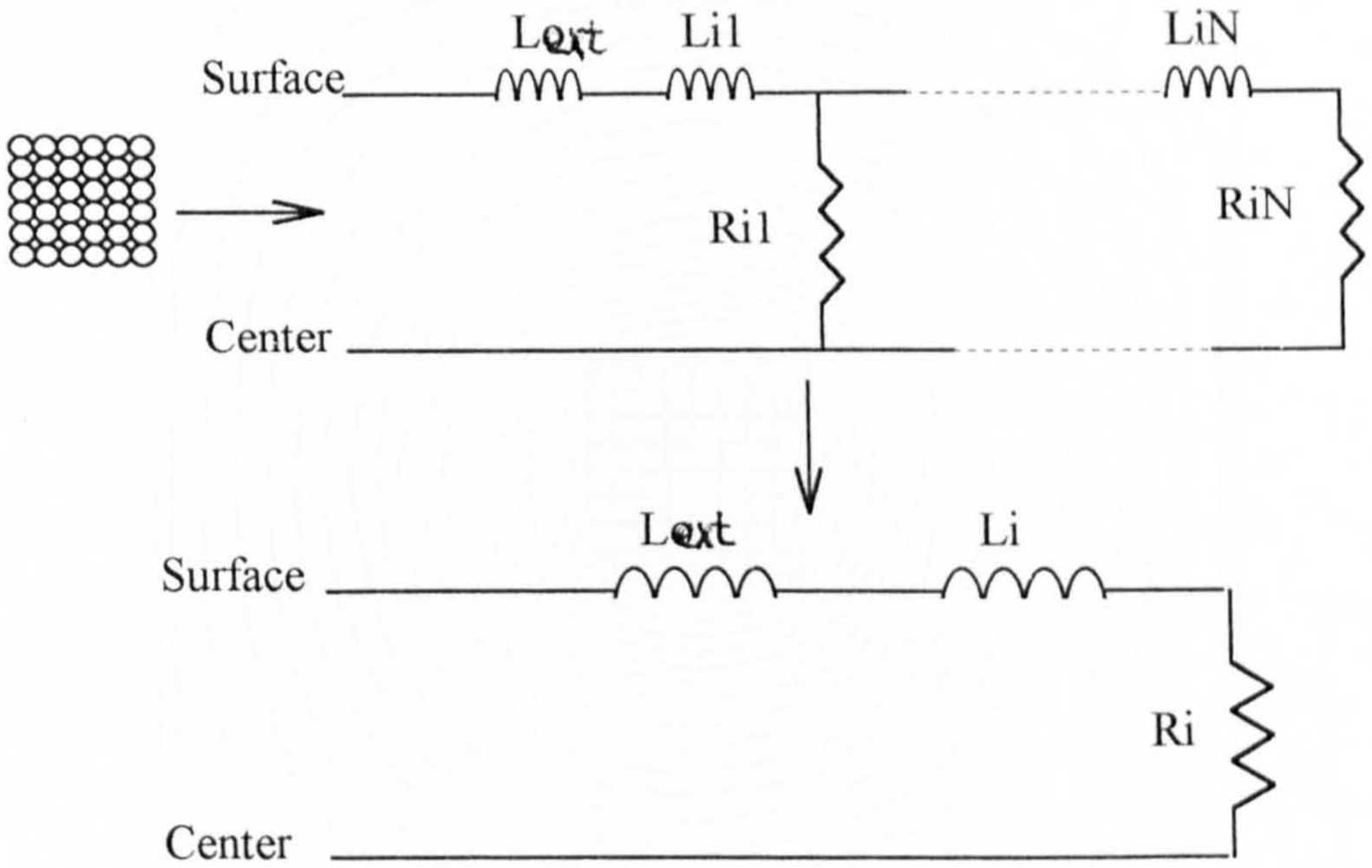

FIG.(3.3) : Single conductor equivalent circuit

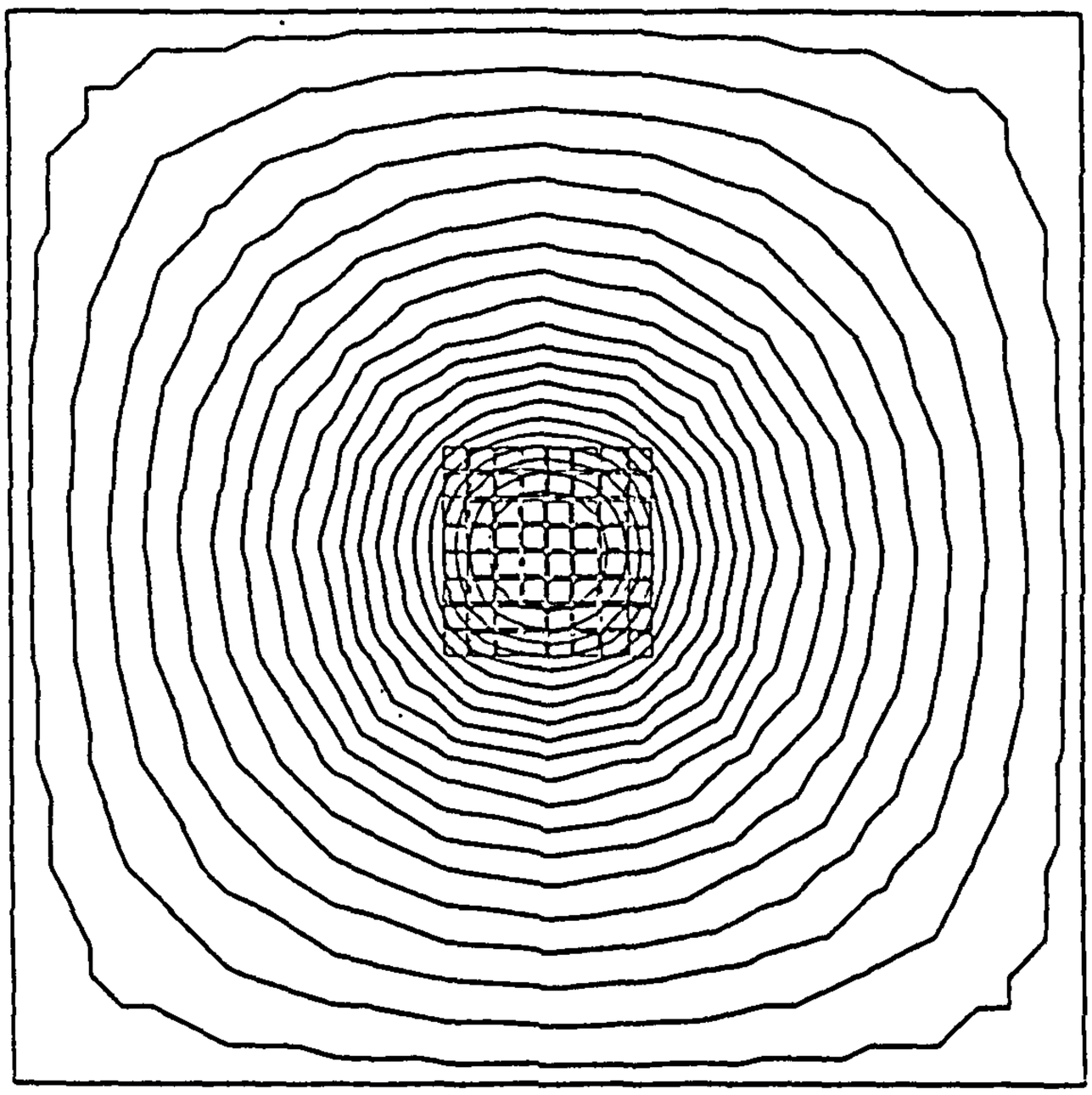

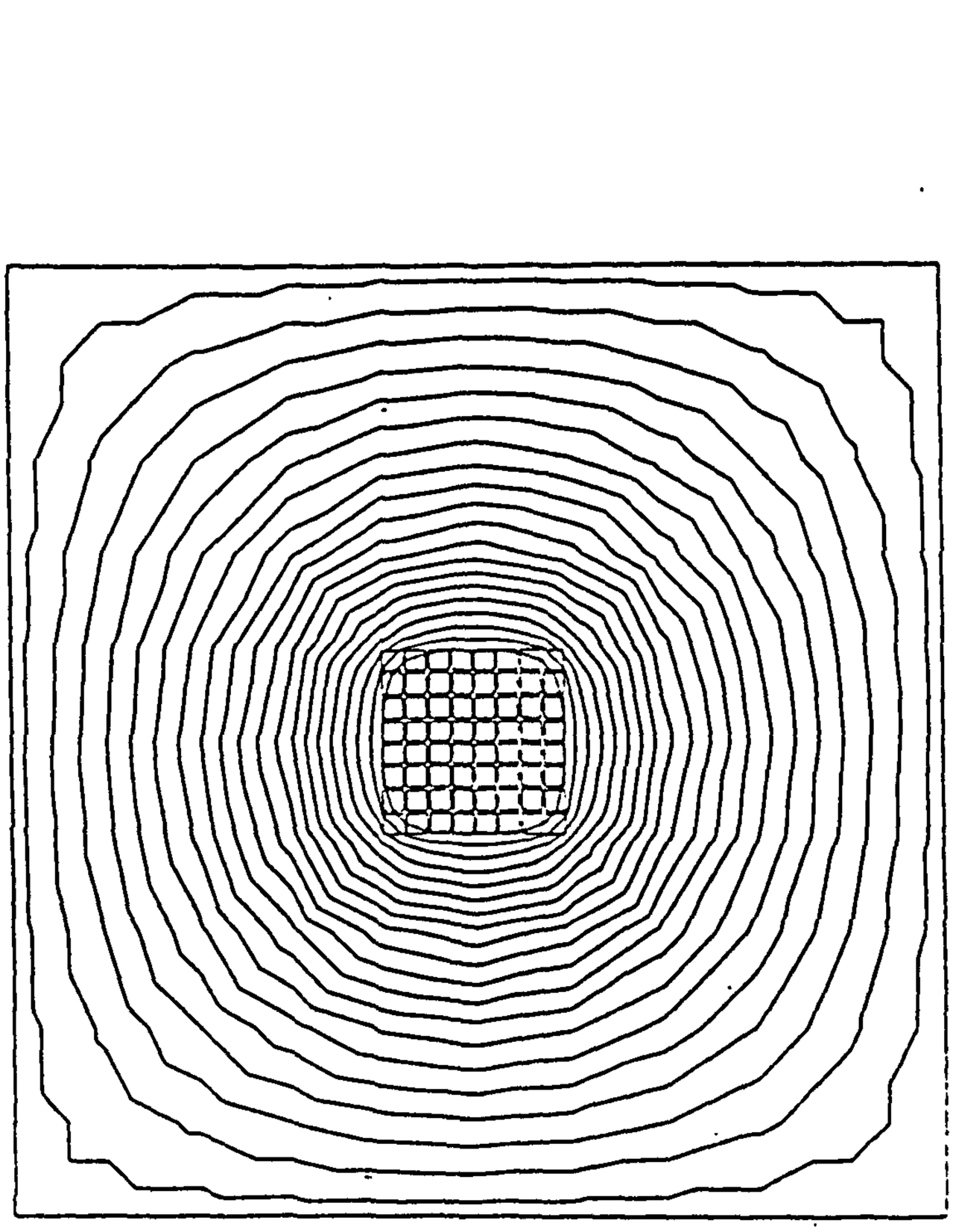

FIG. (3·4) : Flux distribution for single conductor at 1 kHz and 1 MHz

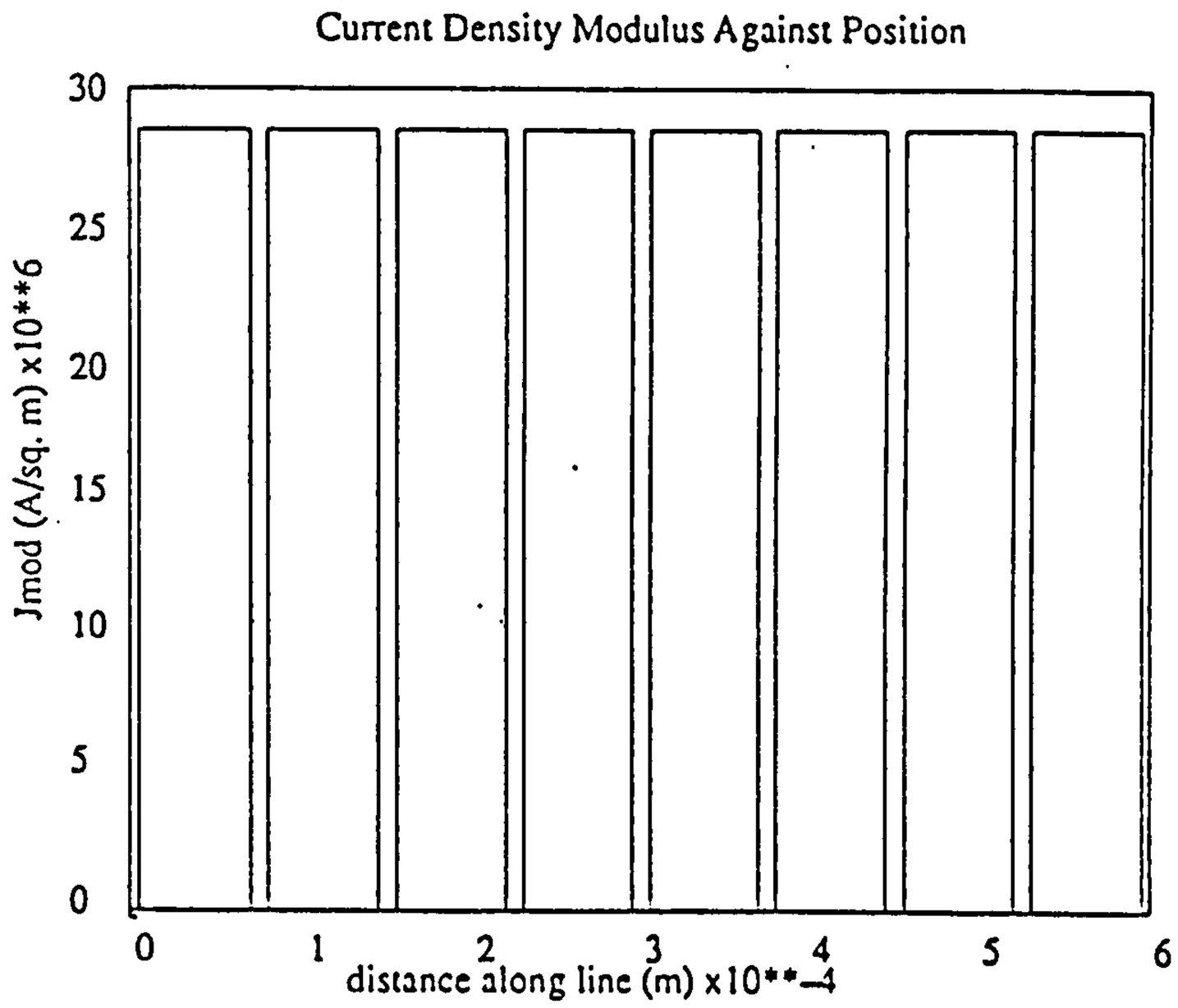

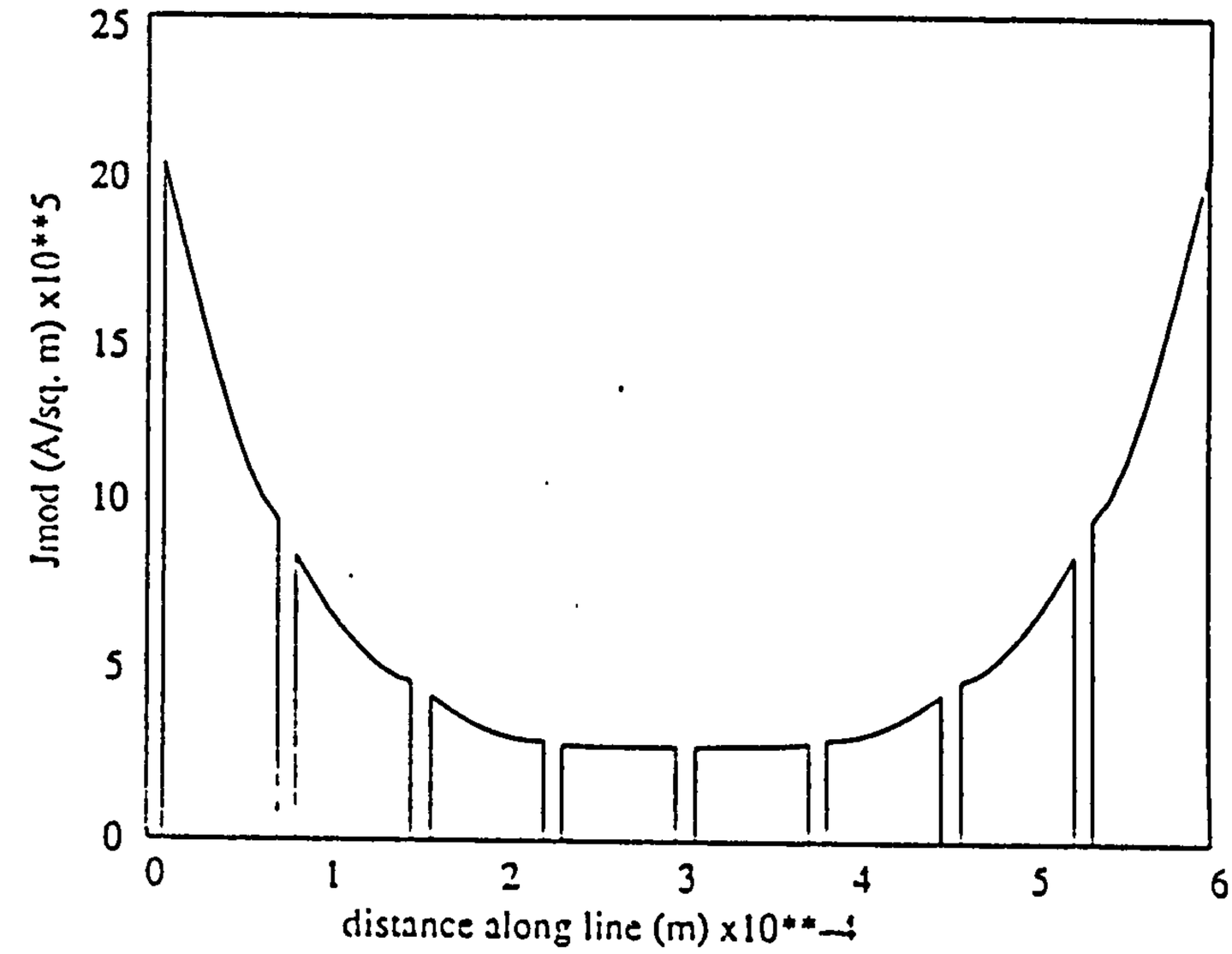

FIG. (3·5) : Modulus current density along the conductor at 1 kHz and 1 MHz

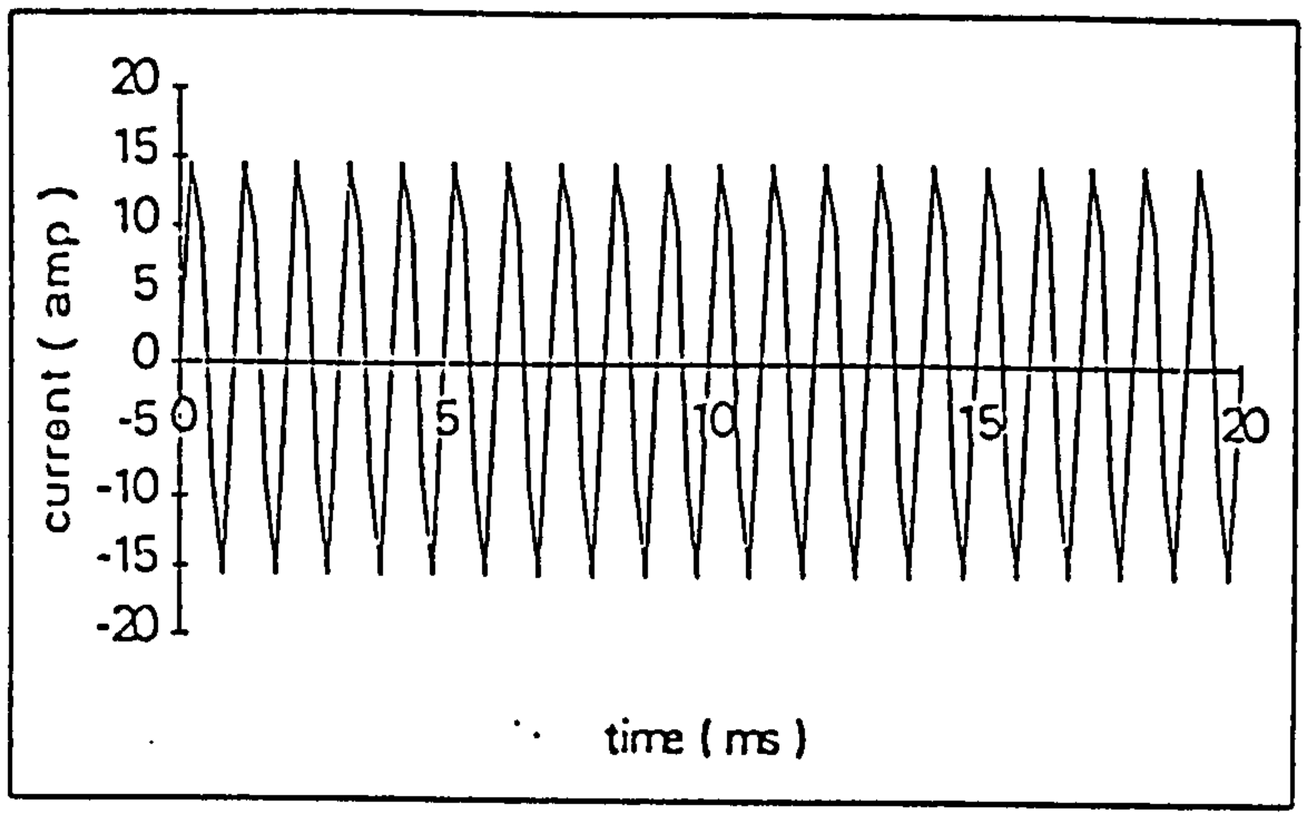

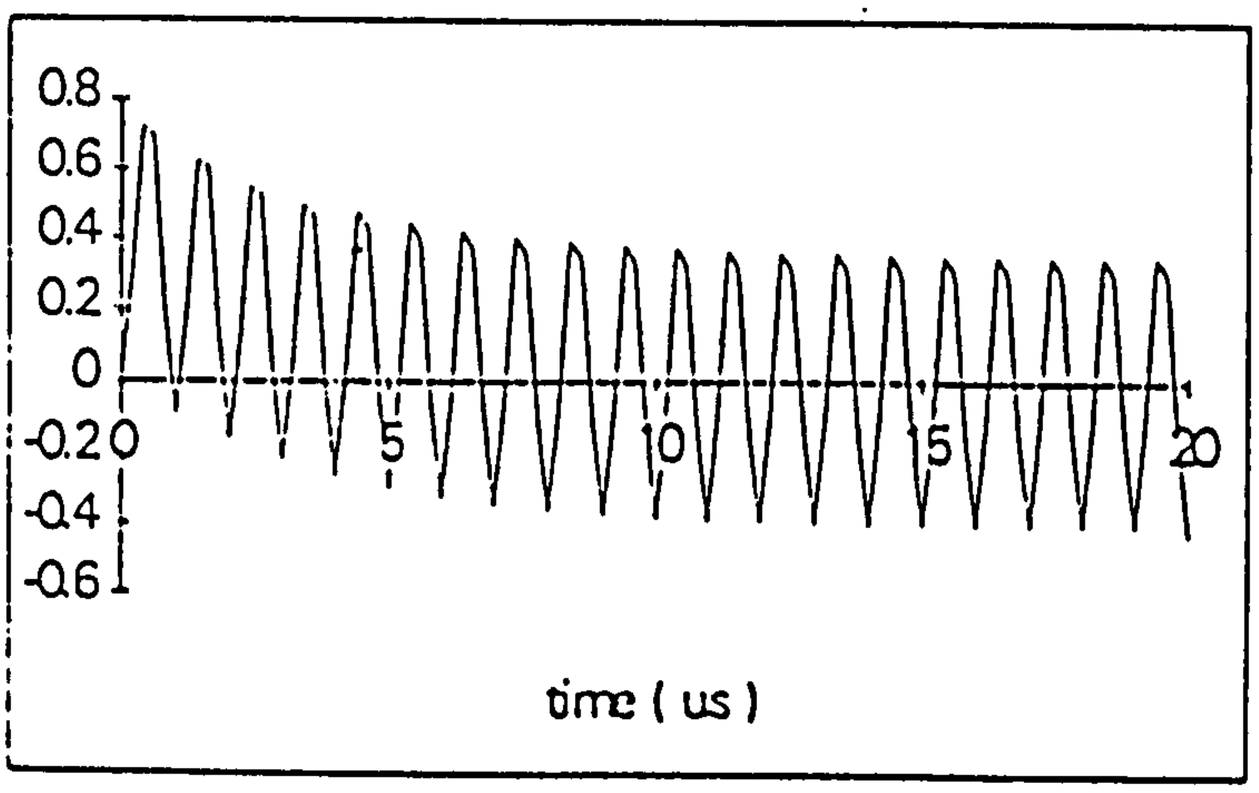

FIG. (3·6) : Current Oscillation Behaviour due to the skin effect

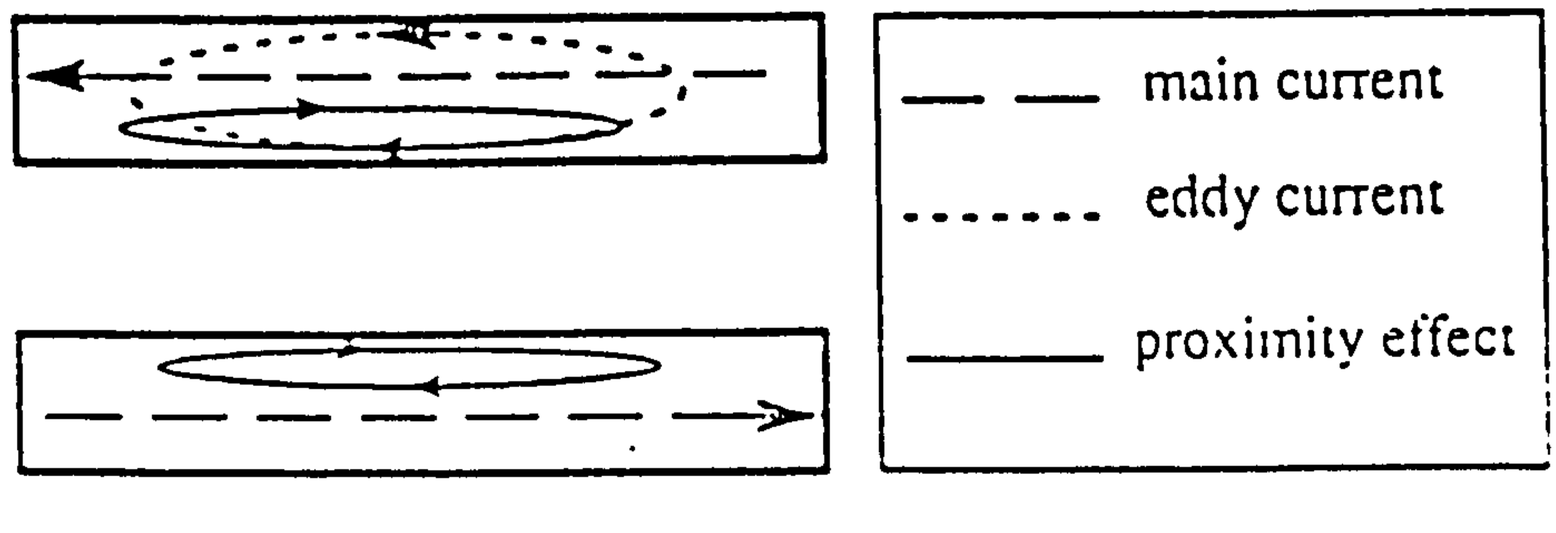

FIG. (3·7) : Proximity Effects Principal

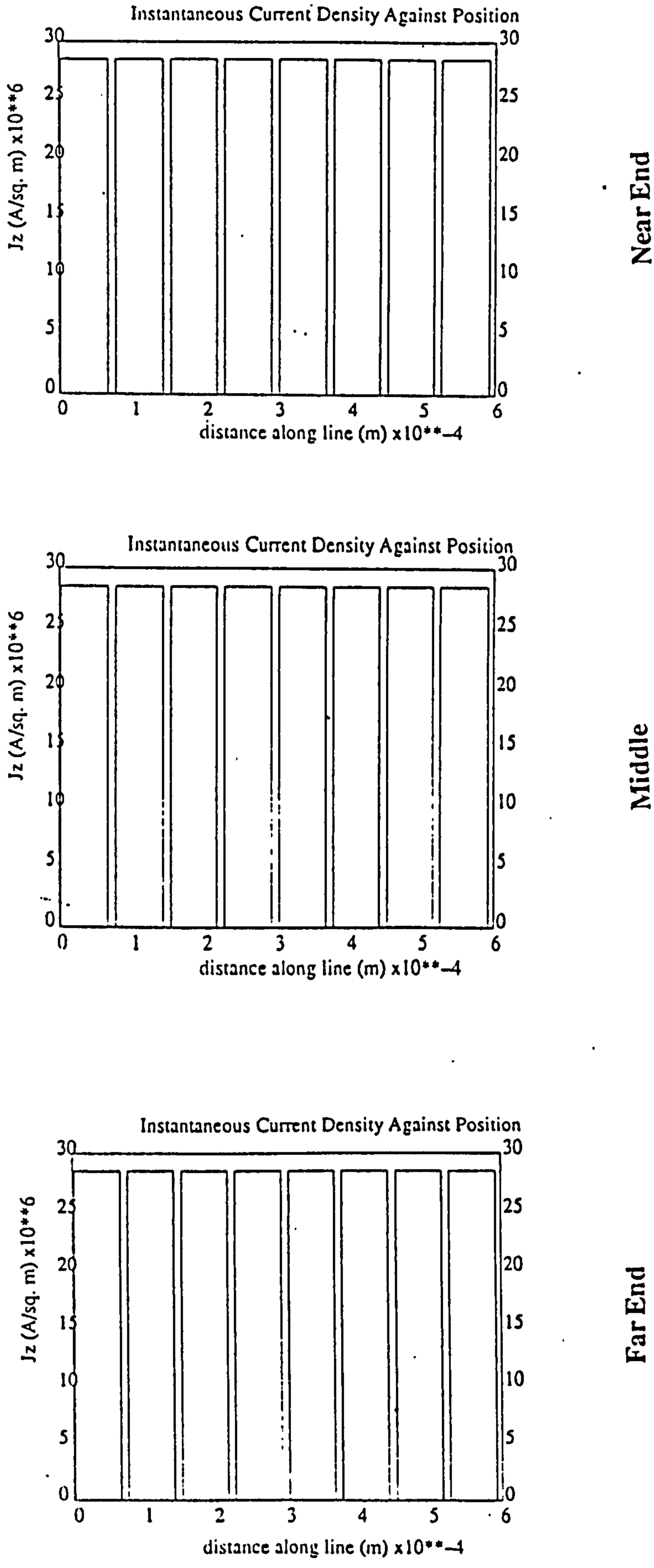

FIG. (3.8A) : Instantaneous current density along the conductor in different positions at 1 kHz.

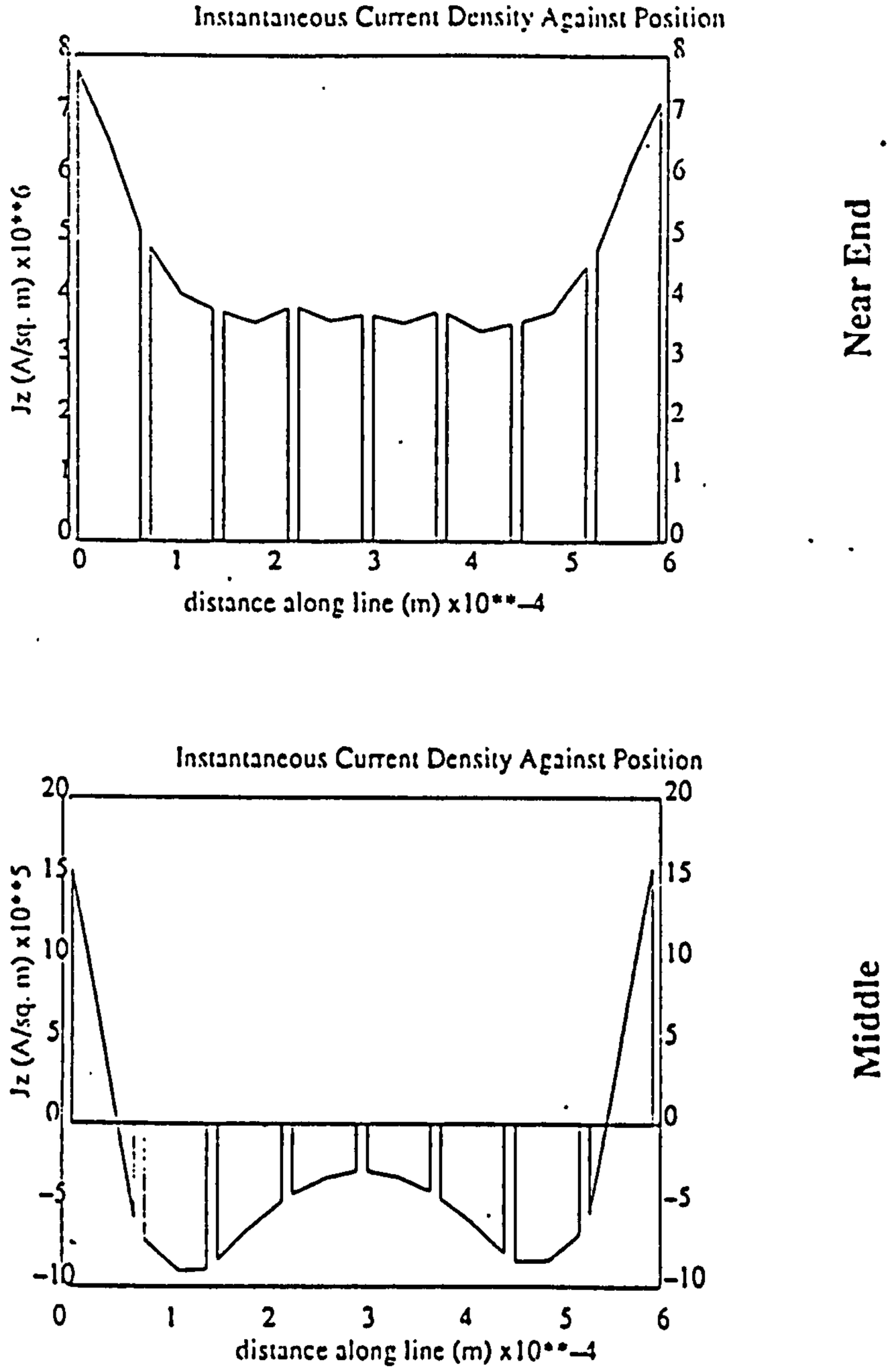

FIG. (3·8B) : Instantaneous current density along the conductor in different positions at 1 MHz.

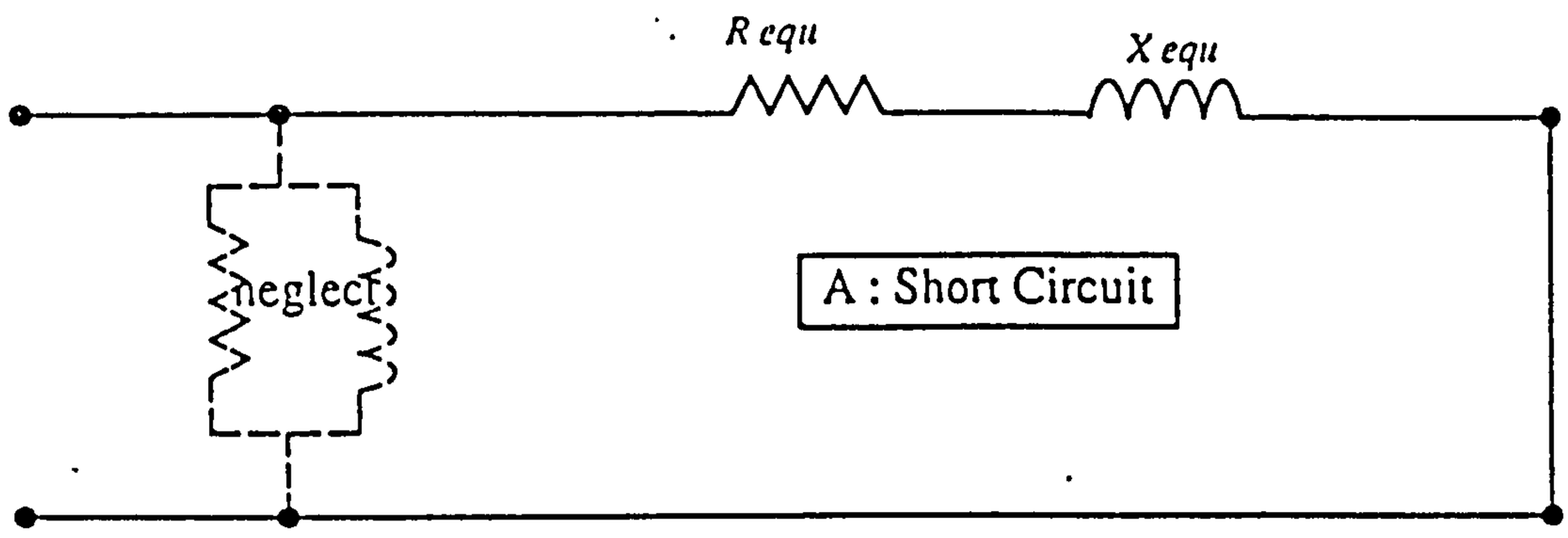

FIG. (3.9) : 2–Dimensional equivalent circuit model at : a– short circuit, b–open circuit

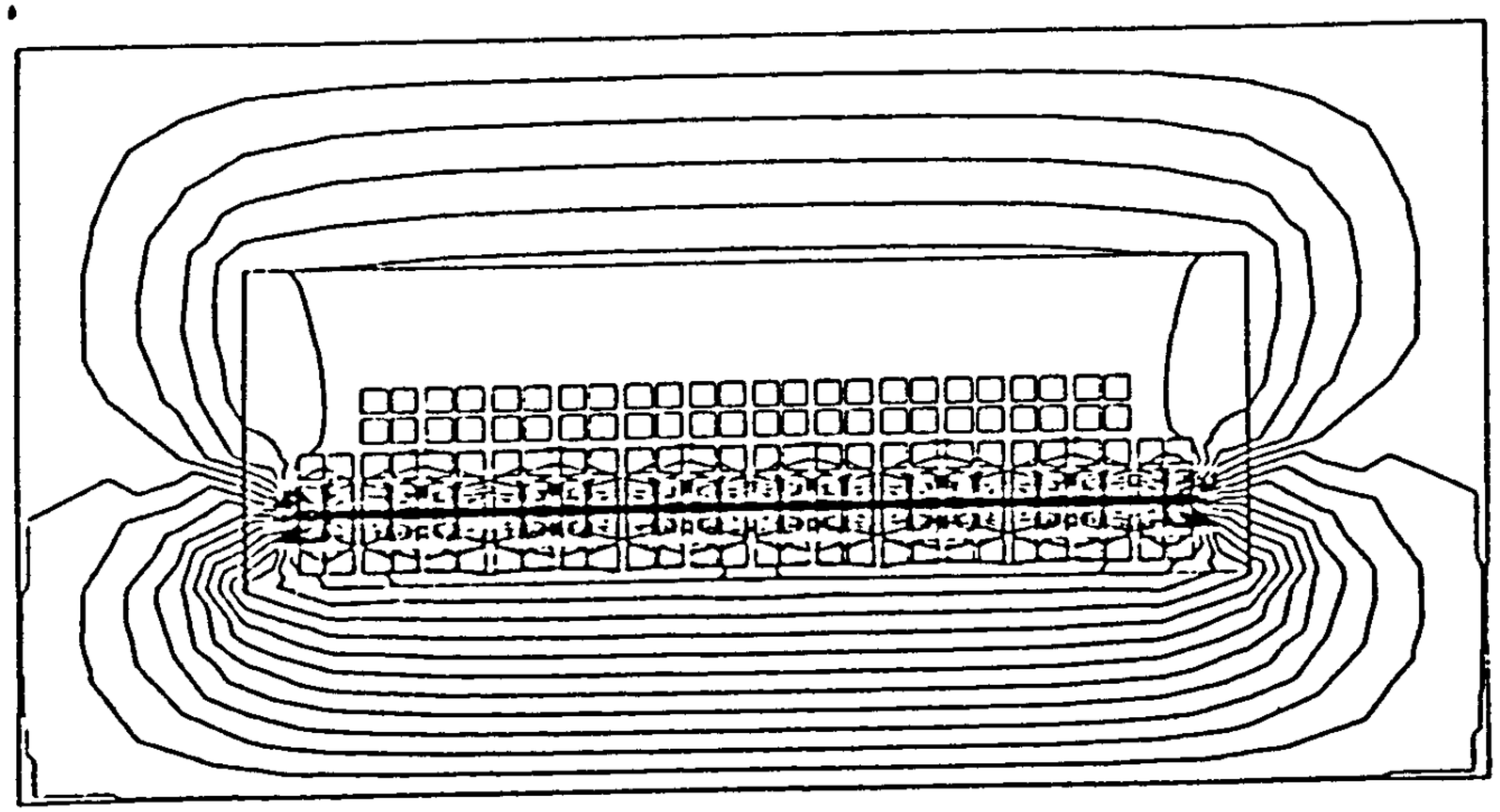

500 kHz

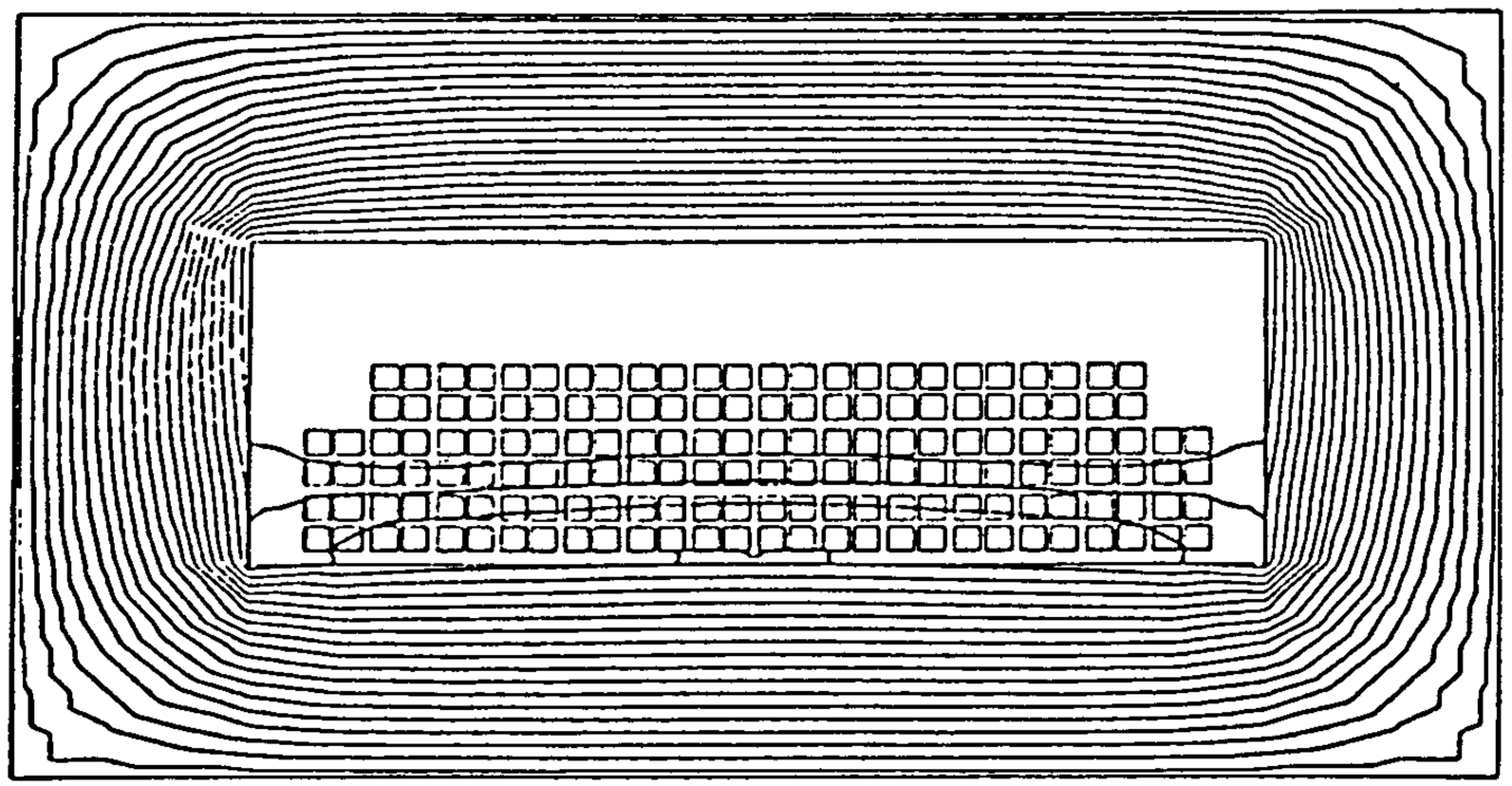

Low frequency

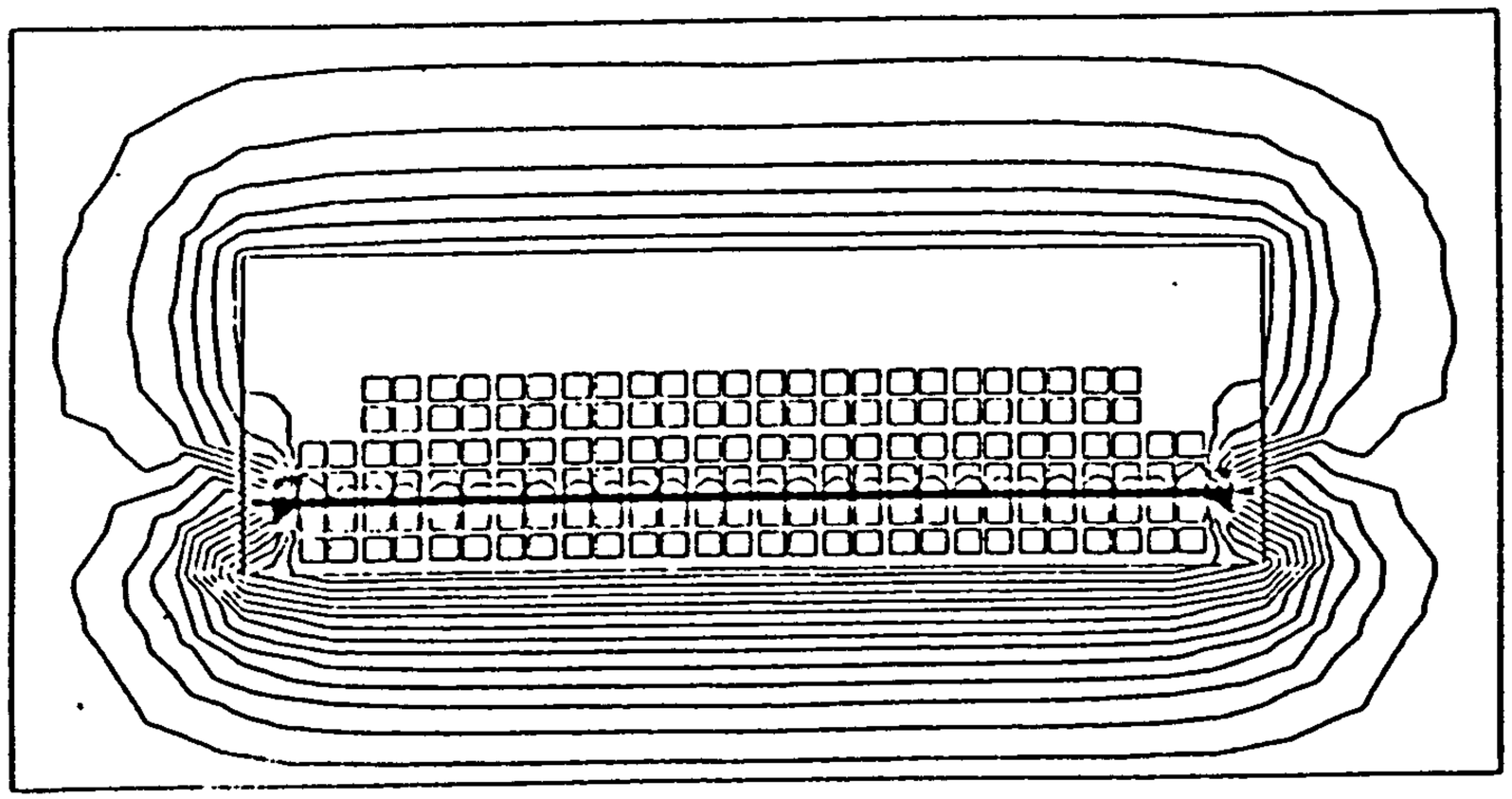

1 MHz

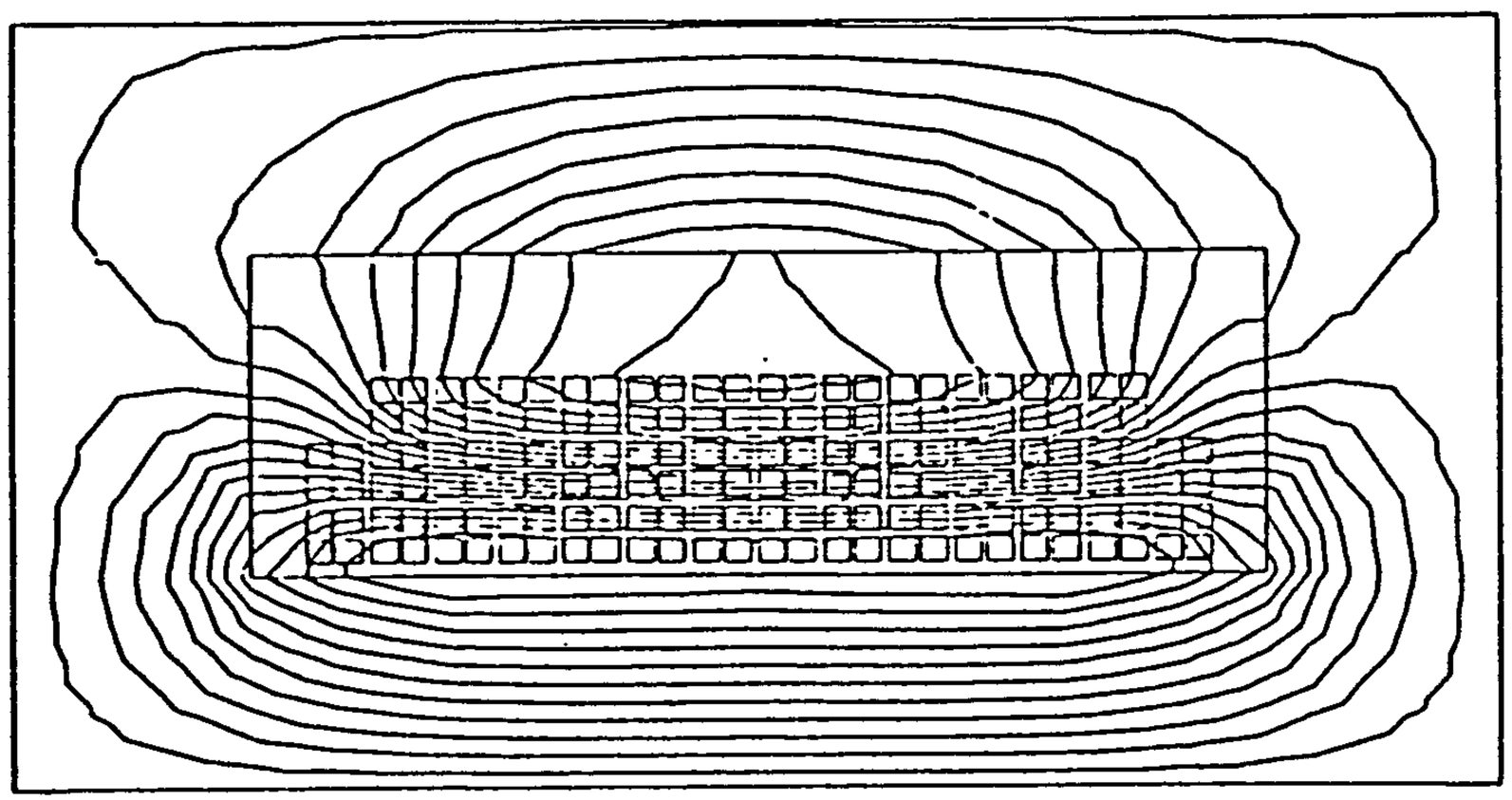

100 kHz

FIG. (3.10) : Short circuit flux distribution at different frequencies

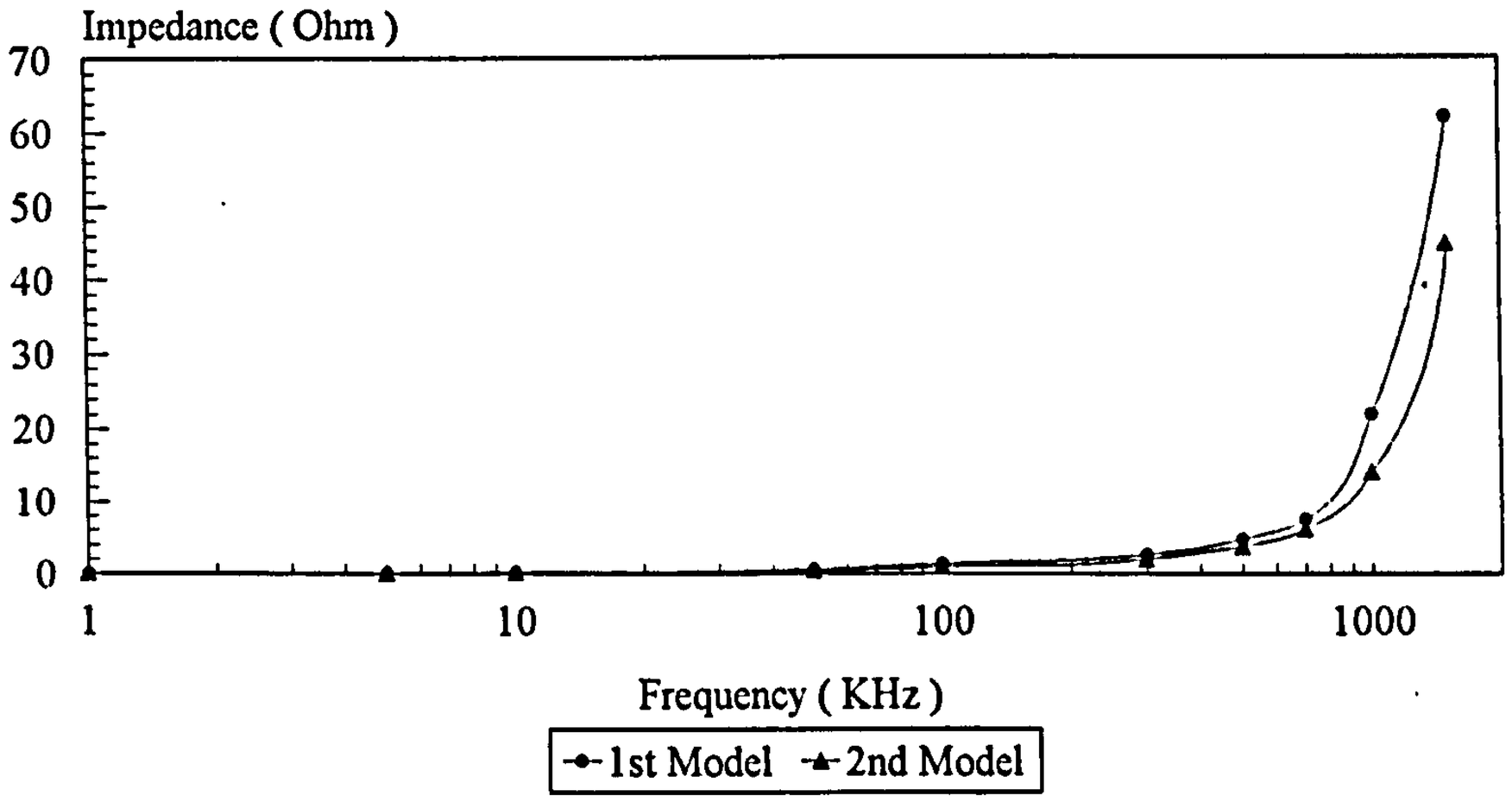

Fig.(3.11) : Short circuit impedance calculated from two FE model

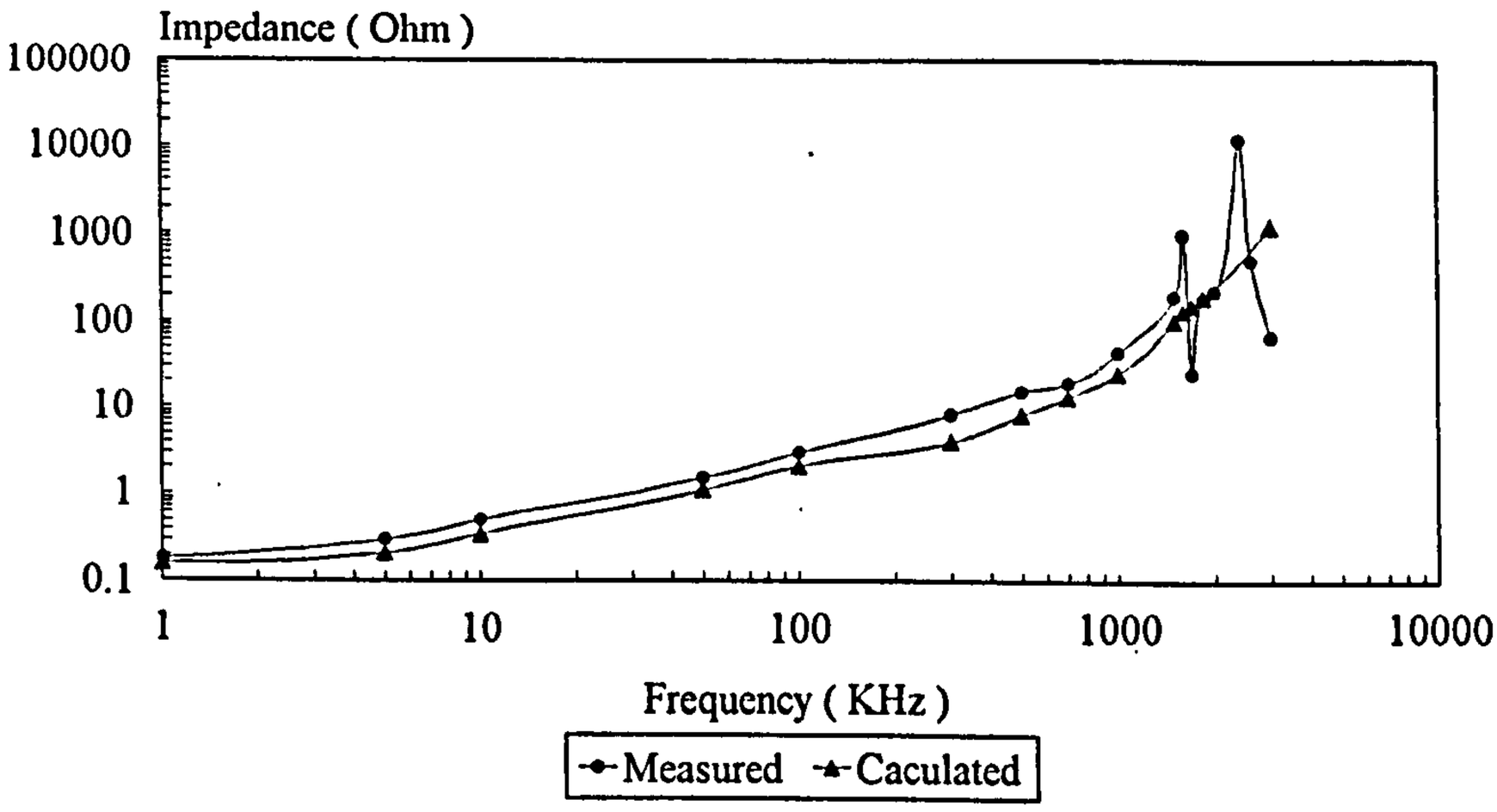

Fig.(3.12) : Short circuit impedance calculated from 2D FE model

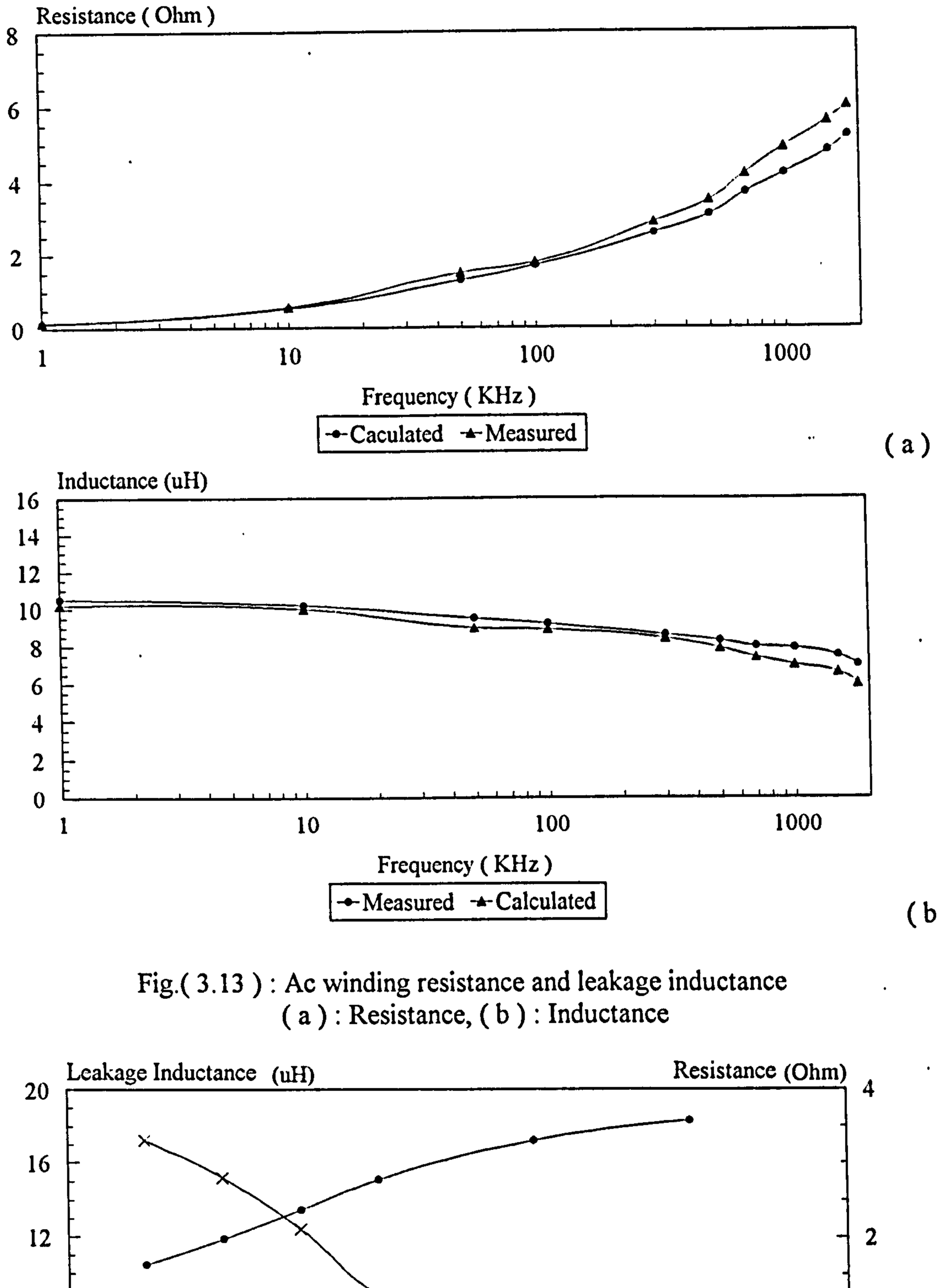

Fig.(3.13) : Ac winding resistance and leakage inductance
(a) : Resistance, (b) : Inductance

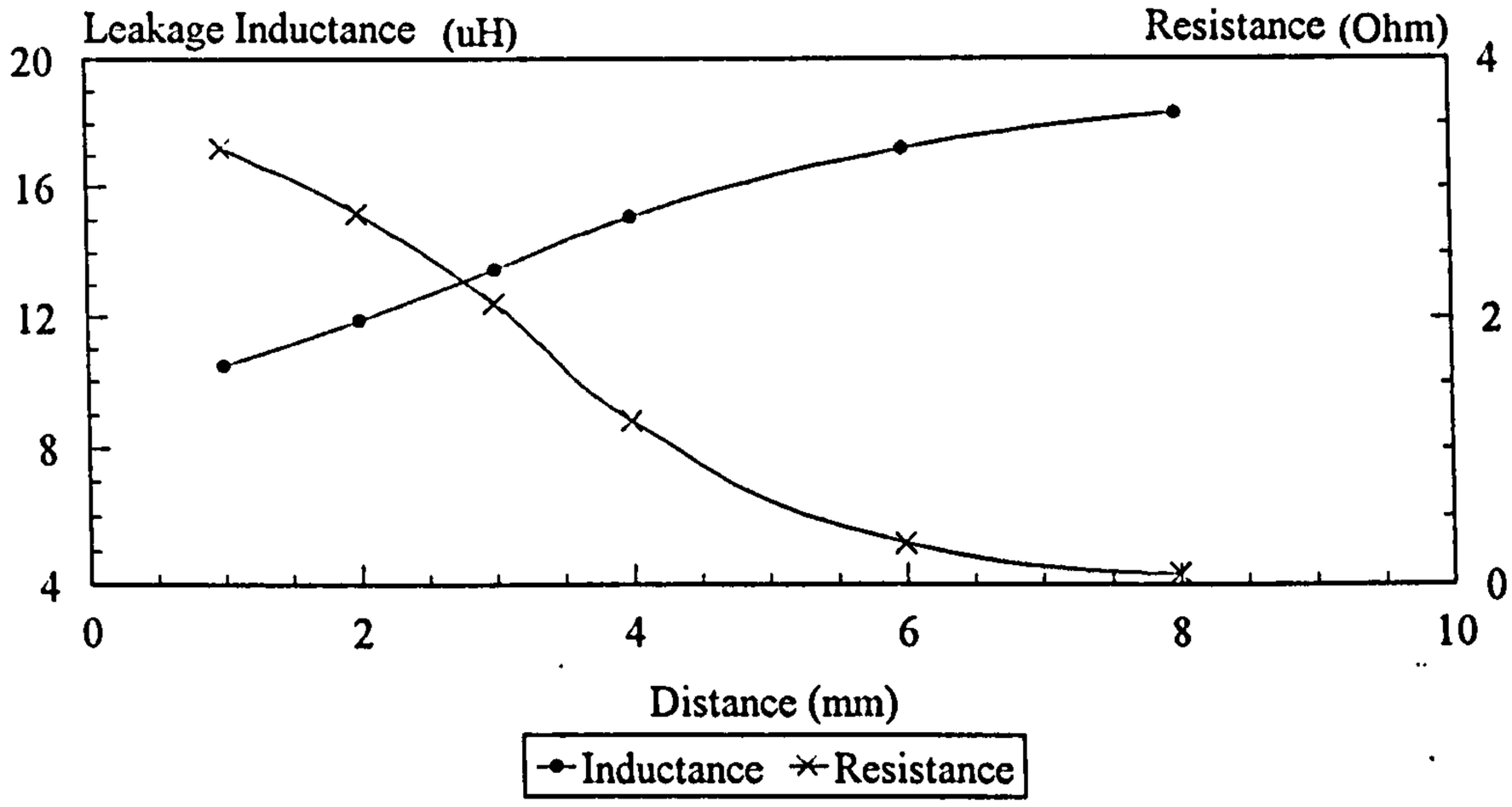

Fig.(3.14) : Effect of the gap between windings on the resistance and inductance

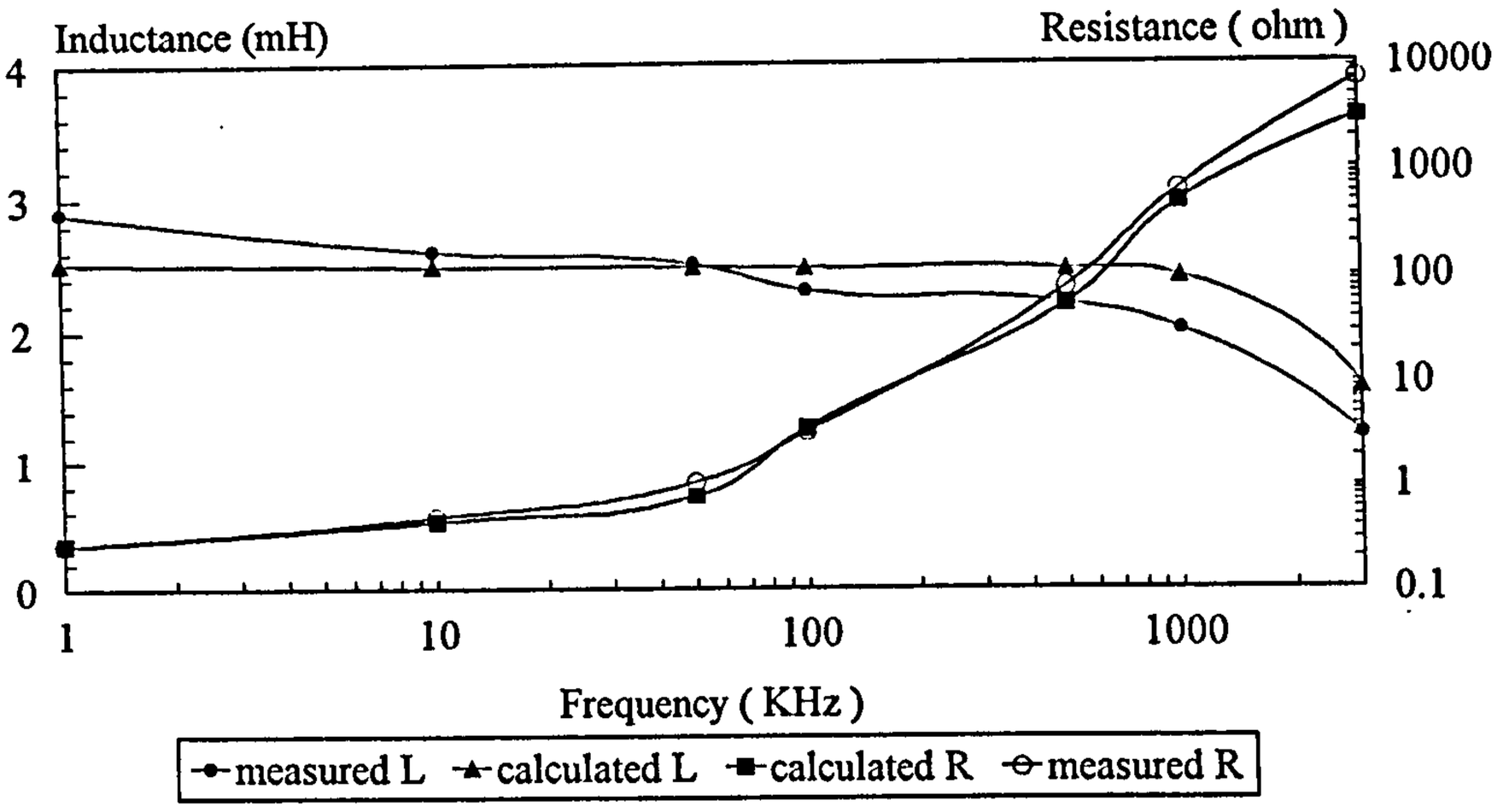

Fig.(3.15) : Self resistance and inductance during the open circuit

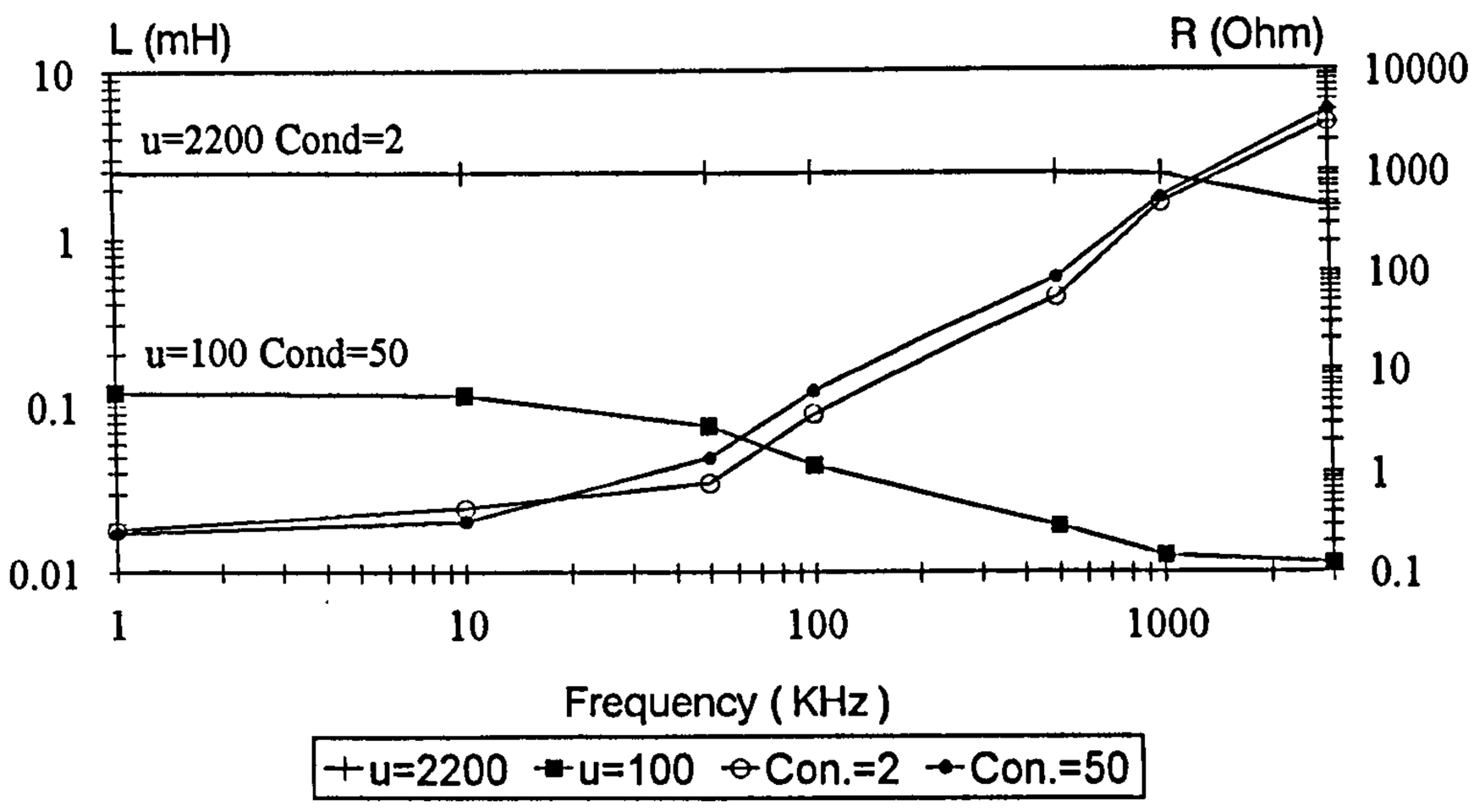

Fig. (3. 16) : influence of core properties on the resistance and self inductance

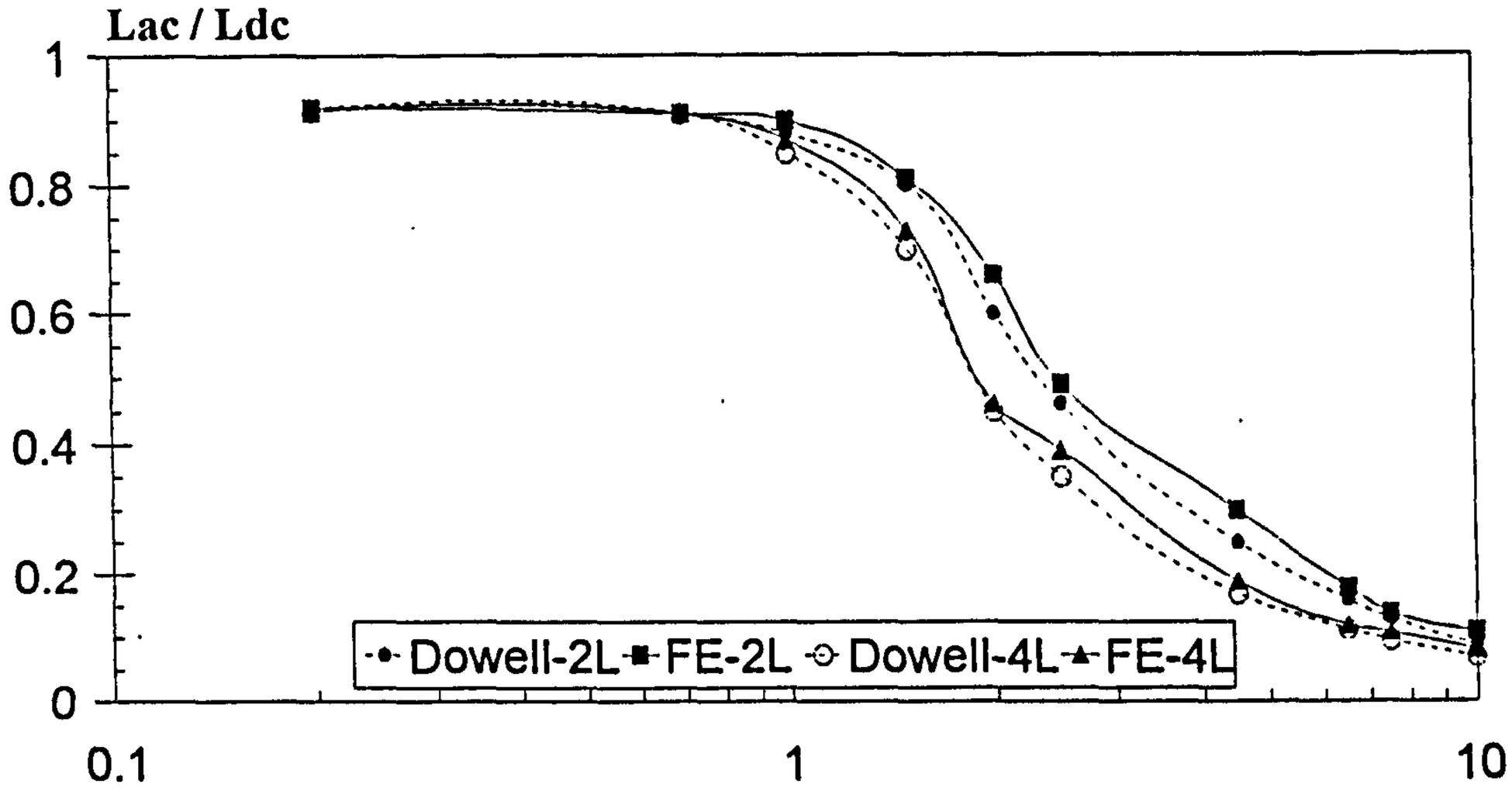

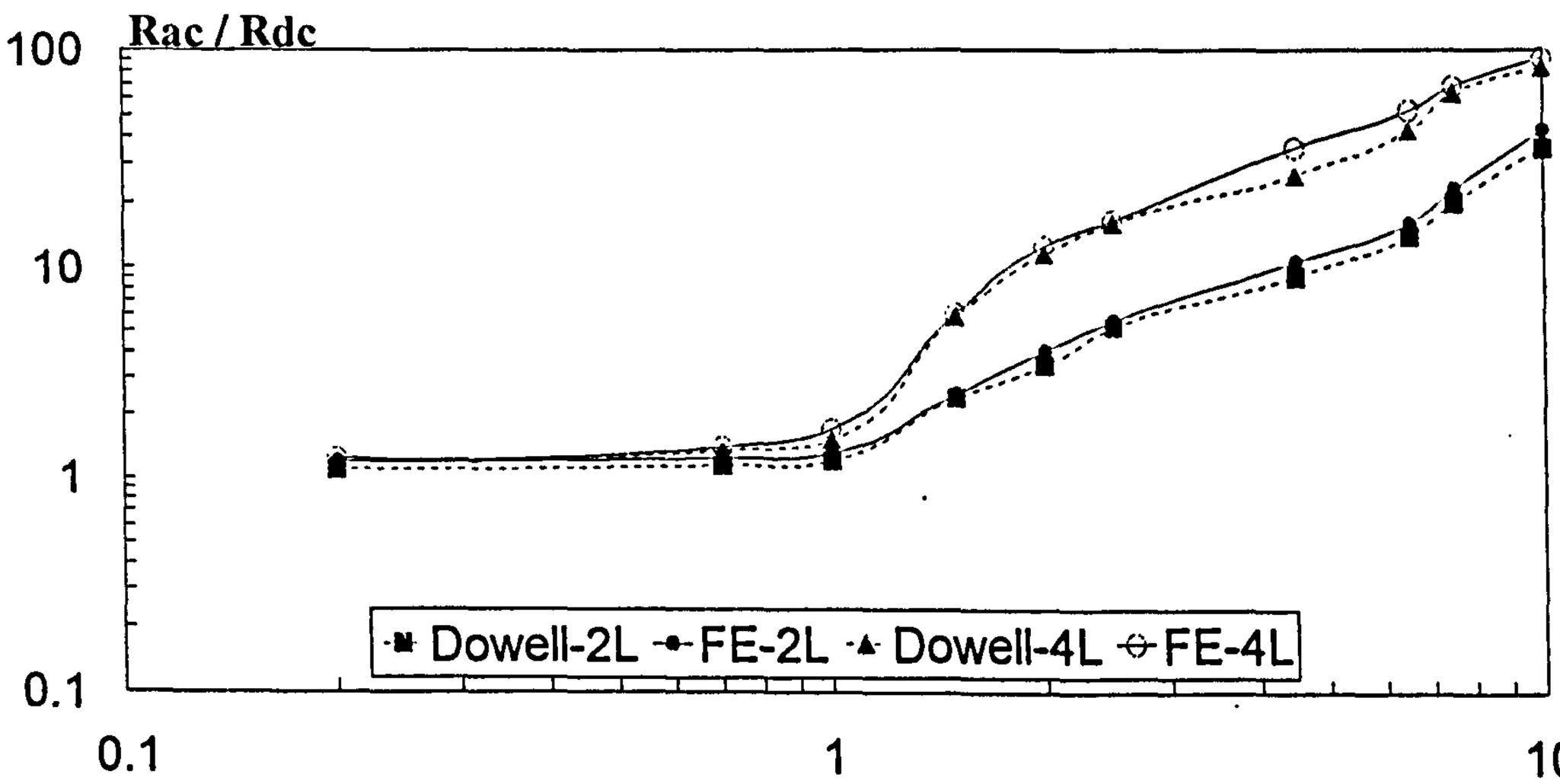

Fig. (3.17) : Primary layer effect on the inductance and resistance

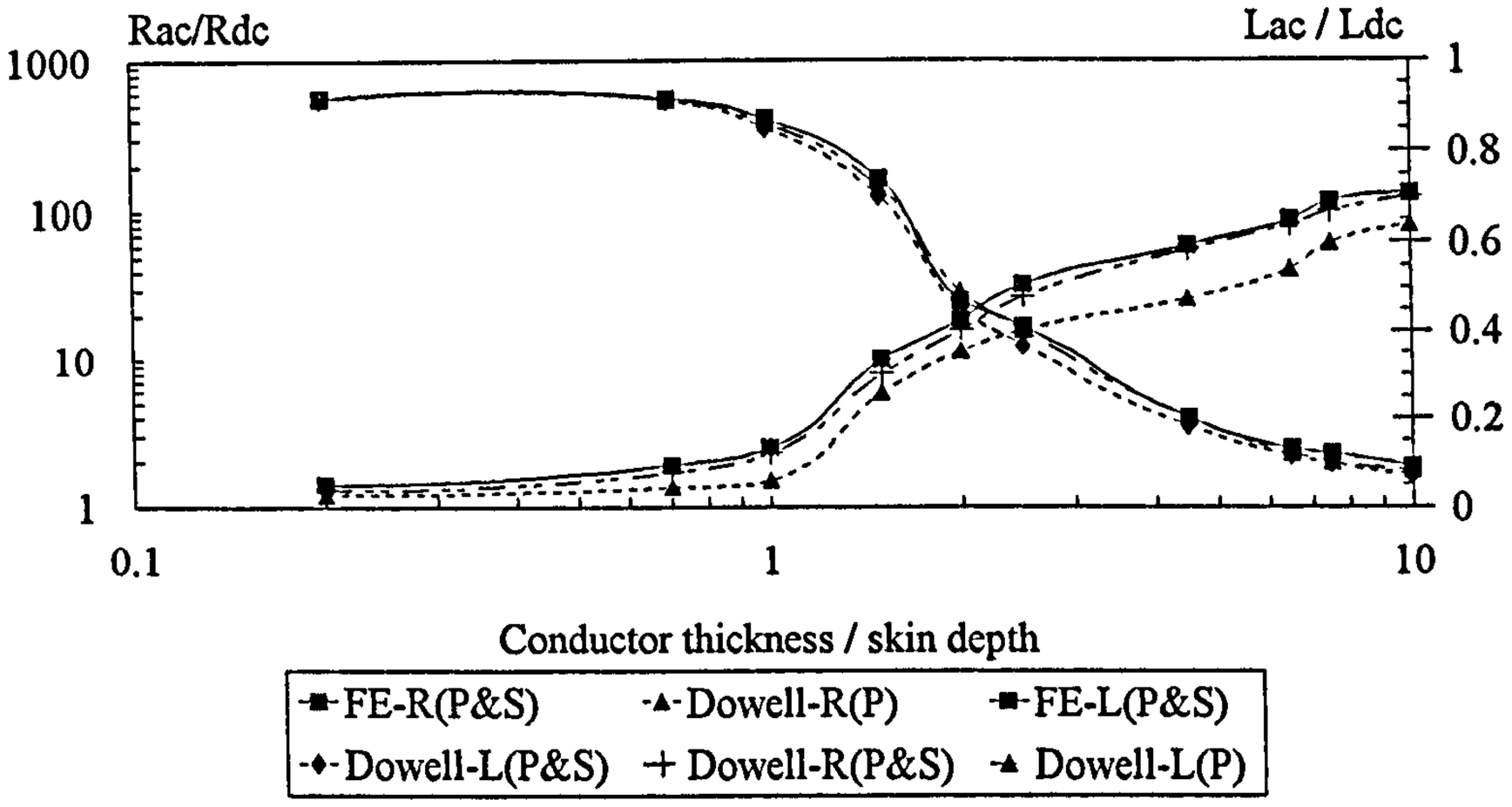

Fig.(3.18) : Effect of transformer layer on the losses and leakage
(4 Layers, P&S Primary and Secondary Windings and
P Primary Winding Only)

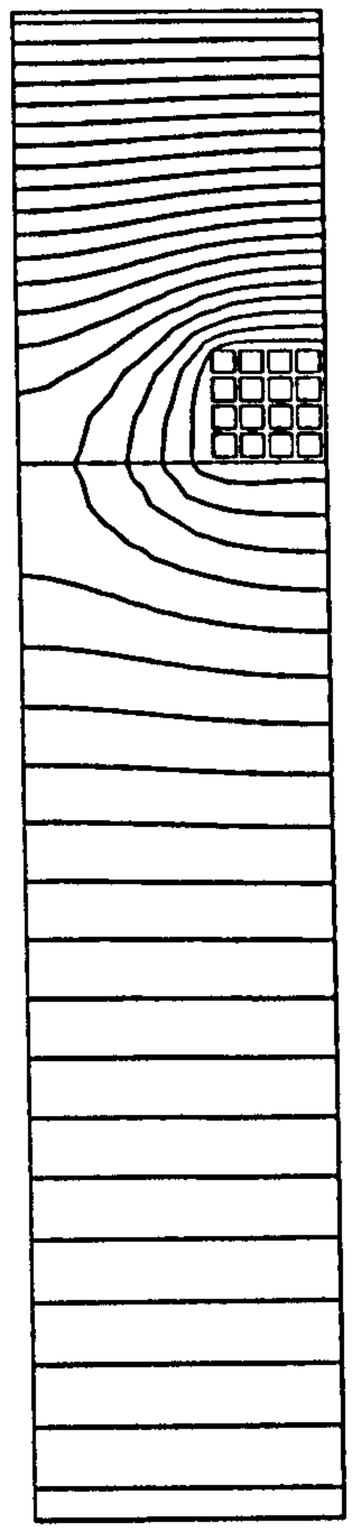

FIG. (3·19) : Flux Distribution for Toroidal core inductor at 1MHz

CHAPTER FOUR

THREE DIMENSIONAL TRANSFORMER MODELLING BY FINITE ELEMENT ANALYSIS

4.1: INTRODUCTION

Many devices are highly three dimensional in nature. One such device is a transformer, where there is almost no axis of symmetry. At low frequency, a transformer is radially symmetric apart from the core, but at high frequency the electrostatic potential varies along the winding whilst the magnetic field varies transverse to the winding.

The reality is that two dimensional field analysis is only reasonable at low frequency, but as capacitive effects start to become significant all the potentials and fields (magnetic and electric) vary in all three axes x,y, and z. Hence a three dimensional FE solution is truly required to model the transformer numerically. The solution is made easier by neglecting the displacement current at low frequency, but it reaches full complexity when the complete set of Maxwell's equation needs to be solved [70]. The difficulty comes from many sides including, the gauge chosen to force unique values, the size and shape of the elements, the derivation of the problem matrix, and economics, because a huge computer memory and time is required. The great developments in computer speed and memory now allow such an analysis to be carried out.

In this chapter the use of a magnetic vector-electric scalar potential formulation with Coulomb gauge to solve the full set of Maxwell's equations is explained and applied to the transformer model. This includes both the eddy current and displacement effects. In this case the magnetic vector potential has three components x, y, and z , due to the three dimensional nature of the field, while the electric scalar potential V has only one

value at each node in the mesh of the model. The concept of using tetrahedral elements and hexahedral elements to implement the FE method are explained. Gauge, mesh generation and other relevant information is also included in this chapter.

An example is given to check the validity of the calculations and it is compared with measurements. The analysis is carried out for a transformer model, with three turns. The interaction between the turns is vital for the capacitance effects which are known to be dominant at high frequency. A real value of permittivity is used, although there is no restriction on the use of a complex value to represent dielectric losses.

4.2 : MESH GENERATION

The main initial requirement to perform an FEA is to describe the problem by creating a mesh. The entire domain of the problem is subdivided into a number of small domains (elements). The way in which the mesh is generated could affect the computer storage requirements, the computation time, and the accuracy of the numerical method. Therefore; it is more convenient to use an automatic mesh generator than a manual approach. Generally, programs that generate a mesh automatically are based on a mesh modification and an error estimation algorithm. The error algorithm is approximated directly using local field derivatives or residuals [73]. In three dimensions such automatic schemes are far from straight forward and currently they will not deal with the type of problem being analysed here.

In the present work, the three dimensional mesh is generated by constructing and combining slices of a two dimensional mesh. The program extrudes the two dimensional mesh to any depth and /or angle and each slice may be required to be modified after extrusion. The program is not restricted on the number of slices that form the model. One of the difficulties lies in representing round wire. Extrusion means that the only way available is by replacing the round wire with an equivalent square cross section. This has been adopted by many researchers as explained in chapter three. In the case of

the 2D mesh shown in chapter three this problem does not exist. Thus the reason behind using a square wire in the model previously explained in chapter three is, first to compare the results with the 3D model currently used, and second, it is the case that the analytical solution is more manageable with square rather than round wire.

The diagram together with the table in Fig.(4.1), represents the way that the three dimensional model was formed, where the material numbered one in the table represents the core, two is the air gap, three and four represent the primary and secondary windings respectively. The process shown in the table has to be repeated for each of the slices required (which is strongly affected by the depth of penetration as discussed in chapter three). The three dimensional transformer model using the above method is shown in Fig.(4.2). The secondary winding can be either short or open circuited.

The same process can be used to include as many fine conductors as the main primary and secondary conductors need to be divided into. The diagram and table of Fig.(4.3), is used to create the three dimensional mesh shown in Fig.(4.4). Since there is a limited number of nodes that the program can handle according to the computer capacity, and the analysis is intend to be carried out in Megahertz zone where small elements are required, only a model of a single wire is used.

4.3: ELEMENTS SHAPES IN 3D FEA

The numerical accuracy of the finite element analysis depends on the characteristics (shape, integration, etc.) of the element used to represent a model. In this section a brief general discussion is introduced regarding the element shapes. In the 3-dimensional analysis, there are three common shapes, which are known as : tetrahedral (four sides, four nodes), pentahedral (five sides, six nodes), and hexahedral (six sides, eight nodes). The choice of the size and shape of these 3-dimensional elements are arbitrary. Tetrahedral elements are the most suitable choice for the derivation of the matrix equation, because these have shape functions which are complete polynomials of a

given order leading to greater accuracy per node in the general case. Gaussian integration is used to numerically integrate over the volume of the elements, by using a simple summation of terms involving the integral evaluated at specific nodes in the domain multiplied by suitable weightings [13].

The general form which yields the solution for the tetrahedral coefficients of the magnetic vector potential is :

$$A(x,y,z) = \sum_{n=i,j,k,l} A_n \left(a_n + b_n x + c_n y + d_n z\right) \quad \text{.....(4.1)}$$

Where i, j, k, and l represent the four corners of the overall shape of the element

Tetrahedrons gives most flexibility in the construction of objects but they are not easy to work with, therefore hexahedral elements are introduced to build volumetric models. Each of the hexahedral elements consists of five tetrahedral elements, and they are used as the global discretization building blocks. The way of creating tetrahedral, hexahedral, prism and others are explained in detailed in reference [24]. The discussion of each shape is out of the scope of this chapter, and only a brief introduction has been given.

The three dimensional mesh shown in Fig.(4.2), consists of 18875 tetrahedral elements, and more than ten thousand nodes. The number of unknown vector potential values (A) is three times the number of nodes, due to the three dimensional analysis (reduced slightly by fixed potential boundaries).

4.4 : FIELD EQUATIONS

In any electromagnetic device (transformer, inductor, etc.), there are two theories to be applied, the internal electromagnetic field of the device and the external circuit it is connected to.

The four governing partial differential equations describing the electromagnetic field (which have become known as Maxwell's equations) [65] are :

$$\nabla \times \mathrm{H} = J + \frac{\partial D}{\partial \mathrm{t}} \qquad \ldots\ldots\ldots\ldots\ldots\ldots (4.2)$$

$$\nabla \times \mathrm{E} = -\frac{\partial \mathrm{B}}{\partial \mathrm{t}} \qquad \ldots\ldots\ldots\ldots\ldots\ldots (4.3)$$

$$\nabla . D = \rho \qquad \ldots\ldots\ldots\ldots\ldots\ldots (4.4)$$

$$\nabla . \mathrm{B} = 0 \qquad \ldots\ldots\ldots\ldots\ldots\ldots (4.5)$$

The constitutive relations are also required, and given by :

$$J = \sigma \mathrm{E}, \quad D = \varepsilon \mathrm{E} \quad \& \quad \mathrm{B} = \mu \mathrm{H} \qquad \ldots\ldots\ldots\ldots\ldots\ldots (4.6a\text{-}c)$$

The equation for current continuity (derived using 4.2 and 4.4) is also useful :

$$\nabla . J = -\frac{\partial \rho}{\partial t} \qquad \ldots\ldots\ldots\ldots (4.7)$$

Equation (4.5) can be satisfied by using the magnetic vector potential ,

$$\nabla \times \mathrm{A} = \mathrm{B} \qquad \ldots\ldots\ldots\ldots\ldots\ldots (4.8)$$

From equation (4.2) and the time derivative of D in equation (4.6), the relation between E and A can be derived and is given by :

$$E = -\frac{\partial A}{\partial t} - \nabla V \qquad \text{..... (4.9)}$$

where V is the electric scalar potential.

The current density relation is formed from equations (4.9) and ohm's law (equation 4.6a), and given as :

$$J = -\sigma \frac{\partial A}{\partial t} - \sigma \nabla V \qquad \text{..... (4.10)}$$

The first term on the right side of equation (4.10), represents the current arising from voltage by the changing of magnetic field, while the second term is the current caused by the electrostatic field.

The main step in any electromagnetic field analysis is the construction of an efficient and economical numerical algorithm. The algorithm describing the particular problem can be derived by manipulating Maxwell's equations to give the required relations. The equations (4.2) to (4.10) can be combined together to form the vector equation given by :

$$\nabla \times \frac{1}{\mu} \nabla \times A = -\sigma \frac{\partial A}{\partial t} + \sigma \nabla V - \varepsilon \frac{\partial^2 A}{\partial t^2} - \varepsilon \frac{\partial V}{\partial t} \qquad \text{..... (4.11)}$$

The first and second terms of the right hand side of equation (4.11) are defined in equation (4.10), the third and fourth terms result from the changing electrostatic field which themselves are due to changing electromagnetic or electrostatic fields.

The program used to simulate the three dimensional model of the transformer is based on the solution of the equation (4.11). It contains both eddy current and displacement currents effects. The displacement current is introduced to account for the production of the electrostatic fields in empty space (between conductors), where the conduction current in this space is equal to zero. The total of electromagnetic fields between any two conductors is due to three components of current, namely the external source, eddy current, and finally displacement current as shown in the equation below,

$$J_{total} = J_{cond} + J_{disp} = -\sigma \frac{\partial \mathrm{A}}{\partial t} - \sigma \nabla V + \frac{d D}{\mathrm{d\,t}} \qquad \text{..... (4.12)}$$

where J_{cond} is the current density within the conductor including source and eddy current, while the second part is the current through the capacitor in the gap between conductors.

4.5 : GAUGE AND FORMULATION

The magnetic vector potential (A) defined only by equation (4.11) is not unique, i.e. its divergence must also be defined. The definition of divergence is called the gauge condition, which is imposed together with a proper selection of the boundary conditions.

The gauge which commonly used is the Coulomb gauge [25], where the divergence of A is made equal to zero. Arguably this is the most natural form of A, since it makes A responsible only for circulating effects, it also results in the simplest formulation for establishing interface conditions. Other gauges can lead to potential efficiencies in formulation but experiments show that large numerical difficulties result, which largely offsets the gain in the number of unknowns [74]. Having selected the term $\nabla \bullet \mathrm{A} = 0$ we can write 4.11 as:

$$\nabla \times \frac{1}{\mu} \nabla \times \mathrm{A} - \nabla \frac{1}{\mu} \nabla \bullet \mathrm{A} = -\sigma \frac{\partial \mathrm{A}}{\partial t} + \sigma \nabla \mathrm{V} - \varepsilon \frac{\partial^2 \mathrm{A}}{\partial t^2} - \varepsilon \frac{\partial \mathrm{V}}{\partial t} \qquad \text{..... (4.13)}$$

Providing μ is taken as a precise constant, equation (4.13) can be written with the assumption of harmonic time variation as :

$$\nabla \times \frac{1}{\mu} \nabla \times \mathrm{A} - \nabla \frac{1}{\mu} \nabla \bullet \mathrm{A} = -j\omega \left(\sigma + j\omega \varepsilon\right) \mathrm{A} - \left(\sigma + j\omega \varepsilon\right) \nabla V \qquad \text{.....(4.14)}$$

Equation (4.14) fixes three of the unknowns, the other must come from the electric field. The choice is made to use the current continuity equation, i.e. :

$$\nabla.\left(J+\frac{\partial D}{\partial t}\right)=0 \qquad \text{.....(4.15)}$$

The first term inside the bracket of equation (4.15) is given in equation (4.10), and the second term is defined by equations (4.6) and (4.9), so equation (4.16) is transformed to :

$$\nabla.\left(-\sigma\frac{\partial \mathrm{A}}{\partial t}-\sigma\,\nabla V\right)+\frac{\partial}{\partial t}\left(-\varepsilon\,\frac{\partial \mathrm{A}}{\partial t}-\nabla(\varepsilon\,\nabla V)\right)=0 \qquad \text{.....(4.16)}$$

Finally, equation (4.16) can be written in the complex form :

$$\nabla.(\sigma+j\omega\varepsilon)\,\nabla V+j\omega\,\nabla.(\sigma+j\omega\varepsilon)\,\mathrm{A}=0 \qquad \text{.....(4.17)}$$

The above two equations (4.14) and (4.17) are the fundamental field analysis equations necessary to determine the vector potential and the scalar potential distributions for the combinations of eddy currents and displacement effects.

In order to obtain a finite element solution, the weighted residual method can be applied, and by using Galerkin's method, where the shape function N is considered as the weighting function, equations (4.14) and (4.17) are replaced by :

$$\int_v N_i\left(\nabla\times\frac{1}{\mu}\nabla\times\mathrm{A}-\nabla\frac{1}{\mu}\nabla\bullet\mathrm{A}\right)+j\omega\,(\sigma+j\omega\varepsilon)\,\mathrm{A}\,N_i-(\sigma+j\omega\varepsilon)\,\nabla V\;N_i\;dv=0$$

.....(4.18)

$$\int_v \mathrm{N_i}\left[\nabla.(\sigma+j\omega\varepsilon)\,\nabla V+j\omega\,\nabla.(\sigma+j\omega\varepsilon)\,\mathrm{A}\right]\mathrm{dv}=0 \qquad \text{.....(4.19)}$$

where v is the volume.

By using Green's function and the vector identities, which are as follow :

$\nabla.(\mathrm{A}\times\mathrm{N})=\mathrm{N}.(\nabla\times\mathrm{A})-\mathrm{A}.(\nabla\times\mathrm{N})$, equation (4.18) becomes

$$\int_v \nabla N_i\left(\nabla\times\frac{1}{\mu}\nabla\times\mathrm{A}\right)+j\omega\,(\sigma+j\omega\varepsilon)\,\mathrm{A}\,N_i-(\sigma+j\omega\varepsilon)\,\nabla V\;N_i\;dv$$

$$+\oint_s \mathrm{N}_i\left(\frac{1}{\mu}\nabla\times\mathrm{A}\right)\times n\;ds+\oint_s \mathrm{N}_i\,(\nabla.\mathrm{A})\,n\;ds=0 \qquad \text{.....(4.20)}$$

The same procedure can be applied to equation (4.19), by using again Green's function and the vector identity, $\nabla.(\mathrm{NA})=\mathrm{N}(\nabla.\mathrm{A})+\nabla\mathrm{N}.\mathrm{A}$, which gives :

$$\int_v \nabla \mathrm{N}_i\left[(\sigma+j\omega\varepsilon)\,\nabla V+j\omega\,\nabla.(\sigma+j\omega\varepsilon)\,\mathrm{A}\right]\mathrm{dv}$$

$$-\oint_s \mathrm{N}_i\,(\sigma+j\omega\,\varepsilon)\,\frac{\partial V}{\partial n}\,ds-\oint_s j\omega\mathrm{N}_i\,(\sigma+j\omega\varepsilon)\,\mathrm{A}.n\;ds=0 \qquad \text{.....(4.21)}$$

Where n in both equations (4.20) and (4.21) represents the normal direction to the boundary surface. Also from equation (4.20) , it may be noticed that the fourth term represents the tangential component of the magnetic field intensity, while the fifth term is zero from the definition of the coulomb gauge. In the same way, the last two terms of equation (4.21) represent the normal component of the total current density (eddy currents and displacement currents).

The global system matrix equation is obtained by integrating the two equations (4.20, 4.21) over the elements of the model. Various solvers are available, but the most common solver is the preconditioned conjugate gradient method, incorporating incomplete cholesky decomposition to carry out the precondition [66].

4.6 : PROGRAM VALIDITY

In order to validate the procedure a simple model is used first to examine the basic background for this 3D analysis. This model consists of two rectangular coils which are in air (i.e. an air cored transformer). Air core and ferrite core transformers are used for high frequency applications and consist of windings on an insulating shell which is air. Both coils consist of two copper wires with 5.7E+07 $(\Omega.m)^{-1}$ conductivity, and 0.9999 relative permeability. The wire cross section area is 0.5mm and the dimensions of the turns (around the peripheral) are 3cm breadth by 2.5cm width. The length of the gap between the turns is 0.2mm. This model is used to calculate results to compare with a ten turns experimental system [75]. The first coil (primary) is supplied by a voltage of 10 volts, the second coil (secondary) which is placed above the first one is left open circuit.

The graph of impedance is drawn for both the measured, and calculated results for the driven coil. The results are shown in Fig.(4.5), where three modes of resonance are clearly seen. Two of the modes are series resonance at 188 KHz, 7.8 MHz, and one is parallel resonance at 1.87 MHz.. Another observation from the impedance curve is that the equivalent circuit can be found easily. Each of the two series resonant points can be represented by LC components, and at resonant frequency the impedances fall to near zero. The impedance at resonance is due to the existence of resistance in each series resonant branch. These two series branches are placed in parallel producing the parallel resonant point on the impedance curve. Physically, the behaviour of such a system is dominated by absence of the core. Usually, the closest ground for the winding is the core and hence the capacitance to the core is dominant. Without a core, the only ground available, is the ground of the actual winding. The ground capacitance is therefore small in comparison with the case were the core exists, and the first cut off frequency is therefore very high.

The fact that the two results (measured and calculated) compare well gives confidence in the method. At low frequencies, the most important parameter is the magnetising reactance that draws a large current that flows through primary winding winding. Magnetising inductance is a function of the magnetisation current, as the magnetising current increases the value of this inductance is decreases until saturation when its value reaches a minimum corresponding to an air core. An air core has higher magnetising current and so a smaller magnetising inductance. The above figure (4.5) shows that at low frequency the magnetising reactance is dominated by high reluctance air core. The figure also shows that the first cut off frequency (parallel resonance) no longer exist and that due to the lower ground capacitance (as no ferrite core exist) together with less magnetising inductance. Therefore, the first cut off frequency is very high.

4.7 : OPEN AND SHORT CIRCUIT IMPEDANCE CALCULATIONS BY 3D FEM

Open and short circuit impedance calculations are the main consideration in the present work. These two impedances provide enough information to build the required elements of an equivalent circuit of the transformer, and hence to give a good equivalent representation of the windings.

The 3D-FE modelling of the transformer is difficuilt in respect of the representation of winding turns. In the 2D model, the turns of the series winding are joined together by an external equation so as to form one single winding. In the 3D such an equation is not available and it is not an easy task to apply in this program. In the actual transformer there are 26 secondary turns and 14 primary turns. Each turn is comprised of 64 fine wires. That makes a total of 2560 fine wires. In addition, the 64 fine wires are in four bundles of 16. Each set of 16 are twisted together, and the four sets of 16 are twisted together. Clearly, it is a practical impossibility to fully represent that arrangement. It is the case that the twisted 64 wires force an even distribution of current over all operating frequencies amongst the substrands and hence it is not necessary to model the detail of every strands. It is also possible to model less than the

full number of turns provided that the turns which are modelled have the correct spacing one with the other and with the respect to the core. Following these arguments three turns of the primary and three of the secondary have been modelled in the half section of the transformer (implying 6 turns each for primary and secondary via symmetry). Therefore, turns are of smaller cross section than the full 64 wire bundle and with an adjusted conductivity to get the dc resistance correct. The turn cross section is necessarily solid in the model (rather than subdivided into the 64 substrands) and the dimension of the turns is chosen so that skin limited eddy currents are not set up over the frequency range modelled.

It is clear that this representation is far from perfect but it does preserve clearances and hence turn to turn and turn to ground capacitance is reasonably faithfully modelled as are leakage flux paths. The results to compare with the actual transformer are then obtained from the model by reflecting through the respective turns ratio i.e. 6:14 and 6:26. This technique is adopted in the present work as for example by the model shown in Fig.(4.2). More elements have to be placed in the conductor area to achieve sufficient accuracy. The number of these elements depends on the skin depth (as discussed previously). They need to be quite fine in the conductor space and they may be five times less dense in the region of the core due to the different material properties involved.

The whole model is placed inside a box to represent an air space around the transformer. The actual Ferrite E core has 0.25mm air gap in the centre limb. In practice, this gap size is obtained by grinding. Another procedure that could be used involves moving the core halves apart by half the size of the required air gap. That means half of the required gap will be in the centre and the other half in the outer legs of the core (assuming the total outer leg cross section area is equal to the centre part of the core). This is the procedure that has been used during the finite element modelling of the air space. Practically this could be an EMI source due to the external magnetic field, particularly at high frequency. The assumption is made that the x,y,z components of the magnetic vector potential, and scalar voltage are equal to zero for all of the

surfaces nodes of the box except the front and back. The front and back surfaces are where the conductor ends emerge. The solution is driven by forcing electrostatic potential across the conductor (in fact zero at one face, and full value at the other). The rest of electrostatic potentials and the z-component of the magnetic potential are left floating on these surfaces. Effectively, the boundary condition chosen restrain the magnetic fields to excite only inside the box and through the ground the sides of the box. The normal component of electric flux is forced to zero on the front and back surfaces excepting within the conductor.

The flux distribution for various frequency components are given in Fig.(4.6) and Fig.(4.7), for open and short circuit cases respectively. The field plots shown in these figures only have limited objective value, but there is considerable tutorial content and an understanding of their meaning adds considerably to the subject via validation of the calculations. There are two tests involved. The first short circuit and the second open circuit. For each test there are four components of field, "A" the vector potentials,"Ax","Ay", and "Az"., and the electric potentials "V". The easiest understanding of the vector potential is as quantifying the flux-linkage per unit length in each co-ordinate direction. Given sinusoidal excitation they therefore indicate components of induced voltage. The real component is effectively the induced voltage at 90^0 to the datum of the source, and the imaginary component is the induced voltage in phase with the datum of the source.

In the short circuit test, the source is an electrostatic potential applied across the terminals of the primary winding. In fact V_{max} + j 0 to the input terminal and 0+ j 0 to the terminal on the place of symmetry. The result is an alternating current through the primary which induces a nearly equal and opposite mmf in the secondary. The induced voltages in the primary and secondary will tend to be at 90^0 to the source and hence components of vector potential can be expected to be maximal in the imaginary components, although the presence of resistance might be expected to give rise to phase shift and hence real components.

Starting first with Fig.(4.6a), which shows contours of the "Z" component of vector potential on the outsides of the model. All other components are forced to zero on their surface. As can be seen "Az" is maximal in the conductor itself. This case is rather easier than the others because the single component of "A" allows simple interpretation of the contour of "Az" as flux lines and the flux can be clearly seen to circulate around the conductor. As expected the imaginary components have higher values than the real components.

Turning now to Fig.(4.6 - 4.7 b,c,d) which show contours of vector potential plotted on the exposed surfaces once the air has been removed from the model a number of features can be seen:-

1- Voltage is induced in the conductors according to the direction e.g. a "y" directed conductor carries "y" directed current and hence "zx" plane flux and hence receives "y" directed induced voltage.

2- It is not easy to see but the pattern of vector potential rising across the excited winding and falling across the shorted secondary is also visible with the highest fields in the space between the windings.

3- Highest vector potentials are mainly in the imaginary components.

4- The vector potential (and hence induced voltage) falls quite markedly towards the corners.

5- The "z" directed potential is found mostly by the input lead but also has secondary effects due to transition between one turn and the next. In fact this is artificial because the real turns will lie in a true spiral whereas here the turns are essentially planar with axial transition at corners.

The input impedance for both cases, which is found from the ratio of the imposed voltage and the calculated current carried by the primary is given in Fig.(4.8) and Fig.(4.9) , for open and short circuit respectively. Measured and calculated results show a satisfactory agreement for both cases.

4.8 : COMMENT ON THE RESULTS

An examination of the impedance curves of Fig.(4.8) and Fig.(4.9) showed relatively good agreement between measurement and calculation rather better in the short circuit case than the open circuit. The agreement is also slightly worse than that found in the air cored coil example (Fig.4.5). This probably points to the difficulty of accurately representing the ferrite core at high frequency.

In the open circuit case, the magnetising components dominate the results. These components (magnetising) have both real and imaginary parts. The real part is a reflection of core loss which is represented entirely by core conductivity and hence very sensitive to the value chosen. The imaginary part has two terms; an inductive element which is sensitive to the core permeability, and a capacitive element which is sensitive to the core permitivitty. But, due to the frequency dependency of all of the core properties in real life, the single value which is used for each property can be expected to result in the differences in the results [18,41]. The values of these properties that is taken in the program are:- the conductivity is $2(\Omega.m)^{-1}$, the permeability is 2200, and the relative permitivitty is 10.

The basic shape of Fig.(4.8) and Fig.(4.9) may best be explained with reference to the high frequency equivalent circuit as shown in Fig.(4.10). The resistances have been excluded from this model for the reason which will be made clear later. Considering the open circuit case, it can be seen that the impedance will become very high when either the leakage branch or the magnetising branch reach resonance. The combination of the two branches could be considered, each has an inductance and capacitance, and therefore a simple port of zero impedance might be expected. Therefore, there are two zeros and one pole.

4.9 : TRANSFORMER EQUIVALENT CIRCUIT

From the open circuit impedance curve, one series and two parallel resonance frequencies can be recognised. The series is at 751.3 KHz, and the parallel are at, 105.5 KHz and 2.4 MHz. In order to simplify determination of the equivalent circuit elements, the resistances will be neglected in the derivation of the inductances and capacitances. They can be added later to model the full equivalent circuit.

The equivalent circuit model and it's parameters are based on the measured and calculated curves of the open and short circuit impedances. The reason for using such a method is the difficulty of calculating all the equivalent circuit parameters directly from the 3DFE model. This difficulty is coming mainly from the hopelessly complex distribution of different elements of capacitance within the model.

The proposed series-parallel equivalent circuit is shown in Fig.(4.10). This is a standard form for a high frequency transformer model. The equations to represent the impedances can be derived and given by :

$$[Z_{oc}]_f = \frac{\omega(L_1+L_m)\left[1-\omega^2\frac{L_1L_m}{L_1+L_m}(C_1+C_g)\right]}{(1-\omega^2L_1C_1)\ (1-\omega^2L_mC_g)} \qquad \text{..... (4.25)}$$

$$[Z_{sc}]_f = \frac{\omega\left(L_1+\frac{L_2L_m}{L_2+L_m}\right)\left[1-\omega^2\frac{L_1L_mL_2}{L_1L_m+L_mL_2+L_1L_2}(C_1+C_g+C_2)\right]}{(1-\omega^2L_1C_1)\ \left(1-\omega^2\frac{L_2L_m}{L_2+L_m}(C_2+C_g)\right)} \qquad \text{..... (4.26)}$$

Examining the poles and zeros of equation (4.25) results in the conclusion that the two frequencies at which equation (4.25) approach infinity (parallel resonance) are:

$$1-\omega^2L_1C_1=0 \ \Rightarrow\ \omega_P=1/\sqrt{L_1C_1} \qquad \text{.....(4.27)}$$

$$1-\omega^2 L_m C_g = 0 \;\Rightarrow\; \omega_P = 1 \Big/ \sqrt{L_m C_g} \qquad \text{.....(4.28)}$$

and the one frequency at which equation (4.25) approach zero (series resonance) is:

$$1-\omega^2 \frac{L_1 L_m}{L_1 + L_m}\left(C_1 + C_g\right) = 0 \;\Rightarrow\; \omega_S = \sqrt{\frac{L_1 + L_m}{L_1 L_m \left(C_1 + C_g\right)}} \qquad \text{..... (4.29)}$$

By considering the open and short circuit impedance curves, it can be found which of the two equations (4.27 & 4.28) represents the first and second parallel resonant frequency. At the first "parallel" frequency (105.5 KHz), an effect is seen on the open circuit curve only. On short circuit the magnetising branch is masked by the secondary impedance and so, the first parallel resonance is related to equation (4.28) and the second to equation (4.27).

Therefore, all of the above equations can be identified as :

$$f_{P\,1} = 1 \Big/ 2\pi \sqrt{L_m C_g} \qquad \text{.....(4.30)}$$

$$f_{P\,2} = 1 \Big/ 2\pi \sqrt{L_1 C_1} \qquad \text{.....(4.31)}$$

$$f_s = 1 \Big/ 2\pi \sqrt{\frac{L_{\,1} + L_m}{L_{\,1} L_m \left(C_1 + C_g\right)}} \qquad \text{.....(4.32)}$$

$$\left| Z_{oc} \right|_f = \frac{\omega \left(L_1 + L_m\right) \left[1 - \left(\frac{f}{f_s}\right)^2\right]}{\left[1 - \left(\frac{f}{f_{p1}}\right)^2\right]\left[1 - \left(\frac{f}{f_{p2}}\right)^2\right]} \qquad \text{.....(4.33)}$$

Equations (4.30 - 4.33) can be used to calculate the value of $L_{\,1}$(primary leakage inductance), $L_{\,m}$ (magnetising inductance), $C_{\,1}$(primary distribution capacitance),

and C_g (ground capacitance) by considering the value of the open circuit impedance at the lowest frequency which is 1KHz. The parameter values then are :

$L_1 = 3.36\ \mu H$ $\quad$ $L_m = 187\ \mu H$

$C_1 = 1.3$ nF $\quad$ $C_g = 12.3$ nF

In order to determine the values of L_2, C_2(secondary leakage inductance and distribution capacitance between the secondary turns), the same procedure is applied.

$$f_{P1} = 1 \Big/ 2\pi \sqrt{L_{eq} C_{eq}}$$

$$f_{P2} = 1 \Big/ 2\pi \sqrt{L_1 C_1}$$

$$f_s = 1 \Big/ 2\pi \sqrt{\frac{L_1 + L_{eq}}{L_1 L_{eq} (C_1 + C_{eq})}}$$

where $C_{eq} = C_2 + C_g$, and $L_{eq} = \dfrac{L_2 L_m}{L_2 + L_m}$

These values then are,

$L_2 = 0.86\ \mu H$ $\quad$ $C_2 = 5.11\ nF$

The values of the above parameters can then be used with the equations (4.25) and (4.26) to recalculate the frequency response. The curves shown in Fig.(4.11 & 4.12) are compared with that of the measurements and the FE calculation. The good agreement shows that the capacitive and inductive components are far larger than the resistive components. The inductances and capacitances have compensated the value of resistances in certain branches, and hence not much difference can be seen when resistances are neglected. This observation is fully discussed in the coming chapter where the resistances are taken into account.

4.10 : SUMMARY

The full set of Maxwell's equations have been used to model the transformer. Both conduction and displacement currents have been considered. The existence of the displacement currents causes a reduction in the voltage between turns away from the terminals of the winding. Therefore; this voltage is not going to be constant as in the case in the two dimensional model discussed in the previous chapter.

The open and short circuit impedance calculations are made, by solving three turns with half of the E core by 3D FEM. The difference in the results (which is rather masked due to the high value of the y-axis) can be explained with respect to the core properties. In this program, just a real part of these properties is considered, but the fact is that complex properties are more likely to be important to better deal with high frequency problems. The difficulty of solving the full set of Maxwell's equation with full account taken of the complex properties of the core taken into account is beyond the scope of this thesis. However, the existence of the imaginary part of the conductivity, permeability, and permitivitty represent additional dielectric losses, magnetic losses, and dielectric losses respectively.

Because of the complex arrangement and distribution of the capacitances and inductances throughout the model, a simple method is used to predict the equivalent circuit. This method is based on the resonant frequencies. The elements of the circuit can be found from the knowledge of the parallel and series frequencies that are located on both the open and short circuit impedances curves. These elements can be used again with the equivalent circuit to predict the open and short circuit impedances. By comparing the results with the measured and FE calculation, the good agreement shows that this equivalent circuit can be used for a wide frequency range.

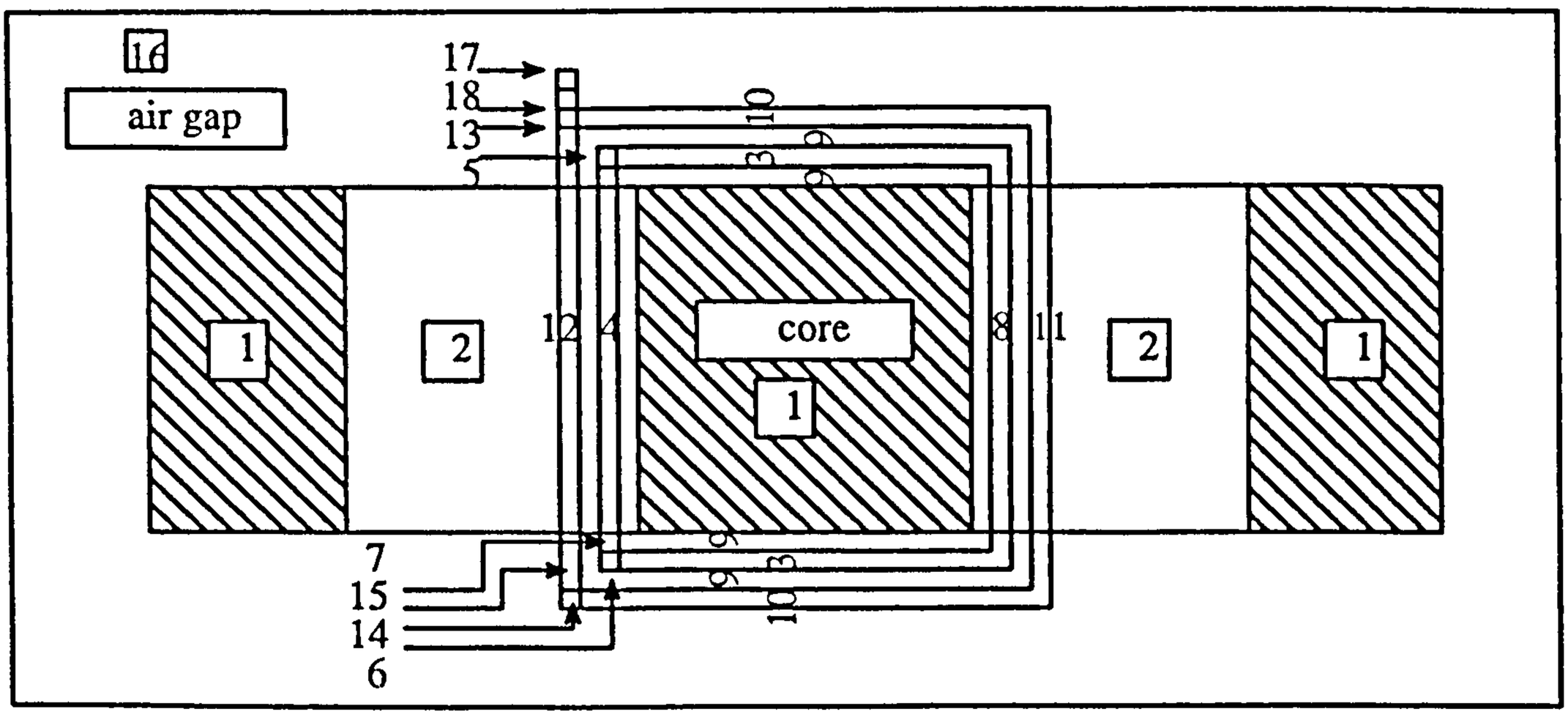

1 2 3 4 5 6 7 8 9 10 11 12 13 14 15 16 17 18	2D material NO.
2 2 2 2 2 2 2 2 2 2 2 2 2 2 2 2 2 2	Core
1 1 2 1 3 2 2 1 2 2 1 1 2 2 2 2 2 2	Air–gap between core & winding
1 2 2 2 3 2 2 2 2 2 2 2 2 2 2 2 2 2	Windings
1 2 3 2 3 3 2 3 2 4 4 2 4 4 2 2 4 4	
1 2 2 2 2 3 2 2 2 2 2 2 2 4 2 2 4 2	
1 2 2 3 3 3 3 2 2 2 2 4 4 4 4 2 4 2	

FIG. (4-1) : Diagram to Form 3D with single wire of both primary and secondary windings mesh from 2D mesh

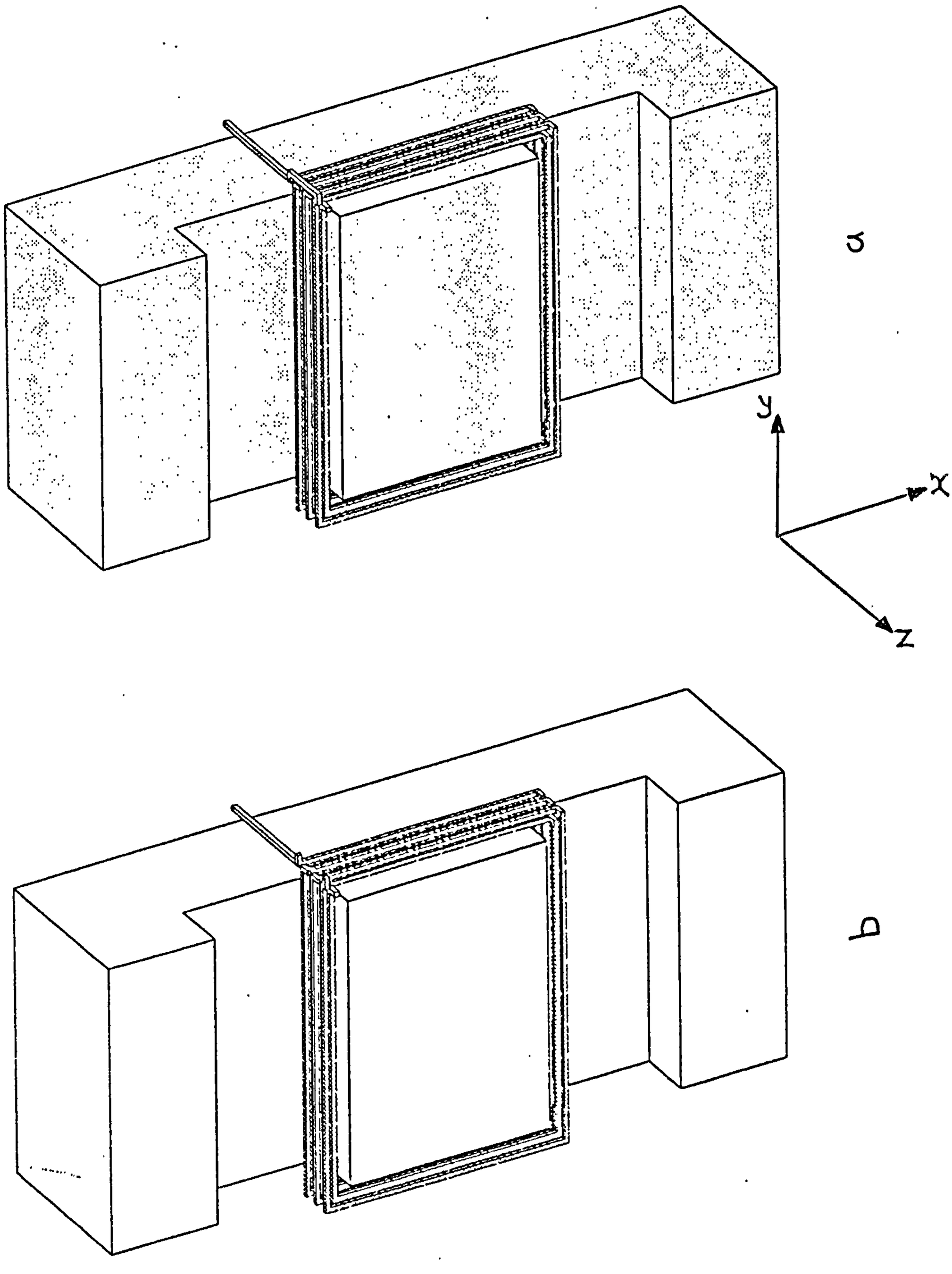

Fig.(4.2) : 3D Finite Element mesh a:- Short circuit b:- Open circuit

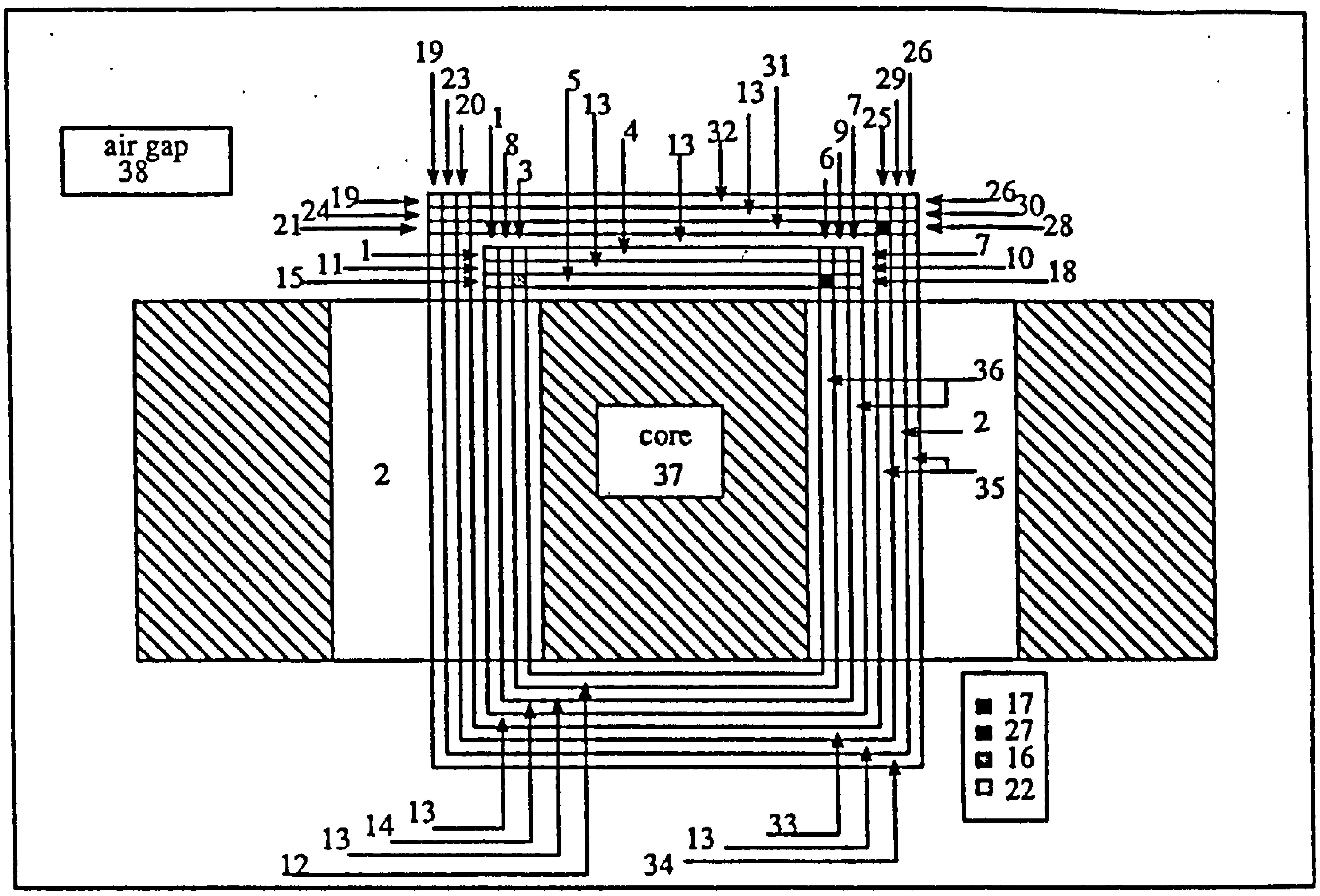

1	2	3	4	5	6	7	8	9	10	11	12	13	14	15	16	17	18	19	20	21	22	23	24	25	26	27	28	29	30	31	32	33	34	35	36	37	38
3	2	3	2	2	2	2	2	2	2	2	2	2	2	3	3	2	2	2	2	2	2	2	2	2	2	2	2	2	2	2	2	2	2	2	2	2	2
3	1	3	2	2	2	2	2	2	2	2	2	2	2	3	3	2	2	2	2	2	2	2	2	2	2	2	2	2	2	2	2	2	2	1	1	1	1
3	1	3	2	2	2	2	2	2	2	2	2	2	2	3	3	2	2	2	2	2	2	2	2	2	2	2	2	2	2	2	2	2	2	2	2	1	2
3	2	3	3	3	3	3	2	3	2	2	2	2	2	3	3	3	3	4	4	4	4	2	2	4	4	4	4	4	2	4	4	2	2	2	2	1	2
3	2	2	2	2	2	3	2	2	2	2	2	2	2	3	2	2	3	4	2	4	2	2	2	2	2	4	2	4	2	2	2	2	2	2	2	1	2
3	2	3	3	3	3	3	3	2	2	2	2	2	2	3	3	3	3	4	4	4	4	4	2	4	4	4	4	2	2	4	4	2	2	2	2	1	2
2	2	2	2	2	3	3	2	2	2	2	2	2	2	2	2	3	3	2	2	2	2	2	2	4	4	4	4	2	2	2	2	2	2	2	2	1	2
3	2	3	2	2	3	3	2	2	2	3	3	2	3	3	3	3	3	4	4	4	4	2	4	4	4	4	2	2	2	2	4	4	4	2	3	1	2
3	2	3	2	2	3	3	2	2	2	2	2	2	2	2	2	2	2	4	4	2	2	2	2	2	2	2	2	2	2	2	2	2	2	2	2	1	2
3	2	3	2	2	3	3	2	2	3	2	3	2	3	3	3	3	3	4	4	4	4	2	2	4	4	4	4	2	4	2	2	4	4	4	3	1	2

Fig.(4.3) : Diagram and Table of 3D, four fine wires FE Transformer model

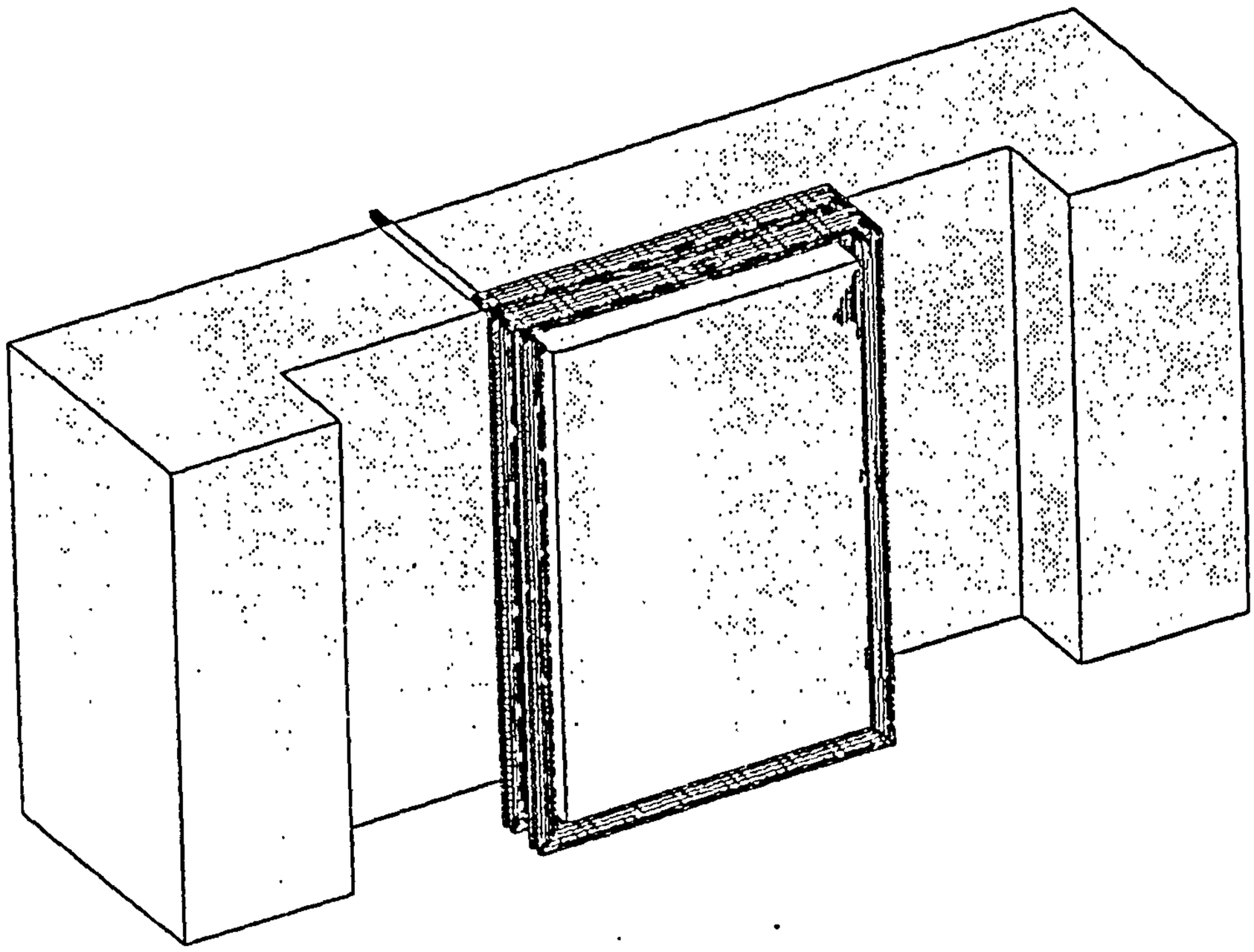

Fig.(4.4) : 3D transformer model with four fine wires

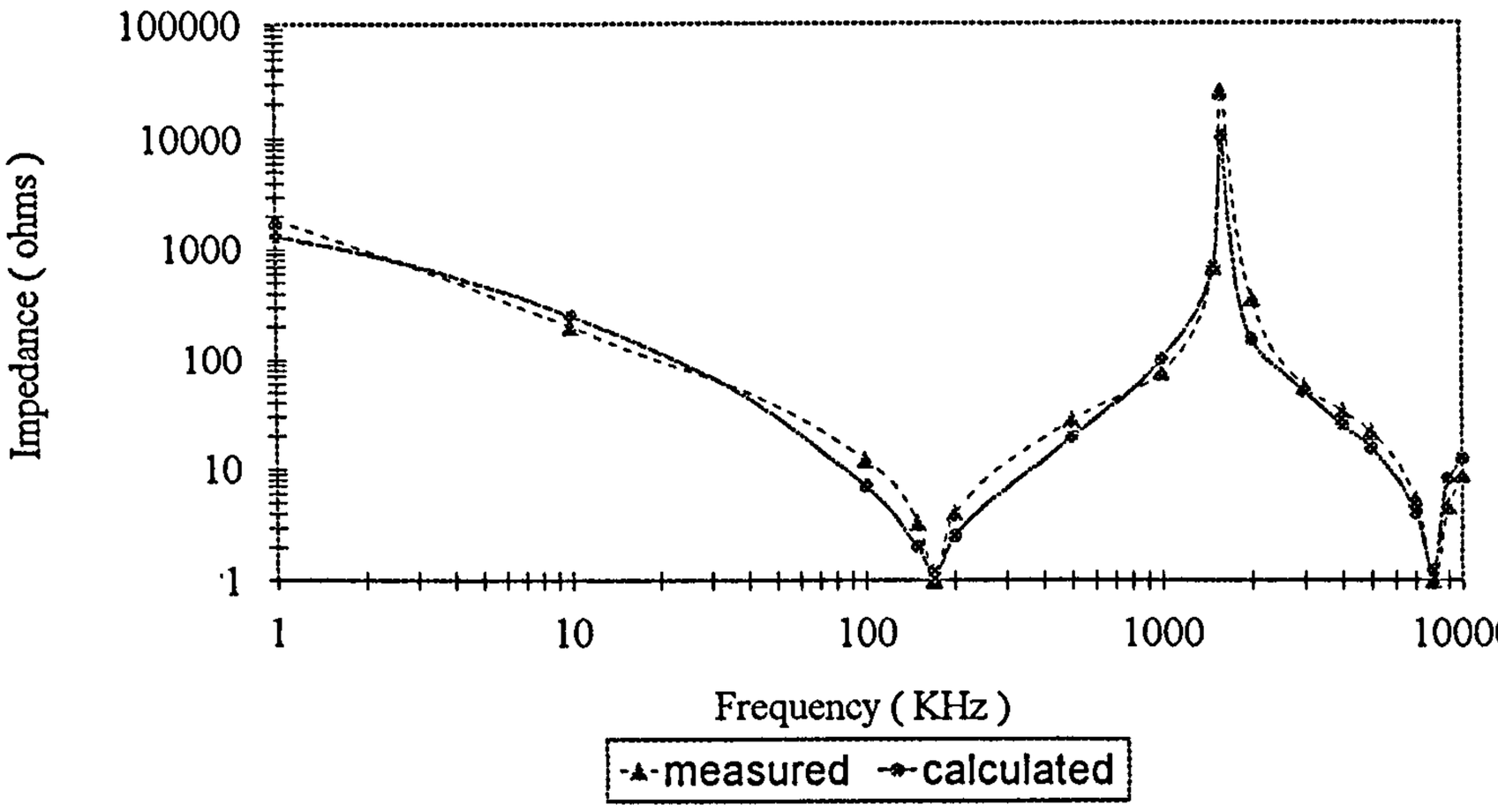

Fig. (4.5) : Impedance Frequency Responce of the example model

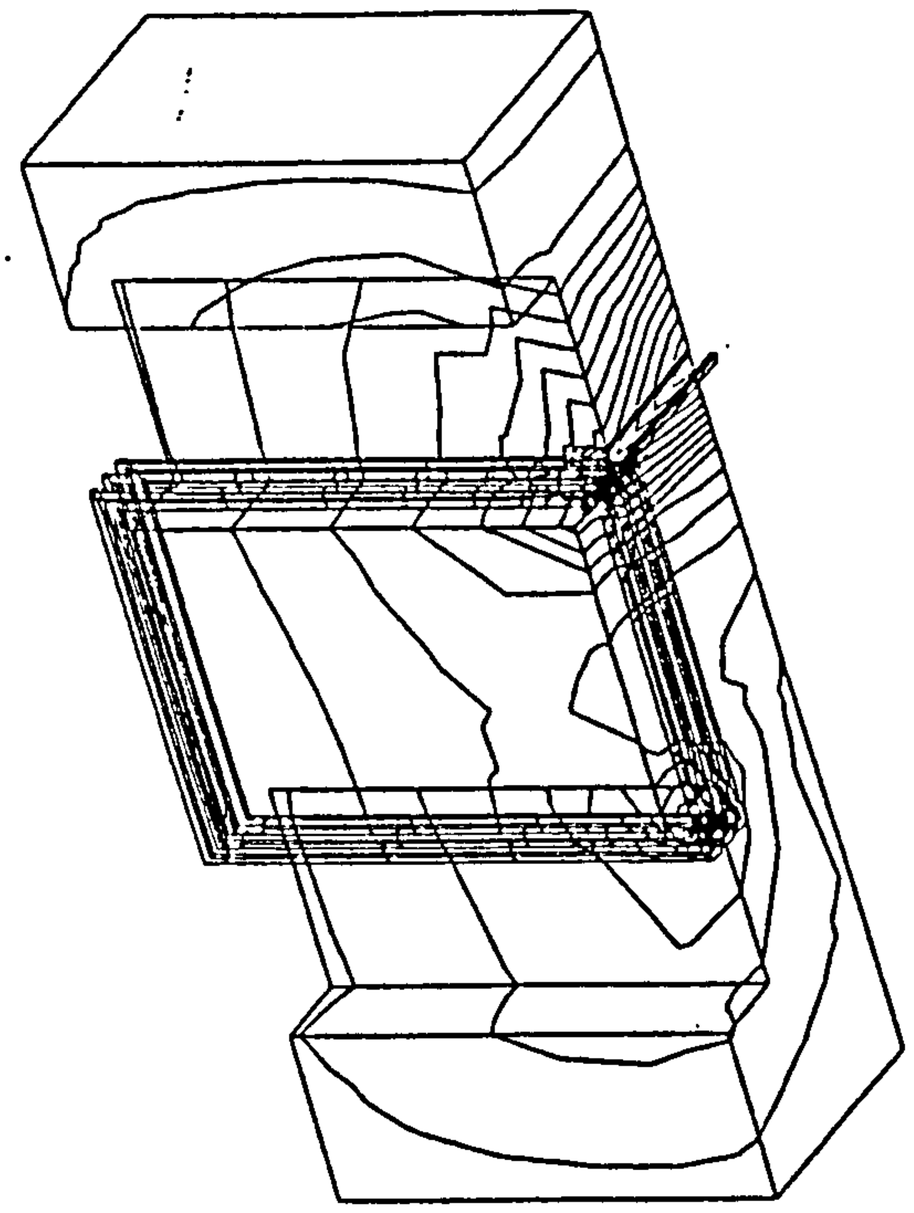

$A_{z\,(imag)}$ 1.0 MHz (Open Circuit)

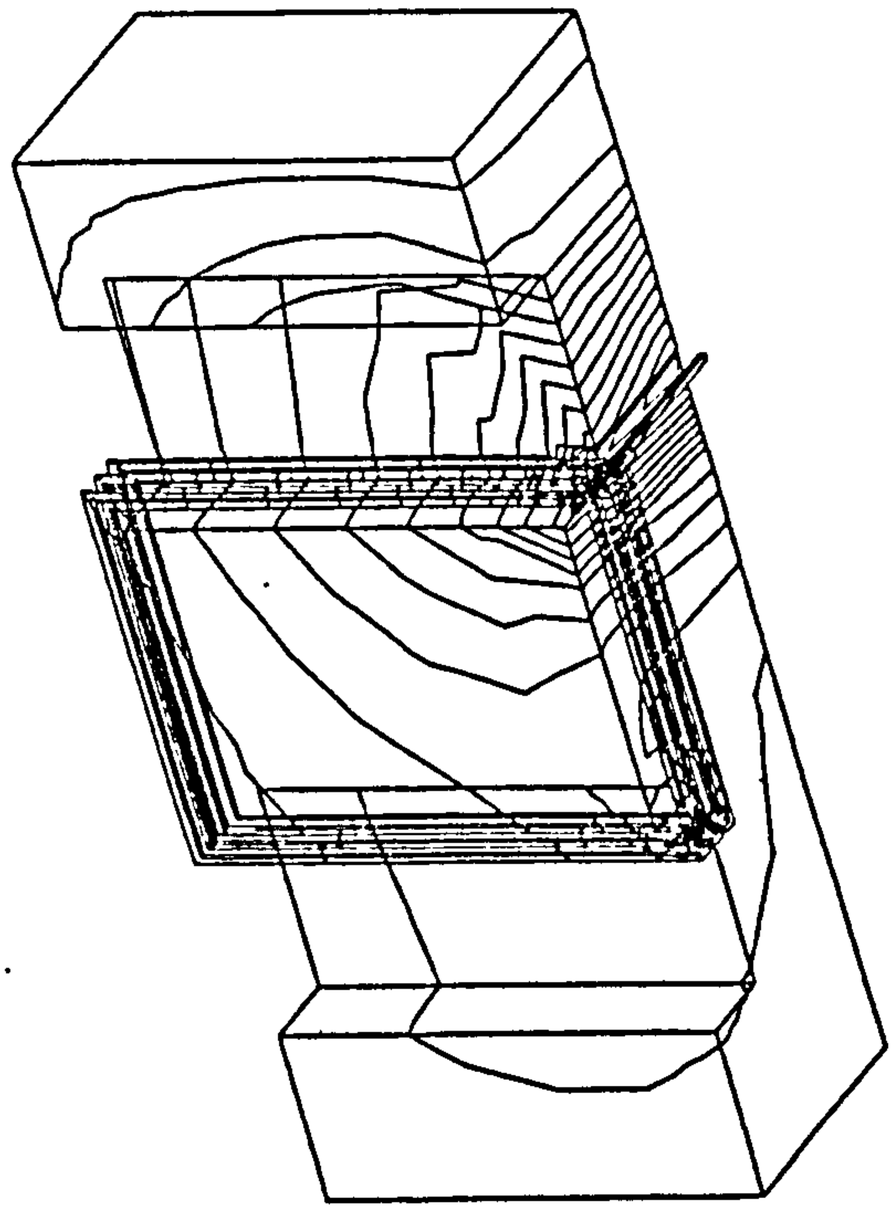

$A_{z\,(real)}$ 1.0 MHz (Open Circuit)

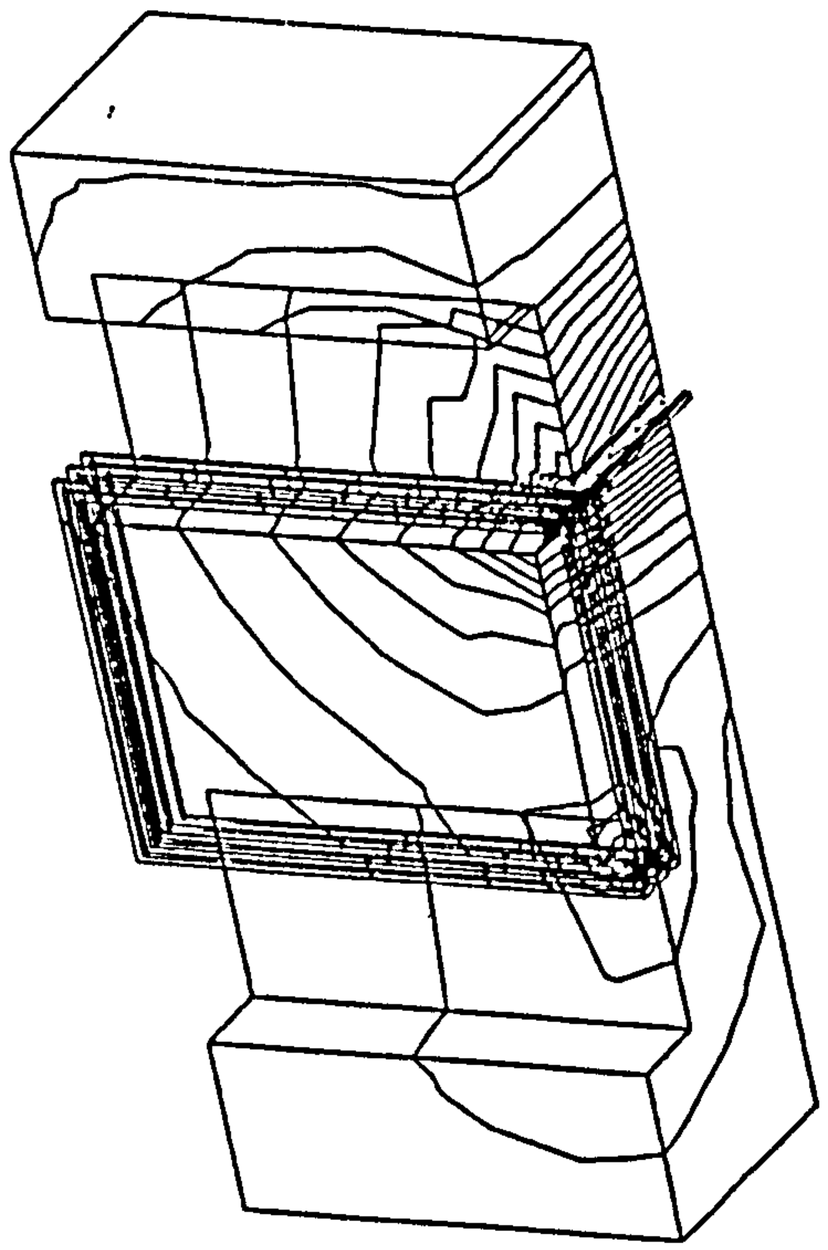

$A_{z\,(real)}$ 1.5 MHz (Open Circuit)

Fig.(4.6): Electromagnetic field distributions at different frequency components (Open Circuit) a and b

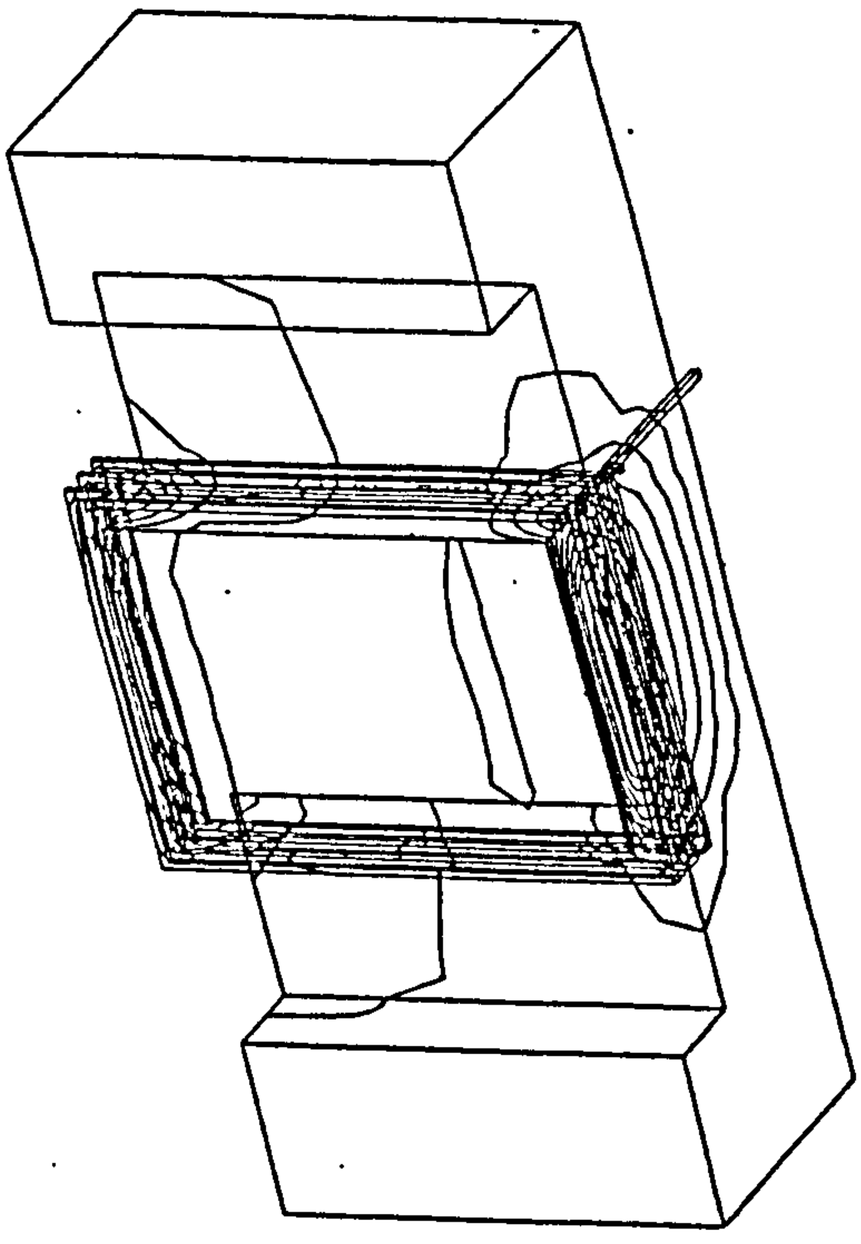

$A_{x\,(real)}$ 1.5 MHz (Open Circuit)

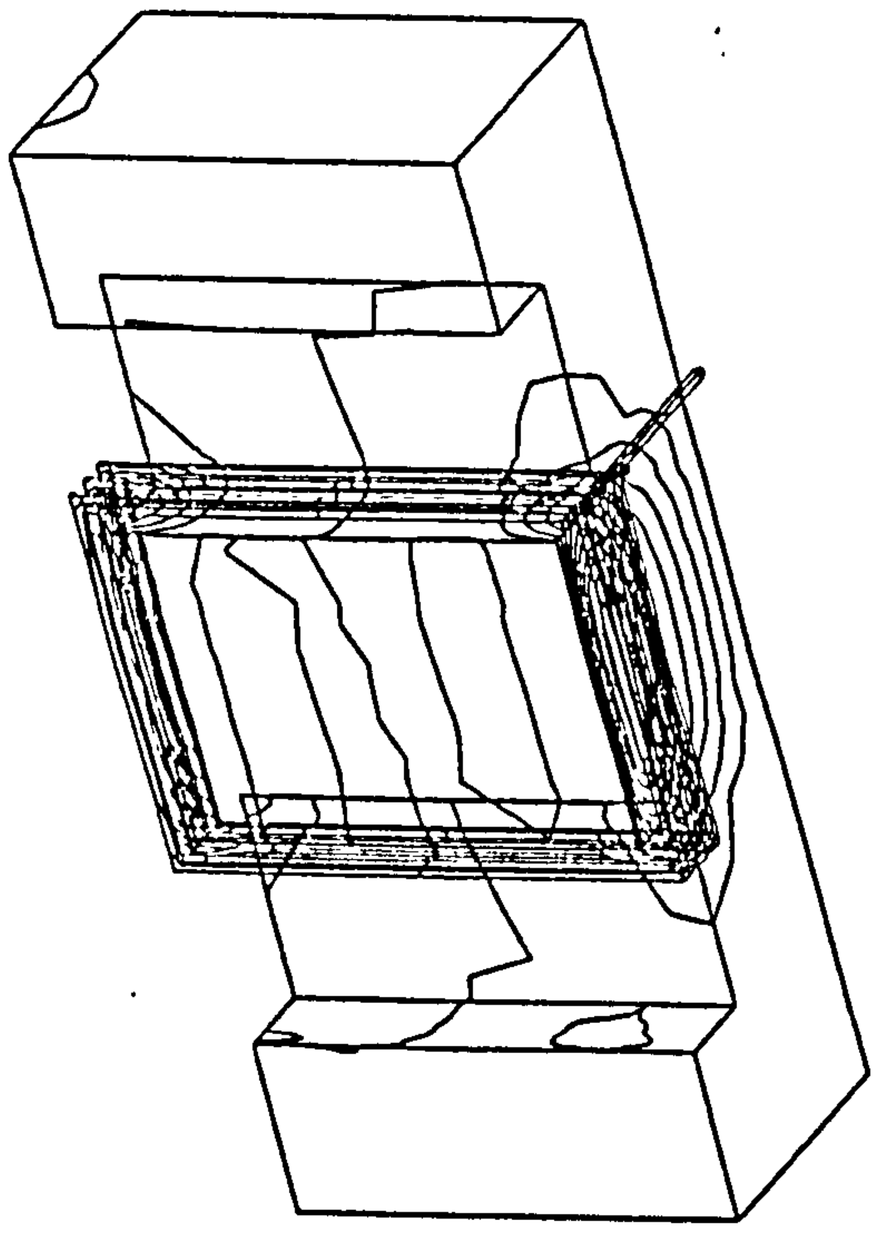

$A_{x\,(real)}$ 1.0 MHz (Open Circuit)

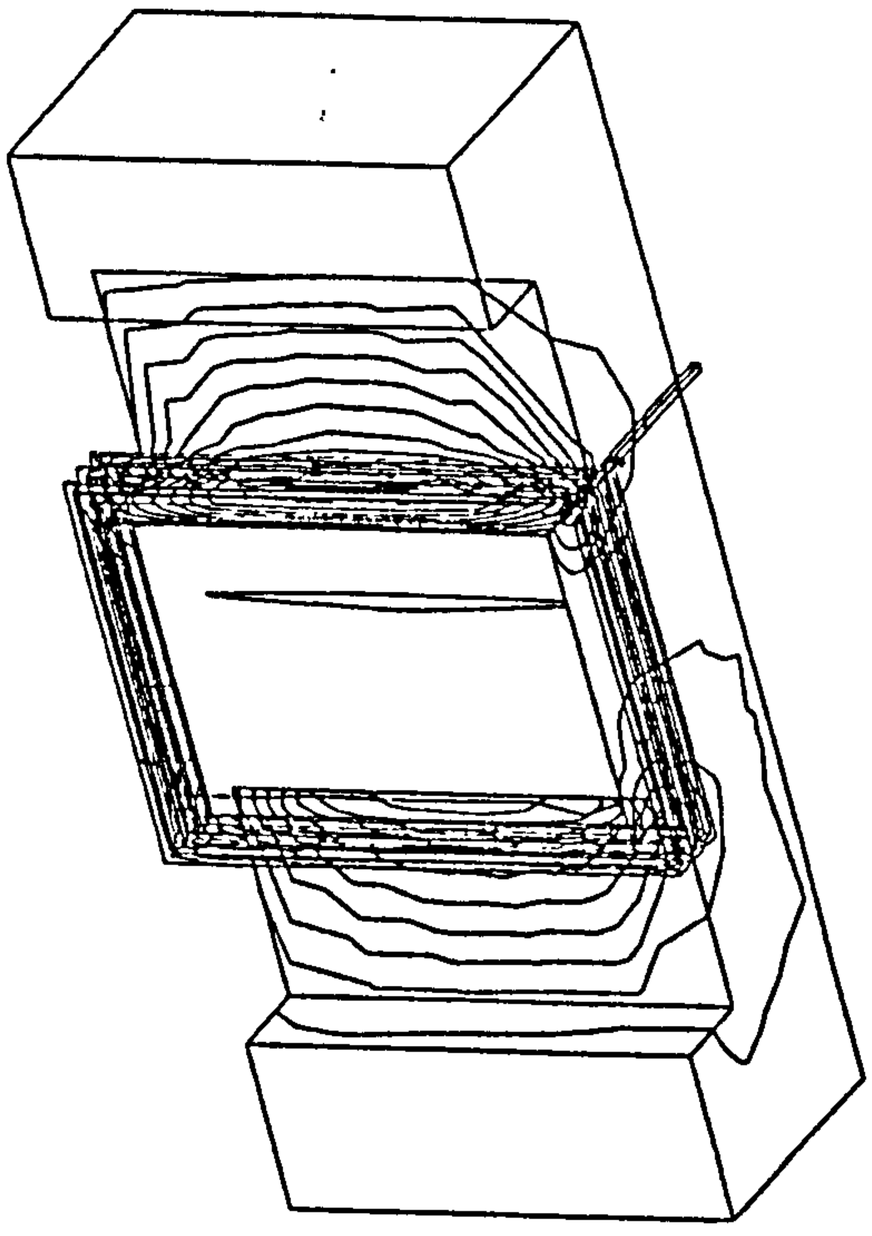

$A_{y\,(real)}$ 1.5 MHz (Open Circuit)

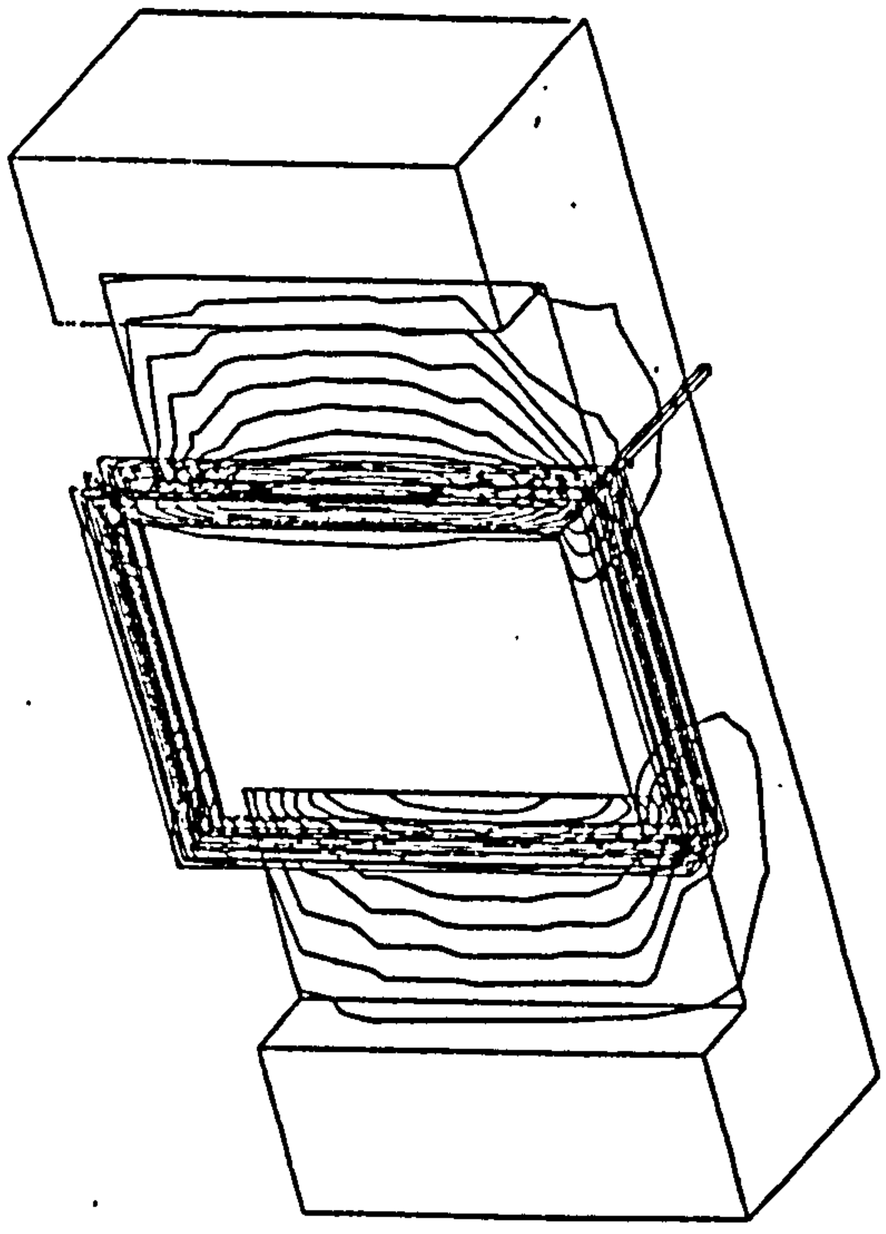

$A_{y\,(real)}$ 1.0 MHz (Open Circuit)

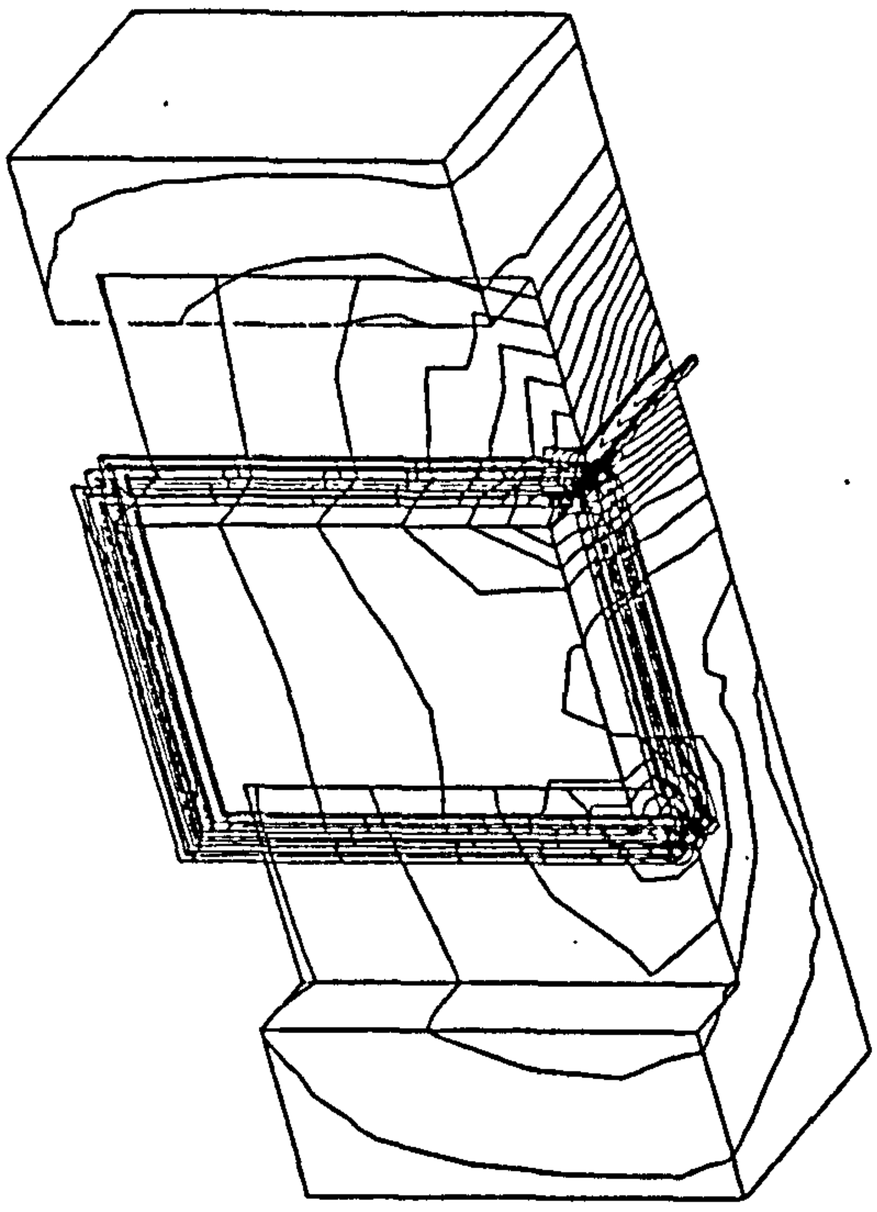

$A_{z\,(imag.)}$ 1.0 MHz (Short Circuit)

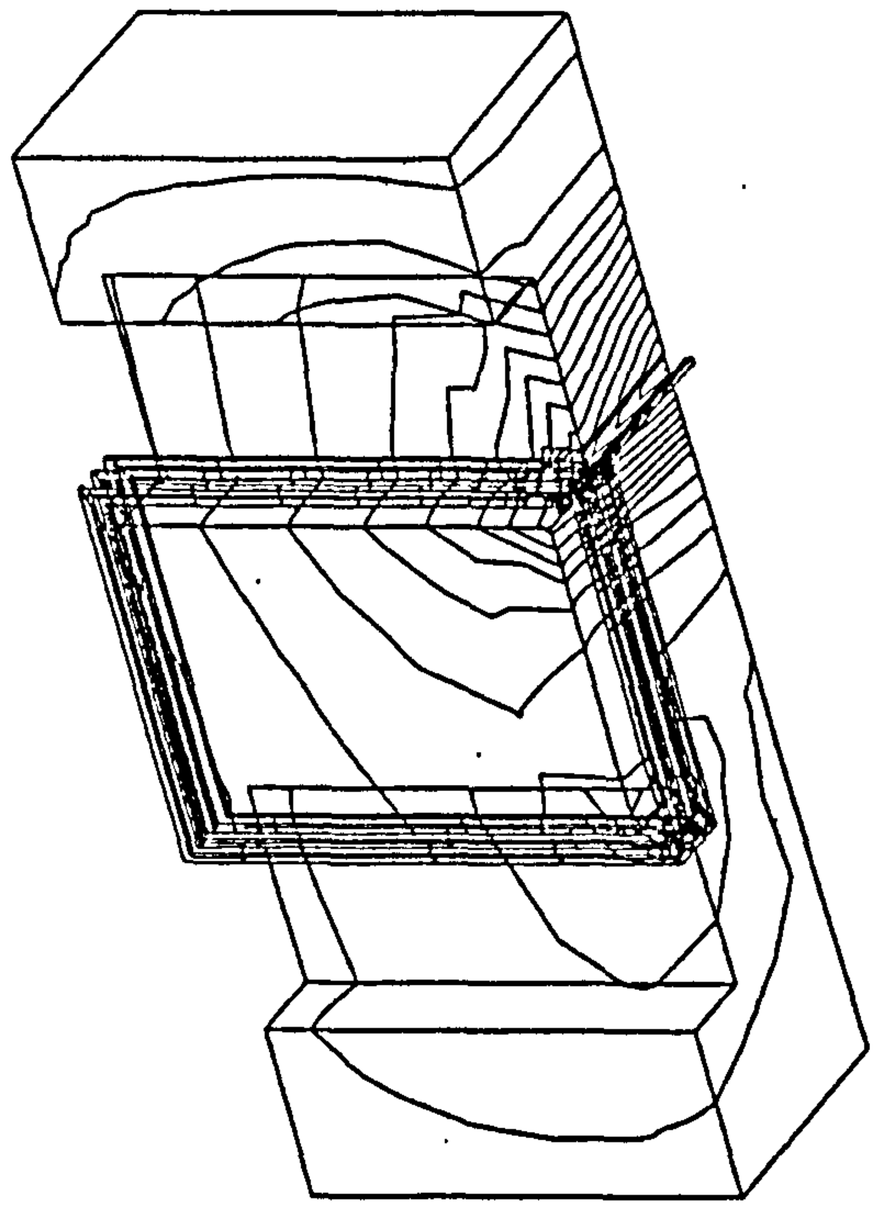

$A_{z\,(real)}$ 1.0 MHz (Short Circuit)

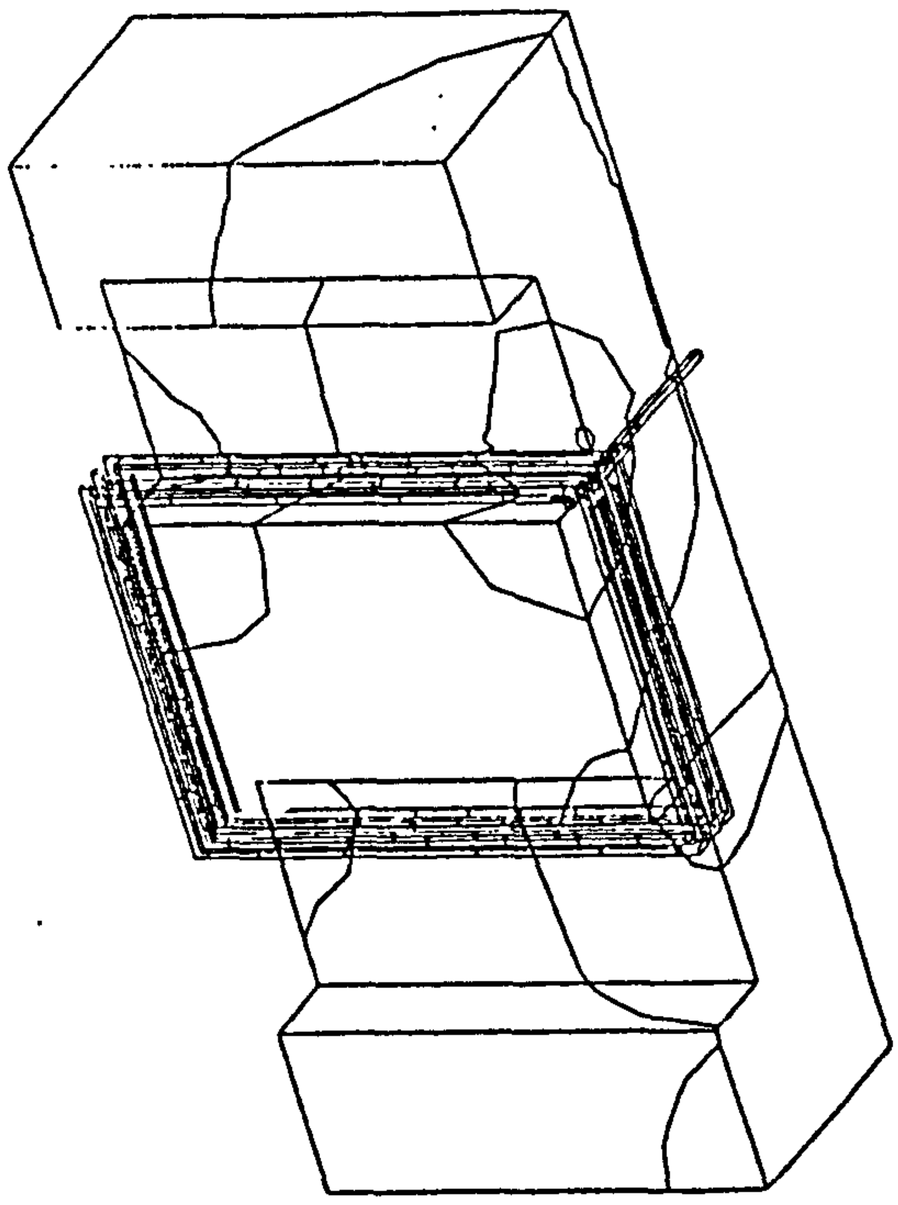

$V_{imag.}$ 1.0 MHz (Short Circuit)

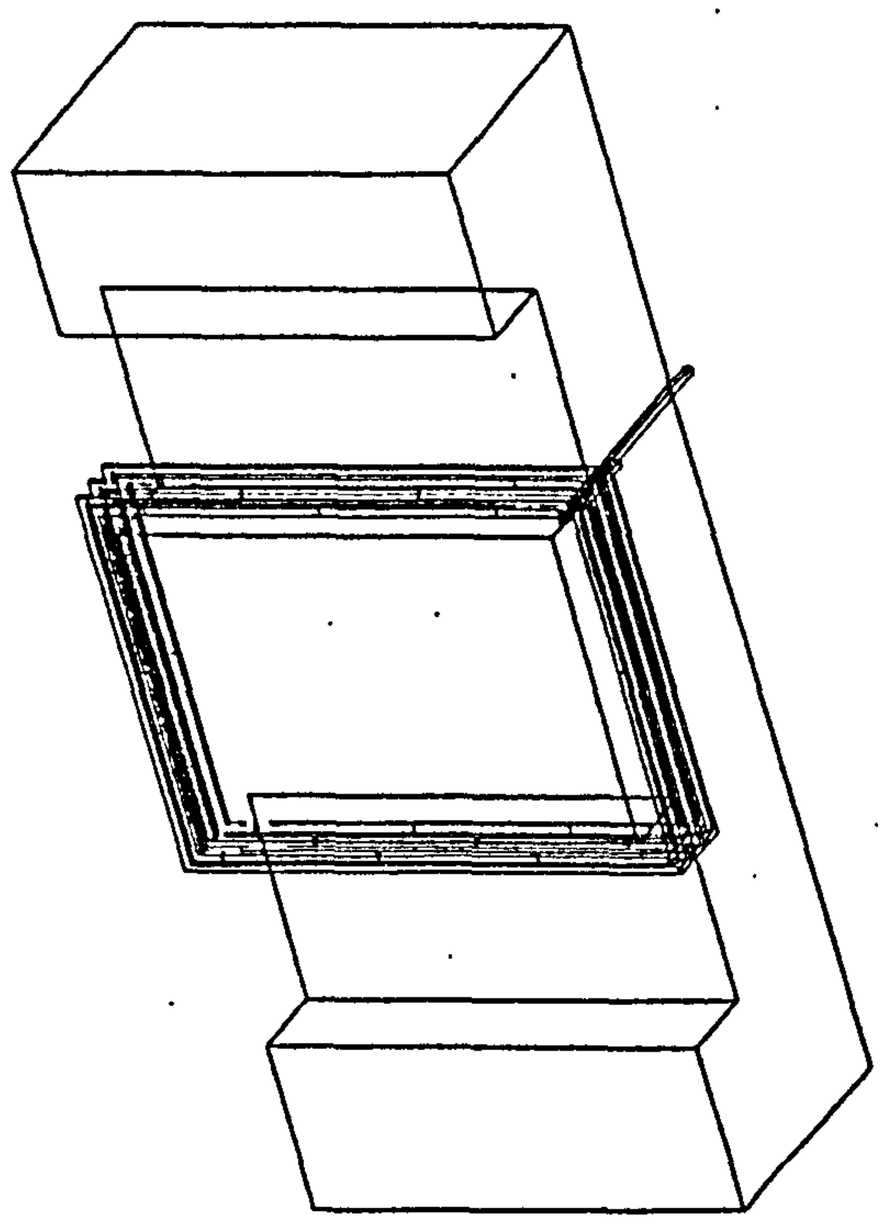

V_{real} 1.0 MHz (Short Circuit)

Fig.(4.7): Electromagnetic field distributions at different frequency components (Short Circuit)

a, b and c

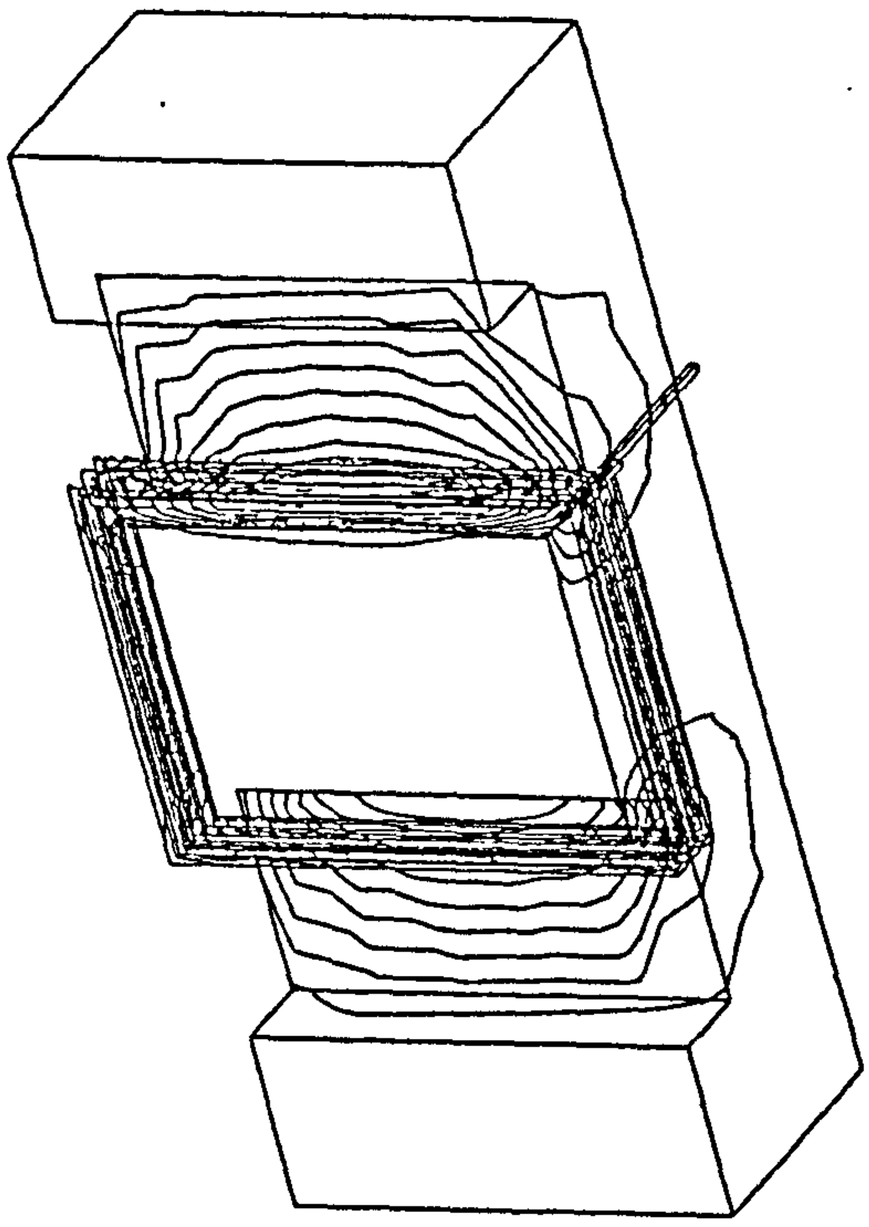

$A_{y\ (imag.)}$ 1.0 MHz (Short Circuit)

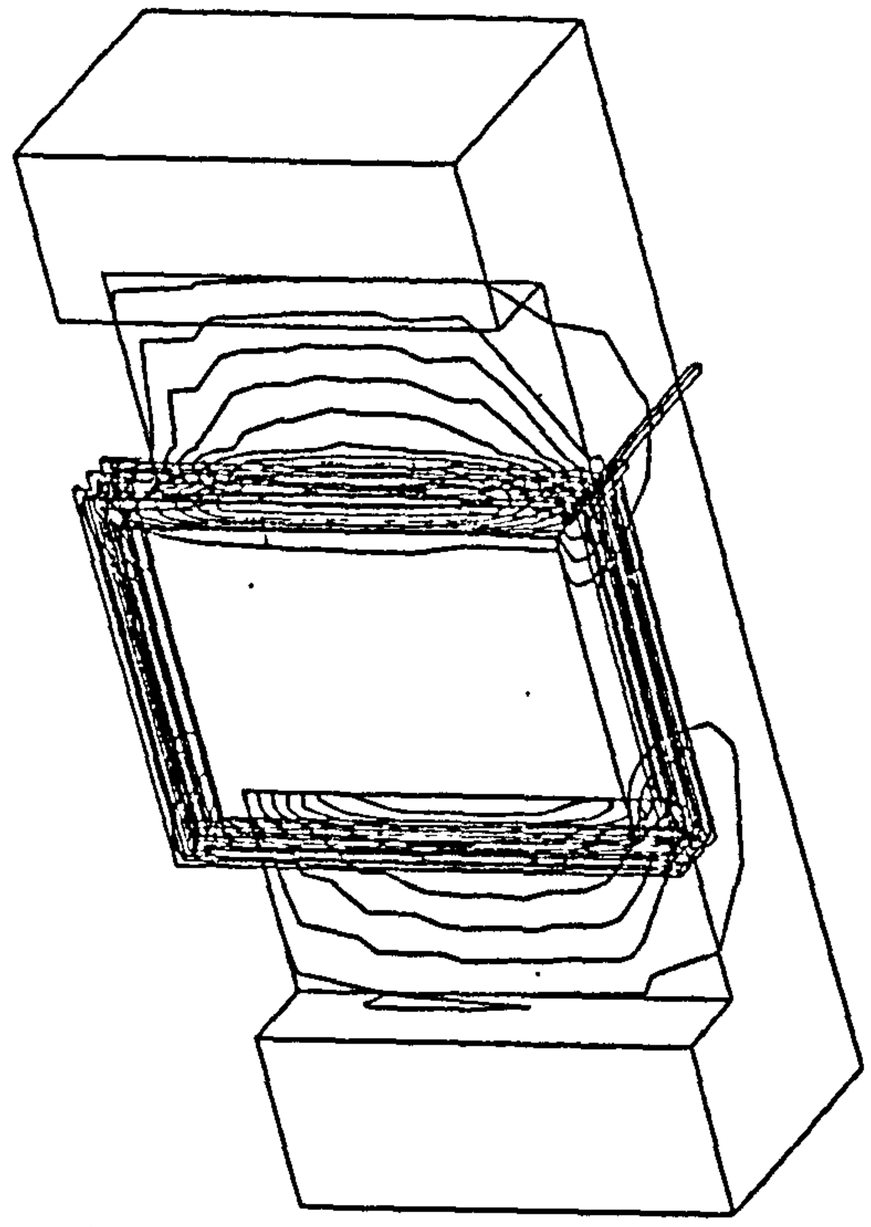

$A_{y\ (real)}$ 1.0 MHz (Short Circuit)

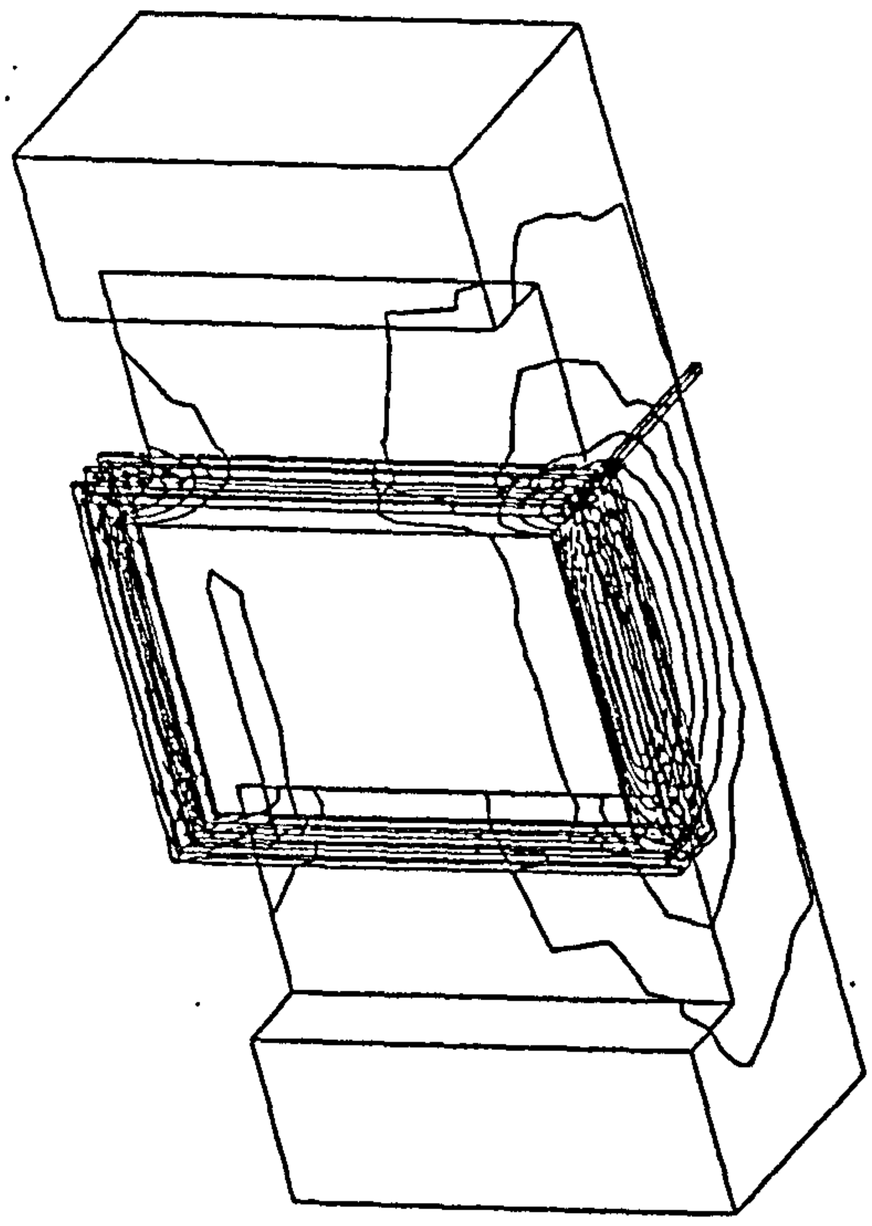

$A_{x\ (imag\ )}$ 1.0 MHz (Short Circuit)

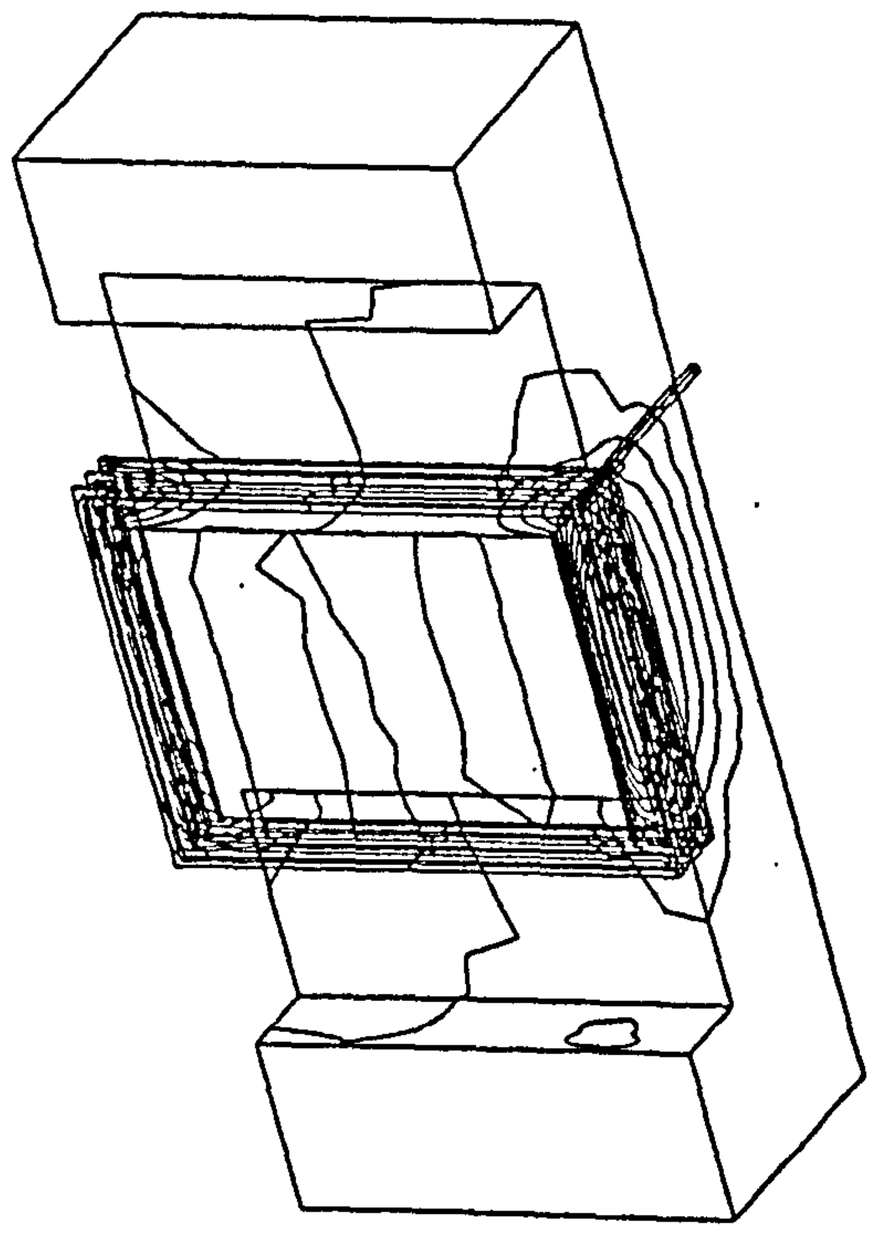

$A_{x\ (real)}$ 1.0 MHz (Short Circuit)

b

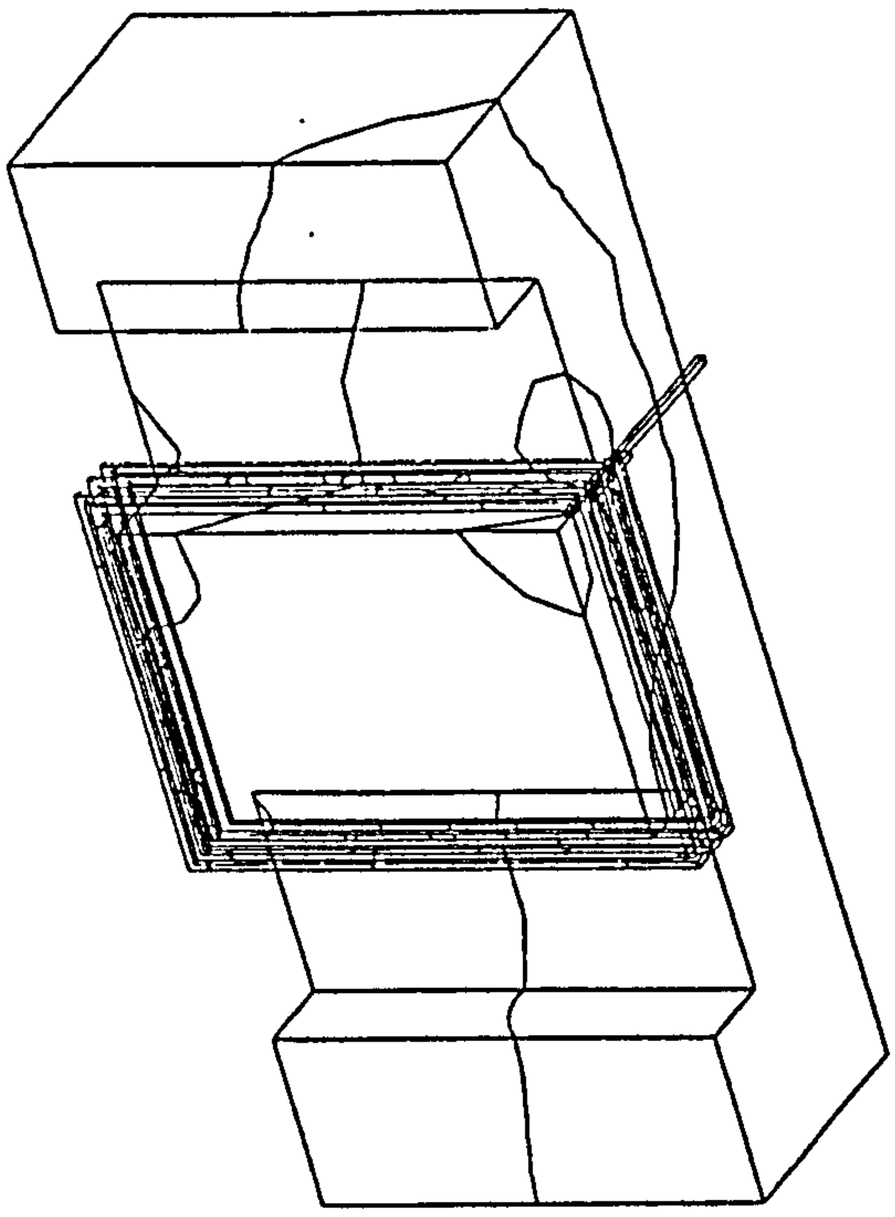

$V_{imag.}$ 2.0 MHz (Short Circuit)

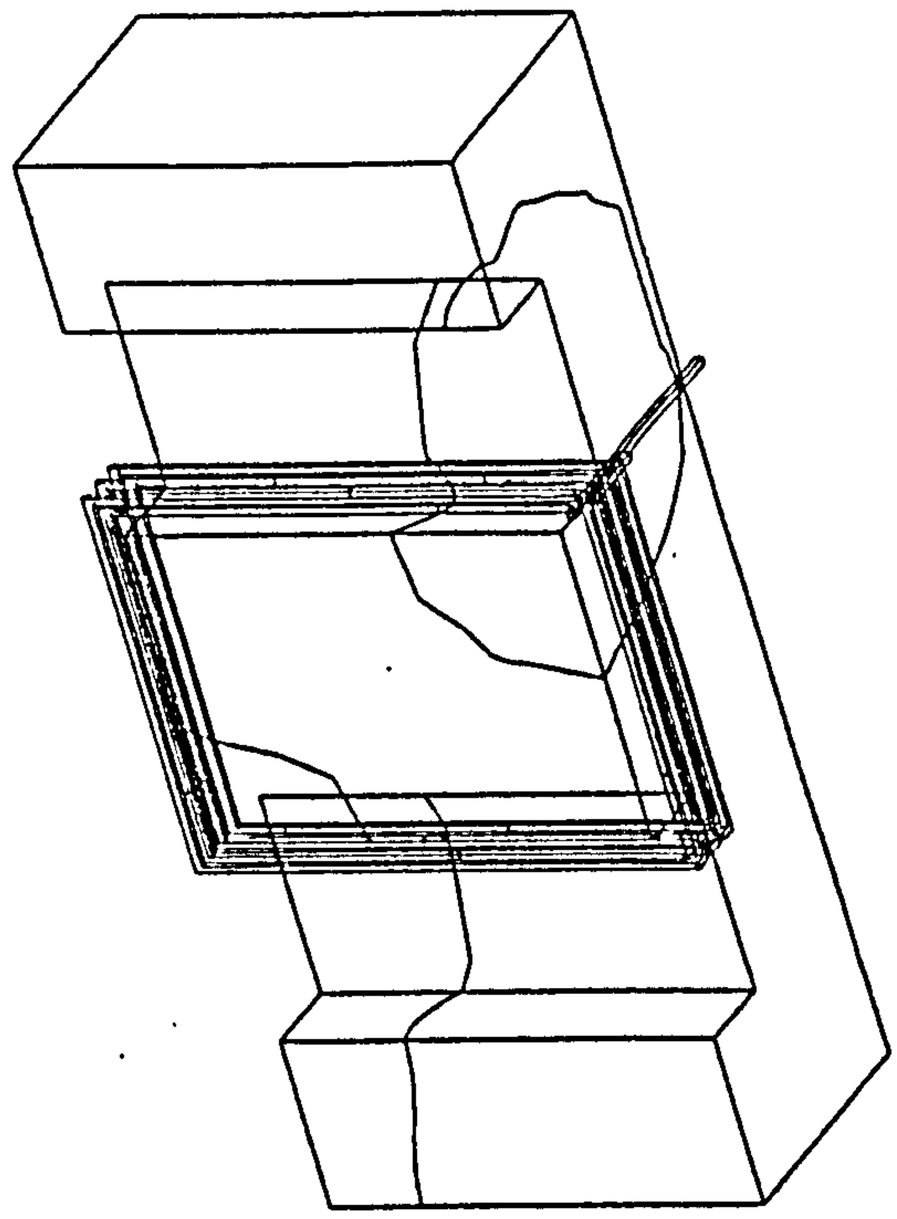

V_{real} 2.0 MHz (Short Circuit)

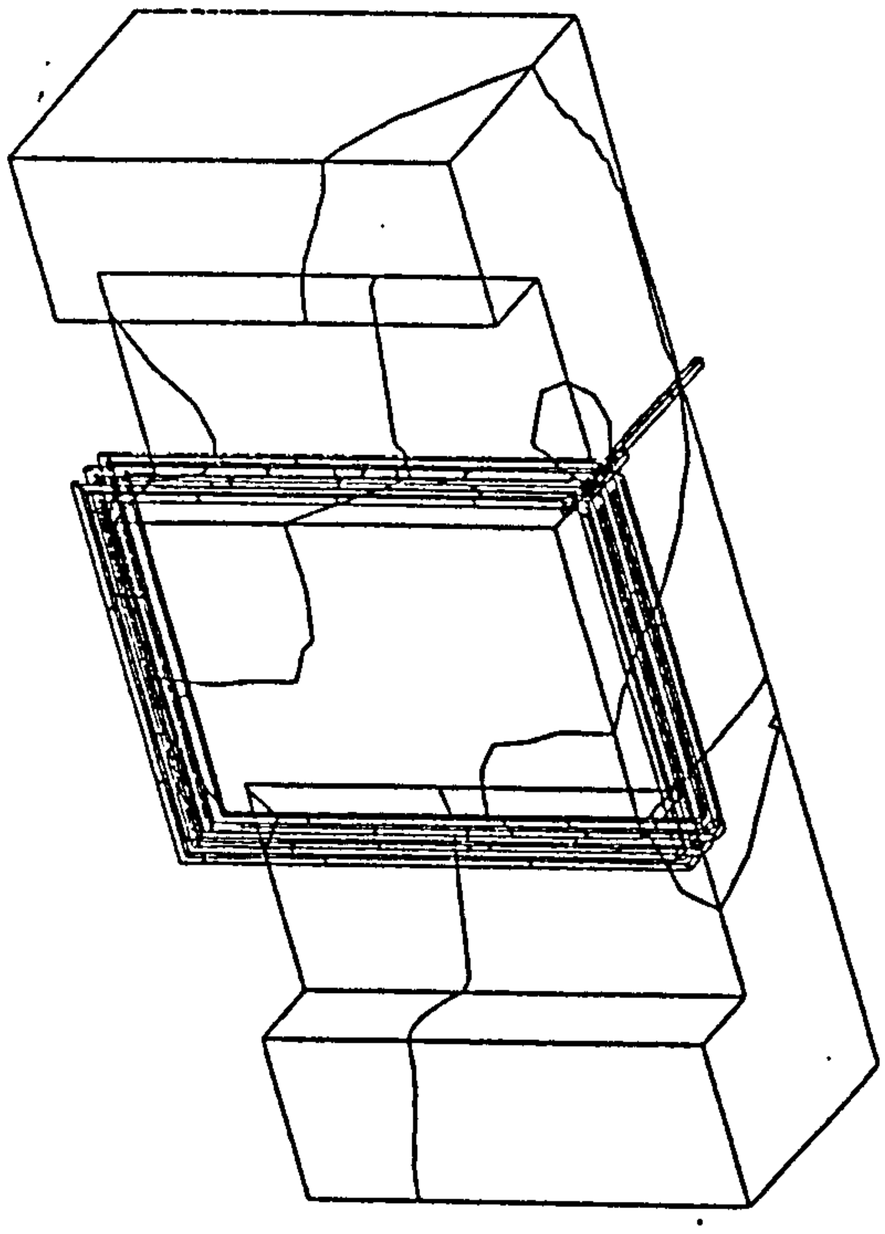

$V_{imag.}$ 1.5 MHz (Short Circuit)

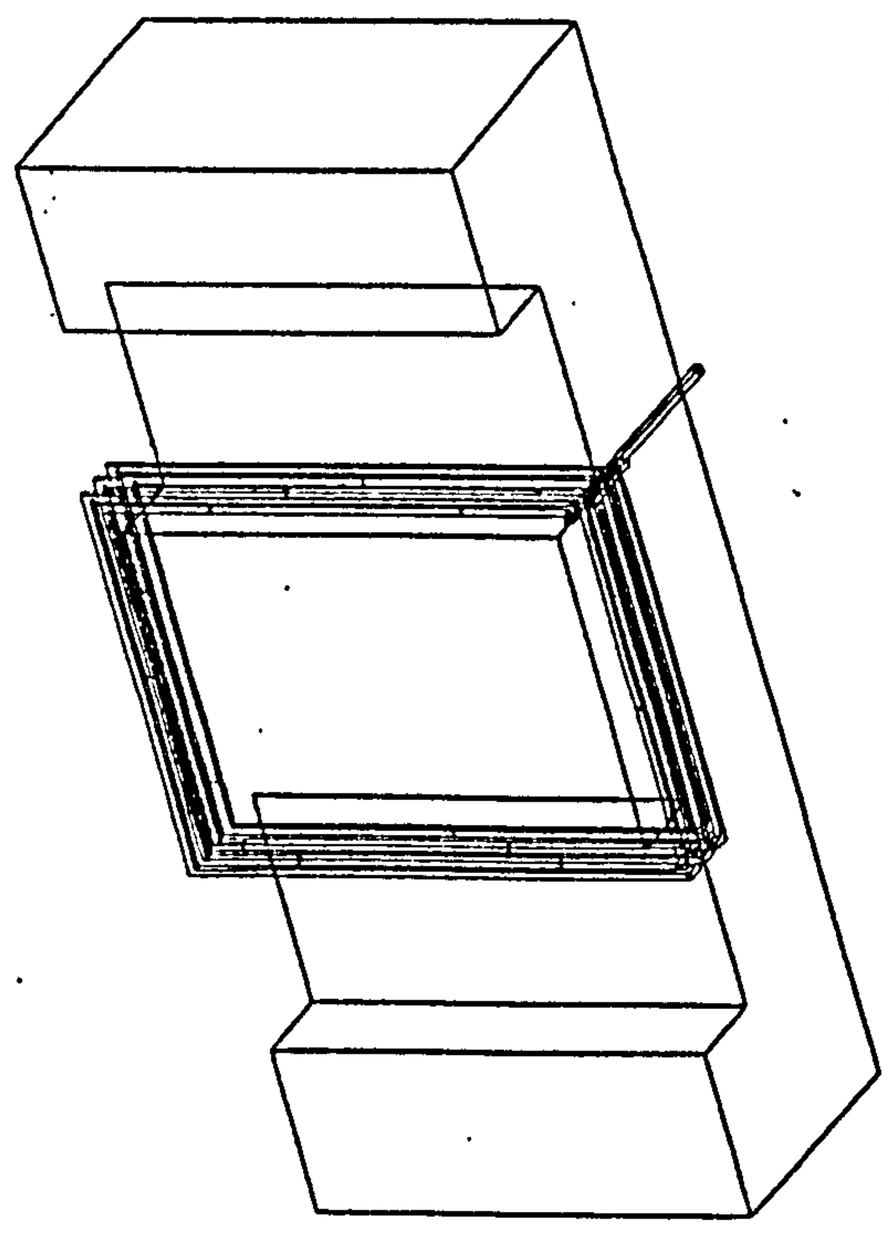

V_{real} 1.5 MHz (Short Circuit)

C

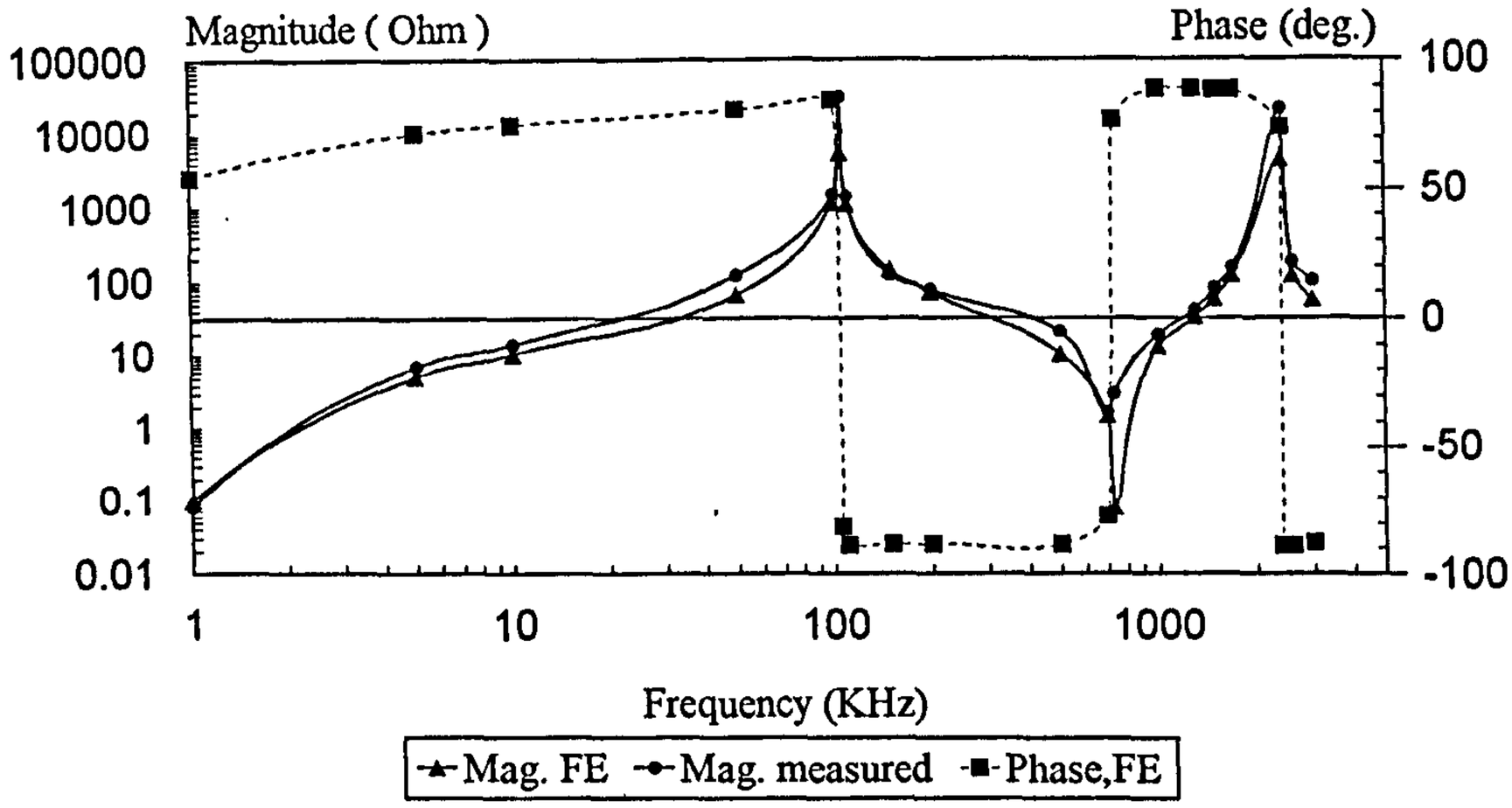

Fig.(4.8) : Open circuit impedance calculated using 3D FE model

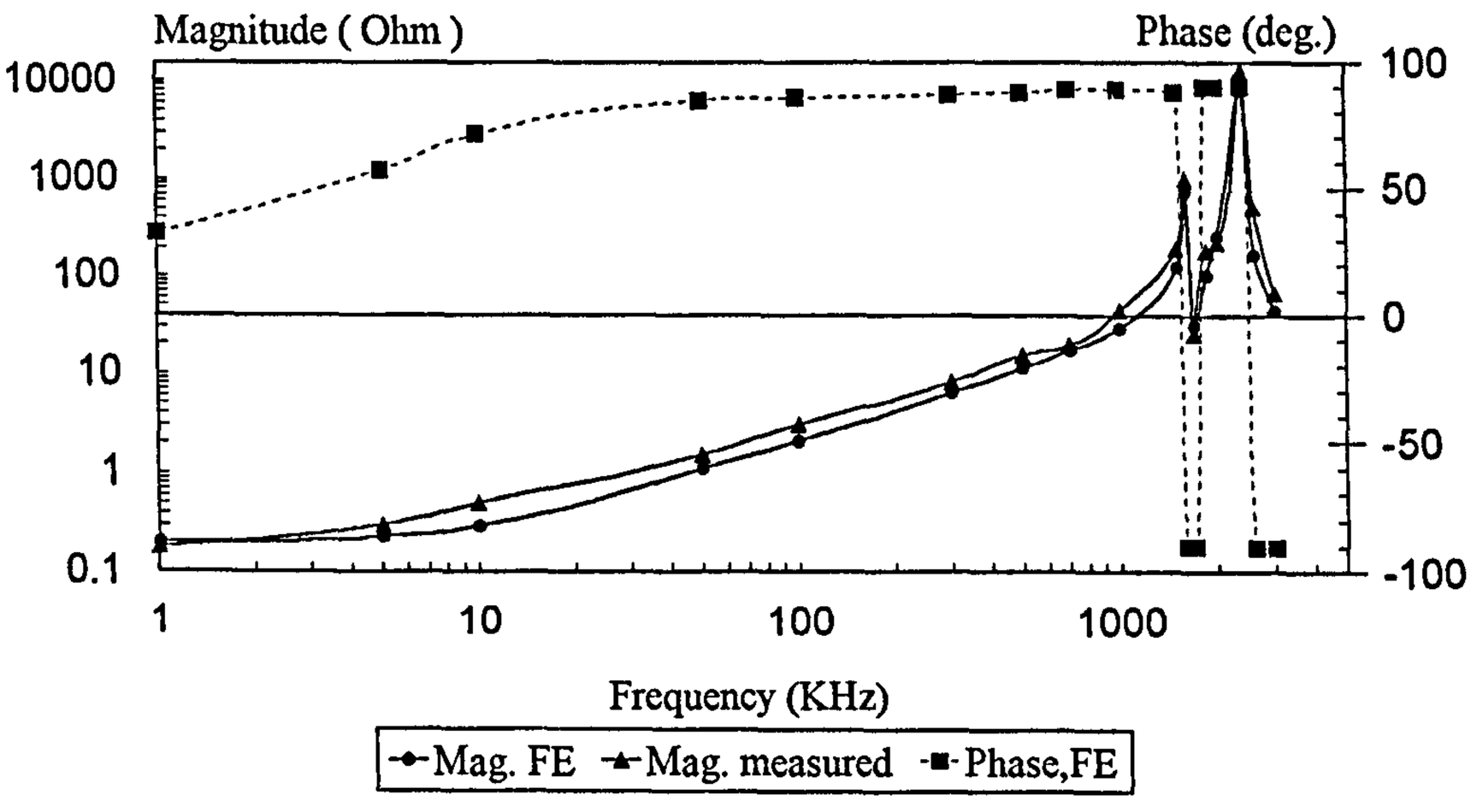

Fig.(4.9) : Short circuit impedance calculated using 3D FE model

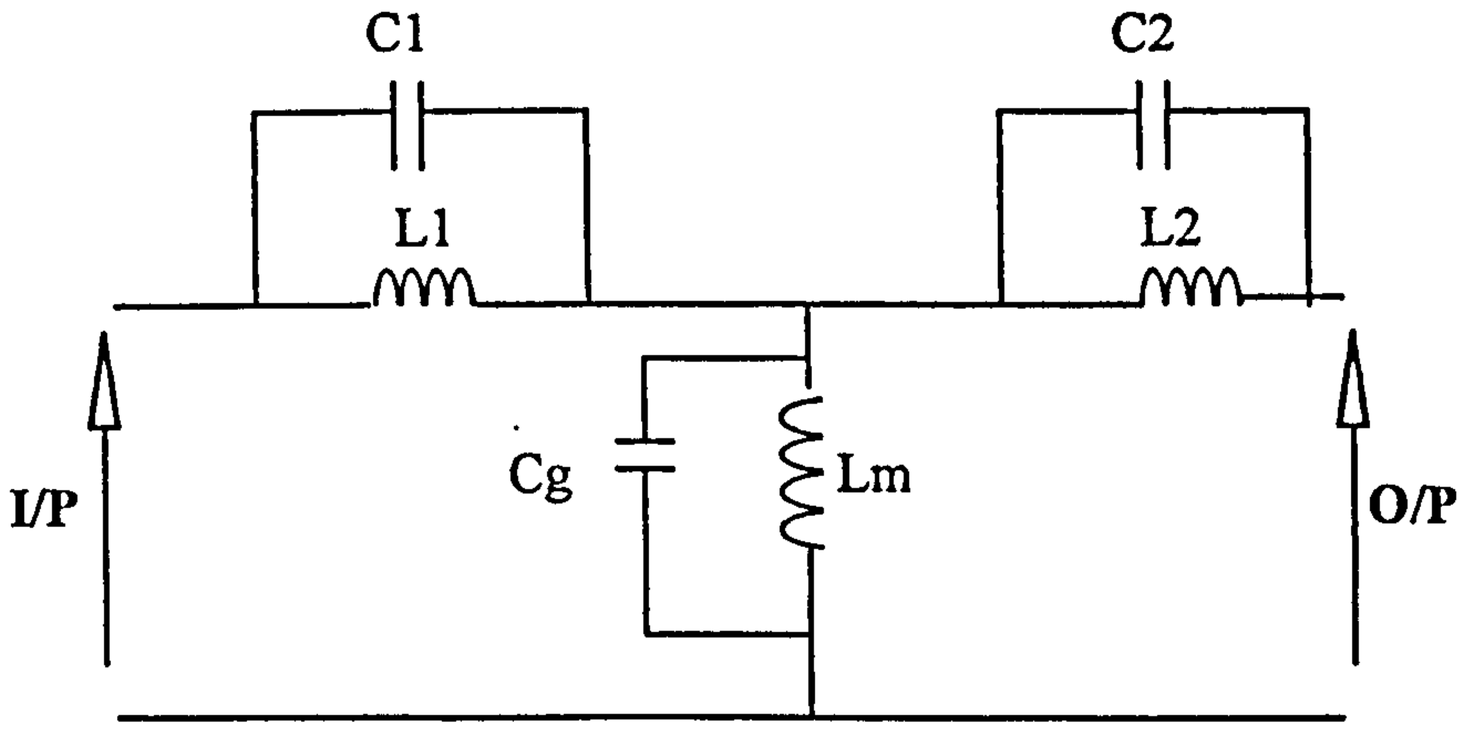

Fig.(4.10): Simplified transformer equivalent circuit

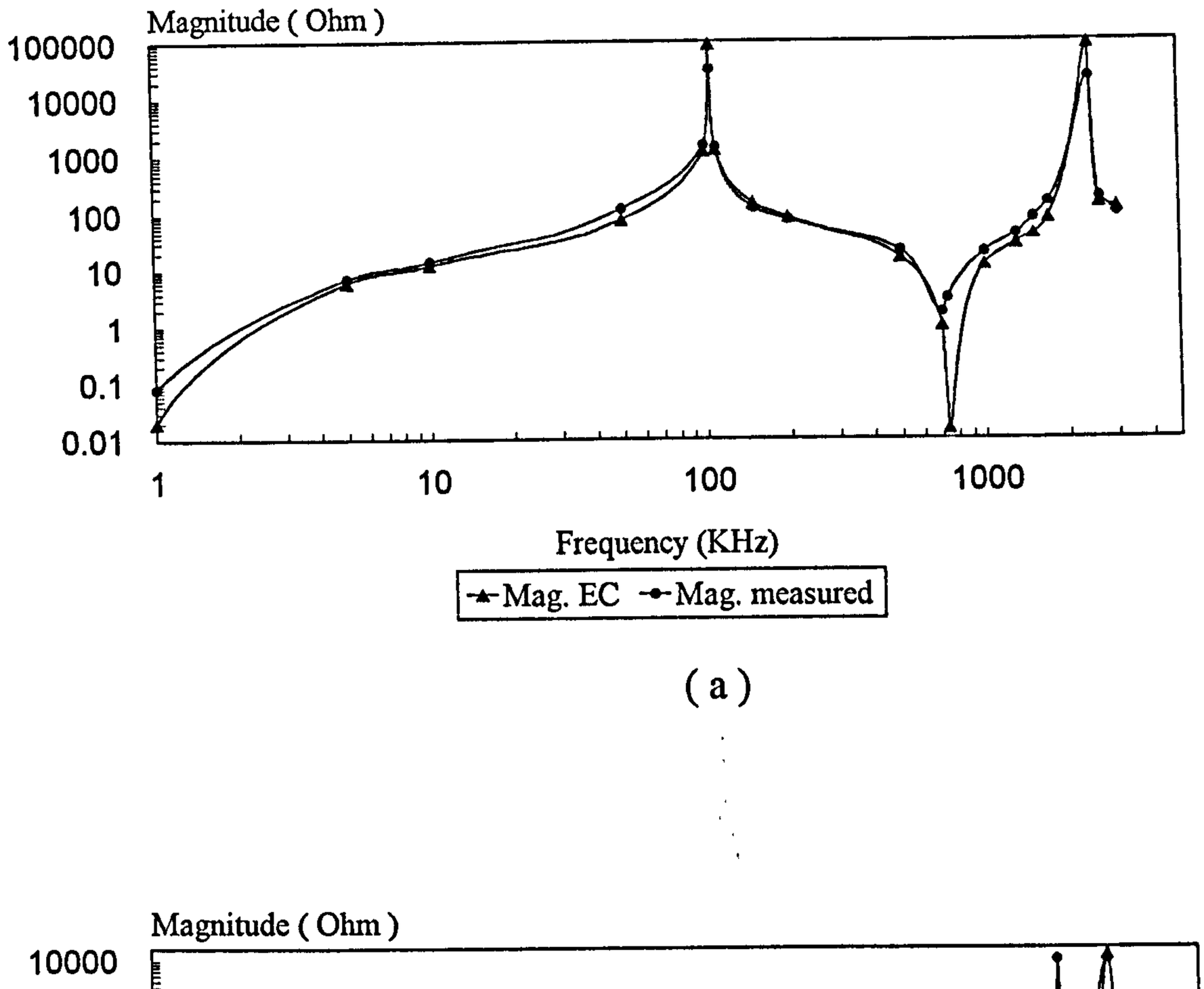

(a)

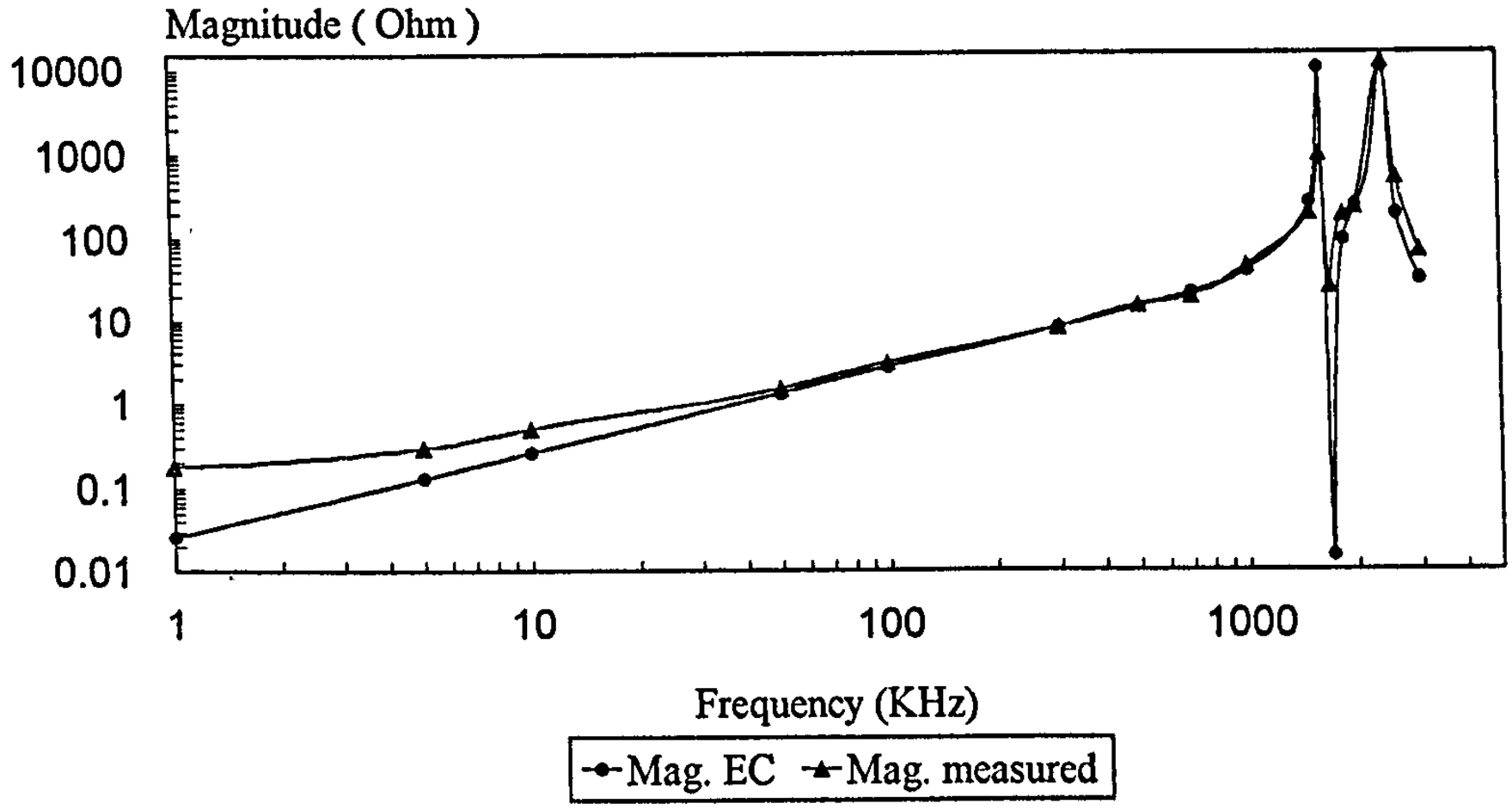

(b)

Fig.(4.11) : Impedance frequency response calculated from the smplified equivalent circuit. (a) : open circuit, (b) : short circuit

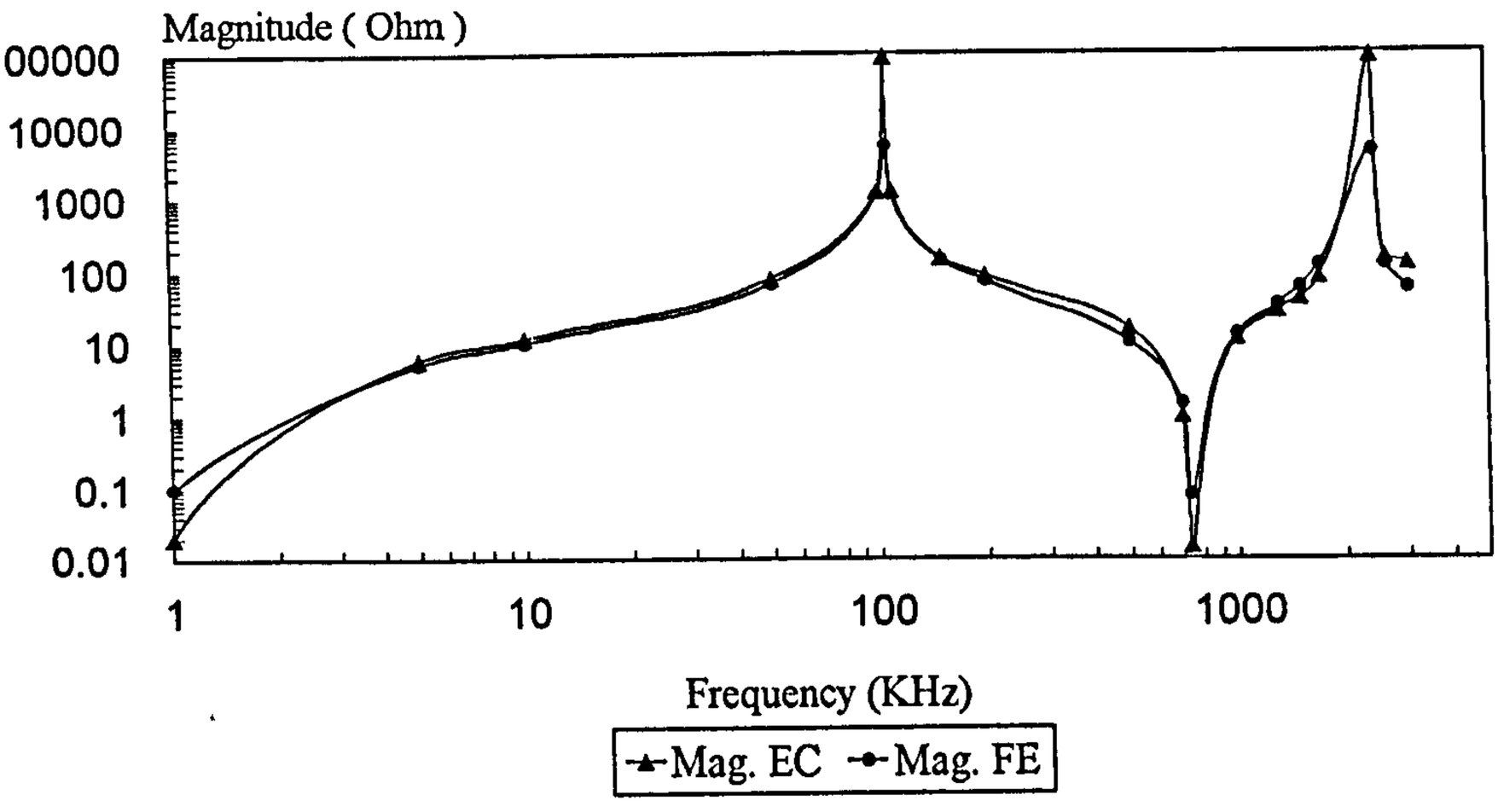

(a)

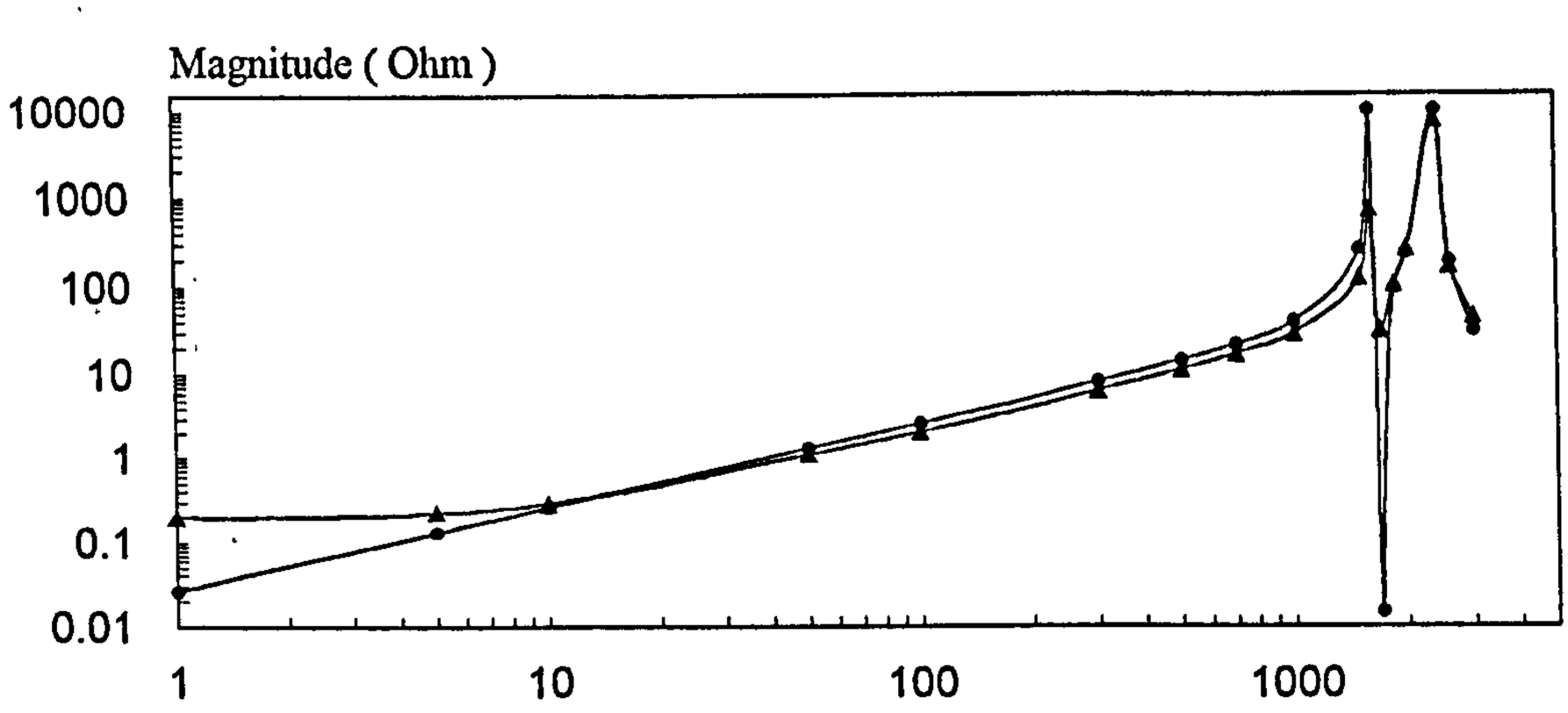

(b)

Fig.(4.12) : Impedance frequency response calculated from the smplified equivalent circuit compared with FE (a) : open circuit, (b) : short circuit

CHAPTER FIVE

PARAMETERS ESTIMATION AND WINDING NETWORK ANALYSIS

5.1 : INTRODUCTION.

The previous chapter has shown that good results can be obtained using a 3D, full electromagnetic, finite element model, but it is also clear that this is a very difficult task for even the few turn model attempted. The resulting model is also very unwieldy in use and it certainly could not be considered as a rapid turm around design tool. Yet, it is clear that the true nature of the distributed capacitance and inductance must be captured if reasonable high frequency models are required.

Finite element models can be seen as equivalent circuit models with the circuit elements related to the product of the number of nodes and degrees of freedom at each node. In respect of terminal performance, the huge number of circuit elements represented by a full 3D electromagnetic finite element model can be distilled into far more compact form. An automatic method to distil the principle modes of the performance involves posing the problem in Eigen form, and it is even more difficult than a straight forward finite element solution.

This chapter aims to go partway to the full solution by identifying simplified per turn equivalent circuits and seeking to establish the parameters of these circuit using non-coupled electric and magnetic finite element models. By these means, it should be possible to obtain a sufficiently accurate model which is amenable to solution.

Later in this chapter, the development of what is known as a lumped circuit, in which the winding is represented by a circuit network model is considered. The way this model is analysed has also been explained and applied using a trapezoidal rule of integration to solve the main equation that contains the nodal conductance matrix [5]. The aim of this

chapter is to examine the effects due to the existence of different parts of capacitance within the transformer structure [9,35]. This effect can be identified from the voltage transient analysis at each node within the network [5,29,35,38]. The effect of these capacitances on the input winding impedance is also one of the chapter's concerns. Later in this chapter, attention is paid to check the possibility of using the same principle of the winding network representation to model the whole transformer.

5.2 : NETWORK PARAMETERS.

At the design stage, it is common practice for the transformer designer to represent the winding by an equivalent network, and this is used for the numerical calculation of the transient phenomena in the transformer winding [4,5,88]. The first requirement is to compute very accurately the R,L, and C elements of this network. These parameters were computed here using a 2D static field simplification of Maxwell's equations taking into account the third dimension by equivalent length, which is the turn mean length given by the core manufacturer's data sheet [51].

One of the main points which needs to be considered relates to the resistance calculation. When considering the static field, the resistance can be found either from the loss equation (magnetostatic solution) or using the closed form given later in this chapter. In both cases, the value of this resistance represents the dc component. If the values of the sections (nodes) inductances and resistances are related to the frequency, then time varying 2DEFM is required [15,69]. In this case the same procedure as that explained in chapter three is used to find the frequency dependence of winding resistances and inductances [39]. The capacitance calculation is frequency independent and can be found from the electrostatic solution [37]. If the values of capacitances are considered frequency dependent then a three dimensional full set of Maxwell equations are used as discussed in chapter four.

However, the frequency dependent values of the inductances, and resistances add some complexity to the network solution. The parameter's values have to be changed at each frequency during the frequency response calculations. If a transient is being solved in the time domain, frequency dependence of parameters implies altering the parameters according to the rate of change of the voltage/current. A transient can also be solved in the frequency domain using transform techniques but the problem must be linearised in some way if nonlinearity is present.

5.2.1 : CAPACITANCES.

Whenever two conductors are brought near to each other, a capacitance exists between them. In transformers, this effect is undesirable, since it places limits on the operation of transformers at high frequency. Since the winding turns are conductors, there will be many capacitances between:- adjacent conductors, non adjacent conductors and ground i.e. the core and support systems.

Researchers [4,35] usually compute capacitance values using the dimensional approach, which is in terms of "a" the conductors cross section area, and ℓ the distance between them and is given by :

$$C = \varepsilon \frac{a}{\ell} \text{ (Farad)}$$

This relationship is not an exact representation of the value of capacitance, because of the edge effect (fringing field) which is neglected in this relation. The capacitor then is treated as though it is used in conjunction with infinitely large conductors.

In order to take proper account of the capacitance distribution within the winding, the 2D electrostatic equation in the previous section is solved using FEM [37]. In this case, the boundaries of the 2D transformer model are limited to the transformer winding window (i.e. the core is ground or 0V). A capacitance is defined as the ratio of the stored charge to the voltage applied, and this definition is used to build the capacitance

matrix. In the finite element model the solution starts with the potential for conductor "1" equal to V and the other conductors left to float. This procedure is used to find the first column in the matrix according to the following relations:

$$C_{11} = \frac{q_1}{V_1} \qquad C_{12} = \frac{q_2}{V_1} \ldots\ldots C_{1n} = \frac{q_n}{V_1} \ldots\ldots\ldots\ldots\ldots$$

Fig. (5.1) shows the electric flux distribution due to placing voltage potential in different places within the primary winding sections. The above procedure is repeated for all of the 14 sections of the primary winding. The charge due to the potential in any conductor is found from the normal component of the electric flux density via:

$$\oint D_n \bullet ds = q \qquad 5.1$$

Using "the line option", the program calculates and draws the required value of electric flux density over the length of the line. On the conductor under consideration it is used to draw the normal electric flux density "D" as shown in Fig.(5.2). The value of the normal flux density used to calculate the capacitance is taken from the graph as the average.

The value of all capacitances in matrix form are given in Table (5.1).

The mathematical approach for computing the total series capacitances in the winding has already been given [29], where the total capacitance between two conductors when the potential placed individually on them is equal to the parallel combination of the capacitances between them, i.e. C_{12} // C_{21} and so on.

Another way of calculating the capacitance between adjacent sections, non-adjacent, and ground can be found directly from the energy relations ($W = \frac{1}{2} V^2 C$). The procedure involves placing a voltage say on conductor "1" and "2", while the rest of conductors are left floating. The total energy is the sum of that in conductor one (used to calculate C11), plus conductor two (used to calculate C22), and that between them (used to calculate C12). Nevertheless, the former method is used throughout the present work.

5.2.2 : INDUCTANCE.

In order to calculate the inductance the finite element magnetostatic equation is solved. The technique explained in this section is well known and is essentially the same as that used to calculate capacitance [37,76].

In this technique a current is placed in one of the conductors while the rest are left float to calculate the inductance. The main inductance components required to determine the transient response of the equivalent circuit are the self and leakage inductances of the section and the mutual inductances between sections.

The current is placed in each conductor, and the flux distribution in the transformer model in one of the conductors is shown in Fig. (5.3). The inductance due to placing current in each section individually is calculated from the flux relation given by :

$$\Phi = \int_s B_t \bullet ds \qquad 5.2$$

The tangential components of the magnetic flux density are calculated using the line option, and the average value of the results from the graph are used as explained for the capacitance calculations.

Therefore, placing current in conductor number one causes flux to cut all the conductors in the model, and the total flux produced by this conductor is :

$\Phi_1 = L_{11} I_1 + L_{12} I_2 + L_{13} I_3$ .....

where L_{11} is the inductance in conductor one due to the current in this conductor and L_{12} is the inductance in conductor one due to the flux cutting this conductor from current in conductor two, and so on, or in general as:

$$L_{11} = \frac{\Phi_1}{I_1} , L_{12} = \frac{\Phi_1}{I_2} \text{ .....}$$

This means that the first column of the inductance matrix can be found due to placing current in the first conductor within the 2D model. This procedure is repeated for all the 14 sections in the model. The values of the calculated model inductances are given in Table (5.1).

It should be noted that in reality skin effects cause the value of the inductances to be a function of dimension , frequency and permeability [92], but as far as the simulation is concerned (which solves the model in static form), none of these functionalities are subject to change, so the value of the section inductances have to be constant.

5.2.3 : RESISTANCE.

The resistance of the conductor depends not only on the type of material from which the conductor is made, but also on its shape and size. It should be observed from chapter three how the resistance of the conductor varies due to the frequency of the current flow in the conductor. However, the model in this section is solved in static terms, which means that the value of the resistance is calculated in the well known form of conductor length "ℓ " and cross section area "a" and conductivity σ .

$$R = \frac{\ell}{a\,\sigma}$$

Due to the conductors being the same size and the frequency not being considered, the resistance values will be the same for all sections and given in a single value.

$R = 0.0567\ \Omega$

It should also be noticed, that the effect from the dielectric loss is negligible, otherwise a shunt conductance has to be placed in parallel with each capacitance. The reason for this conductance being neglected is due to its dependence on the bulk conductivity of the interconnecting wire insulator used. Since this FE model considers air an insulator, whose conductivity is zero, the conductance is also zero. However, the conductance per unit length "G" depends on the geometrical features of the conductor in the same way as the capacitance per length "C", and it may be given as:

$$G = \sigma \frac{C}{\varepsilon_o\, \varepsilon_r}$$

Where σ is the insulator conductivity (typically between 10^{-12} – 10^{-16} siemens/cm), and ε_r is its relative permitivity (typically between 1 and 10).

Branch	L μH	C pF	Branch	L μH	C pF
$\sum_{k=1}^{14} A_{kk}$	4.713	40.73	$\sum_{k=1}^{7} A_{k\,k+7}$	2.838	0.98
$\sum_{k=1}^{13} A_{k\,k+1}$	4.356	30.45	$\sum_{k=1}^{6} A_{k\,k+8}$	2.674	0.57
$\sum_{k=1}^{12} A_{k\,k+2}$	3.821	16.56	$\sum_{k=1}^{5} A_{k\,k+9}$	2.455	0.26
$\sum_{k=1}^{11} A_{k\,k+3}$	3.615	9.98	$\sum_{k=1}^{4} A_{k\,k+10}$	2.089	0.15
$\sum_{k=1}^{10} A_{k\,k+4}$	3.342	4.88	$\sum_{k=1}^{3} A_{k\,k+11}$	1.897	0.088
$\sum_{k=1}^{9} A_{k\,k+5}$	3.188	2.79	$\sum_{k=1}^{2} A_{k\,k+12}$	1.253	0.051
$\sum_{k=1}^{8} A_{k\,k+6}$	3.117	1.89	$\sum_{k=1}^{1} A_{k\,k+13}$	0.849	0.027

Table (5.1) :Elements values (Inductance and Capacitance) for the winding

5.3 : EQUIVALENT NETWORK OF THE TRANSFORMER WINDING.

In general, a two winding single phase HF transformer can be represented by a model such as that shown in Fig.(5.4). In this model, four turns of primary and secondary windings are shown. The model includes distributed inductance and resistance, mutual inductance, and three capacitances including, inter- winding, self, and ground capacitance. The model equivalent circuit was chosen from the physical consideration of the distribution of both the electric and magnetic field.

The difficulties in selecting a correct network lie in two factors mainly, the analytical solution that is used to solve it, and the degree of complexity. Many analytical methods have been used to solve the network of the winding equivalent circuit. Some of these methods are, nodal method [35], nodal admittance matrix method [10,38], eigen values and eigen vectors [77], series expansion of the state transition matrix [5] and others. Each method has its own limitation regarding the degree of complexity of the equivalent circuit. The adopted numerical method to solve the model should show accuracy, stability, deal easily with complex structure of the winding network, and be fast in execution.

In this chapter, the transient voltage distribution has been calculated using the trapezoidal rule of integration. Fig.(5.5) shows the equivalent network of a single winding of the transformer [5], including the mutual coupling between sections (nodes). In fact, it is not easy to solve such a network numerically; the difficulty comes from the mutual coupling. An obvious solution to this problem is to transfer the original network to an equivalent uncoupled network [5] as shown in Fig.(5.6). In order to validate this network for the high frequency calculations, it must contain the maximum number of branches (sections) that is possible in an actual transformer model.

5.4 : TRAPEZOIDAL INTEGRATION.

The numerical integration algorithms discussed in the preceding section can be generalised by a system of first order differential equation given by:

$$\frac{\mathrm{d}\,x}{\mathrm{d}\,t} = f(x,\,t) \qquad 5.3$$

There are many numerical integration methods which may be used to solve this equation, for instance, Gear, forward Euler, backward Euler, trapezoidal, and many more [77,78]. The trapezoidal algorithm is the integration used currently due to its high stability in transient simulation. It is recommended as the best choice for solving winding network from all other possible methods [5].

The general form of the trapezoidal rule of integration that is used to solve equation (5.3) is given by :

$$x_{n+1} = x_n + \frac{\Delta t}{2}\left[f(x_n,\, t_{n+1}) + f(x_n\,, t_n)\right] \qquad 5.4$$

It is clear from equation 5.4 that this algorithm is a two time steps formula, where the values of $f(x,t)$ are needed at two instants of time t_n and t_{n+1}. Hence equation (5.4) can be solved in a step by step procedure with a variable or fixed time step (Δt), until the maximum time required is reached. In general, at any instant of time "t", the past history of the solutions are known from the previous time step, i.e. at " $t-\Delta t$ ". The initial condition is the past history for the first time step (first program iteration) in the analysis. Before continuing with the programming details, It is better to introduce the trapezoidal algorithm to the network elements as detail below.

5.4.1 : TRAPEZOIDAL RULE FOR INDUCTANCE

The voltage across the inductance due to the time varying current flowing through it, is a first order differential equation, and therefore; the trapezoidal rule of integration can be applied directly. The inductance voltage is given by:

$$v_L(t) = v_1 - v_2 = L\frac{di}{dt} \qquad 5.5$$

If the current needs to be found at time "t", the integration has to be carried out from the past history $t-\Delta t$, which yields:

$$i(t) = i(t-\Delta t) + \frac{1}{L}\int_{t-\Delta t}^{t}(v_1 - v_2)\,dt \qquad 5.6$$

where the first part of equation (5.6) is the initial condition at the past history time. By applying the trapezoidal rule of integration, the current at any time instant "t" is:

$$i(t) = I(t-\Delta t) + \frac{\Delta t}{2L}\left[v_1(t) - v_2(t)\right] \qquad 5.7$$

The known previous (history) current is :

$$I(t-\Delta t) = i(t-\Delta t) + \frac{\Delta t}{2L}\left[v_1(t-\Delta t) - v_2(t-\Delta t)\right] \qquad 5.8$$

In order to simplify both equations (5.7) and (5.8), the voltage v_L across the inductance is :

$$i(t) - I(t-\Delta t) = \frac{\Delta t}{2L}\left[v_L(t) - v_L(t-\Delta t)\right] \qquad 5.9$$

This equation (5.9) can be interpreted as being the equivalent circuit for an inductance as shown in Fig.(5.7a).

5.4.2 : TRAPEZOIDAL RULE FOR CAPACITANCE.

The procedure for applying the trapezoidal rule of integration in a capacitance is not different to that applied to an inductance, where the first order differential equation represents the current through the capacitance, and is given by :

$$i(t) = C \frac{d(v_1 - v_2)}{dt} \qquad 5.10$$

The solution at any instant of time, is the integration from the past to the time required,

$$v_1(t) - v_2(t) = \left[v_1(t-\Delta t) - v_2(t-\Delta t)\right] + \frac{1}{C}\int_{t-\Delta t}^{t} i(t)\,dt \qquad 5.11$$

Using the trapezoidal rule of integration this gives :

$$i(t) = I(t-\Delta t) + \frac{2C}{\Delta t}\left[v_1(t) - v_2(t)\right] \qquad 5.12$$

and the past history current is :

$$I(t-\Delta t) = -i(t-\Delta t) - \frac{2C}{\Delta t}\left[v_1(t-\Delta t) - v_2(t-\Delta t)\right] \qquad 5.13$$

The composed form of these two equations (5.12), (5.13) is :

$$i(t) - I(t-\Delta t) = \frac{2C}{\Delta t}\left[v_C(t) - v_C(t-\Delta t)\right] \qquad 5.14$$

This equation can be transferred to the equivalent circuit shown in Fig. (5.7b).

It should be observed, that the resistance in the Ohm's law relation remains the same without any conversion,

$$i(t) = \frac{1}{R} v_R(t)$$

The winding network elements in Fig.(5.6), can be replaced according to the equivalent trapezoidal representation for each element. This network can then be represented by a resistive circuit that can be solved using the well known methods, which will obey both Kirchhoff's current and voltage laws.

5.5 : THE NUMERICAL SOLUTION.

A numerical solution to analyse linear or dynamic networks which contain many elements is a priority for many researchers. A dynamic network means one that contains at least one capacitor or inductor or both. The trapezoidal rule of integration transfers this network to an equivalent linear resistive network, the concern must then be to solve the linear network. There are many books on computer network aided design which can offer much support in solving any network numerically. The general detail of the numerical method that is currently used is given by Chua [78]. Other methods available to solve the winding network can be found in many publications [5,35].

The common procedure in all references solving the winding network is the nodal equation. This equation can be derived from Kirchhoff's current law (KCL), or voltage law (KVL) this depends on the source used for an input and the degree of network complexity. The current law is the simple option used to solve the network in Fig.(5.6), with an input current source, the KCL is that the sum of the currents entering a node is equal to the sum of the currents leaving this node. The voltage at each node, is merely a straight forward calculation from the current through the ground capacitance that connects this node. The total node equations has to be arranged in a matrix form. In order to solve this matrix, many techniques are available, Guassian elimination is probably the most popular. The technique that is used here to solve this matrix is LU factorisation [79,80,81] (this is some times called Crout reduction, or triangularization). The reason for using such a technique is discussed in the following sections.

5.6.1 : LU FACTORISATION.

In general, a set of simultaneous linear equations in the equivalent form is given by:

$$
\begin{aligned}
&s_{11}x_1 + s_{12}x_2 + \ldots\ldots\ldots\ldots\ldots + s_{1n}\,x_n = p_1 \\
&s_{21}x_1 + s_{22}x_2 + \ldots\ldots\ldots\ldots\ldots + s_{2n}\,x_n = p_2 \\
&\cdot \\
&\cdot \\
&s_{n1}x_1 + s_{n2}x_2 + \ldots\ldots\ldots\ldots\ldots + s_{nn}\,x_n = p_n
\end{aligned}
\qquad 5.15
$$

Where x,p could be branch currents or node voltages respectively, and s is the branch element (resistance, or conductance), n is the number of nodes or branches. In matrix form, equation (5.15) is:

$$
\begin{bmatrix}
s_{11} & s_{12} & \ldots\ldots\ldots\ldots & s_{1n} \\
s_{21} & s_{22} & \ldots\ldots\ldots\ldots & s_{2n} \\
\cdot & & & \\
\cdot & & & \\
s_{n1} & s_{n2} & \ldots\ldots\ldots\ldots & s_{nn}
\end{bmatrix}
\begin{bmatrix} x_1 \\ x_2 \\ \cdot \\ \cdot \\ x_n \end{bmatrix}
=
\begin{bmatrix} p_1 \\ p_2 \\ \cdot \\ \cdot \\ p_n \end{bmatrix}
\qquad 5.16
$$

Or in general, $S\,X = P$

The usual procedure using Gaussian elimination begins by eliminating x_1 from equation (5.15). For instance, if the first part of equation (5.15) is divided by s_{11}, multiplied by s_{21}, and subtracted from the second line in equation (5.15) x_1 is eliminated, and so on to eliminate $x_2, \ldots\ldots x_n$. This procedure can be written in general form for all the elements in the matrix as follows; to eliminate the Kth column equation, multiply by s_{K1} , and subtract the result from the Kth equation. This kind of elimination will continue until the matrix is in triangular form, where the lower triangle of the matrix is equal to zero. The last step is to divide the results by the diagonal values to yield unity diagonals. The number of multiplication and division required to obtain a unit diagonal is high and the

Gauss ordering of these operation is often too restrictive. Again, if the solution needs to be repeated for an intermediate point, the S matrix needs to be re-factorised for any change in P. In order to overcome these problems, a more flexible and realistic solution is used, it is called LU factorisation.

The LU factorisation technique starts with dividing the S matrix into a lower triangular matrix L, and an upper triangular matrix with unit diagonal U. For equation (5.16), the S matrix can be transferred into L and U matrices as shown:

$$L = \begin{bmatrix} \ell_{11} & 0 & . & 0 \\ \ell_{21} & . & . & 0 \\ . & . & . & . \\ \ell_{n1} & . & . & \ell_{nn} \end{bmatrix} \qquad U = \begin{bmatrix} 1 & u_{12} & . & u_{1n} \\ 0 & . & . & u_{2n} \\ . & 0 & . & . \\ 0 & 0 & 0 & 1 \end{bmatrix} \qquad 5.17$$

The elements in the LU matrices are to be found in a recursive way involving the first column of L and the first row of U and so on. In general, the calculation at the Kth column is:

$$u_{jk} = \left(s_{jk} - \sum_{m=1}^{j-1} \ell_{jm}\ u_{mk} \right) / \ell_{jj} \qquad j < k$$

$$\ell_{jk} = s_{jk} - \sum_{m=1}^{j-1} \ell_{jm}\ u_{mk} \qquad j \geq k \qquad 5.18$$

Following the determination of matrix elements (eqn 5.18), the solution can be carried out using both forward solution and back substitution. During the forward calculation, the equation to be solved is L Y = P (compare with the original equation S X = P), which yields, the values of y. The back substitution involves solving U X = Y, which yields the required x values.

The computer program using this technique is a direct implementation of equation (5.18). An important point which needs to be handled carefully is the division of ℓ_{jj} , where if the column involving this division is zero, the value of u_{jk} is infinity (this

problem is however less of a possibility due to the full matrix representation). This problem can be solved by a rearrangement of the row-column to avoid such an error. This form of row-column interchange to locate a non zero ℓ_{jj} is necessary, and a subroutine to serve this purpose [77,78,82] has been developed.

5.5.2 : ANALYSIS OF LINEAR NETWORK.

In this section, attention will be paid to describing the rules of forming a system of nodal equations (admittance matrix) for a linear network, and how the computer can be used to generate them.

The transient analysis can be carried out in either of two ways, state equation or nodal equation. The state equations for any electrical network are derived from capacitor voltage and inductor current, since knowledge of the energy stored in the network can be determined solely from these variables. The state equation has a drawback of instability and restriction in complex network solution [5,77]. This difficulty is reflected in its suitability to solve a small network analytically but not numerically.

The nodal equation is the well known relation defined by :

1- Kirchhoff's current and voltage laws and the relationship between them.

2- Methods of combining structural and elemental values to give the complete circuit definition.

All the above steps are necessary to formulate any general form of the equations for computer analysis using graph theory [78,79]. This theory allows the node-branch connections for the network to be introduced to the computer program in the form of a table. In a large network involving many elements, an alternative way of placing this connection information is in a matrix called the node-branch incident matrix (A). The size of this matrix is given by nodes times branches, where the column shows the branch

that connects to each node and the connection polarity. In general, this matrix is given by $A=[a_{ij}]$, where i denotes the node and j denotes the branch, and specified as follows: a_{ij} is equal to "1" if j incident at i (current out of i), equal "-1" if j incident at i (current into i), and equal "0" if j is not incident at i. In any considered network, one of the nodes is a reference to scale the rest of nodes, and has to be removed from this matrix, since it is assumed to be ground (0V). In terms of the node-branch connection matrix (A), and the primitive admittance (or conductance) matrix Y (or G), the nodal equation is :

$$A^t Y A e^- = A^t (I - Y E) \qquad 5.19$$

Where e^- is the vector of nodes of the reference voltages, I is the vector of current sources, and E is the vector of voltage sources in each branch. The matrix A^t gives the node-node relations, where two possibilities of connection are available. First, the branch connection is from the i node to the reference, so the only non zero element in column k of A is a_{ik} =1 (-1 from reference to node i). Second from node i to node j (either of nodes is not a reference), the only two non zero elements in column k of A are a_{ik} =1 and a_{ik} = -1, the voltage between ij nodes $v_k = v_{in} - v_{jn}$ (n is the number of nodes).

The vector of element voltage is V=E+e, where e is the branch voltage related to e^- by:

$$e = A\ e^- \text{ , therefore } V = E + A\ e^- \qquad 5.20$$

With respect to equation (5.20), equation (5.19) can be rewritten as :

$$A^t \left[Y \left(A e^- + E \right) - I \right] = 0 \text{ or } VY = I \qquad 5.21$$

Once the element voltage is known, e^- can be computed and so on for the branch currents and node voltages.

5.6 : PROGRAM DESCRIPTION.

Fig.(5.8) shows the flow chart of the simulation program. The program starts with the information supplied in an input data file. The input information includes the network element values where each is specified with initial and final node, in addition, the

elements connected to the datum node are required(0V or ground). The time step, initial condition at t = 0, and the maximum time required is also provided in the input data. The program interprets each of these elements and replaces them with an equivalent according to the trapezoidal rule of integration. Thus the whole network is changed into a linear resistive network with a set of linear equations. At any instant of time these equations are given in a matrix form as :

$$[\mathrm{Y}]\,[v(t)] = [i(t)] - [I_h] \qquad 5.22$$

Where $[\mathrm{Y}]$ is the nodal admittance matrix, $[v(t)]$ is the node's voltage, $[i(t)]$ branches current, and $[I_h]$ is the known current from the past history. Since equation (5.22) involves the past history term, some of the quantities in this equation are known and some not at any step of time. Therefore; equation (5.22) can be rewritten as :

$$\begin{bmatrix} [\mathrm{Y}_{11}] & [\mathrm{Y}_{12}] \\ [\mathrm{Y}_{21}] & [\mathrm{Y}_{22}] \end{bmatrix} \begin{bmatrix} v_1(t) \\ v_2(t) \end{bmatrix} = \begin{bmatrix} i_1(t) \\ i_2(t) \end{bmatrix} - \begin{bmatrix} I_1 \\ I_2 \end{bmatrix} \qquad 5.23$$

Where the nodal admittance matrix with "1" contains the unknown node voltage, "2" contains the known node voltage, $[v_1(t)]$ is the required quantities, and $[v_2(t)]$ is known from the past history, the solution may written then as :

$$[\mathrm{Y}_{11}]\,[v_1(t)] = [[i(t)] - [I_1]] - [\mathrm{Y}_{12}]\,[v_2(t)] \qquad 5.24$$

As explained earlier in this chapter, at any time step there are two steps to yield the final solution using the LU factorisation technique, forward solution and back substitution. Before the program goes into the time step loop and forward solution, some preparations are necessary. These include:

1-Building the upper part of the conductance matrix in the same way as explained before, so that the matrices $[\mathrm{Y}_{11}]$ and $[\mathrm{Y}_{12}]$ are solved only once.

2- The specified current source $[i_1(t)]$ and the past history $[I_1]$ are entered on the right hand side of equation (5.24).

The solution of equation (5.24) has to be repeated at each time step until the maximum time required is reached. In each time step, the first part of the right hand side of the equation (5.24) is found through forward solution, and then back substitution to obtain $[v_1(t)]$, and $[v_2(t)]$ has to be updated before entering the next time step.

5.7: PROGRAM ACCURACY.

The numerical solution of any integration method is not exact, there will always be an accompanying error, this is because the numerical solution transfers the function of a continuous curve into a curve with discrete points. There are two types of errors that form the total errors. The first type is the round off error, sometimes called the machine error which is due to the finite number of digits and depends on the computer used. The second error is the truncation error, which is the error that results when the arithmetic is imprecise (algorithm error). The total error may increase or decrease as the computation proceeds. If the error decreases with an increase in the number of steps, the numerical solution is called stable. If the error increases as the number of steps increases the numerical solution is called unstable and has no meaning practically. Hence, it is vital to check the value of the error during the numerical solution to ensure the method's validity.

The error analysis in a computer program is performed from Taylor's series formula [78,82]. In the case of a differential equation given by : $\frac{dx}{dt} = f(x,t) \quad x(0) = x_0$, the truncation error (T) is :

$$T = x(\tau_{n+1}) - x_{n+1}$$

The first term $x(\tau_{n+1})$ is the exact solution of x(t) at point τ between t_n and t_{n+1} . The second term x_{n+1} is the solution found at the next time step $(t_n + \Delta t)$.

In the present program a linear interpolation [83] for a point τ located between t_n and t_{n+1} is used to calculate this error. However, the mathematics and numerical approach of this error is discussed in much detail in many references [77,78,81,82]. The

important thing here is the application of this error in the case of inductance and capacitance which is :

$$T = \frac{\Delta t}{2C}\left[i(\tau) - i(t-\Delta t)\right]$$

$$T = \frac{\Delta t}{2L}\left[v(\tau) - v(t-\Delta t)\right]$$

This error is always used as a reference to be compared with the next time step. In order to prove the accuracy of the trapezoidal method in comparison with the original capacitor or inductor an example is considered. In this example a simple series RC circuit is used, with an initial condition of 1V at t = 0 on the capacitor. For simplicity, the values of R and C are considered 1Ω and 1F respectively. The solution of this example is to find the voltage across the capacitor at any time (v(t) for t > 0). In order to solve this problem with a computer, the voltage function (V) has to be discretized by selecting a finite number of moments (m). The distance between two moments is Δt, therefore the total time is : $t = \Delta t \cdot m$

The exact solution (state equation) of this circuit $V(t) = e^{-\frac{t}{RC}} = e^{-t}$ is compared with the trapezoidal method. For this circuit the capacitor discharge through the resistor, the voltage across the resistor then is V= - R i, and the capacitor current is $i = C\frac{dV}{dt}$. If the voltage belonging to m (V(m)) is found, the next step voltage (V(m+1)) can be found. The trapezoidal integration method for the capacitor and resistor is as follows :

$$V(m+1) = V(m) + \frac{\Delta t}{2C}\left[i(m) + i(m+1)\right] \quad \text{(capacitor)}$$

$$i(m) = -(1/R)\,V(m)$$

$$i(m+1) = -(1/R)\,V(m+1) \qquad \text{(resistor)}$$

The total circuit voltage is :

$$V(m+1) = V(m) - \frac{\Delta t}{2CR}\left[V(m) + V(m+1)\right]$$

Consequently, $V(m+1)\left(1+\frac{\Delta t}{2CR}\right) = V(m)\left(1-\frac{\Delta t}{2CR}\right)$, and then:

$$V(m+1) = \frac{1-\Delta t/2RC}{1+\Delta t/2RC}\,V(m) \qquad 5.25$$

In order to compare the computed values from equation (5.25) with the exact solution, the following table examines different time steps:

Δ t	m	Exact	Trapezoidal
0	0	1	1
0.2	1	0.82	0.82
0.4	2	0.67	0.67
0.6	3	0.55	0.55
0.8	4	0.45	0.45
1	5	0.37	0.37
2	10	0.14	0.13

* The values in this table are calculated analytically as follows, when the time step is 0.2 , V (m+1) = (0.9 / 1.1) V(m), Therefore V(1) = (0.9/1.1)*V(0) = 0.82, and so on. These values are not different to those found numerically using the described program.

Another way of examining the accuracy is for the voltage at a time of "1 sec." to be computed for different time steps. Fig.(5.9) shows that the error which is generated from 0.1 time step to 0.001. Since the error is reduced, the present numerical solution is stable, so the time step should be 1ns.

5.8: NETWORK TRANSIENT RESULTS.

The whole network containing 14 sections is solved numerically. These sections representing the primary winding turns, and their element values are given in table 5.1. Fig.(5.10) shows the voltage waveforms at a number of sections with respect to the ground. It can be seen from this figure that the voltage of one section is different from that of the next. If the network is resistive, there will be no voltage difference between the sections except the resistive voltage drop. This case has been discussed in chapter three when the model is solved for the magnetic field only (resistance and inductance

only). Such voltage difference causes an electric field to set up and hence capacitive effects appear. The voltage drop due to the resistance (copper and eddy current winding losses) follows a straight line reduction from a high value (supply voltage) to a low value (ground). Since the network is dynamic, the voltage drop is not a linear reduction as in the resistive/inductive network. The way this voltage reduces can show which of the capacitance (shunt or series) dominates the analysis at the supply frequency. If the voltage drops in a curve that never exceeds the supply voltage at any section, the series capacitance has more effect than the shunt capacitance, otherwise the voltage in the middle sections of the winding goes higher than the voltage at the terminal. The series capacitance may cause the same effect if its value between adjacent conductors (only while the rest of capacitance between nonadjacent conductors and ground are the same) goes very low, in particular lower than five times than its original value. The additional case of winding overvoltage is by changing the frequency of the input supply to double the design frequency of the winding. In this case, the voltage in the middle section goes higher than that at the terminal. These can be the main reasons why overstressing of the winding occurs. If the applied voltage has the same frequency as one of the network internal resonant frequencies, then the winding experiences an internal overvoltage. In order to avoid and control an internal winding overvoltage, it is important to obtain the winding internal resonant frequencies. These frequencies are vital for the transformer designer at the design stage.

Fig.(5.11) shows the currents waveform in selected branches including adjacent, nonadjacent conductors, and the load current. The current here is not as important as voltage unless another transient phenomena is considered such as the inrush current. This case is vital in particular at first switch on where the supply current entering the transformer is high and sometimes overstresses the winding. This case is vital to the transformer designer so as to carefully considered the winding insulation thickness.

The resonant frequency of a winding depends on the self and mutual inductances, and capacitances. These frequencies can be clearly identified from the terminal network (winding) impedance. The frequency response of the impedance can be found from the

network solution of the terminal voltage source and the total network current. The inverse Fourier transform [83] can be used to obtain the frequency response of the transient results, or directly using the same technique but in the frequency domain. Fig.(5.12) shows the network impedance for the frequency range of 10KHz to 50MHz. The terminal resonant frequency is shown as a terminal maximum voltage and a terminal impedance minimum (series resonance). The anti-resonance of the parallel resonant frequency has the opposite property. This calculation allows the determination of the first resonant and anti resonant frequencies. The first parallel resonance (i.e. impedance maximum) is caused by Cg and L1 to n. The rest of the parallel resonances are found by L1 to n with C1 to n, and will therefore produce a further 14 principle resonant frequencies (only the first six are present in the graph shown). The series resonances are again the combination of L1 to n with C1 to n, and they will produce 14 principle series resonance parts. The first two resonant frequencies differ as compared to measurements by 1.36 (parallel) and 1.19 (series). As a result, the transient response of the network is expected to be different from that of the winding it represents [9]. The reasons behind this could be that not enough network elements were used in the analysis, or frequency dependent values should be used.

The winding impedance curve can also validate components of the proposed winding equivalent circuit. This allows the calculation of the total series equivalent and ground capacitances. The equivalent series winding capacitance is found to be of most concern to researchers. The procedure for finding the equivalent circuit of the winding from the impedance curve is explained in detail in chapter four. For the first series and parallel resonant frequencies and the lowest frequency range used in the curve, the equivalent circuit could be represented by a series RL in parallel with a series winding capacitance, and the whole is connected to the ground capacitance. Using the chapter four procedure, the equivalent series capacitance is equal to 5.8pF in comparison to 4.1pF using the mathematical approach [29]. The equivalent ground capacitance is 1.25pF, inductance 4.2uH and resistance of 0.98Ohm. By examination of the impedance curve an approximate equivalent circuit can be constructed. At frequencies below the first parallel

resonant frequency, the impedance function behaves as a combination of RL branches without resonance. At frequencies above the first parallel resonant frequency, the capacitance comes into effect and a number of resonances are present.

Fig.(5.13-to-5.16) shows, the network terminal impedance when the capacitances of the different network allocation are changed. By examining the capacitances between adjacent conductors for an increase and decrease to five times their original values some differences are noticed. When adjacent capacitance values are increased (i.e. 0.152nF), the frequency range between the series and parallel resonant frequencies decreases. In addition, the impedance curve falls sharply between them, and corresponding parallel resonant frequencies (second parallel and over) are well spaced with respect to each other. The first parallel frequency is also affected but it is not easy to spot such a change in the figure due to the wide frequency range considered. The reduction in the first parallel frequency is small because the adjacent conductors capacitance only is changed(part of series capacitance) and not the total capacitance (refer to Fig.(5.6)). Opposite events occur when the capacitance values are decreased (6.1pF). When the ground capacitance is decreased to five times its original value (i.e. 8.146pF), the frequency of the first parallel resonance is increased, but the first series resonant frequency still has the same value. When the ground capacitance is increased (i.e. 0.203nF), both parallel and series resonant frequencies are reduced and the number of internal resonant frequencies are reduced.

This study of the capacitance effect has shown that the best response for the high frequency winding structure is obtained when the capacitance is reduced. As was said earlier, reducing the capacitance between adjacent conductors can increase the stress of the winding. Bearing in mind that the winding is part of the transformer and any reduction in the capacitance reflects in an increase in the transformer size. The frequency dependence of the leakage inductance and resistance of the windings are also important and need to be included.

5.9 : MODELLING THE TRANSFORMER BY NETWORK REPRESENTATION.

In this section, attention is paid in seeking the possibility of modelling the whole transformer using the network representation that has been discussed. The secondary winding can be modelled using an equivalent network in the same way as that used to model the primary winding. Indeed, all the winding's elements including the mutual inductance and distributed capacitance of both windings can be found from FEM. This network technique has the possibility to model the transformer, but it is most suitable if the primary winding turns are equal to the secondary winding turns. Each turn of the primary winding can be connected easily to the corresponding turn in the secondary winding. In the case where the secondary turns are more than primary turns (as the case currently existing with a 26 / 14 turn ratio), and the core window contains multiple layers of winding, such technique is hopelessly complex. In addition, modelling the transformer by this technique needs a massive capacity for the nodal matrix. For these reasons, a model of this type has not been presented further. It would be viable if the calculations necessary to produce equivalent circuit terms could be automated. Adaptive finite element method techniques might allow this.

Another approach which could be used instead is by modelling each of the windings separately to calculate the input impedance using the same technique. The frequency response input impedance curve can be used to derive an equivalent circuit as discussed earlier in this chapter. The elements of the equivalent circuit can be found based on the resonant frequency. The rest of magnetising elements and distribution capacitance may be found with the help of the FE program. In the ways described, it is clear that this method lacks flexibility, because a new model has to be built each time a new design is required, and consequently this method is quite expensive in time.

5.10 : SUMMARY

In the present chapter, the approach has been taken to model the transformer by the equivalent network representation. The procedure started with taking the primary winding only into account. The primary winding was transferred into an equivalent R, L, and C network. The network elements were calculated using the finite element program to solve both electrostatic and magnetostatic fields equations individually. Numerical solution of this network was carried out using the trapezoidal rule of integration, where each element is transferred into an equivalent resistance and independent current source. The whole network then appears as a resistive network which can be solved by the well known method. The program used has been detailed and an example has been given to check its accuracy. The transient analysis is used first to solve the network numerically, and an inverse form of fast Fourier transform is used to obtained the frequency response of the input impedance. The effect due to the changes in the distribution and ground capacitance on the input impedance have been introduced. It was observed that whatever the number of the network elements used the actual resonant frequency cannot be reached. therefore, the method lacks the flexibility and accuracy to model the whole transformer. The method seems more suitable to study the transient phenomena associated with single winding (overvoltage, surge current, etc.).

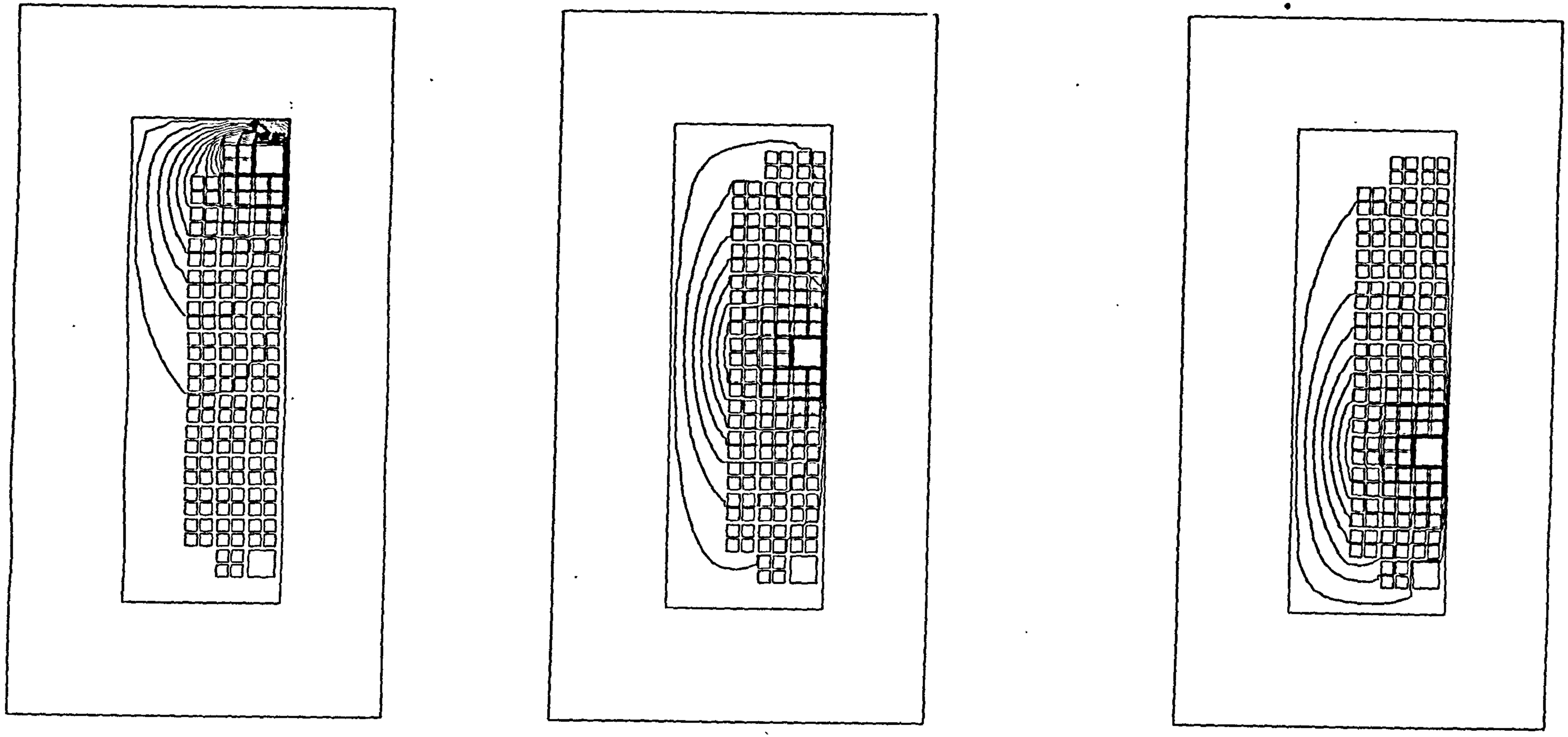

Fig.(5.1): The electric flux distribution, by placing Voltage in different position within the winding.

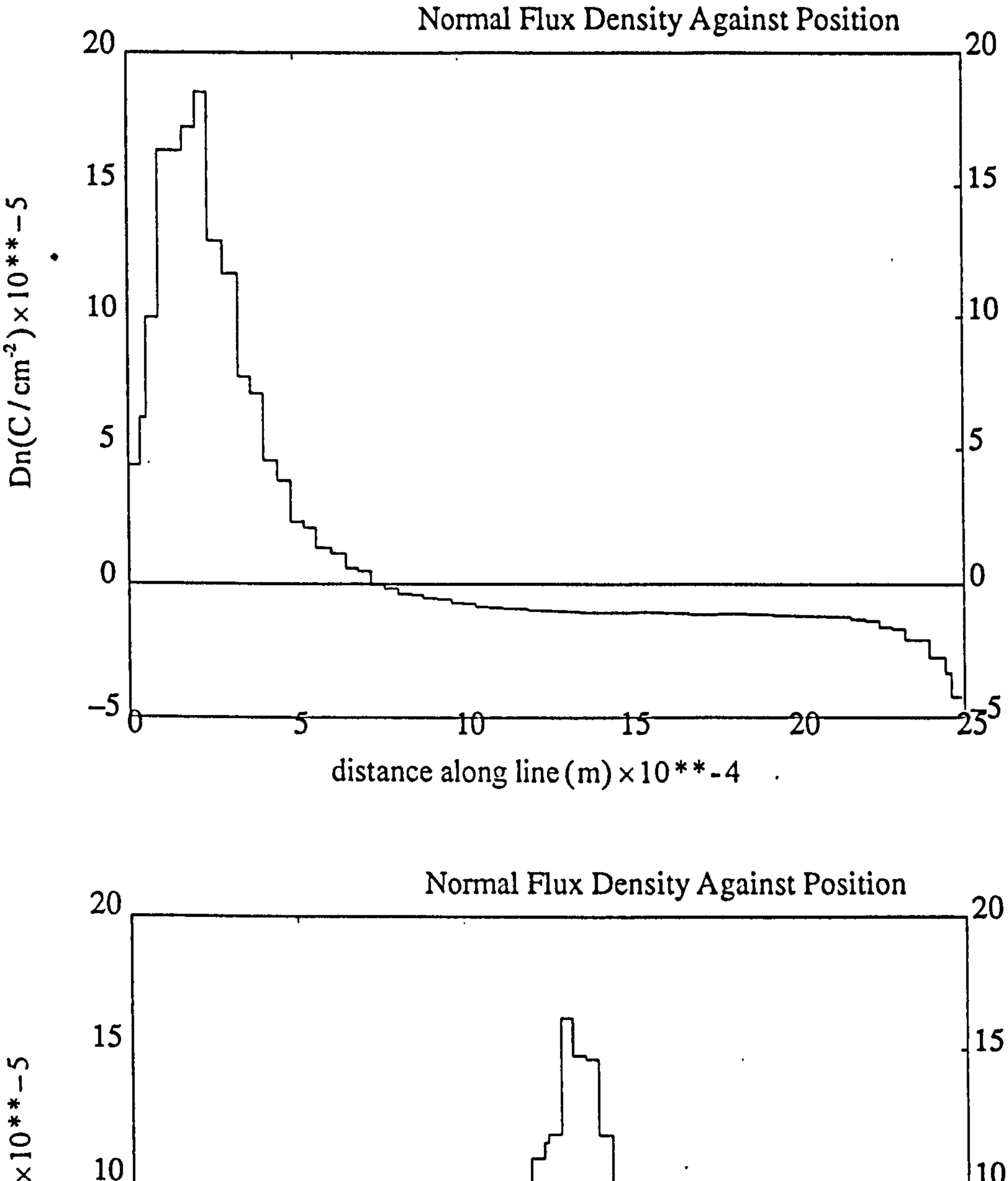

Fig.(5.2): Normal electric flux density at different winding position.

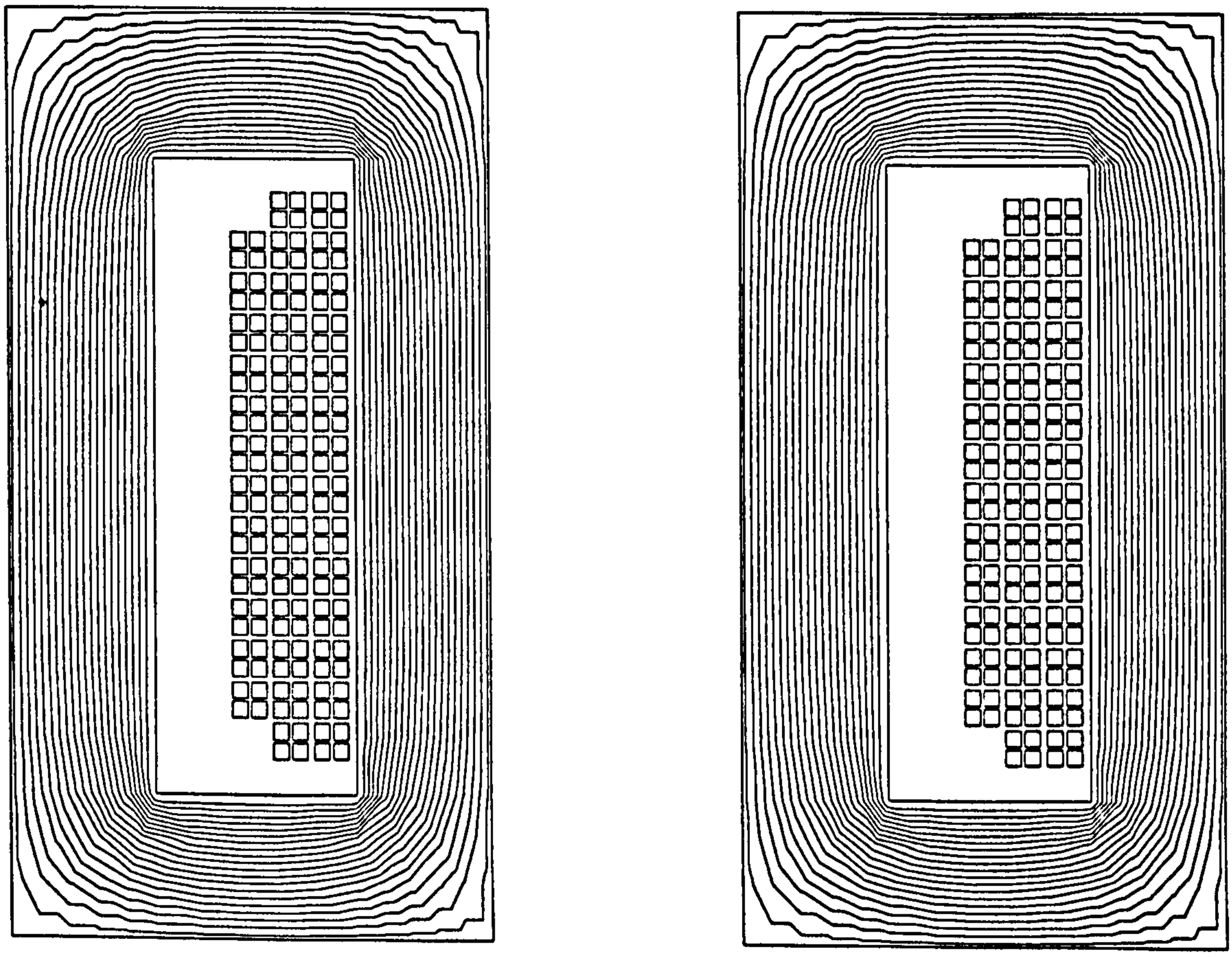

Fig.(5.3): Magnetic flux distribution, excitation at different winding position.

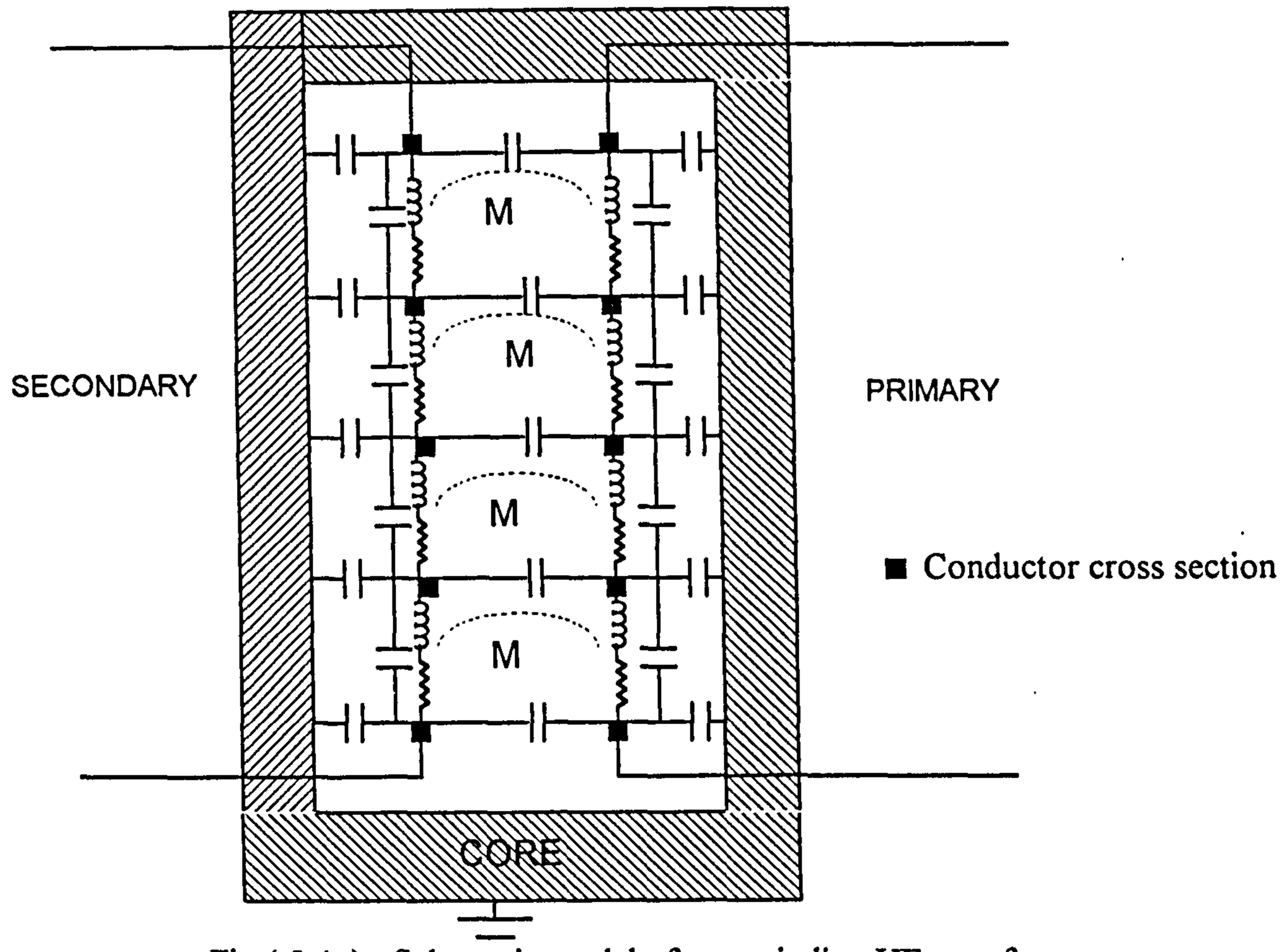

Fig.(5.4) : Schematic model of two winding HF transformer

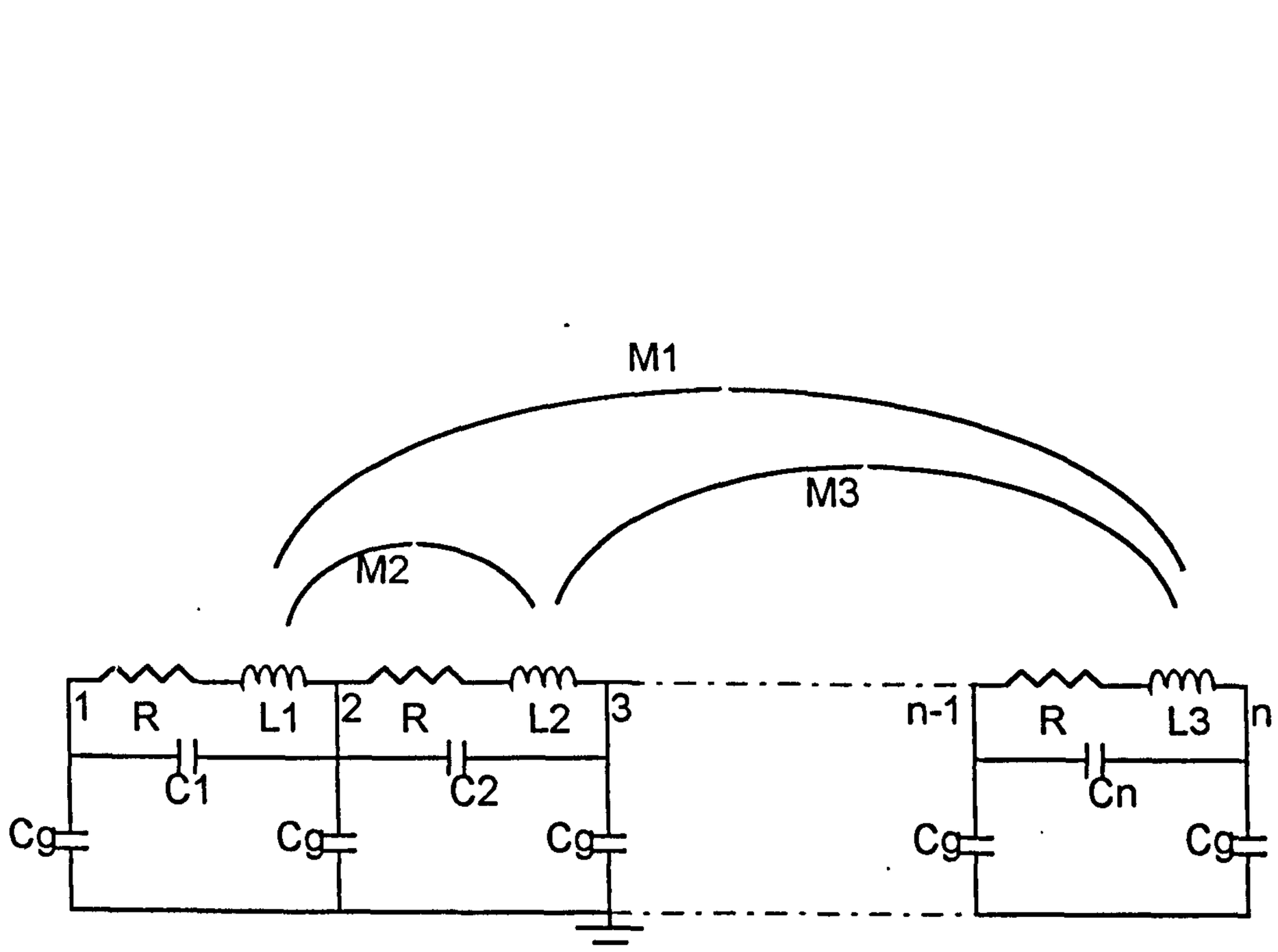

Fig.(5.5): Equivalent network of a transformer winding

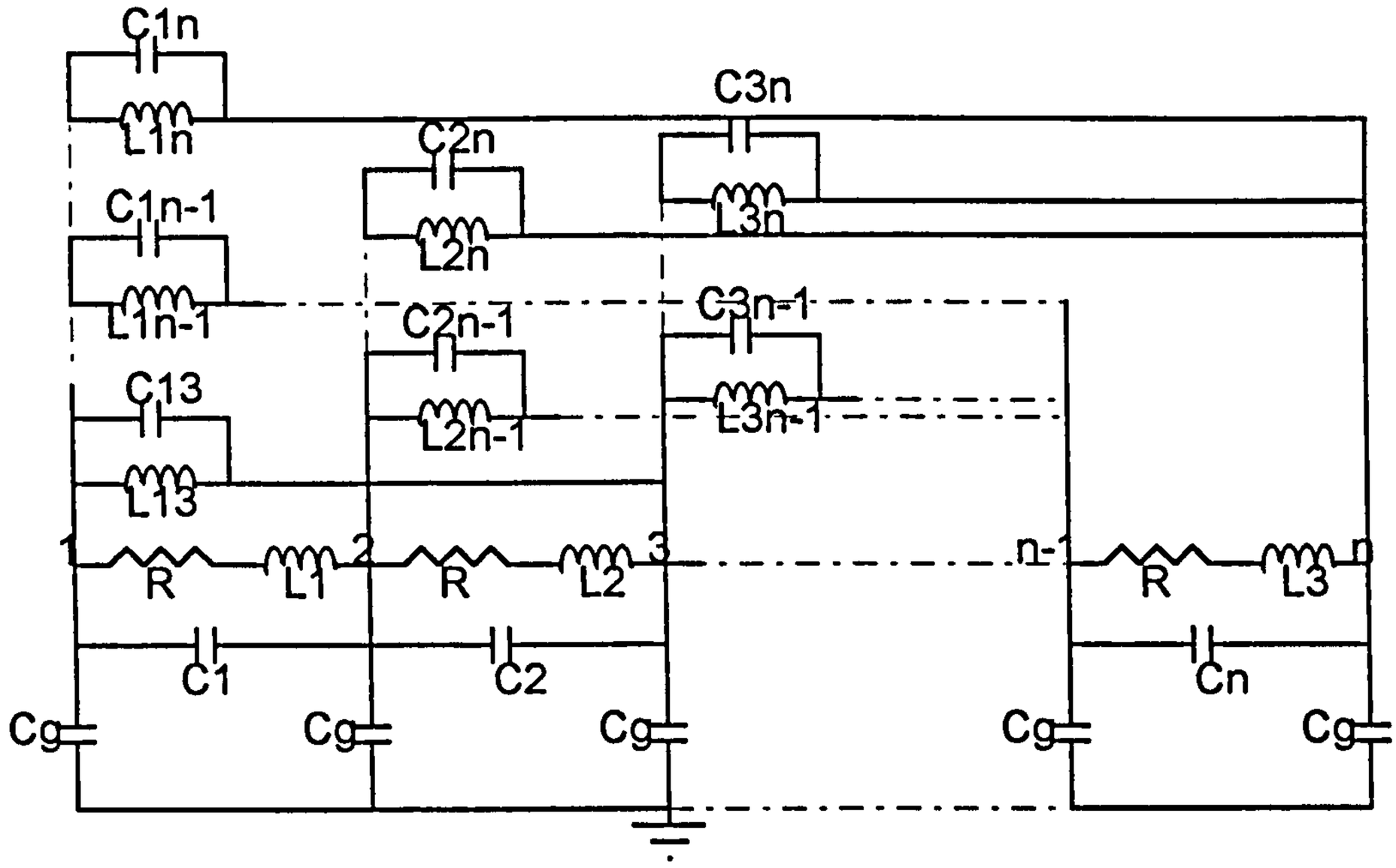

Fig.(5.6): Proposed winding equivalent circuit

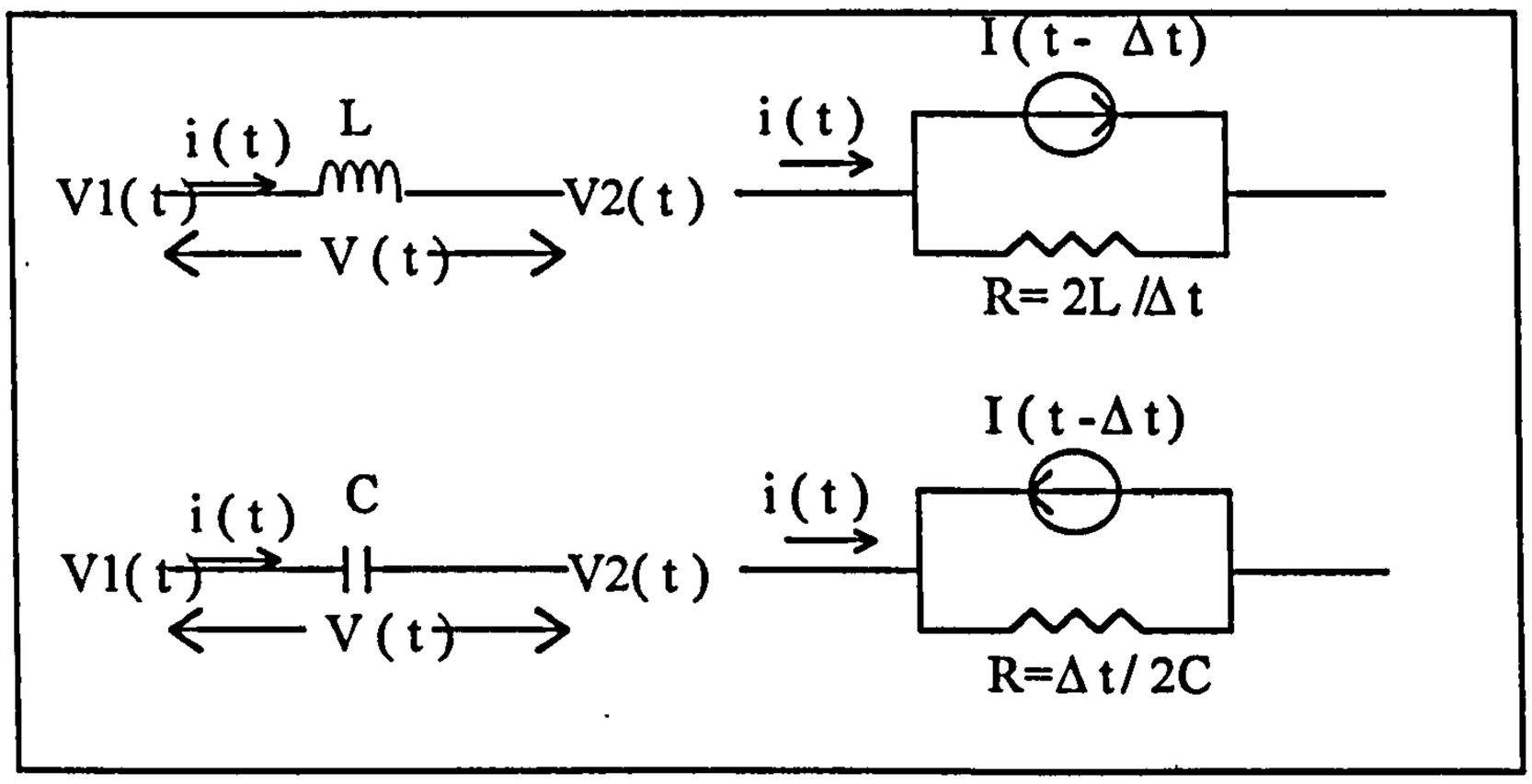

Fig.(5.7) : Equivalent circuit of a) Inductance, b) Capacitor

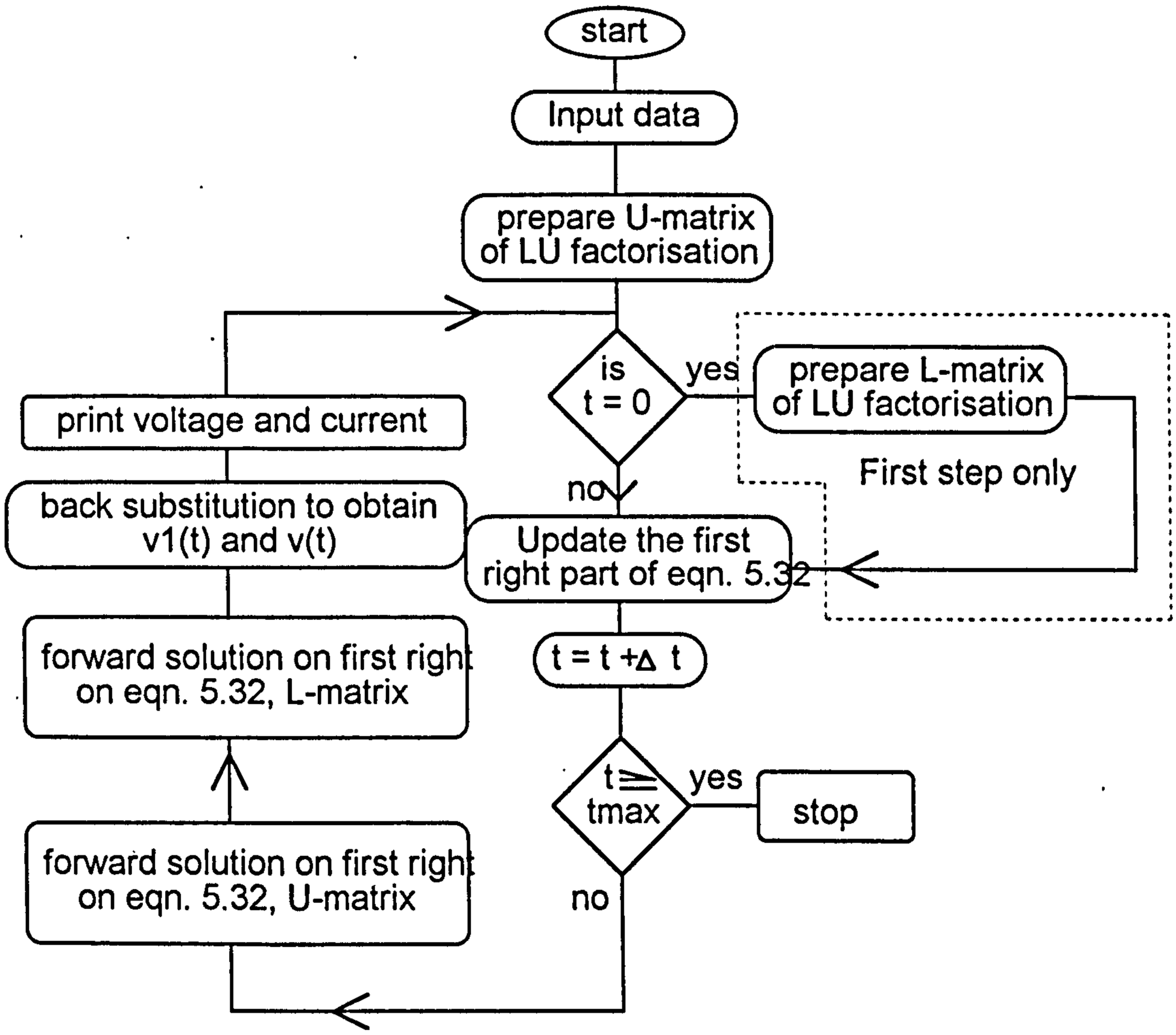

Fig.(5.8): Program flow chart

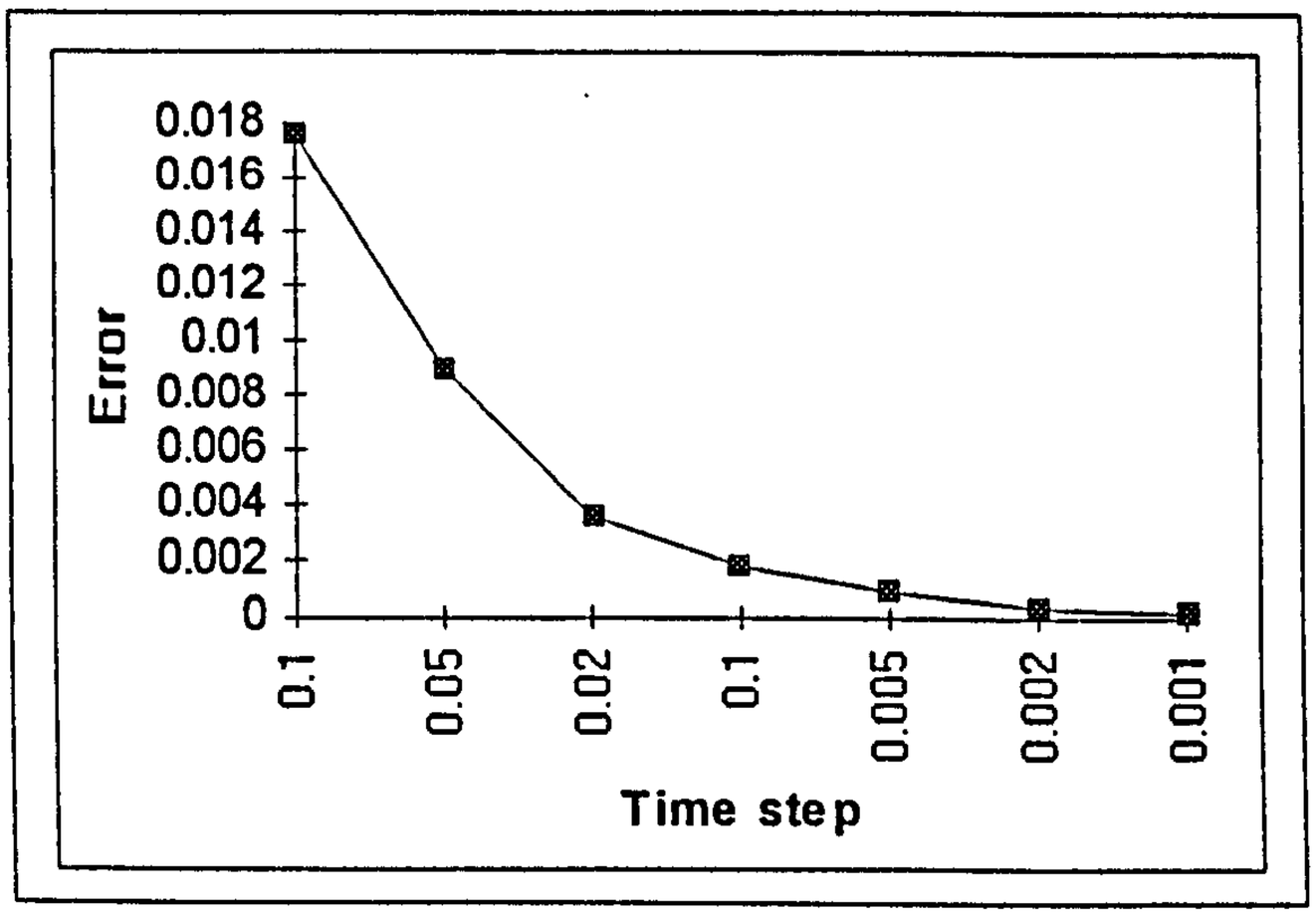

Fig.(5.9) Numerical error as a function of time step

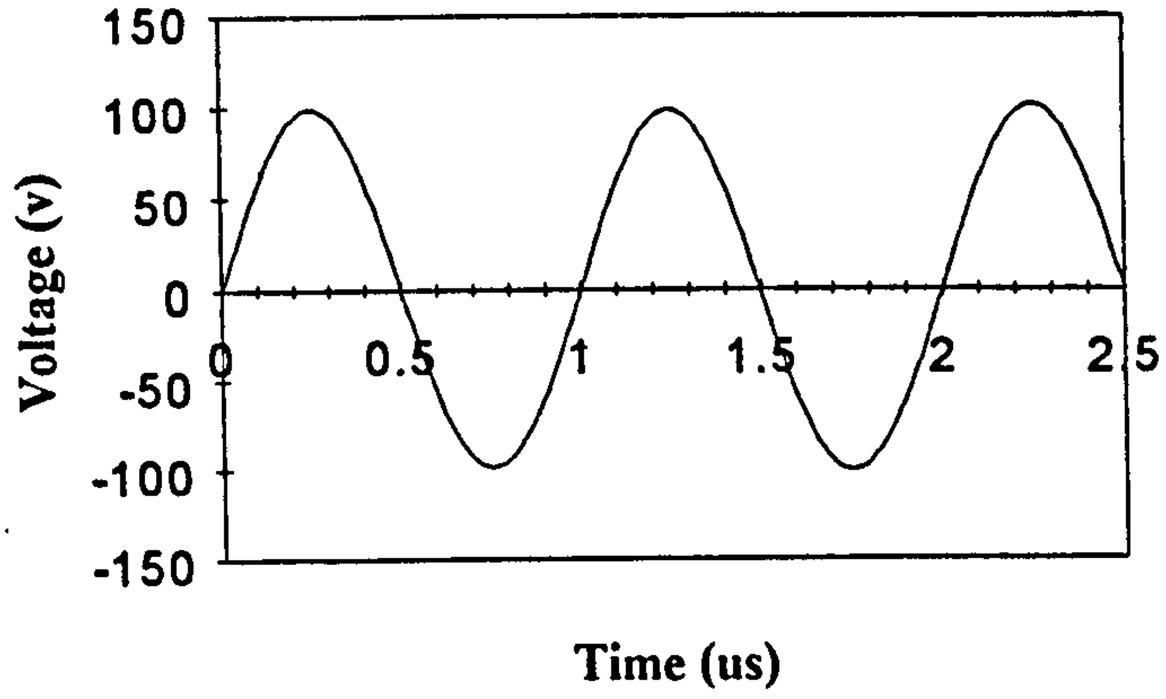

Node 1

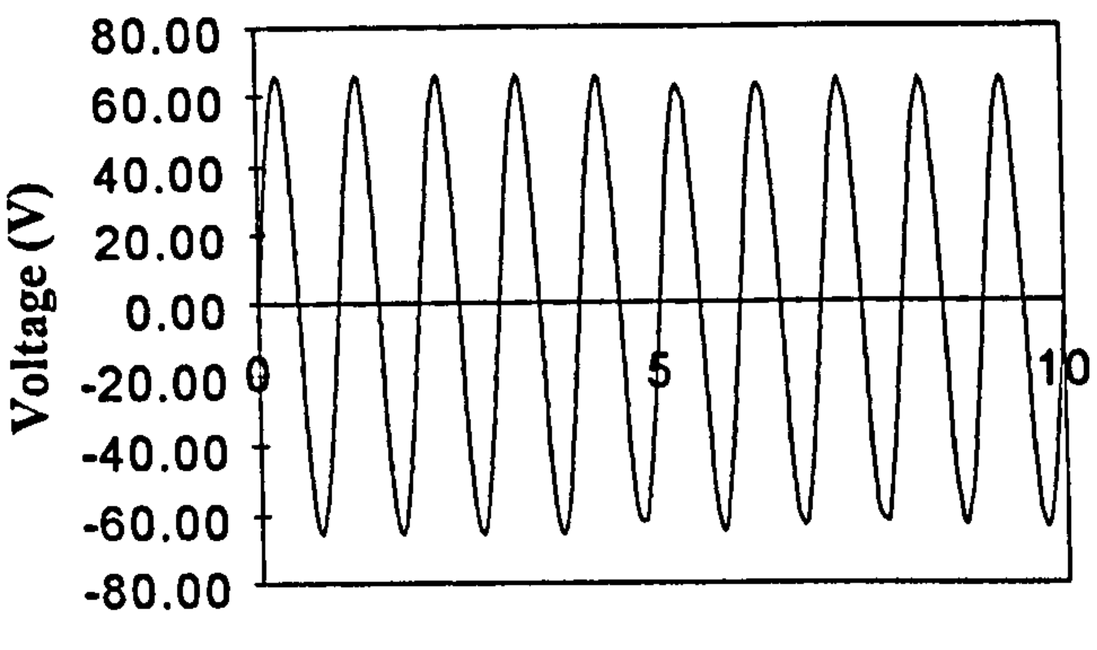

Node 6

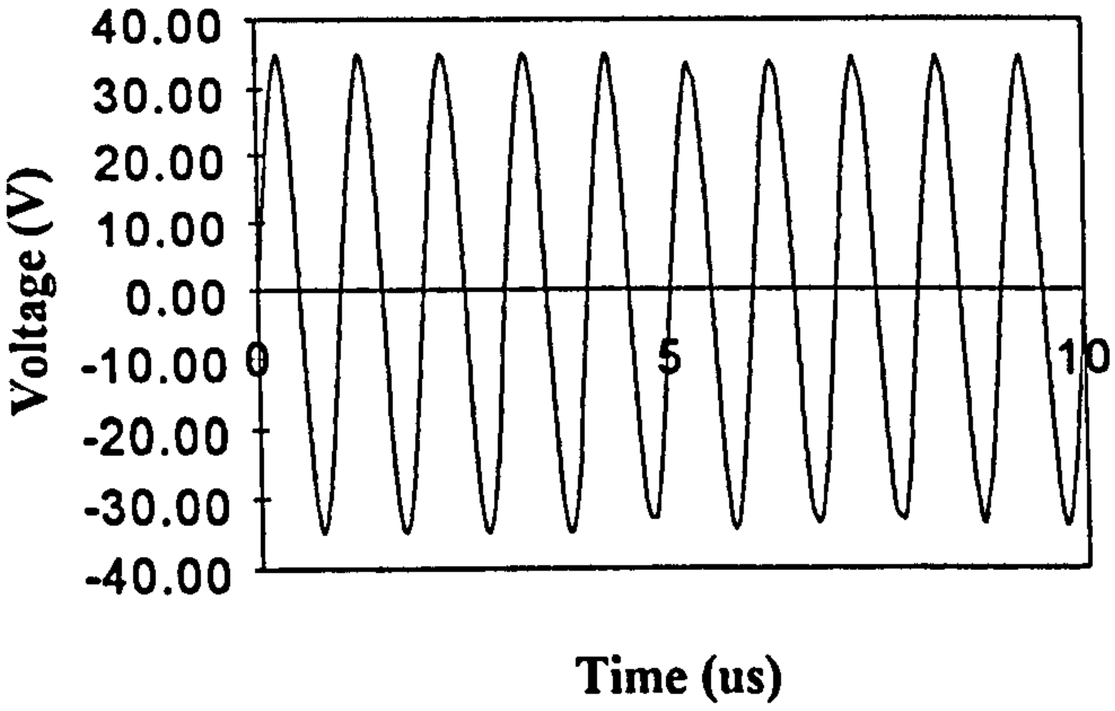

Node 11

Fig.(5.10) : Voltage of the selected nodes

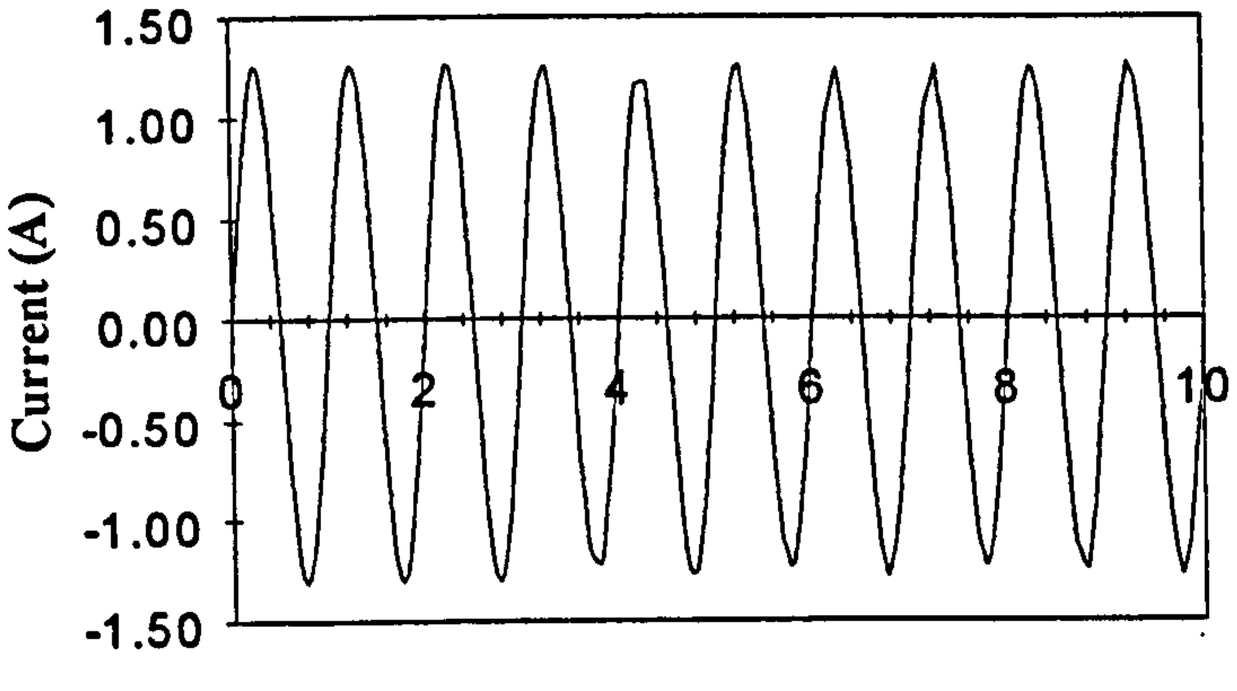

(a)

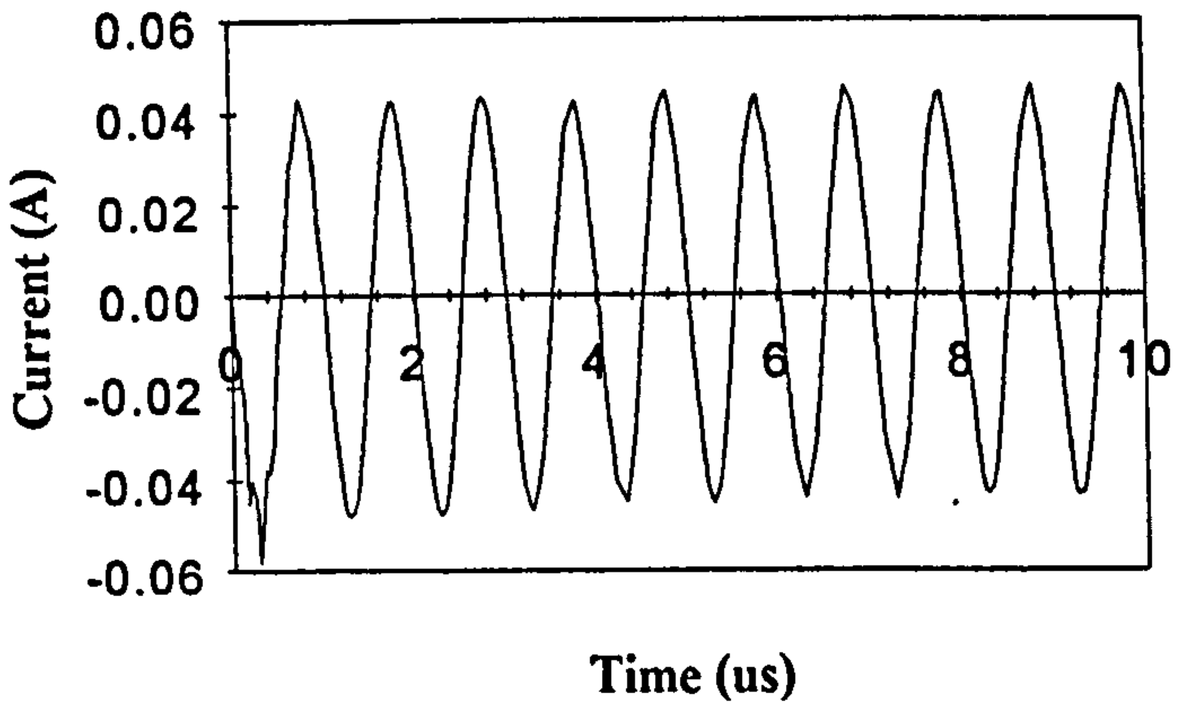

(b)

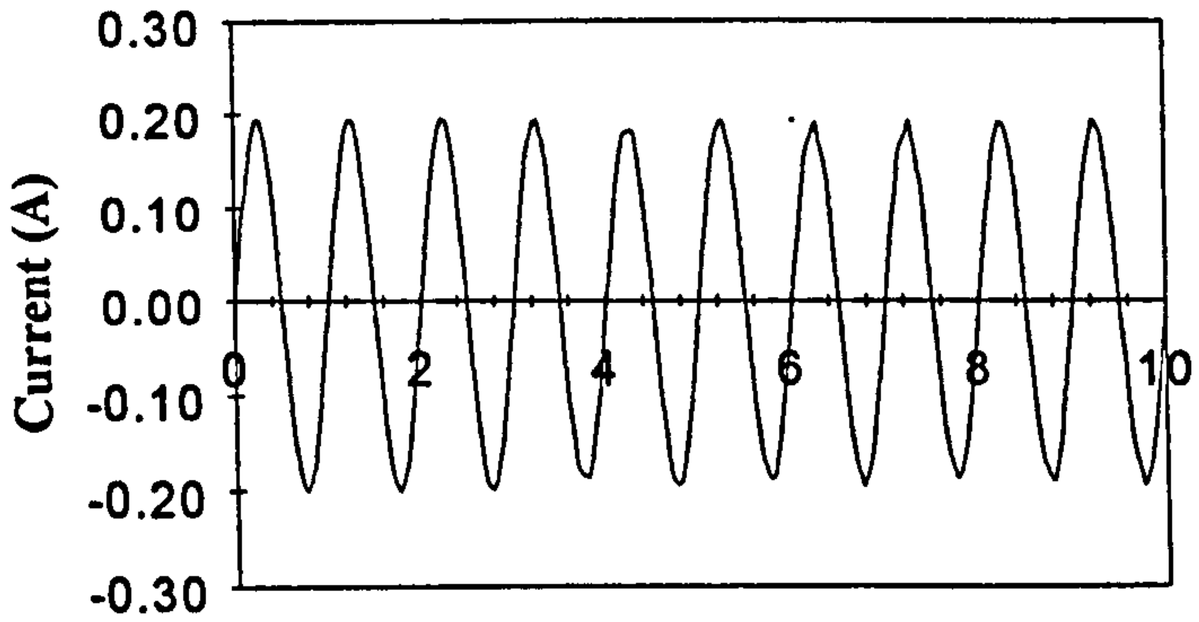

(c)

Fig.(5.11) : Branches current, (a): Load, (b): branch 1-7
(c) : branch 1-14

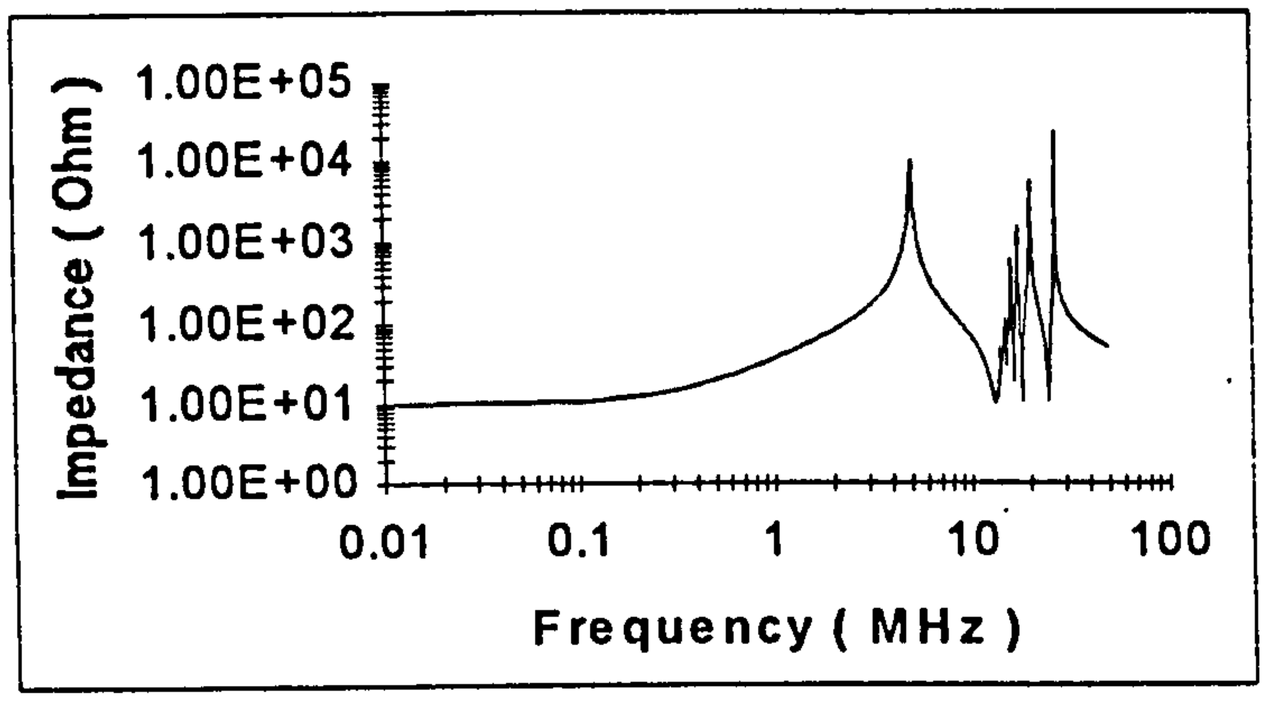

Fig. (5.12) Winding input Impedance

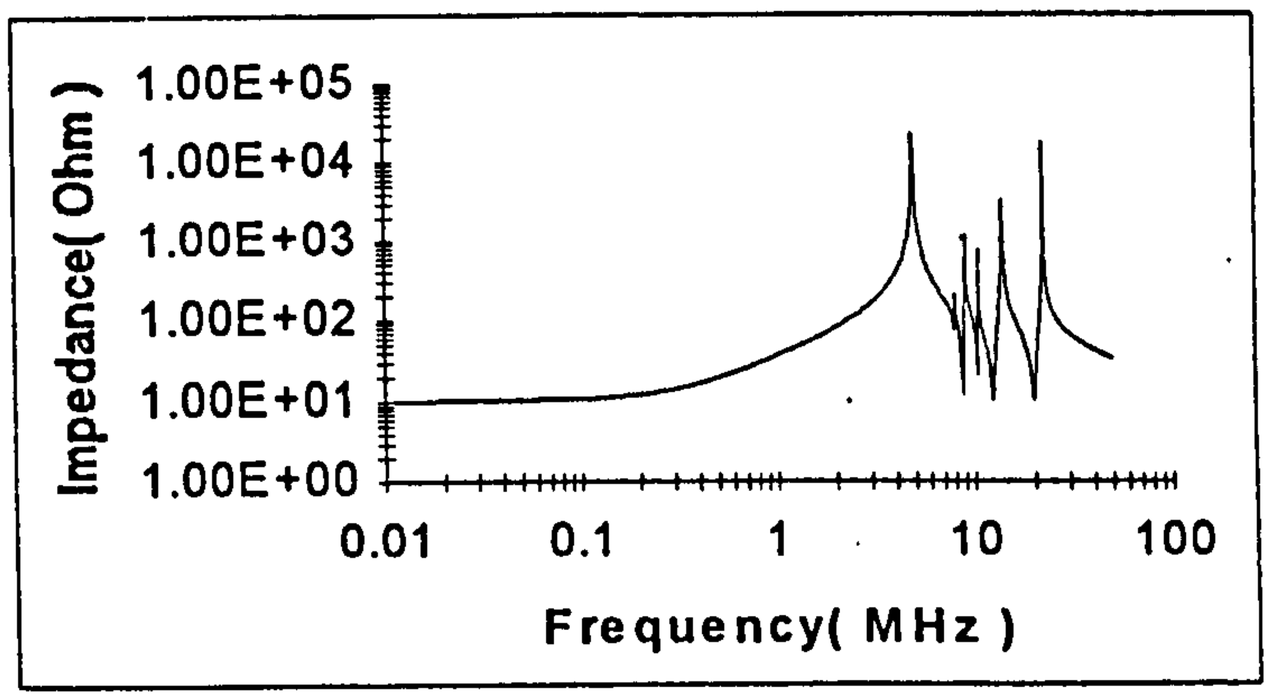

Fig. (5.13) Winding input impedance When C between Adjacent conductors is increased (0.152nF)

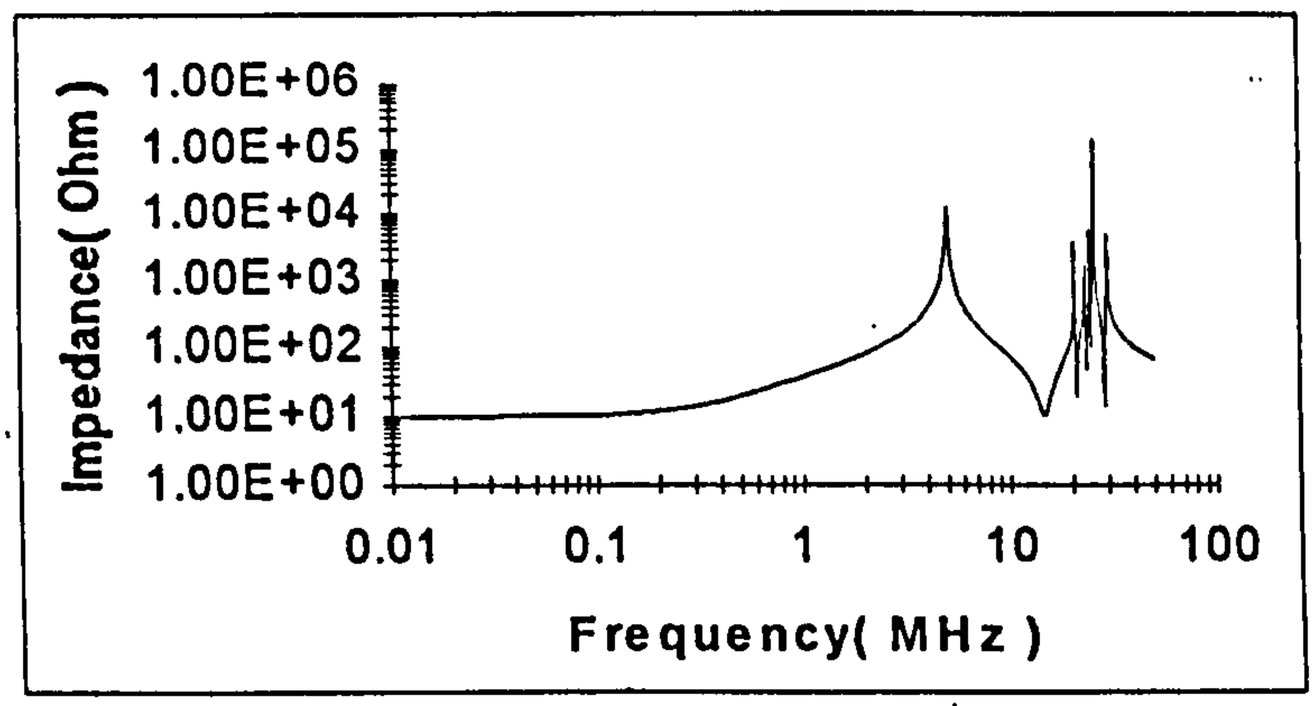

Fig. (5.14) Winding input impedance when C between adjacent conductors is decreased (6.1pF)

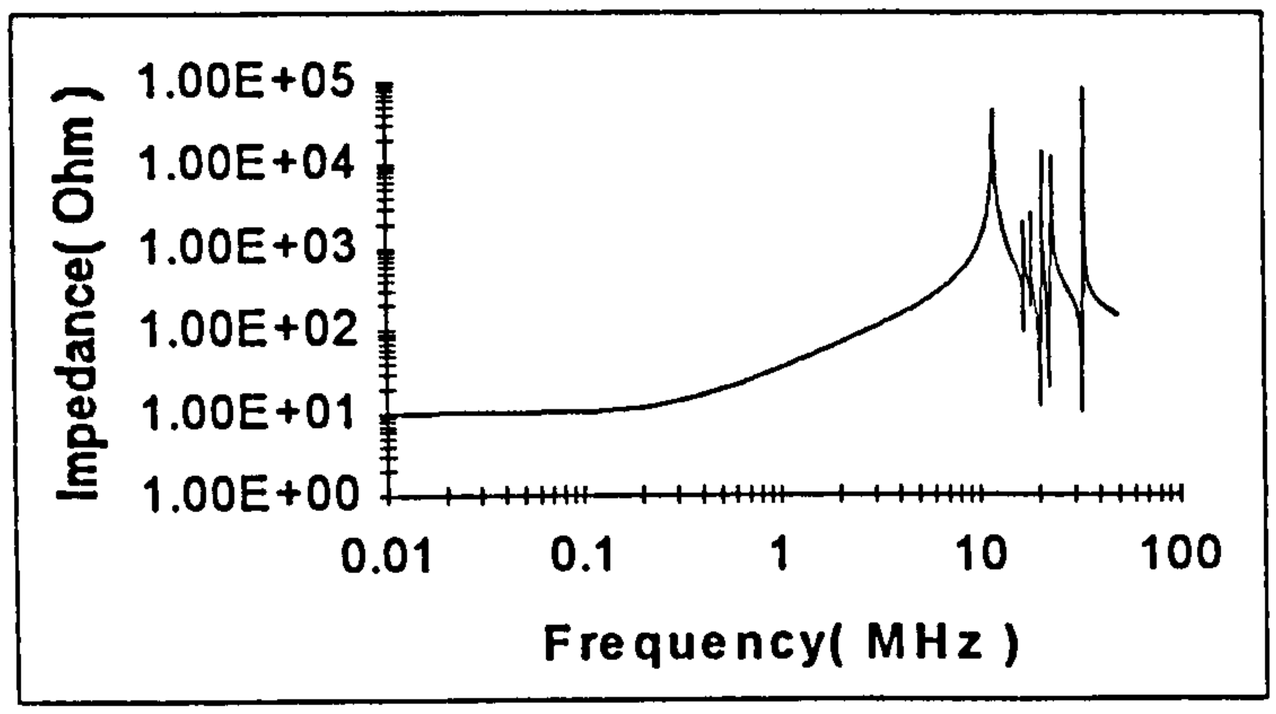

Fig. (5.15) Winding input impedance when ground capacitances decreased (8.146pF)

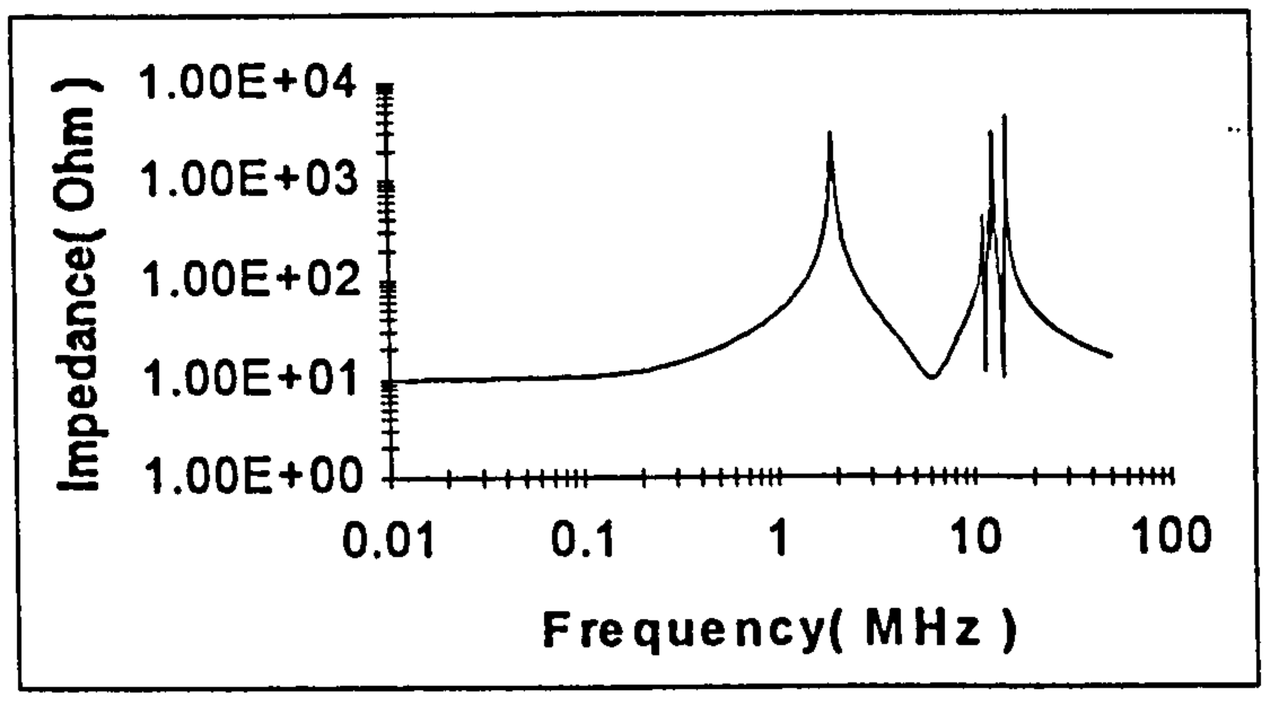

Fig. (5.16) Winding input impedance when ground capacitances increased (0.203nF)

CHAPTER SIX

TRANSFORMER ELEMENT SIMULATION USING SPICE CONVERTER MODEL.

6.1: INTRODUCTION.

The Spice simulation program is a useful and important tool for power supply design. This program can be considered as an intermediate step between analytical design and practical testing. It provides more insight into design problems and their solution before any practical work is implemented. Hence it saves time, cost and forms a basis for system improvement. Spice can also be used as a tool for evaluation of potential problems, which could destroy the semiconductor devices if a practical circuit was built without a prior understanding of the problem. For instance, volt-second and imbalance that can push the transformer to work in the saturation area.

The Spice program starts by placing the required circuit elements between nodes. The program reads all the circuit information through a file called the "net list" file. In this file, the program translates the original circuit drawing, their elements, and initial conditions. A circuit model can either be built from discrete components or using the components that already exist in its library. The computer run time tends to be long due to the number of iterations attempted. Of course this is aided through the use of a very fast computer but Spice none the less can be very cumbersome. This problem will be exacerbated if many sub-circuits have been selected and linked together to form the whole circuit as is the case here, where a full bridge converter needs to be simulated. Finally, the associated analysis specified in the input net-list file will then be executed by entering the “spice” command. The Spice program, stores the simulation results requested in either an output listing file, or as a graph data file. It has a complete set of prints and graphs called "probe" for viewing the analysis results.

The main concern of this chapter is to examine the transformer element's behaviour and their interaction with the resonant tank elements during normal converter operation. General information is given about this converter including its principles of operation, the reasons for interest in it, and the problems associated with the transformer. Nowadays, there is much interest in resonant converters, series, parallel or a combination of series-parallel. The classification depends on whether the dc-dc power conversion is being achieved through the resonant current or the resonant voltage. A converter is called series loaded when the load is in series with the resonant circuit elements (inductor and capacitor in series). The operating characteristic of this type of converter tends towards a current source with a high output impedance (high output voltage). A parallel loading converter has the opposite characteristics. The series-parallel converter combines the operating characteristics of both types.

The magnetic components (transformer and inductor) that exist in any power supply unit reduce the opportunity for improvement. Therefore, a better understanding through the simulation of these components can turn these undesired effects to an advantage.

The work in this chapter is an extension of previous research in this area [44]. In this reference, simulation was carried out to examine the transformer elements for a 20KHz half bridge converter. The ratio of the switching frequency to the resonant frequency was 0.4. In the present chapter, the work is extended to simulate a full bridge series resonant converter. The transformer equivalent circuit currently used is a high frequency transformer and it obviously contains more elements than that at 20KHz. In addition, the simulation is carried out above and below resonant frequency and at a different frequencies ratios. The simulation program used in this chapter is not the same as that used by [44].

6.2 : SIMULATION ADVANTAGE.

Megahertz frequency power supplies have received a high amount of researchs attention recently [33,48]. In this zone of operation, the resonant converter types are the only choice available. The transformer was designed (chapter two) to work at this frequency, and it was simulated using the finite elements program. The effects of the transformer elements are the main concern of the present work. The transformer was designed as a step up transformer, and therefore the converter has to be of high voltage type (series converter). The practical circuit of the present power supply (chapter two) was given previously above and below the resonant frequency of 500KHz [45]. The same circuit has been improved and built here again at 1 MHz frequency operation. The results in chapter two provide the basis of the simulation validity for the case currently studied. Bearing in mind that the aim here is to examine the behaviour of the transformer elements within the converter, the reasons behind not examining these elements practically is as follows:

1- The principles of the transformer equivalent circuit is well known which simplifies the analysis. It is difficult to implement practically, unless five or more different transformers are designed. Each of these transformers will provide an examination of a combination such as high / low inductance (leakage and magnetising), and capacitance (ground and distribution). This is rather difficult practically. Even assuming that all the above is possible, difficulties still exist due to the following :

a- The difficulty of controlling the values of these elements, where examining these elements practically means there are some degrees of flexibility to change their values within a specific range.

b- Many converters have to be designed for different duties, so a different control technique is required in each case. It is well known that each of these elements has a great influence on the power supply particularly in resonant converters.

2- The optimum power supply solution and performance is found when the supply frequency matches the transformer resonant frequency. From the open circuit impedance

curve, the voltage resonant (parallel resonant) exists either about 100KHz which is not under the present concern or at approximately 2.4MHz, which is the one currently investigated in this chapter. Care must be taken at this frequency where the semiconductor devices could be destroyed if resonant frequency is approached too closely.

In any case, the simulation can provide a clear insight in the behaviour of the transformer elements in the Megahertz zone and their interaction with the resonant tank elements. The existence of inductances (leakage, magnetising), and capacitances (ground, distributed) can turn to an advantage. These elements can be arranged to form a series or parallel resonant tank, with no additional discrete components required. For instance, many researchers have already used the leakage inductance as a resonant tank element [55]. The magnetising inductance has also been used as resonant elements [47,48], but under special treatment. The treatment was based on the fact that the primary winding is shorted during the resonant stage due to the simultaneous conduction of the output rectifier (when a full bridge output rectifier is used).

6.3 : CONVERTER MODEL

The model used to simulate the converter above and below resonant frequency is not significantly different to the practical model. The simulated model follows the same stages that were discussed in chapter two. The simulation difficulties involved with each stage will be explained. Every effort has been made to reduce the differences between the practice and the simulation. In both resonant cases (above and below) the resonant tank inductor consists of the reflected leakage inductance of the transformer in the primary in series with an external inductor. The transformer has been placed between the resonant inductor and the capacitor. Practically, this arrangement has an advantage, where in the

full bridge converter, an ON pair in one half cycle may have a different storage time than the second half. This means, the on-voltage drop in both MOSFET legs may be unequal, and the volt-second product applied to the transformer primary is unequal as well. This can cause the centre of the hysteresis loop to change which saturates the core and this can damage the device. In order to avoid this flux imbalance a capacitor is usually placed in series with the transformer.

It is obvious, that the switching signal of the present converter is arranged to give a quasi-square wave voltage across the tank both above and below resonant frequency. The inductor (and/or transformer leakage inductance) and the capacitor forming together the tank of the series resonant circuit. Another advantage of the inductor is to charge and discharge the capacitance of the devices to achieve zero voltage switching and hence reduce the switching losses.

In general, when any of the devices (MOSFET) is turned off, its capacitance is charged by the main supply dc voltage. This capacitance has to be discharged prior to turning the device on to achieve zero voltage switching, and this reduces the switching losses. there are two ways of doing this, either supplying a negative current to discharge the capacitance, or to cause it to oscillate with an external inductor. The same technique can be employed to achieve zero current switching, but instead of a capacitor an inductor is used, and a negative voltage applied to discharge the inductor energy or to cause it to oscillate with a capacitor. These two techniques (zero-current, zero-voltage) are very important for any converter operating in the Megahertz zone to damp the switching losses.

6.3.1 : INPUT STAGE.

The input stage has already been discussed in chapter two and consists of two parts, a rectifier and a filter circuit. The simulated input dc voltage can be taken from a full bridge rectifier model of a sine wave source input. The voltage drop in the input rectifier diodes can also be taken into account. For the best accuracy, the whole converter has to

be simulated in less than one nanosecond time steps. One problem that arises is that of matching the input rectifier time step (msec.) with the converter time step of nanoseconds. Hence, the rectifier circuit alone can run faster than the whole converter. This problem may be overcome by running the program to msec., which allows the dc voltage to build up. However, this is a quite expensive way as it requires a large amount of computing time. An alternative way of saving run time is to use a pure dc input source that contains a completely ripple free output.

6.3.2 : POWER, ISOLATING, AND CONTROL STAGES.

The equivalent n-channel MOSFET circuit model that is used for the transient analysis is shown in Fig.(6.1), in which all the data can be obtained from the manufacturers data sheet. This model was given previously by Ram et al [84]. The drain to source capacitance (Cds) is introduced in the present work for high frequency validation [85]. In this model, three capacitances are typically used, and their values are given in the manufacturers data sheet. First is the gate to source capacitance, usually referred to in the manufacturer data sheet as the input capacitance (Ciss). Second, is the gate to drain capacitance referred to as the reverse transfer capacitance (Crss). Third, is the drain to source capacitance usually referred to as the output capacitance (Coss). The gate to drain capacitance (Cgd) is equal to Crss at high Vds, Cgs is equal to Ciss minus Crss at high Vds, and Cds is Coss minus Crss at zero Vds. A non-linear current source (J) is used to model the forward drain source current and the static body diode. The step by step detail of calculating the elements of the MOSFET equivalent circuit is given in many references [85,86].

The clamped shotcky diode is available in the spice program library. The rest of the diodes are modelled by the diode model given in Fig.(6.2) [84]. In this model the parameters consist of resistance, two non-linear current sources to model the forward

and backward currents, leakage inductance, and depletion layer capacitance. The detail of the way to calculate these parameters is explained in [85,86].

The problem of isolating the two top MOSFETs of the converter bridge looks easier in simulation than in practice. There are two ways this can be achieved, either using the Spice library optoisolator model or assigning the circuit to a different ground.

The switching signal is provided by a very simple control circuit involving a type three error amplifier and comparator as shown in Fig.(6.4). There are six unknown components in the error amplifier to be selected. By choosing any of the two resistances (say R1, and R3) arbitrarily, the remaining four can be found readily at the design frequency [50,85]. The four equations required are two zero's frequencies at C2 R3 and R1R2C1, and two pole frequencies R3C2C3, and C1R2. The output of the error amplifier which is within a 3V amplitude is to be compared with a 5V sawtooth waveform. During the simulation nothing changes rapidly, and hence the four MOSFETs may be supplied from different sources as switching signals, i.e. without the control circuit. Nevertheless, this has proved to give an error which is relatively small at low frequency but grows as the frequency goes higher.

6.3.3 : TRANSFORMER MODEL

The simplified transformer equivalent circuit model derived in chapter four is used in this analysis. In this model the core and copper losses are neglected, and hence no resistances exist. However, the resistance has a well known effect which was studied heavily in chapter three. The model consists of leakage inductances and distribution capacitances for both primary and secondary windings, magnetising inductance, and ground capacitance. All the secondary elements are referred to the primary side by the turns ratio of 14/26 as explained previously. Surprisingly, researchers in this area [36,44], have been concerned about transformer elements and ways of estimating their value in the audio frequency range (20KHz), but no further study, very few have been concerned about

these elements for higher frequencies such as those in the megahertz zone. It is logical to think that the most visible effect of these elements is present at this higher frequency. Again, all the power supplies operating in the megahertz zone are of the resonant type, and the value of these elements can be added with the resonant tank elements. This could lead to a serious consequence as it may push the power supply to work out of its design frequency which can cause failure. A further study of these elements can turn their undesired effect into an advantage, and then there will be no need for extra inductors or capacitors.

The transformer simplified equivalent circuit replaces the original transformer of the power supply circuit. However, the equivalent circuit can be arranged in a different way if required using a dependent current and voltage source [84]. But in this case the purpose of examining the transformer elements is not possible, because this circuit does not contain these elements.

6.4 : PRINCIPLE OF OPERATION.

Fig.(6.3-6.4) show a series resonant converter and its gating signals above resonant frequency [45]. The converter circuit, gate signals, and principle of operation below resonant frequency has already been discussed in chapter two. Hence, the operation principle of this section is concerned with the case where the switching frequency is higher than the resonant tank frequency. The ratio of the switching frequency to the resonant frequency is considered to be 1.2, in a similar manner to the value of 0.8 for the case below resonant frequency.

The way of selecting L and C of the resonant tank is not arbitrary. During the resonant frequency calculation, the selection of any L or C will be at the expense of the other. Usually for optimum operation, the characteristic impedance of the resonant tank (Z) has to be matched with the load impedance (Zload), which leads to the following relationships:

$$Z = \sqrt{\frac{L}{C}} = Zload\,,\ \omega_o = 2\pi f = \frac{1}{\sqrt{LC}}$$

$$L = \frac{Z}{\omega_o}\ \text{, and}\ C = \frac{1}{\omega_o Z}$$

The switching frequency can be selected then from either of 1.2 or 0.8 at the resonant frequency (ω_o).

Although, the switching signals in Fig.(6.3) have shown the sequences of operation of all MOSFETs and diodes, a further point will be mentioned here. At the beginning of a new cycle, T1 and T2 are conducting, and so the current is circulating through the resonant inductor. The two antiparallel diodes (D1 and D2), are conducting until the resonant inductor current changes its polarity. At this moment the resonant capacitor charges to a maximum voltage. When D1 and D2 are turned off, the current discharges the capacitor voltage, where it reaches zero when T1 is turned off. The inductor current starts to flow through T2 and D3 charging the capacitor. The negative cycle of the resonant tank follows the same procedure, and the process repeats itself.

It clearly follows that the antiparallel diodes of any two MOSFETs are conducting for a short period until the resonant current changes its polarity. Therefore, the principle is to turn the devices off at zero voltage. This procedure may not help to reduce the losses practically at frequencies approaching Megahertz unless a capacitor is placed across each of the MOSFETs. This capacitor can help to force zero voltage switching to reduce the turn on losses of the device. Another solution is to introduce a short dead gap between each of the two legs of the MOSFETs, where the diode is conducting prior to its associated MOSFET. The zero voltage switching ON can then be forced to work.

6.5 : TRANSFORMER ELEMENTS AND POWER SUPPLY PERFORMANCE.

In the simplified transformer equivalent circuit given in chapter four, some points are to be observed. The low cut off frequency (first parallel resonant frequency) is determined

by the magnetising inductance and ground capacitance. The high cut off frequency (second parallel resonant frequency) is determined by the leakage inductance and distribution capacitance. The arrangement of all the elements in the transformer equivalent circuit determines the series resonant frequency. Therefore, any change in the values of these elements will reflect a change in the appropriate resonant frequency. The clear insight to the influence of these elements then is by examining each of the elements individually.

Fig. (6.5) and Fig. (6.6) show the results of the power supply simulation. Since all of the transformer elements are referred to the primary side, the resonant voltages and currents are referred to the transformer primary side by the turns ratio. These figures show the resonant tank and resonant capacitor voltages. In addition, the figures also show the resonant inductor current (primary current), and the secondary current of the transformer. The results of these two figures are calculated for both cases i.e. where the switching frequency is above and below resonant frequency. The ratio of the switching frequency to the resonant tank frequency is considered as 0.8 and 1.2 below and above the resonant respectively. The output load is assumed to match the resonant tank characteristic impedance ($Z = \sqrt{L_r / C_r}$).

In order to show the effect of the transformer elements, waveforms under the normal operation of the power supply are considered first. The first element to be examined is the magnetising inductance. When the magnetising inductance is removed (i.e. open circuited) as shown in (b) of both figures, the ground capacitance now is part of the resonant tank capacitor. The voltage across the resonant tank capacitor is reduced by 0.72 and increased by 1.2 of the normal operation for below and above resonance respectively. The reason is that as the resonant capacitor is increased, the resonant frequency is reduced, and hence the resonant frequency is away from the series resonant frequency of the transformer when working below resonant frequency, and close to the series resonant frequency in the case of working above resonant frequency. That means (referring to the impedance curve in chapter four), the voltage is reduced below resonant and increased above resonant frequency. It should be noticed, that the switching

frequency is selected to be near the series resonant frequency of the transformer for a better performance. The observation of the currents in both windings indicates an oscillation in the secondary current. This oscillation is due to shifting the first cut off frequency to the value that it very close to the dc, by removing the magnetising inductance. The switching frequency is far away from the series resonant frequency, and the frequency ratio may be less than 0.05. The oscillation no longer exists in the above resonant case for the same reason. This fact indicates that the magnetising inductance has the major effect in the below resonant case but not in the above resonant case.

The same situation is shown in the case when the ground capacitance is removed (c). For the same reason above, the voltage across the resonant tank is increased by 1.1 and reduced by 0.7 below and above resonant frequency respectively. The oscillation is reduced by 50% as compared to that when the magnetising inductance is removed. This oscillation no longer exists in the case when the switching frequency is higher than the resonant tank frequency.

Neglecting the distribution capacitance between the winding turns has not introduced any resonant tank voltage effect in both cases under study (above and below). This is because it has nothing to do with the resonant tank frequency, but this effect becomes greater if the converter is parallel loaded rather than series. Therefore, it can be used as resonant tank element in the parallel resonant converter but not in a series converter. However, in the case under study the waveforms given in (d) of both figures have shown a large reduction in the secondary current oscillation when this capacitance is removed. Practically, this reduction in the capacitance will be at the expense of an increased leakage inductance.

Through the examination of the above and below resonant cases, it seems that the best case is the above resonant case. The transformer elements have shown a limited effect on the power supply in comparison with the below resonant case. In the below resonant case when both the magnetising inductance and the ground capacitance are removed, the result is shown in (e). Removing the magnetising inductance means no magnetising current i.e. an infinitely permeable core Here, the first cut off frequency no longer exists.

The series resonant frequency of the transformer is dominated by the leakage inductance and the distribution capacitance of both primary and secondary windings. It should be noticed that this case is not equivalent to an air core transformer. An air core will increase the magnetising current i.e. make the magnetising inductance smaller. The ground capacitance cannot be removed by an air core due to the existence of the winding ground, but this is less than using a core. Usually the closest ground is the core, and the problem of increasing the leakage will be much higher in the air core than when using a core. It would be better if the reduction of the ground capacitance was of the same magnitude as the reduction in the distribution capacitance as shown in (f) of the same figures. This can be considered as the best case of working below resonant frequency.

The ratio of the switching frequency to the resonant frequency has also been under attention. The simulation has shown that when the ratio is reduced to 0.4 instead of 0.8, a change is introduced to the resonant tank voltage. Within the normal tank voltage waveform there is a partial charge and discharge. In addition the oscillation gets worse as the ratio is reduced lower than 0.8. When the ratio goes higher than 1.2 above resonant, the low frequency oscillation (a little bit is shown in the secondary current in Fig. (6.6)) is getting worse. In this case, the resonant tank capacitor has to be split between the primary and secondary to reduce the low frequency oscillation [36].

6.6 : EFFECTS OF TRANSFORMER ELEMENTS ON THE OUTPUT.

In this section, the investigation is continued to study the effect of the elements on the output voltage of the power supply. The examination took place by changing the values of each of the elements individually. The calculated results are given in normalised values. The normalised relation of (Vo/nVin), where n is the turns ratio is used for this

purpose. Three cases at frequency ratios of 0.4, 0.8, and 1.2 are considered as shown in Fig. (6.7abc).

In Fig.(6.7 a), the value of the distribution capacitance is changed to higher and lower than its original value. The output reduced to a value which is different by 1.65 at frequency ratio of 0.8, compared with a frequency ratio of 0.4 at below resonant frequency. At one value of the distribution capacitance the output reaches the minimum value. The graph indicates that the magnitude of the maximum to minimum level is the best at 0.8 rather than that at 0.4. As previously discussed, the distribution capacitance determines the second cut off frequency, where as its value increases the cut off frequency is reduced. Therefore, the minimum value of the curve represents the point at which the switching frequency matches with parallel resonance of the transformer. The same and opposite situation happens in the case of the frequency ratio of 1.2 above resonant frequency. If the magnetising inductance and ground capacitance are both removed, the output voltage drop is small. The drop is 2.3%, 4.2%, and 1.8% at frequency ratio of 0.4, 0.8 and 1.2 respectively.

Fig.(6.7 b) shows the case of changing the value of the ground capacitance. In both below resonant cases (0.4, and 0.8), the output is reduced as the capacitance is increased. The reduction is steeper at a frequency ratio of 0.4 but less of a reduction at a frequency ratio of 0.8. The effect of changing the capacitance is less at the ratio of 1.2, and the output increases as the ratio is increased above the resonant frequency. If the magnetising inductance is removed, the voltage drop on the output is greater. At a ground capacitance of 12nF, the drop is 17%, 11.3%, and 7.5% at frequency ratios of 0.4, 0.8, and 1.2 respectively.

In Fig.(6.7 c), the magnetising inductance value is plotted against the output voltage. As is well known this inductance is a function of the core current. As the core current is increased, the value of this inductance is decreased until saturation when its value is zero. Practically this inductance value can be changed without affecting the other transformer elements by changing the core air gap. In both below resonant cases, the output reaches a maximum at one value of the magnetising inductance, this is called the optimum value

[44]. The magnetising inductance at which this maximum value occurs is different at 0.8 than at 0.4. This means that less air gap is required as the ratio is increased. The same effect can be seen in the ratio of 1.2, but the output voltage is increased as the magnetising inductance increases. The reason for this maximum value occurring is that as the magnetising inductance value is reduced from that originally used by the equivalent circuit, the first cut off frequency increases to match that of the switching frequency. This means that the switching power supply is working in the area of resonance. If the ground capacitance is removed, the effect of the magnetising inductance on the output is negligible. the voltage drop with respect to the normal operation is 2.2%, 4.1%, and 1.8% at the frequency ratios of 0.4, 0.8 below, and 1.2 above resonant respectively.

6.7 : SUMMARY.

The simulation was carried out to study the effect of the transformer elements on the power supply performance. Many cases have been considered by examining each of the transformer elements individually. The full circuit was simulated in a step by step procedure using the well known Spice program. The two cases at which the simulation is performed are where the switching frequency of the power supply is higher and where it is lower than resonant tank frequency.

It was found that the best performance is achieved at frequency ratio of 0.8 below resonant and 1.2 above resonant. As the switching frequency is increased to megahertz for instance, the best choice available is the case of 1.2 above resonant. This case has shown a stable power supply performance and a very limited deterioration of the transformer elements. If the below resonant power supply required then the frequency ratio of 0.8 is advisable. When this is required at a higher frequency operation, more effort is required to reduce both ground and distribution capacitances. A circuit requiring low capacitance to ground presents a special challenge to the transformer designer. In order to reduce this capacitance a core with a large window is required. In this case there is no point in increasing the frequency to achieve lower sized magnetic components. The

results also show that reducing this capacitance can cause an undesired oscillation in the secondary current. Reducing the distribution capacitance is a better choice than reducing the ground capacitance. The distribution capacitance can be reduced by increasing the space between conductors and by changing to a dielectric material with lower dielectric constant. There is an unavoidable increase in the leakage inductance when the capacitance between winding turns is decreased.

In order to avoid all of these difficulties, the above resonant frequency ratio of 1.2 is the best solution at higher frequencies (above 500KHz).

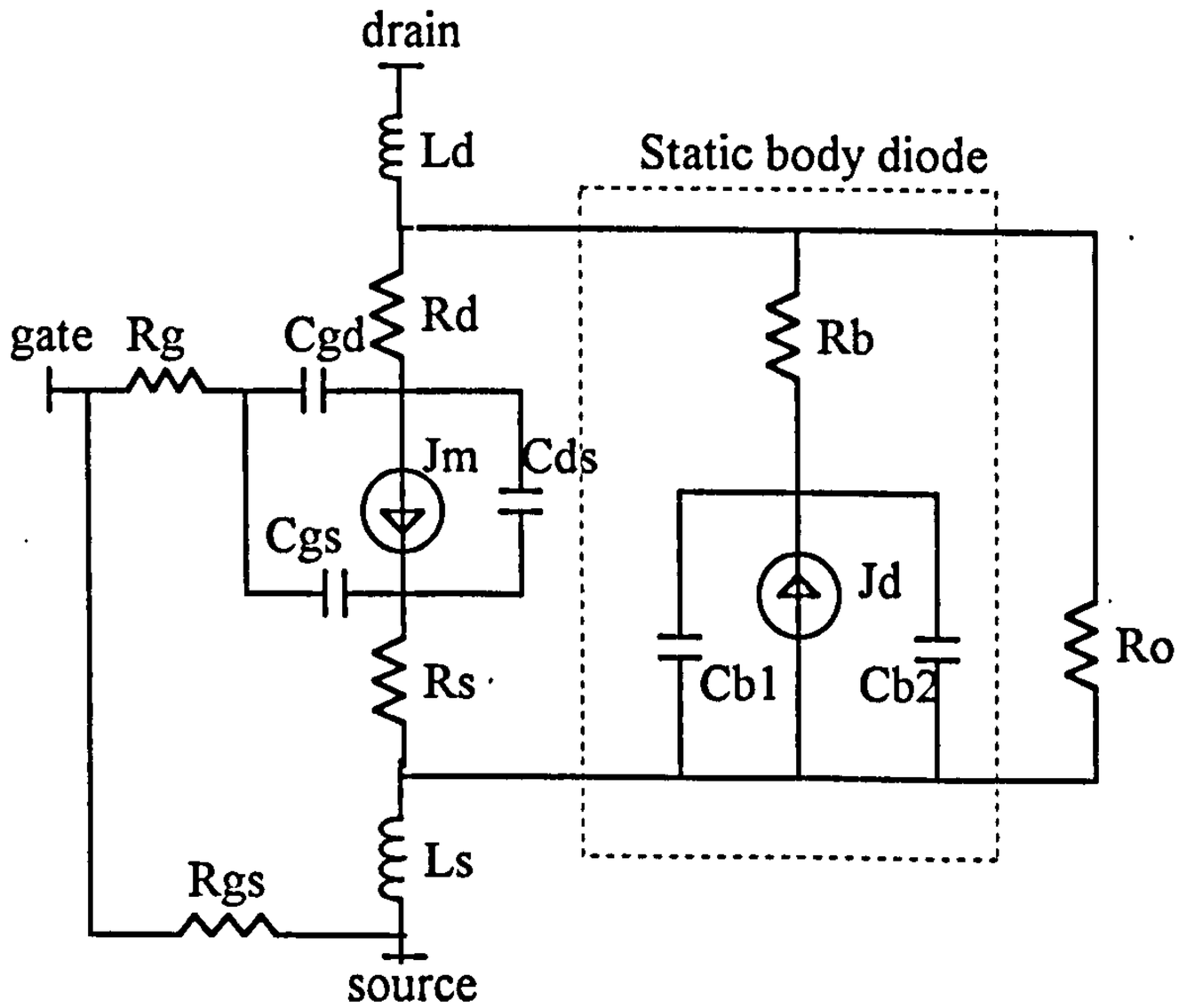

Fig.(6.1) : High frequency MOSFET model

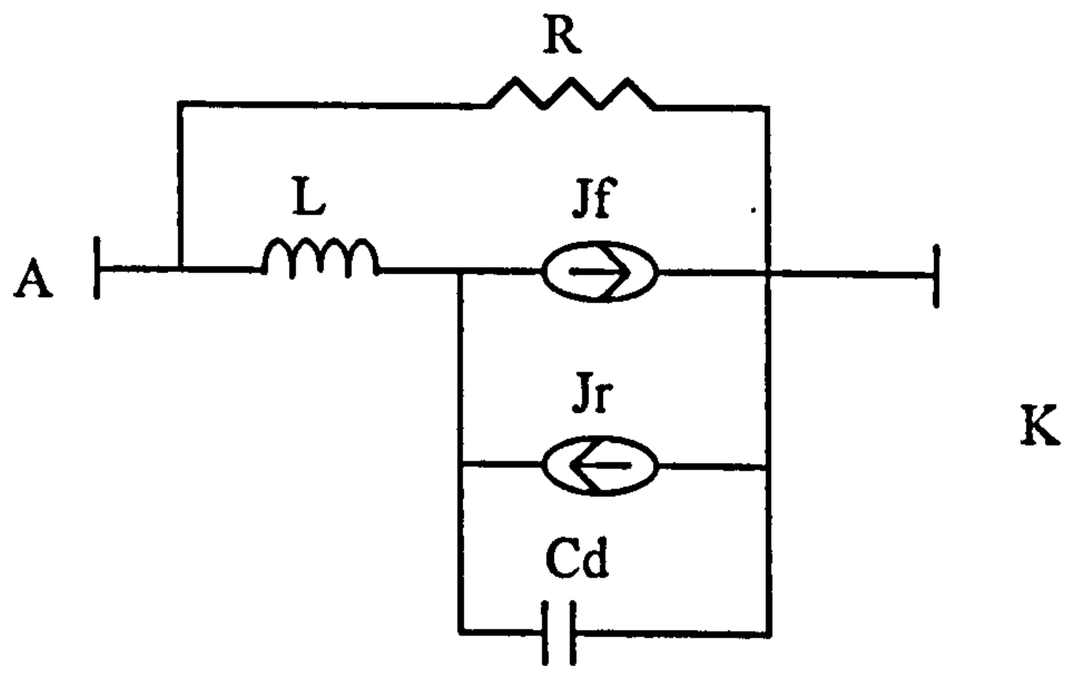

Fig.(6.2) : Diode model

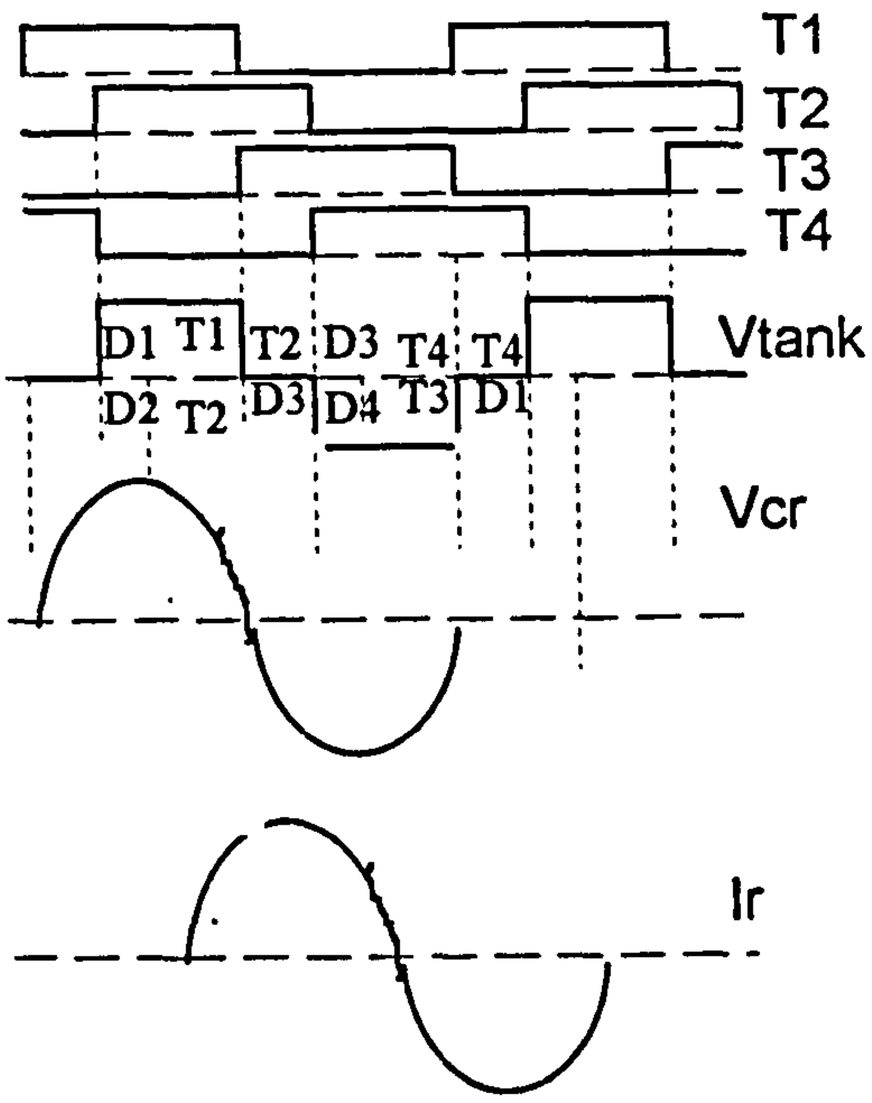

Fig. (6.3) : Switching signals

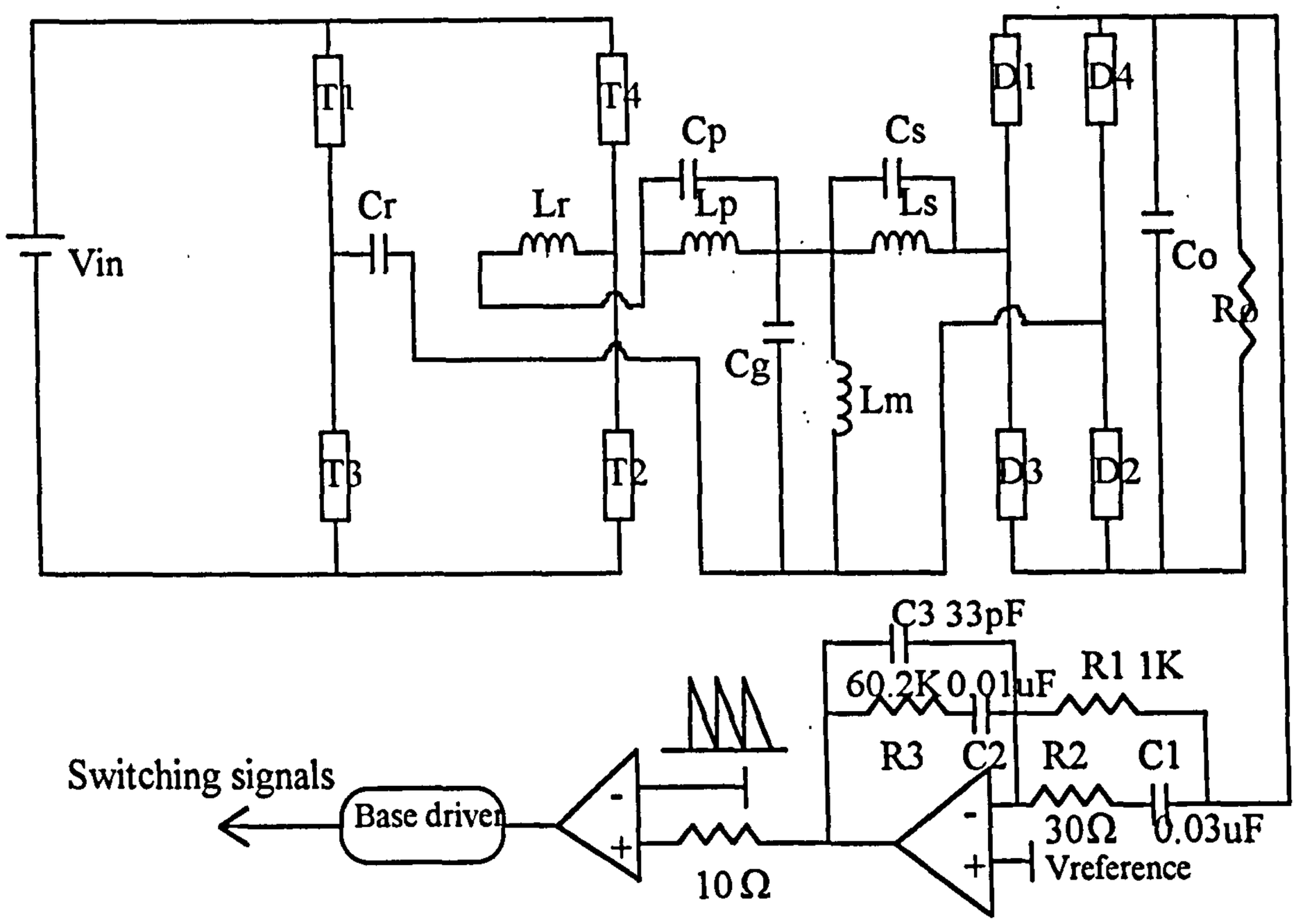

Fig.(6.4) : Spice power supply model

Fig.(6.5): Below resonant, simulated waveforms: (a) Normal operation, (b) no Lm, (c) no Cg, (d) no Cd, (e) no Lm, and no Cg, (f) no Cg, and no Cd

(a)

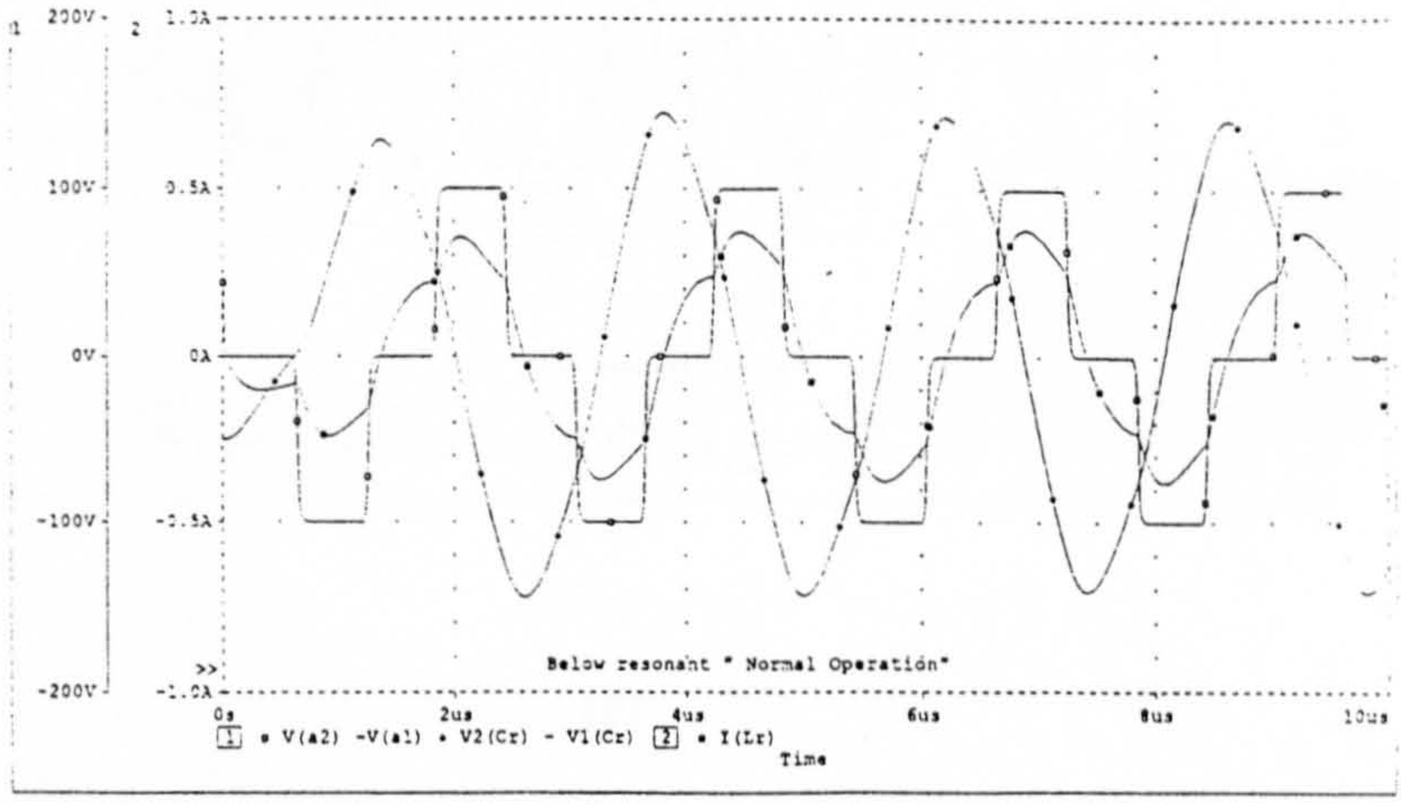

(b)

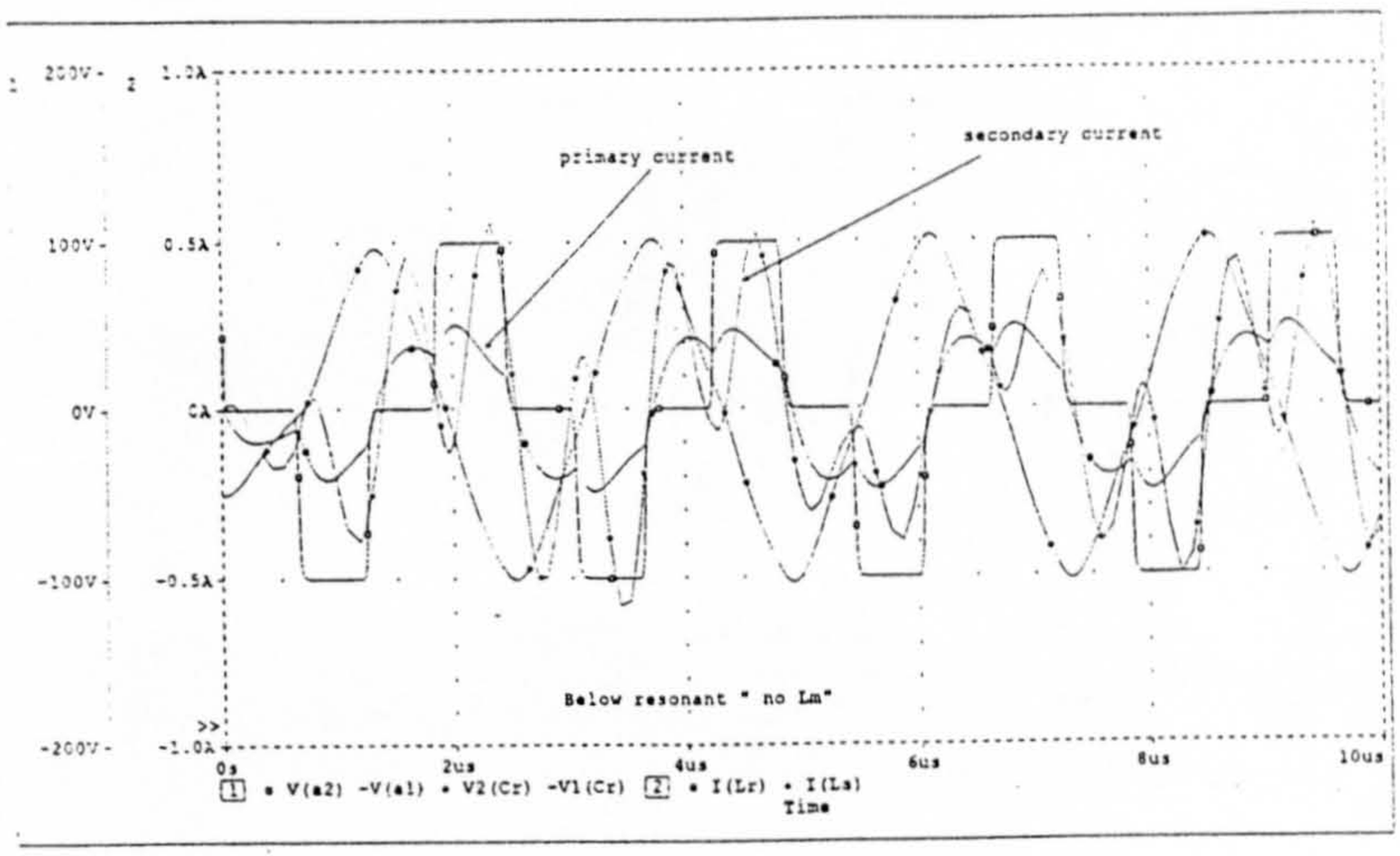

(c)

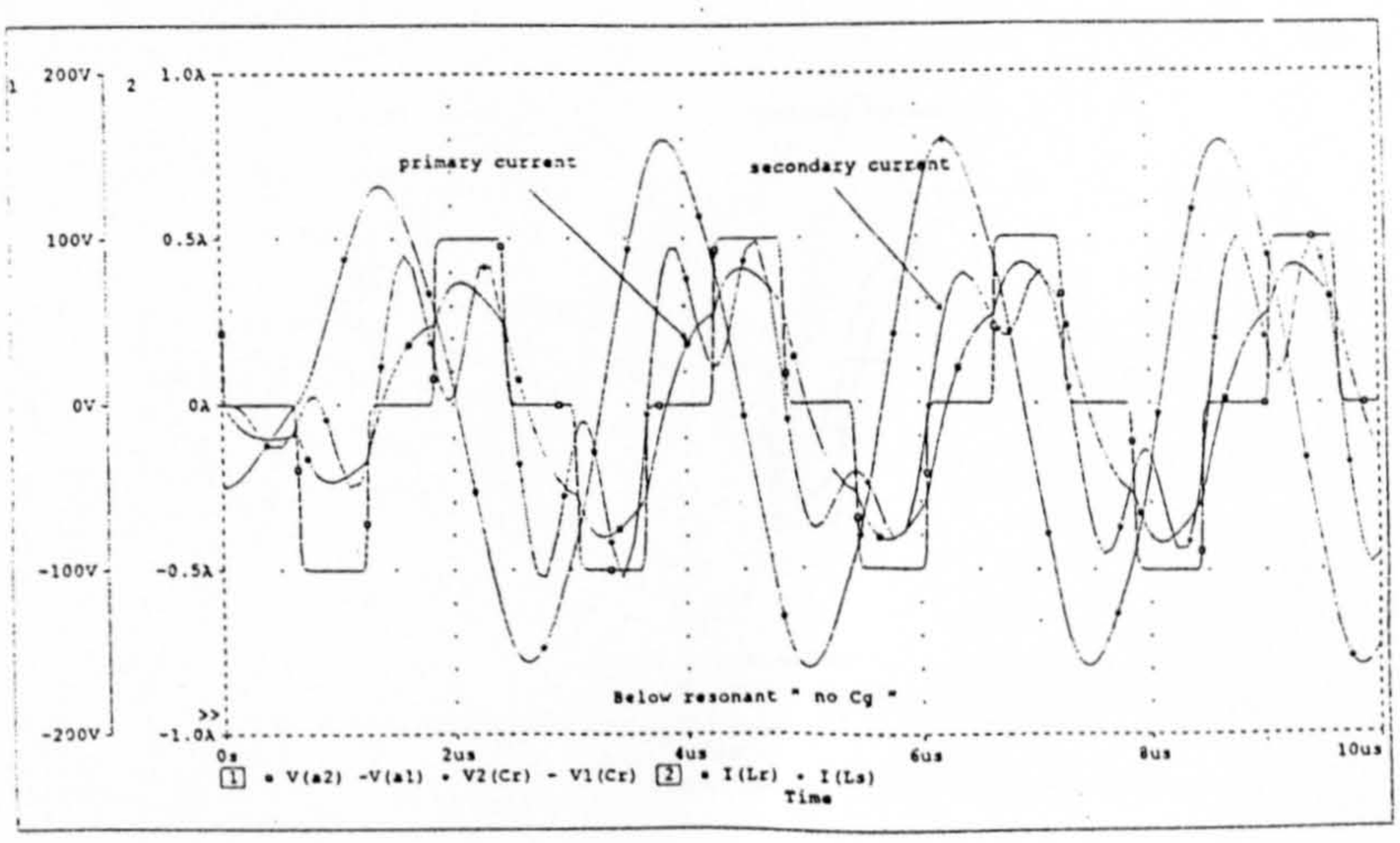

(d)

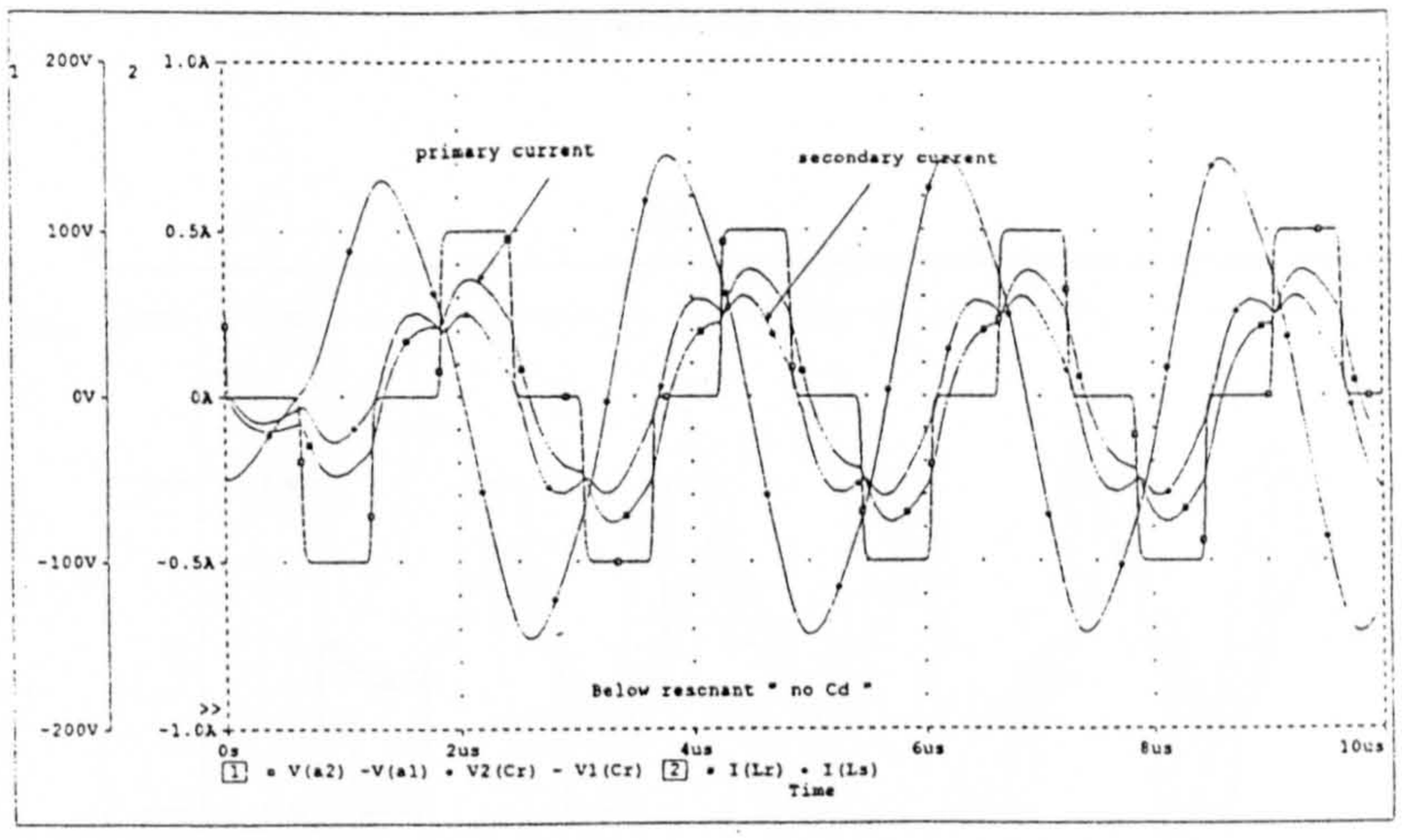
200V
1.0A
primary current
secondary current
100V
0.5A
0V
0A
-100V
-0.5A
-200V
-1.0A
0s
2us
4us
6us
8us
10us
V(a2) -V(a1) • V2(Cr) - V1(Cr) • I(Lr) • I(Ls)
Time
Below resonant " no Cd "

(e)

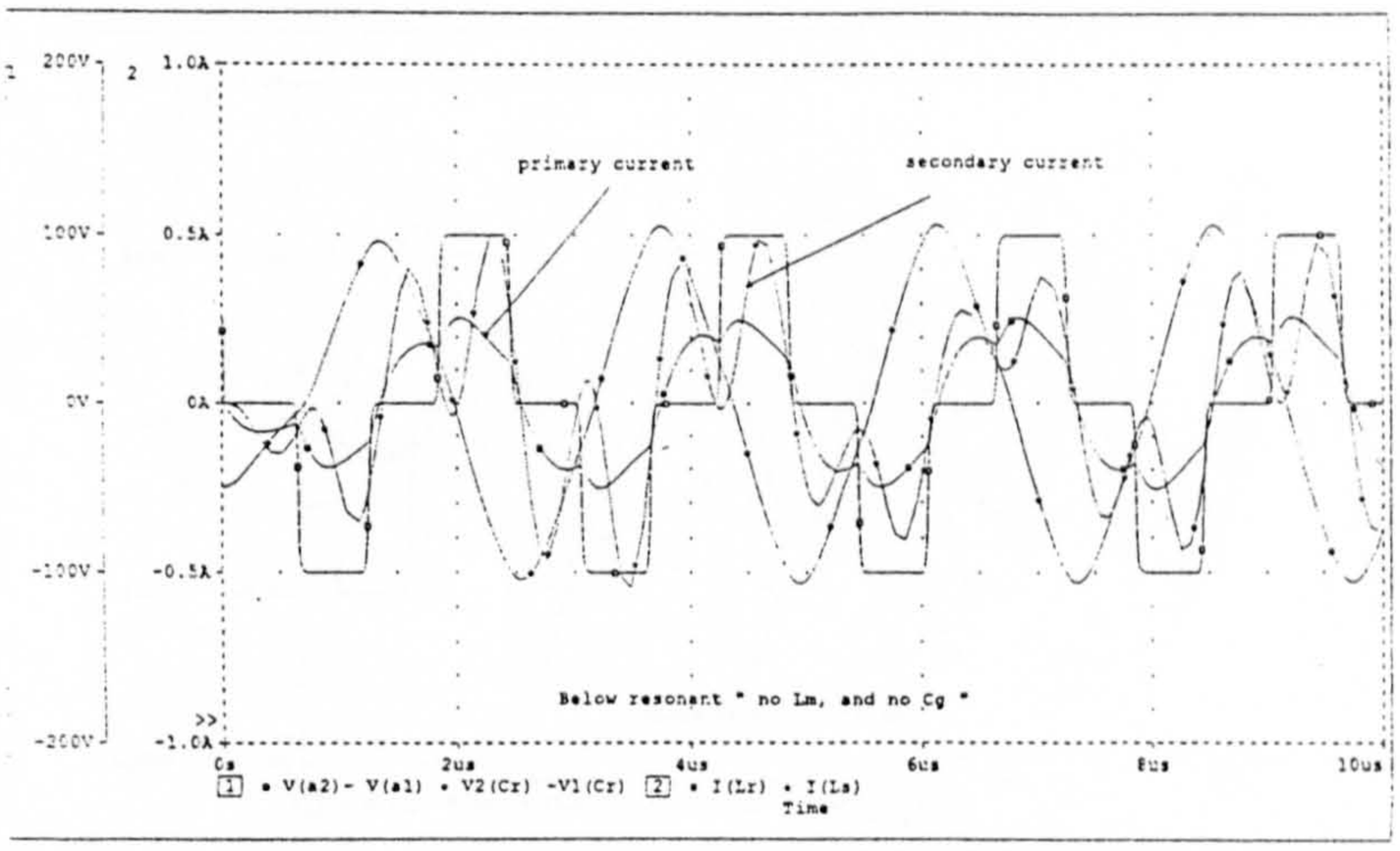
200V
1.0A
primary current
secondary current
100V
0.5A
0V
0A
-100V
-0.5A
-200V
-1.0A
0s
2us
4us
6us
8us
10us
V(a2)- V(a1) • V2(Cr) -V1(Cr) • I(Lr) • I(Ls)
Time
Below resonant " no Lm, and no Cg "

(f)

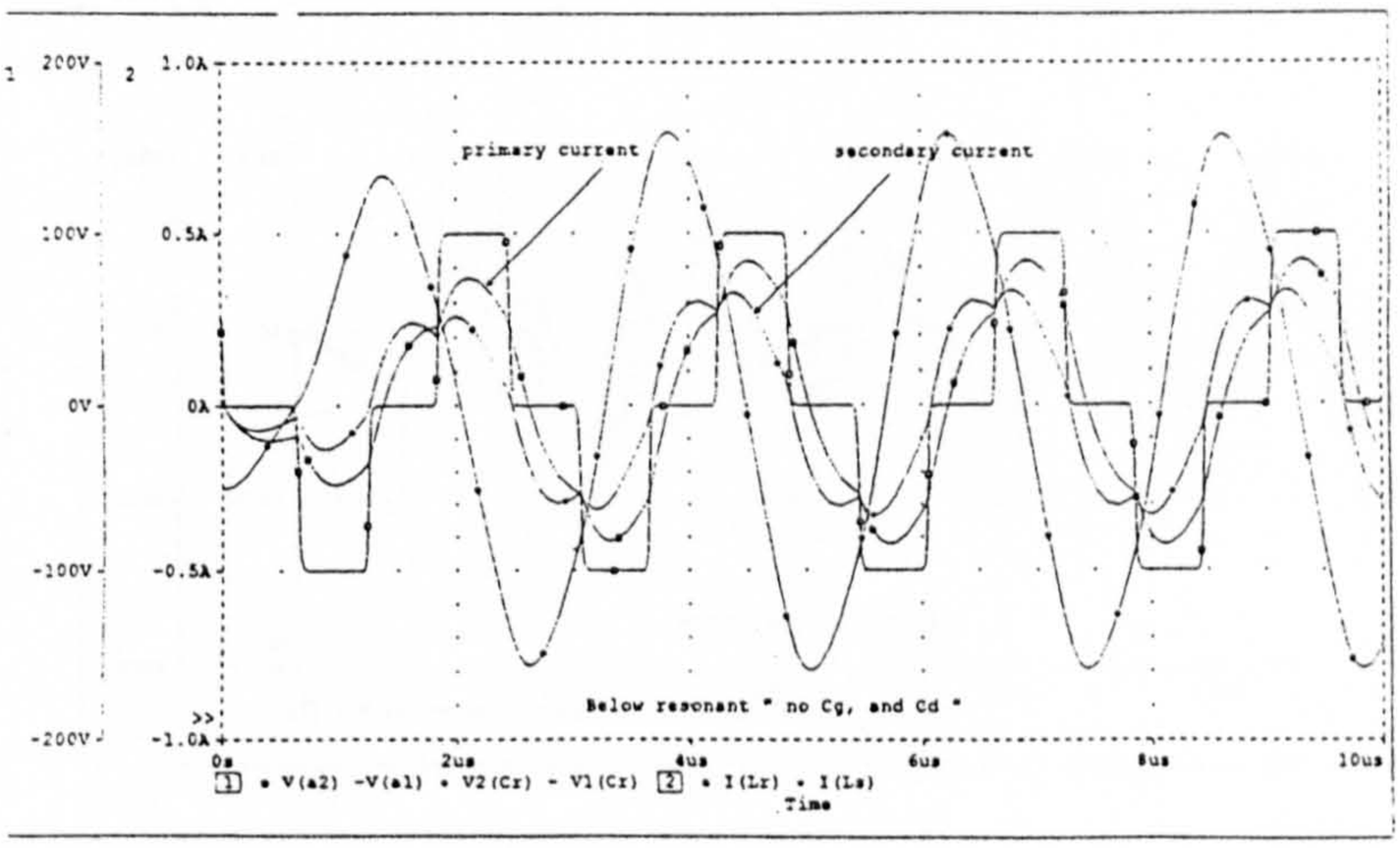
200V
1.0A
primary current
secondary current
100V
0.5A
0V
0A
-100V
-0.5A
-200V
-1.0A
0s
2us
4us
6us
8us
10us
V(a2) -V(a1) • V2(Cr) - V1(Cr) • I(Lr) • I(Ls)
Time
Below resonant " no Cg, and Cd "

Fig.(6.6): Above resonant, simulated waveforms: (a) Normal operation, (b) no Lm, (c) no Cg, (d) no Cd, (e) no Lm, and no Cg, (f) no Cg, and no Cd

(a)

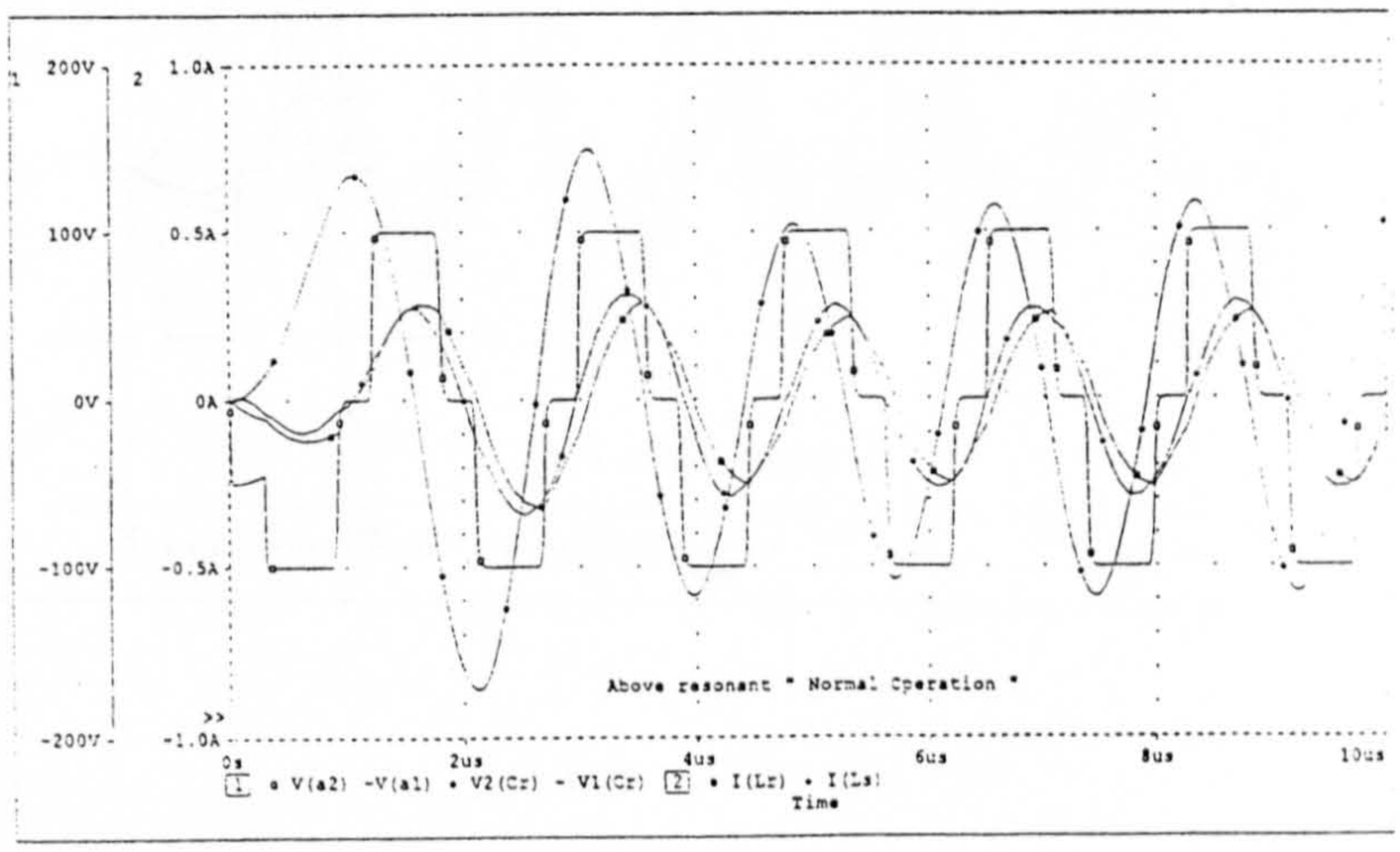

(b)

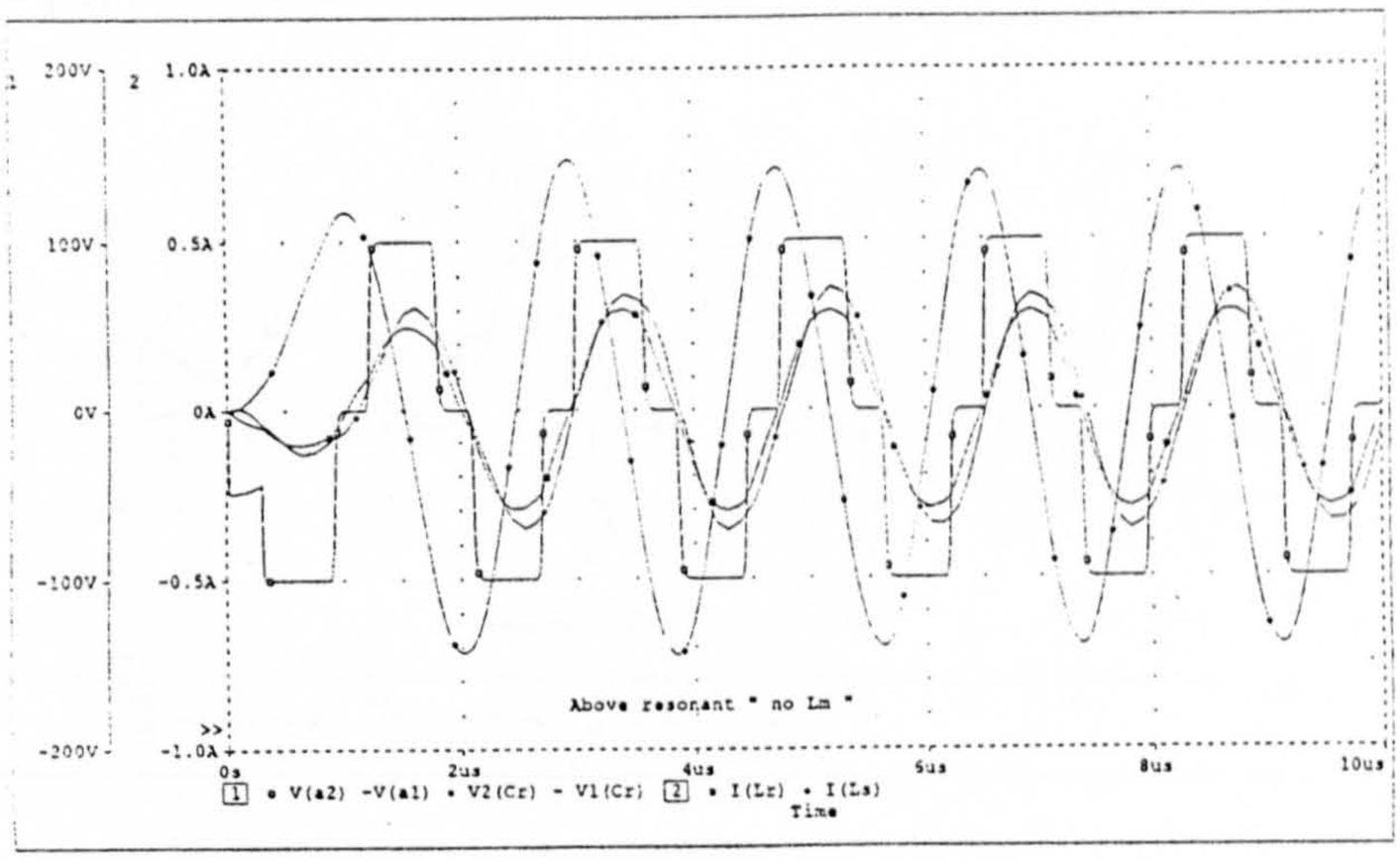

(c)

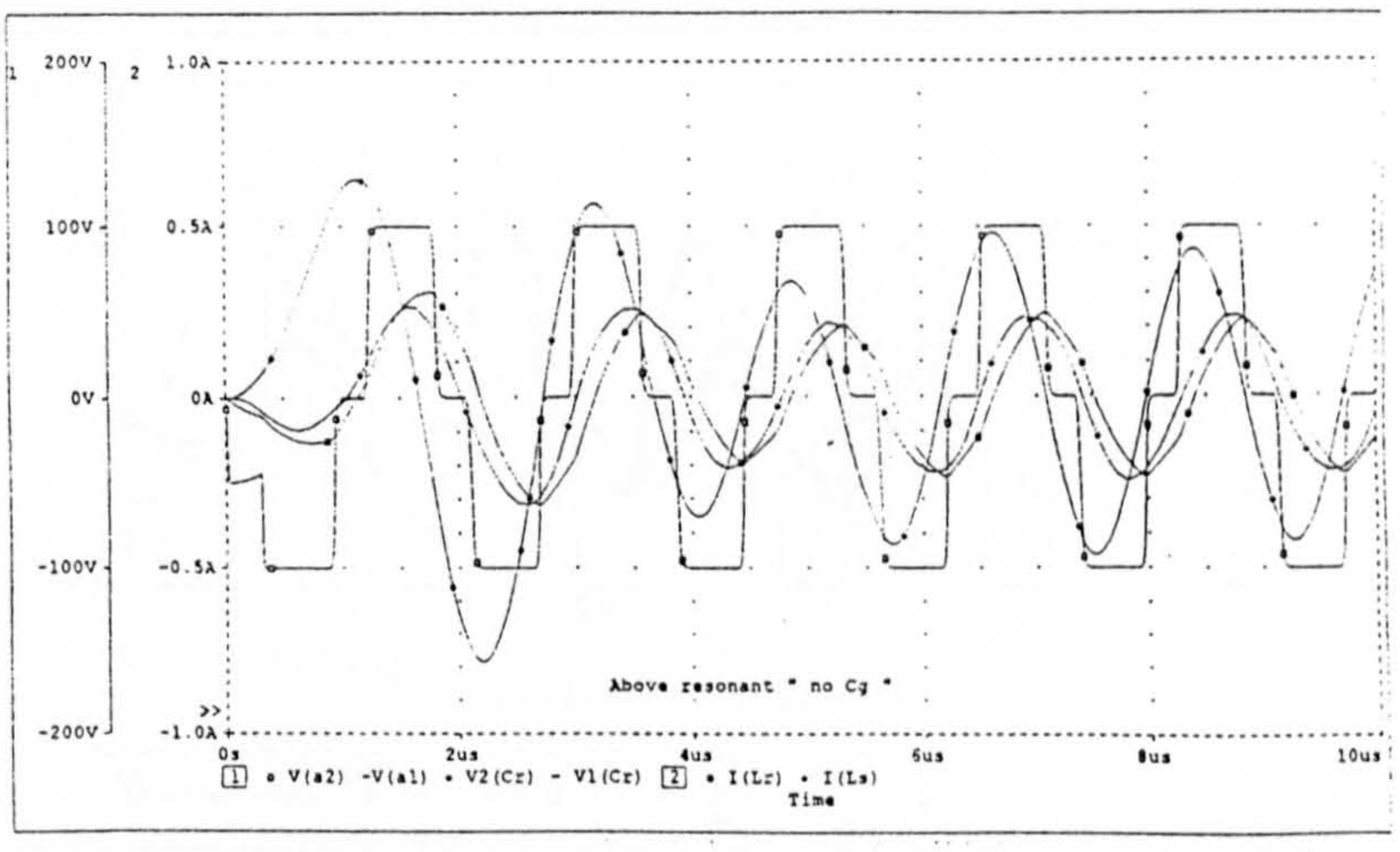

(d)

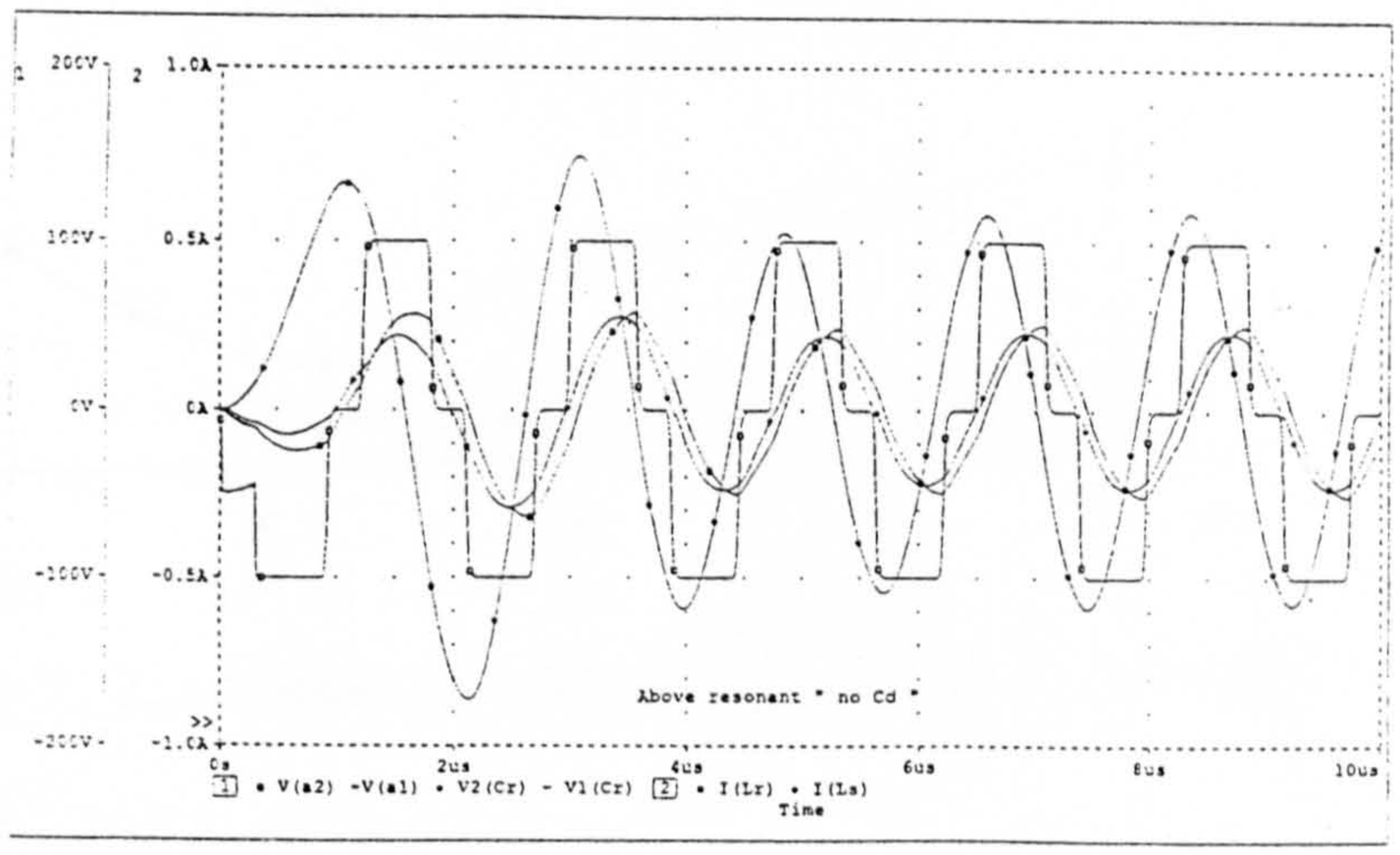
200V
100V
0V
-100V
-200V
1.0A
0.5A
0A
-0.5A
-1.0A
Above resonant " no Cd "
0s
2us
4us
6us
8us
10us
V(a2) -V(a1) • V2(Cr) - V1(Cr) • I(Lr) • I(Ls)
Time

(e)

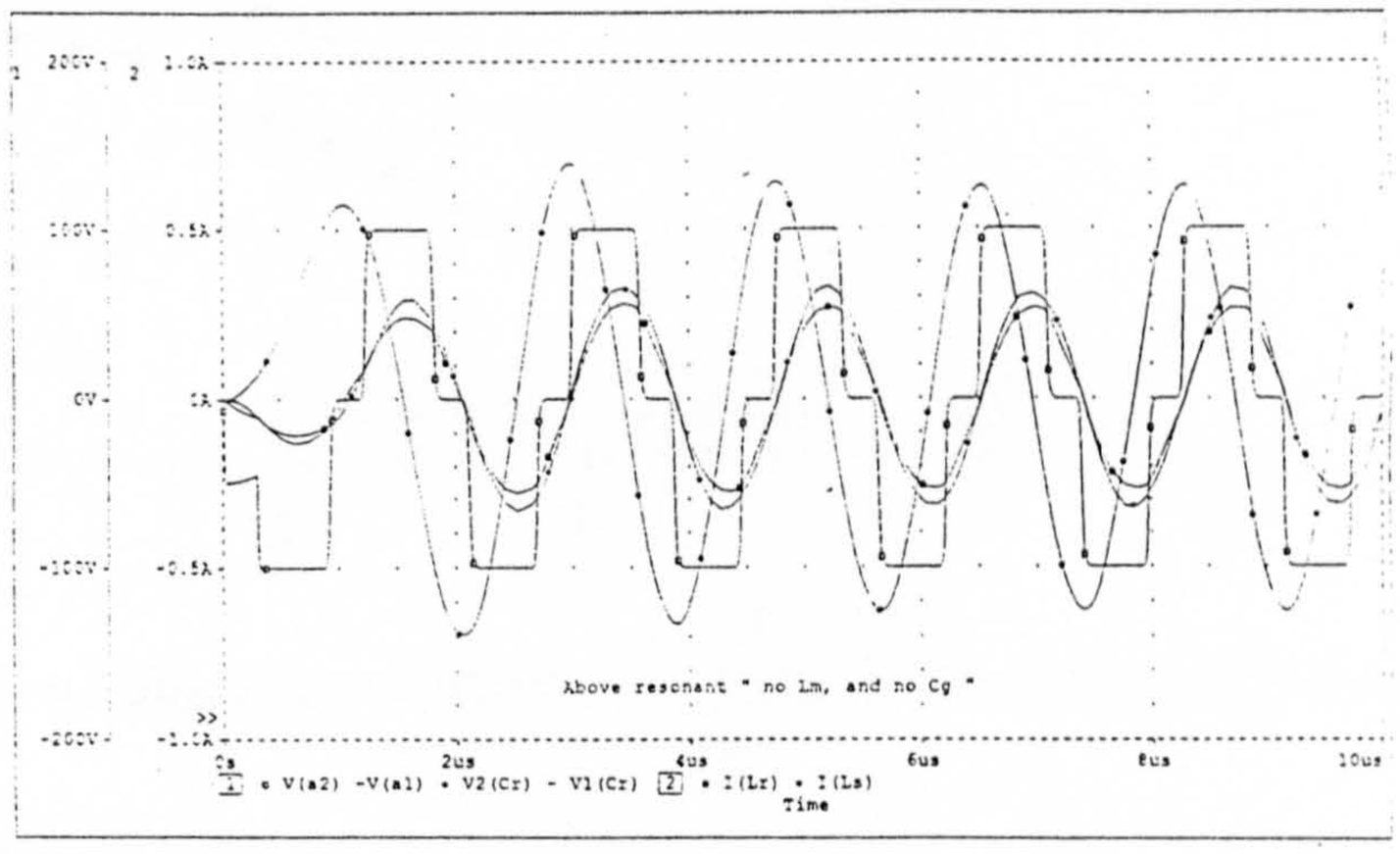
200V
100V
0V
-100V
-200V
1.0A
0.5A
0A
-0.5A
-1.0A
Above resonant " no Lm, and no Cg "
0s
2us
4us
6us
8us
10us
V(a2) -V(a1) • V2(Cr) - V1(Cr) • I(Lr) • I(Ls)
Time

(f)

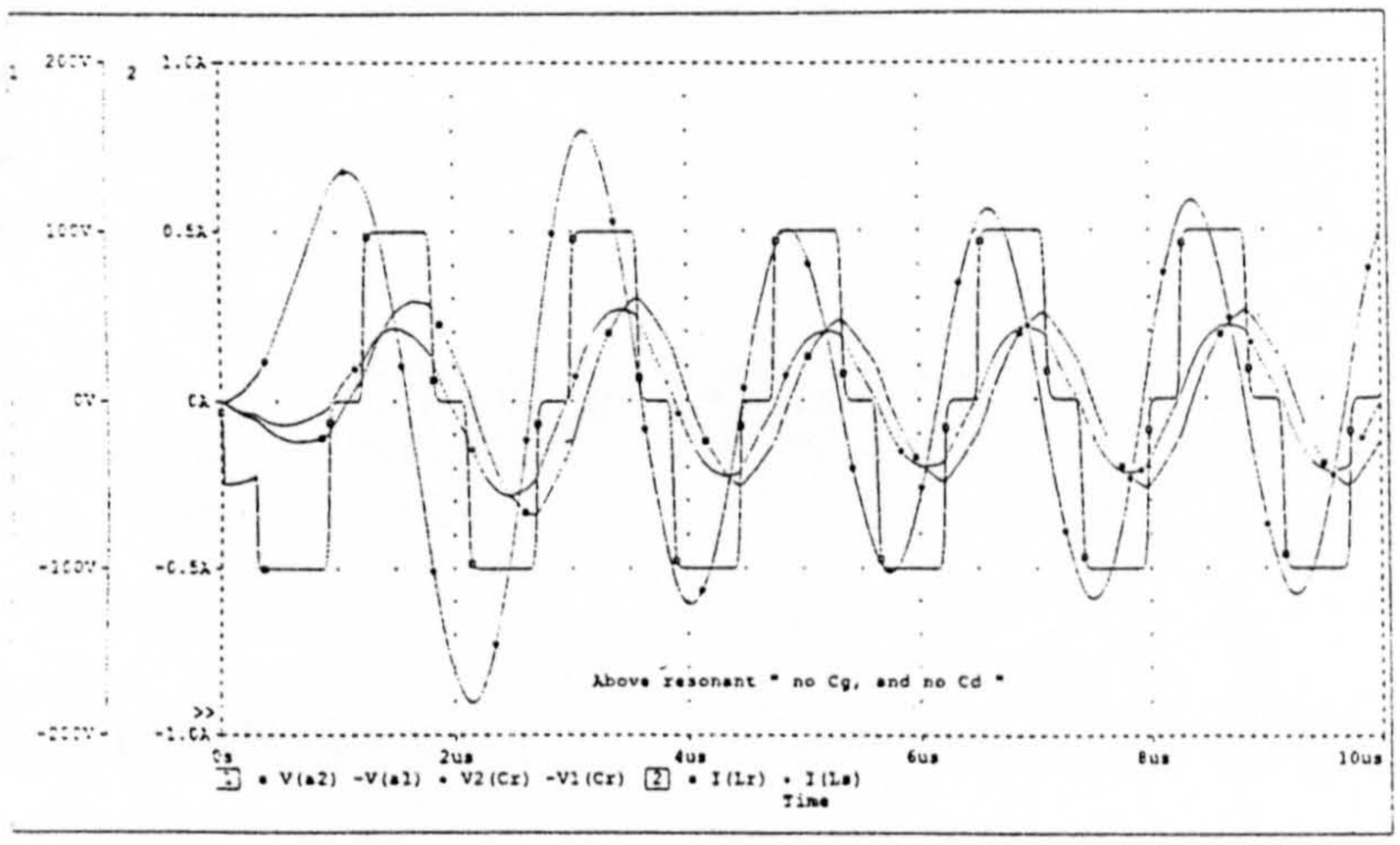
200V
100V
0V
-100V
-200V
1.0A
0.5A
0A
-0.5A
-1.0A
Above resonant " no Cg, and no Cd "
0s
2us
4us
6us
8us
10us
V(a2) -V(a1) • V2(Cr) -V1(Cr) • I(Lr) • I(Ls)
Time

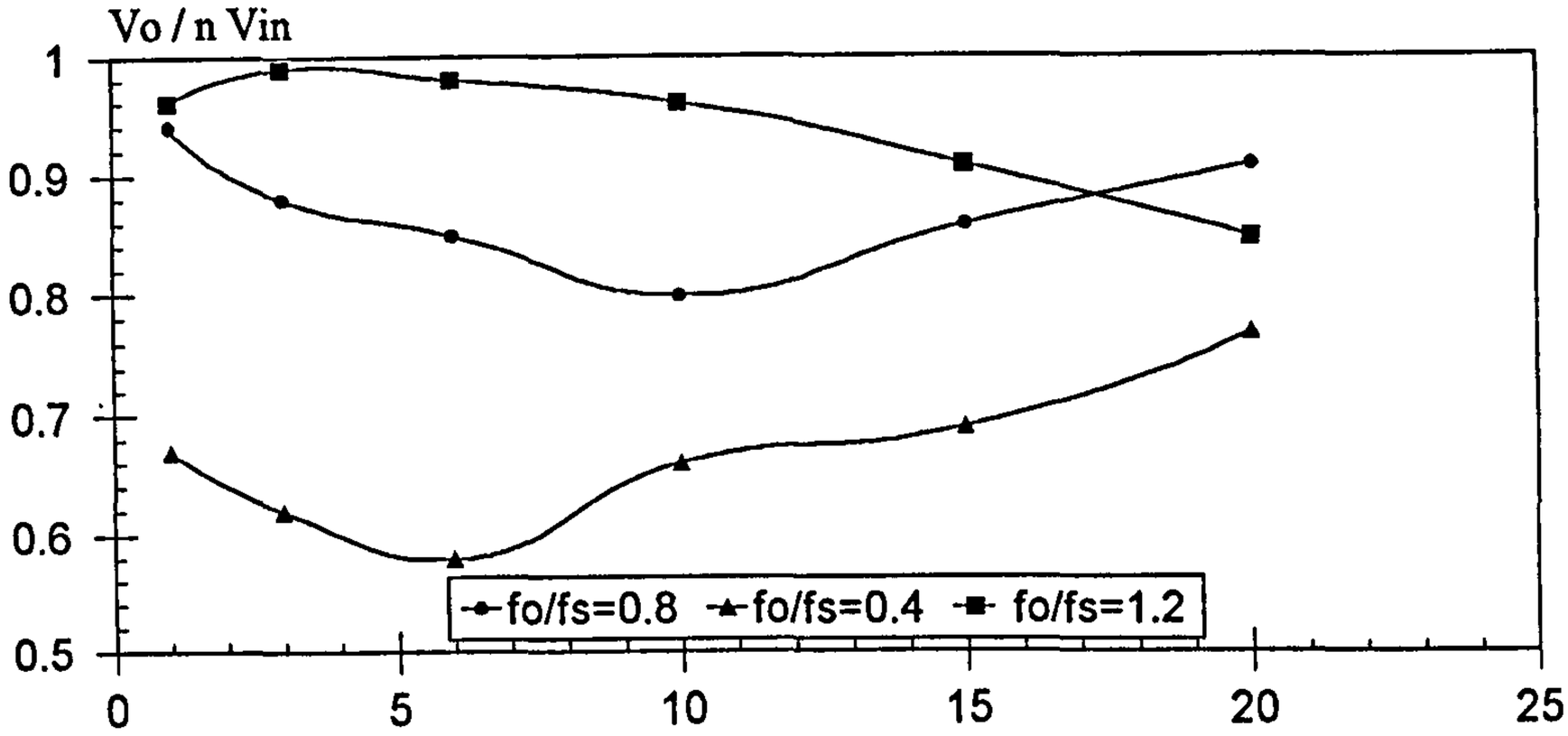

Cd (nF)

$L_1 = 3.36\mu H, L_2 = 0.86\mu H, L_m = 187\mu H, C_g = 12.3nF$

(a)

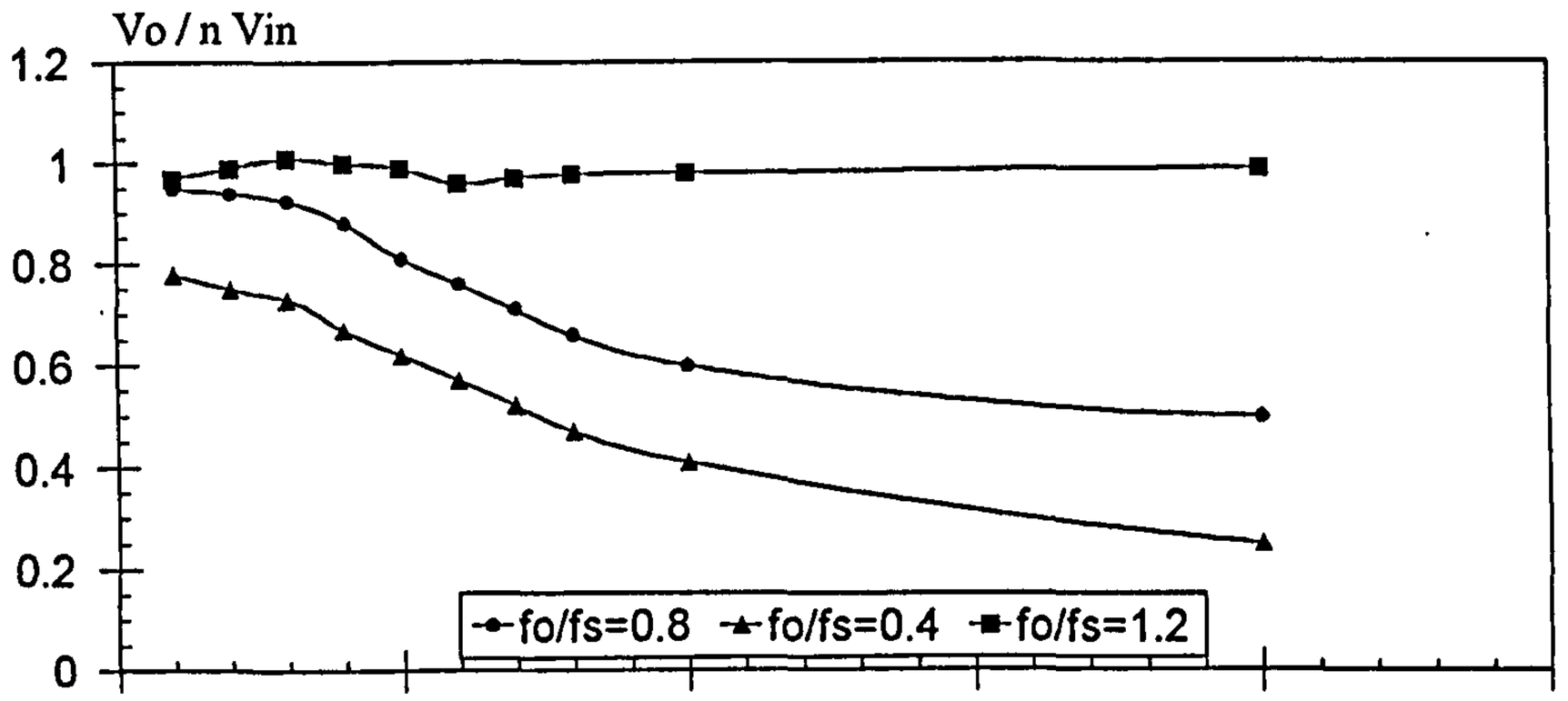

Cg (nF)

$L_1 = 3.36\mu H, L_2 = 0.86\mu H, L_m = 187\mu H, C_d = C_1 1.3nF \& C_2 5.11nF$

(b)

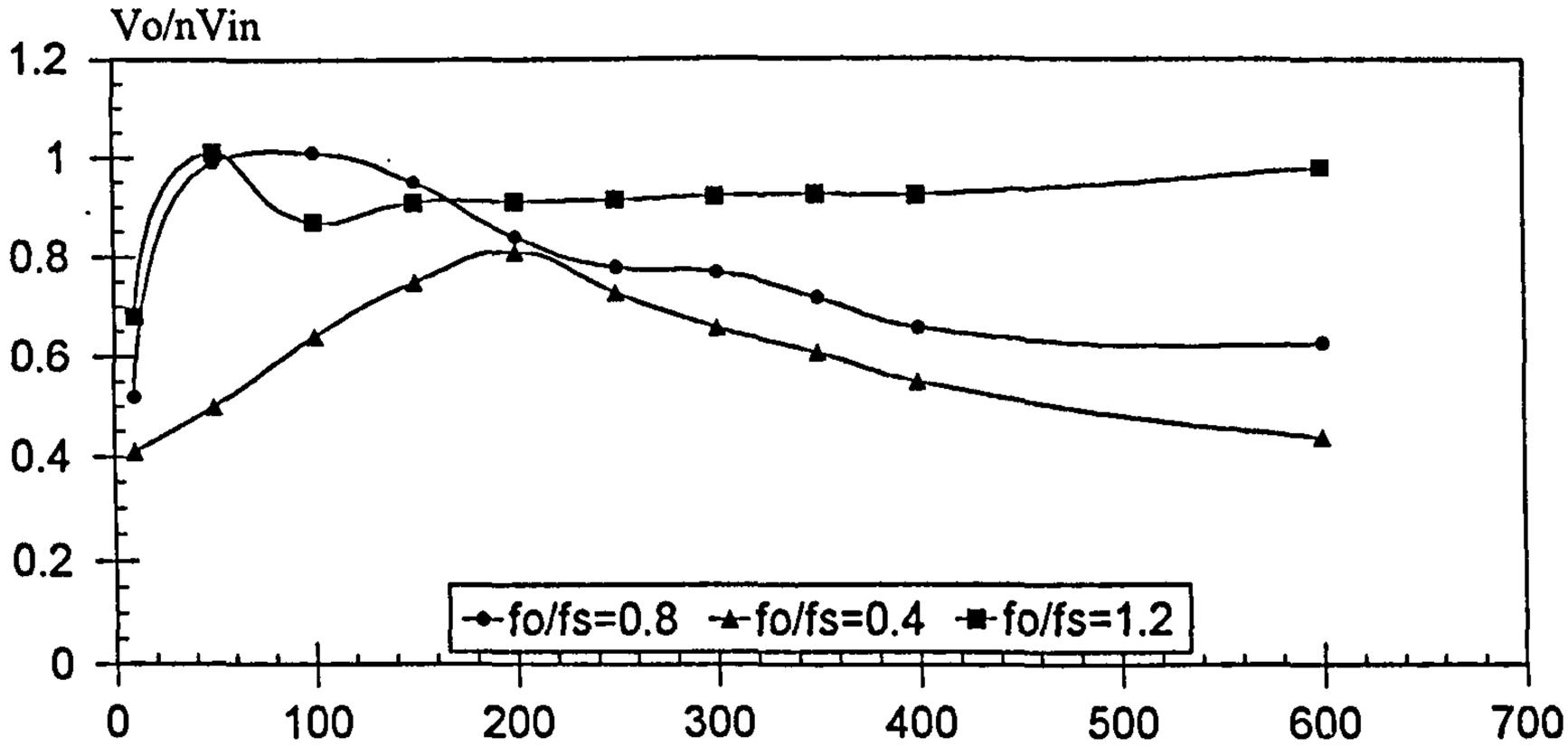

$L_1 = 3.36\mu H, L_2 = 0.86\mu H, C_g = 12.3nF, C_d = C_1 1.3nF \& C_2 5.11nF$

(c)

Fig.(6.7) : Output voltage against the transformer elements

CHAPTER SEVEN

"EXACT" TRANSFORMER EQUIVALENT CIRCUIT

7.1 : INTRODUCTION.

In any circuit, the behaviour of the transformer can be found from its dimensions and the material properties, by means of solving the electromagnetic field equations as previously discussed. An alternative way of predicting such behaviour is by using an equivalent circuit representation. There are many advantages of treating the transformer by means of an equivalent circuit. The simultaneous partial differential equations that describe the electromagnetic field can be avoided and the equivalent circuit gives an alternative method of solving these equations. In addition, the equivalent circuit is closer to the scale of practical imagination than differential equations, as well as easy to use and remember.

A given transformer may be represented by many equivalent circuits depending on the required purpose. Usually the approximation is considered to avoid analysis complexity. For instance, in an actual transformer, the existence of capacitances between windings and to earth are not important at low frequency but are significant at high frequency. Nevertheless, the "exact" equivalent circuit at very high frequency (Megahertz) could never be achieved as it would be too complicated. In this chapter, the exact does not means an exact practical representation but an exact physical definition of the transformer elements. In fact, the presence of an element is a sign of comparison with an ideal transformer. The ideal transformer is not a practical state but only a convenient way of comparing the actual transformer with the ideal. The ideal transformer could possibly be realised at low frequency by the use of a very high permeability core material and an arrangement allowing both primary and secondary windings to be very close to each other. The same magnetic field is then led through the windings, and the capacitive reactance is so high as to be

neglected. The case is not as simple as that as at high frequency, any reduction in the leakage flux will be at the expense of increased capacitance.

Electrostatic coupling is the phenomena behind the appearance of capacitance. It resides between the components within the actual transformer such as the core, winding turns, shields etc. Theoretically, it is desirable to treat the transformer electromagnetic and electrostatic aspects on the basis of separation for simplicity, but in practice, the case is far away from this simple assumption.

In the present chapter, care is taken to derive the circuit in such a way that its elements have a physical meaning. A three dimensional FE model could be used directly to build a highly accurate equivalent circuit, although, there are still many difficulties with calculating the capacitance of the different parts. This could be solved by using the electrostatic energy calculation by means of treating the transformer as a three port network [87]. This technique attempts to model the whole transformer which is very time consuming and expensive as it requires a huge computer memory to model the transformer FE mesh, and much preparation and computation time. Therefore, although the later technique is just about practicable, it is not used as researchers are usually looking for a simple and general method that can be used to derive the circuit. A model derived from calculation has a great meaning practically since a computer can be used instead of building prototypes. Nevertheless, a 3D finite element program is not generally available in many institutions and companies.

One of the well established methods to derive equivalent circuits is by fitting elements to match the performance measured (or calculated) in short circuit and open circuit tests (or calculations). In analysis terms this approach has the merit of simplifying the field model that must be solved from a 3D transient load model to the open and short circuit results at fixed frequency. The equivalent circuit is also easier to solve for transient analysis than trying to time step a 3D finite element model. This chapter persues this approach by using the open and short circuit input impedance

measured (or calculated) across a range of frequencies to obtain parameters in a selected equivalent circuit topology.

7.2 : PHYSICAL MEANING OF ELEMENTS

Fig.(7.1) shows the proposed equivalent circuit of the high frequency transformer. The circuit elements shown are referred to the primary winding using the transformer turns ratio. The circuit elements will be explained from the physical point of view.

The primary and secondary windings are made from conductors, and losses exist due to the finite copper conductivity (5.7×10^7 mho.m^{-1}). The windings losses can be modelled using two resistances one each to represent the two windings. The primary winding resistance (Rp) carries both load and no load (magnetising) current, and hence it has to be placed prior to the magnetising branch. The secondary winding resistance (Rs) carries only the load current, and so it is in a series with the load. In addition to the winding losses, there are another two kinds of losses that exist in the core, eddy and hysteresis losses. The combination of both eddy and hysteresis losses are called the transformer core loss. The core loss can be modelled by a resistance in parallel with the magnetising branch.

In simplistic terms, it could be assumed that the flux generated by the primary winding links all the turns in the secondary. Practically, there is an amount of flux that does not link the secondary (and vice versa), and so it is considered as a leakage flux. In order to model the leakage flux two inductances (Lp & Ls) are placed in series with the two windings resistances (Rp & Rs) respectively.

If these inductances did not exist the input / output voltage ratio would equal the transformer turns ratio (ideal transformer). In the same way, if the no-load current did not exist or it is not taken into account, the input / output current ratio would equal the reciprocal of the turns ratio (ideal). Practically both load and no load currents are present and they flow in the primary winding. If the core is made from a very high permeability material, then the no load current is negligible in comparison

with the load current, but it will be quite appreciable if the core has an air gap. This no load (magnetising) current can be modelled by an inductance (Lm).

The presence of conductors within the actual transformer separated with respect to each other and to the core makes capacitance between them. In this equivalent circuit representation, there are two types of capacitance namely, the distribution and ground capacitances. The distribution capacitances are either those belonging to successive turns of the same winding (C1 & C2), or that between windings (C12). The ground capacitance (Cg) is the capacitance appearing between the total winding turns and earth. The core represents the closest ground for both windings, and so capacitance may be placed in parallel with the magnetising branch. Nevertheless, the modelling of these capacitances in the equivalent circuit does not in general correspond exactly to any actual transformer capacitance, they are only a convenient way of approximation. All these elements can be justified from the physical point of view, but the reality is very complicated. It should be remembered that the main issue here is to generalise the prediction of the equivalent circuit. Since, the impedance curves are the only data being considered, the equivalent circuit can be built for any transformer regardless of differences in design.

7.3 : EQUIVALENT CIRCUIT ELEMENTS CALCULATIONS

The equivalent circuit can provide a reasonable tool for finding the magnetic field characteristics (flux density, field intensity, etc.), as well as currents and voltages. In the first instance, the main two questions that may be raised and need to be explained are as follows: First, suppose the flux in the core is calculated using the inductive elements of the equivalent circuit. The single value obtained is assumed to be the same at all points within the core. Second, in an actual transformer, the magnetising inductance will fall with saturation while its value is linear within the equivalent

circuit. At high frequency, the capacitance has the effect of shunting the current to ground and transferring current between primary and secondary. Clearly the distribution of the magnetic field is affected and the results implied by the equivalent circuit can only provide answers for local field distribution within the limits of the topology chosen for the circuit. It is in these details that finite element modelling can provide further insight.

Fortunately, due to the high permeability Ferrite core material used, the magnetising current is small, and hence the assumption of linearity does not create much error in the calculations. The previous 3D finite element impedance calculations provide a basis to validate the linear model.

The problem in any proposed equivalent circuit parameter derivation is the complexity of deriving the equations that represent both impedances (open and short) to specify adequately the poles and zeros. These points are vital to estimate the resonant and anti-resonant frequencies. Once these points are found, the equivalent circuit elements estimation follows a straight forward procedure. The procedure given here is in easy steps that avoids such complexity. The assumptions made from the point of view of Fig.(7.1) is that the current in the capacitance of the same winding is negligible compared with that flowing in the capacitance between windings during the short circuit. In the same way, the opposite assumption can be made during the open circuit. During the open circuit, the secondary winding current is zero and so the capacitance between windings is part of the capacitance of the same winding and it leaks current through the ground capacitance.

During the short circuit, the equivalent circuit can be reduced to the one shown in Fig.(7.2 a & b) [88]. The winding to winding capacitance can be referred to the primary winding using the turns ratio as shown in the Fig.(7.2 b). Since the flux required to induce a certain voltage is inversely proportional to the frequency, as the frequency goes higher, the assumption of neglecting the magnetising branch during the short circuit is increasingly valid [88]. In general, the magnetising current is negligible in comparison with the load current during the short circuit. Using

Fig.(7.2b), where both winding resistance and inductance are in series, the short circuit impedance is given by:

$$Z_{sc} = \frac{1}{\frac{1}{R_{eq}} + j\left(\omega C'_{12} - \frac{1}{\omega L_{eq}}\right)} \qquad \text{.....(7.1)}$$

where $R_{eq} = \frac{R^2_{Ps} + \omega^2 L^2_{Ps}}{R_{Ps}}$ and $L_{eq} = \frac{R^2_{Ps} + \omega^2 L^2_{Ps}}{\omega^2 L_{Ps}}$

The parallel resonant frequency can be found by setting the imaginary part of equation (7.1) to zero, and the result is :

$$\omega_p = \sqrt{\frac{1}{L_{PS} C_{12}'} - \left(\frac{R_{PS}}{L_{PS}}\right)^2} \qquad \text{.....(7.2)}$$

and $|Z_{SC}|_{\omega_p} = R_{eq} = \frac{R^2_{Ps} + \omega^2 L^2_{Ps}}{R_{Ps}} = \frac{L_{PS}}{R_{PS} C_{12}'}$

Where the magnitude of the short circuit impedance at the parallel resonant frequency is equal to 12KΩ.

The total of the primary and secondary windings resistance (Rps) can now be deduced directly from the short circuit impedance curve at low frequency. This resistance is automatically referred to the primary if the impedance curve is found from the primary winding side, and hence $Z_{SC} = R_P + \left(\frac{N_2}{N_1}\right)^2 R_S = 0.2\,\Omega$.

From equations (7.1, and 7.2), the elements of the circuit shown in Fig.(7.2b) are calculated directly at a resonant frequency of 2.408 MHz, and are given by :

Lps = 3.24 μH, and $C_{12}' = 1.34$ nF

It is well known (as previously discussed in chapter four) that the highest cut off frequency obtained is due to the leakage inductance and distribution capacitance of the winding. In the same way the lowest cut off frequency is due to the ground capacitance, because the ground capacitance is usually bigger than the distribution capacitance. Hence, the parallel resonant frequency of 2.408 MHz is used to predict the leakage inductance and distribution capacitance.

During the open circuit, it is assumed that the current leaking to the secondary through C12 is small in comparison with the current through C1, and hence the

circuit shown in Fig.(7.3) is the equivalent circuit during an open circuit. Following the same procedure as the short circuit, the open circuit impedance is the total of primary and magnetising impedances in a series connection as shown in the figure. The resonant frequency relationship is given by :

$$\omega_{P1} = \frac{1}{\sqrt{L_m C_g}} \qquad |Z_{oc}|_{\omega_{P1}} = R_C \qquad \text{.....(7.3)}$$

$$\omega_{P2} = \sqrt{\frac{1}{L_P C_1} - \left(\frac{R_P}{L_P}\right)^2} \qquad |Z_{oc}|_{\omega_{P2}} = \frac{L_P}{R_P C_1}$$

Where the magnitude of the open circuit impedance at the first and second parallel resonant frequencies are about 32 KΩ and 22 KΩ respectively. The series resonant frequency is equal to :

$$\omega_S = \sqrt{\frac{L_m + L_{eq}}{L_m L_{eq} (C_1 + C_g)}} \qquad \text{.....(7.4)}$$

where $L_{eq} = \dfrac{R^2_P + \omega^2 L^2_P}{\omega^2 L_P}$ and $\omega_S = 2\pi \times 751\,\text{KHz}$

The value of the open circuit impedance curve at low frequency gives Rp only. Because Rc is compensated by Lm and Cg [87], its value only appears at the resonant frequency of Lm and Cg, and so Rp is equal to 0.09 Ω at low frequency. Using equations (7.3) and (7.4) leads directly to the following :

Rc = 32 KΩ C1 = 1.49 nF Lp = 2.9 μH Lm = 161 μH Cg = 14.3 nF

Rs = Rps - Rp = 0.11 Ω and Ls = Lps - Lp = 0.34 μH.

C2 can be estimated from the resonant frequency, when Rs and Ls are known, or by referring the open circuit impedance curve to the secondary using the turns ratio. The same procedure that is used to estimate C1 can then be applied. If the later is used, its value has to be referred again to the primary, and then C2 is equal to 12.9 nF.

7.4 : OPEN AND SHORT CIRCUIT IMPEDANCE CALCULATIONS

The proposed equivalent circuit together with it estimated elements is used to re-predict the open and short circuit impedances. Because the circuit is simple, it is easy to determine both impedances point by point at all frequencies within the required frequency range. Fig.(7.4) and (7.5) show the open and short circuit impedance curves respectively, given in phase and magnitude in comparison with the results of the 3D finite element model. The agreement is clearly seen in both figures and in both curves, a number of observations can be noted as follows:

1- If the windings resistances are neglected and keeping the element values as they are, the parallel resonant frequency which is 2.408 MHz changes to: $\omega_P = \frac{1}{\sqrt{L_P C_1}} = 2.413\,\text{MHz}$, with a difference of 5.1 KHz. In the megahertz zone such a difference as this is clearly unrecognisable. In the circuit previously derived in chapter four, such a difference does not appear where the resistances have been neglected. This is because, the values of the windings resistances are compensated by the leakage inductance and distribution capacitance at the resonant frequencies [87]. Comparing the element values derived in this chapter with that in chapter four gives a clear view of how these values change when the winding resistance is considered.

2- By taking the winding resistance into account, both impedance curves have a finite value at each resonant frequency and do not go to infinity (parallel resonance) or zero (series resonance) as is the case derived in chapter four.

3- At very low frequency the impedance curves are constant which give the resistance value. At a certain frequency, where the curves start to increase, the inductance begins to appear, and so the impedance value at this frequency is the total of resistance and inductance. When the capacitance comes into play, it resonates with the inductance at a certain frequency, which depends on which of them is

predominant for the circuit to be inductive or capacitive and then the resonant frequency is either series or parallel.

4- If the losses are not considered, the real part of the impedances is equal to zero, and so the phase is a straight line always equal to 90^0 .

7.5 : TRANSIENT RESPONSE

Transformers are subject to many transient phenomena during their working life. These include surges, inrush current, sudden short circuit, etc. During the transient a high frequency oscillation occurs and these can result in an over voltage stress on the windings. Such stress can be enough to destroy the insulation of the windings. A large amount of work has been directed towards modelling the transient response of transformers [9,39,63,89]. These efforts were mainly devoted to modelling the over voltage transient response in the windings (as discussed in chapter five). Measurement of the transformer transient response is the most reliable method that is used at the present time. There are many difficulties involved in this measurement [9]. These difficulties are increased as the frequency rises, for instance the high sampling rates of the measuring instruments required, therefore an adequate transformer model is unquestionably required to determine the transient response numerically and analytically.

Current attention is being concentrated on a high frequency transformer model suitable for transient calculation. The determination of the equivalent circuit elements from the transient response at 100 KHz was found previously [90]. At high frequencies, the capacitance becomes predominant, and it is harder to use the transient response to obtain these elements. Therefore, researchers have paid more attention to modelling the frequency response rather than the transient response [9,35,87,90]. Using the frequency response, the transformer can be modelled for a

certain frequency range. The transient waveforms (currents or voltages) in the transformer comprise all the frequency components, and there will be no frequency range specified. All the frequency components are excited at once during the transient response. The difficulty in the time responses is then clear and the question which is left is how to model the transformer covering all the frequencies to which it is subject.

In order to avoid such a difficulty, the transformer is modelled first in the frequency domain. The frequency response characteristics have been calculated for the proposed equivalent circuit. These characteristics for the open and short circuit impedances are given as follows:

$$Z_{oc} = \frac{V_{in}}{I_{in}}\Big|_{I_{SEC}=0}$$

$$Z_{s.c} = \frac{V_{in}}{I_{in}}\Big|_{V_{SEC}=0}$$

Two methods are available to determine the transient response. First by transferring the frequency response characteristics into the time domain using a well known method, such as Fourier transformer [83], state space[11,77] etc. The input voltage or current can usually be considered as a step change function. Mathematically, the step change in the frequency domain gives an impulse function in the time domain and vice versa. These relationships between step change and impulse functions are given by Gupta [91]. The second method is that the equivalent circuit can be time stepped directly (as detailed in chapter five). The present transient simulation is based on using the trapezoidal rule of integration. Each of the equivalent circuit elements is transferred to an equivalent of a current source and a resistance. Appendix B shows the way of applying this method to the proposed equivalent circuit.

The HP34810A Bench link software can provides a communication link between the PC and the HP54500 Oscilloscope. The results can be stored as a table of data which is easy to use and compare with the calculated results. Fig.(7.6) shows the

comparison of the actual and calculated transient responses of the primary voltage during the short circuit at high frequency excitation. In order to simplify the analysis, it is assumed that the step occurred at t=0. This can be clearly recognised from the curves. However, if the fault at this instant of the ac cycle is not required another instant can be analysed. The small differences shown could be caused by the sampling rate of the devices or the sampling rate is insufficient in the transient simulation results. Nevertheless, the agreement is fairly acceptable.

This technique has two advantages. It is a general solution so that it could be applied to any circuit regardless of the design differences. The accuracy of the simulation depends on the accuracy of the proposed equivalent circuit and its elements and the sampling rate. Second is that the results can be found either directly in a numerical or by an analytical solution.

7.6 : SUMMARY

This chapter presents a method to calculate the frequency response characteristics for a lumped parameter transformer model. Previous characteristics of open and short impedances are used to predict the values of these elements. The existence of these elements in the proposed equivalent circuit is justified at high frequency from a physical point of view. The circuit is reused to compare the predicted frequency responses with the actual.

This chapter has also paid attention to the transient response for the proposed equivalent circuit. During the transient response a time stepping technique is used which transforms the differential equations into equations in which each of the circuit elements is transferred into an equivalent current source and constant resistance (as discussed in chapter five). The circuit is used to predict the transient primary voltage due to a step change function in the input of the primary.

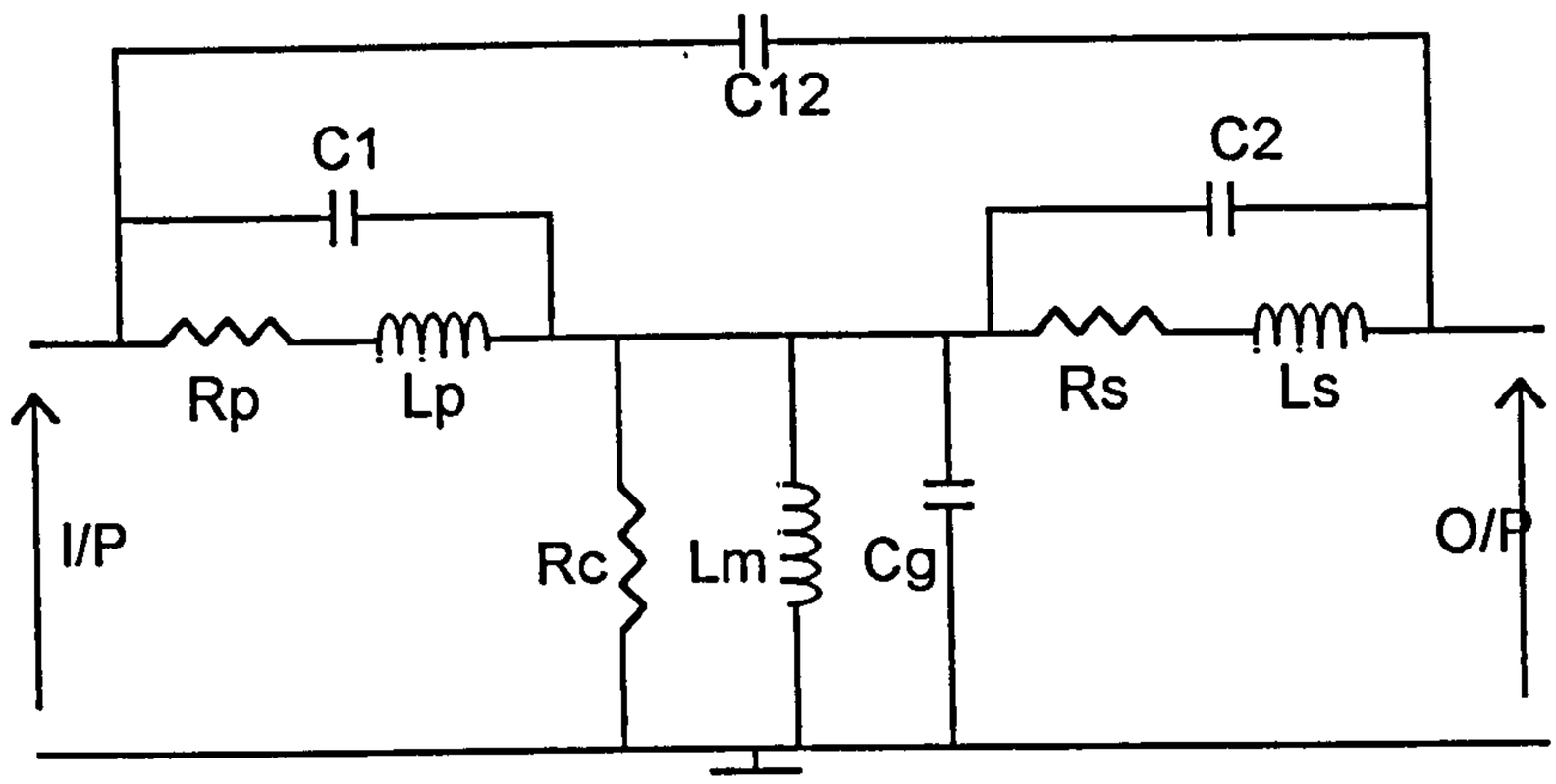

Fig.(7.1): The proposed HF transformer model

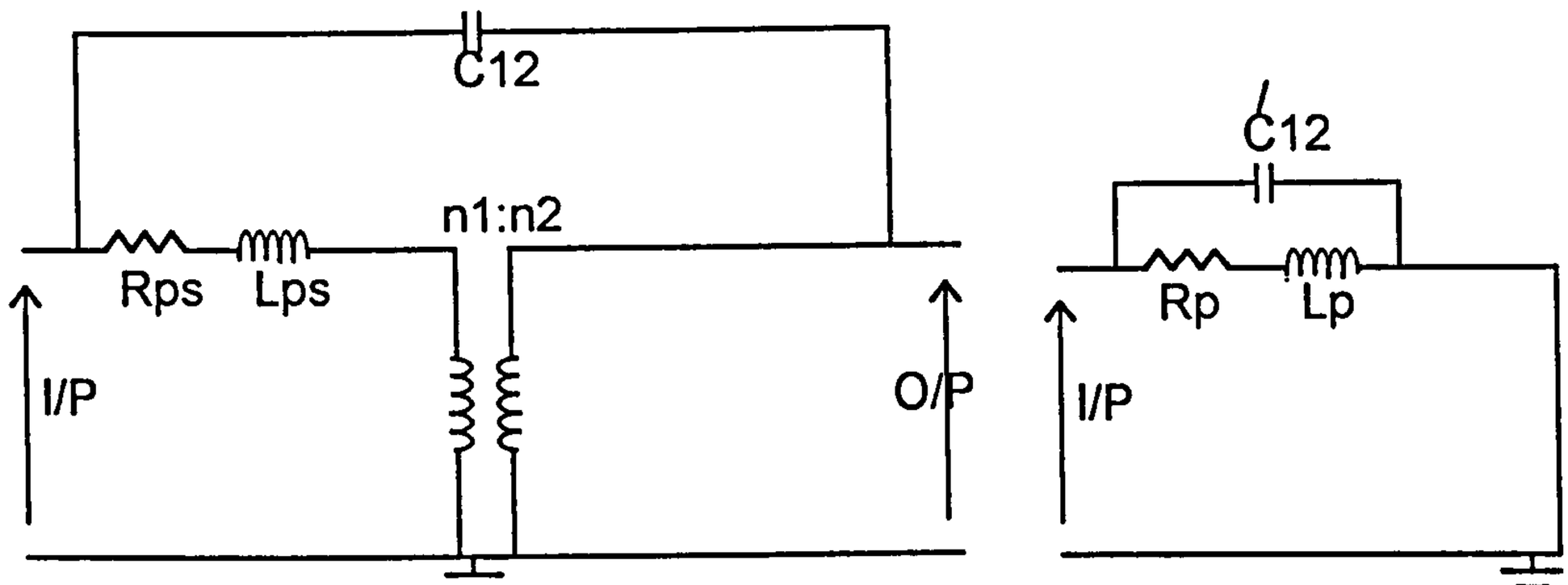

(a) (b)

Fig.(7.2) : Equivalent circuit during short circuit of the secondary winding

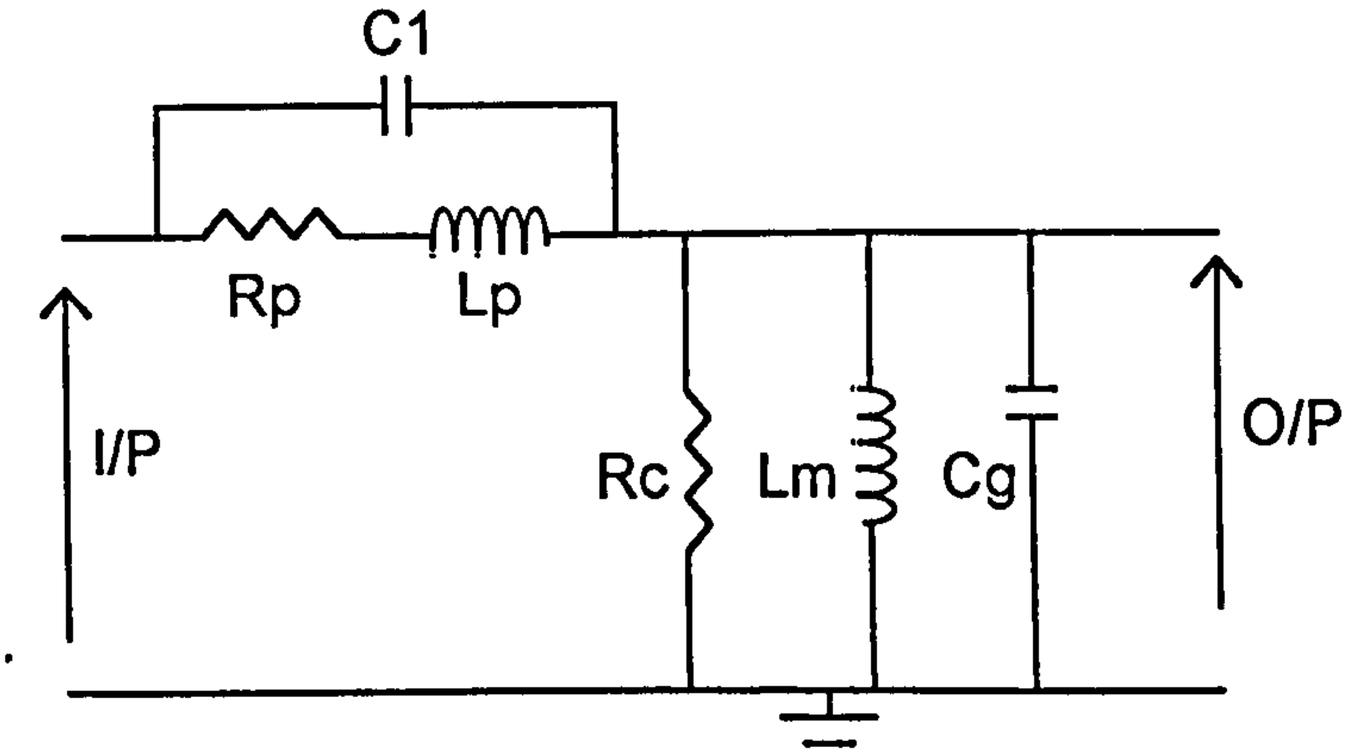

Fig.(7.3) : Equivalent circuit during open circuit of the secondary winding

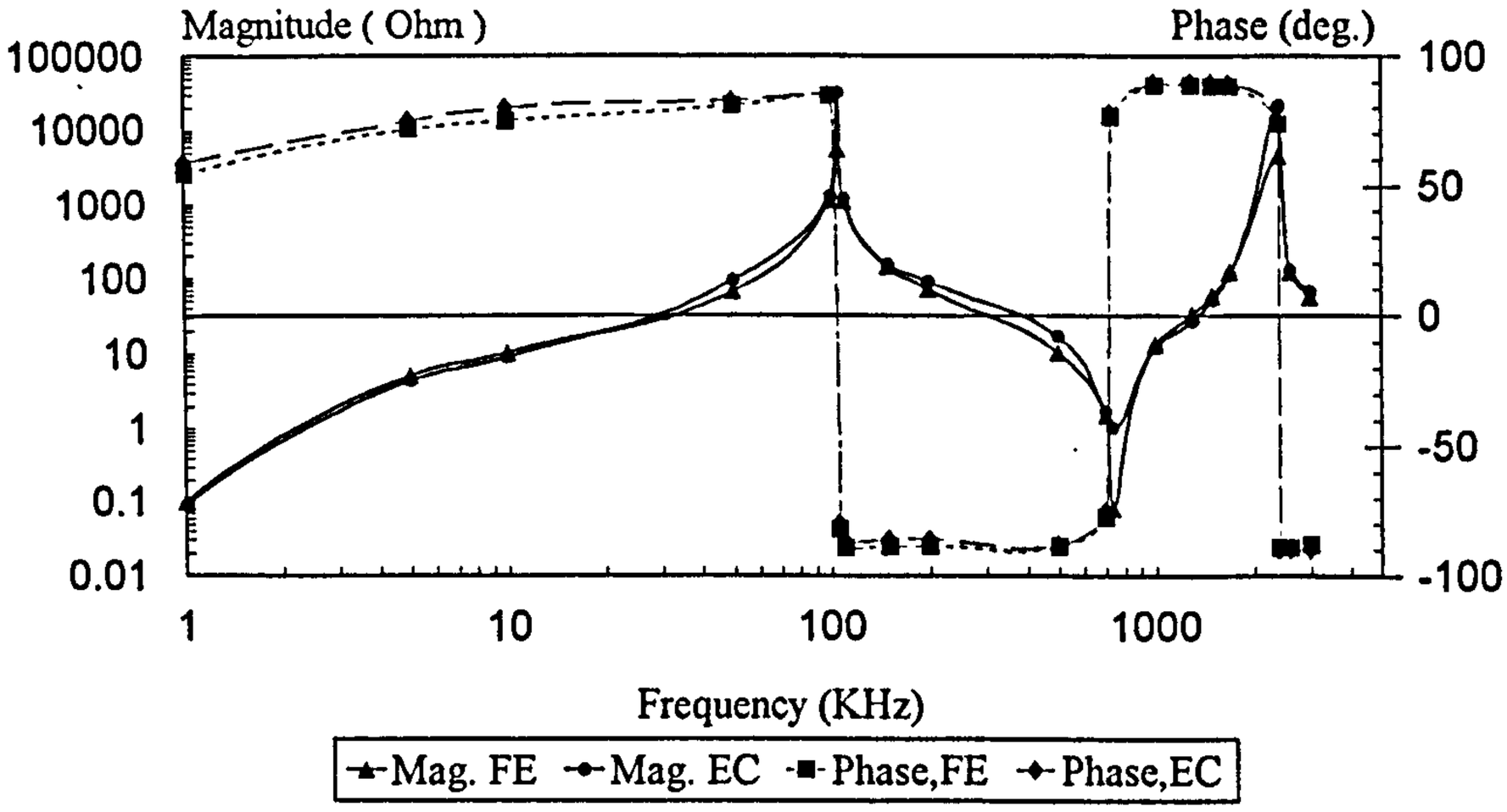

Fig.(7.4) : Calculated open circuit impedance

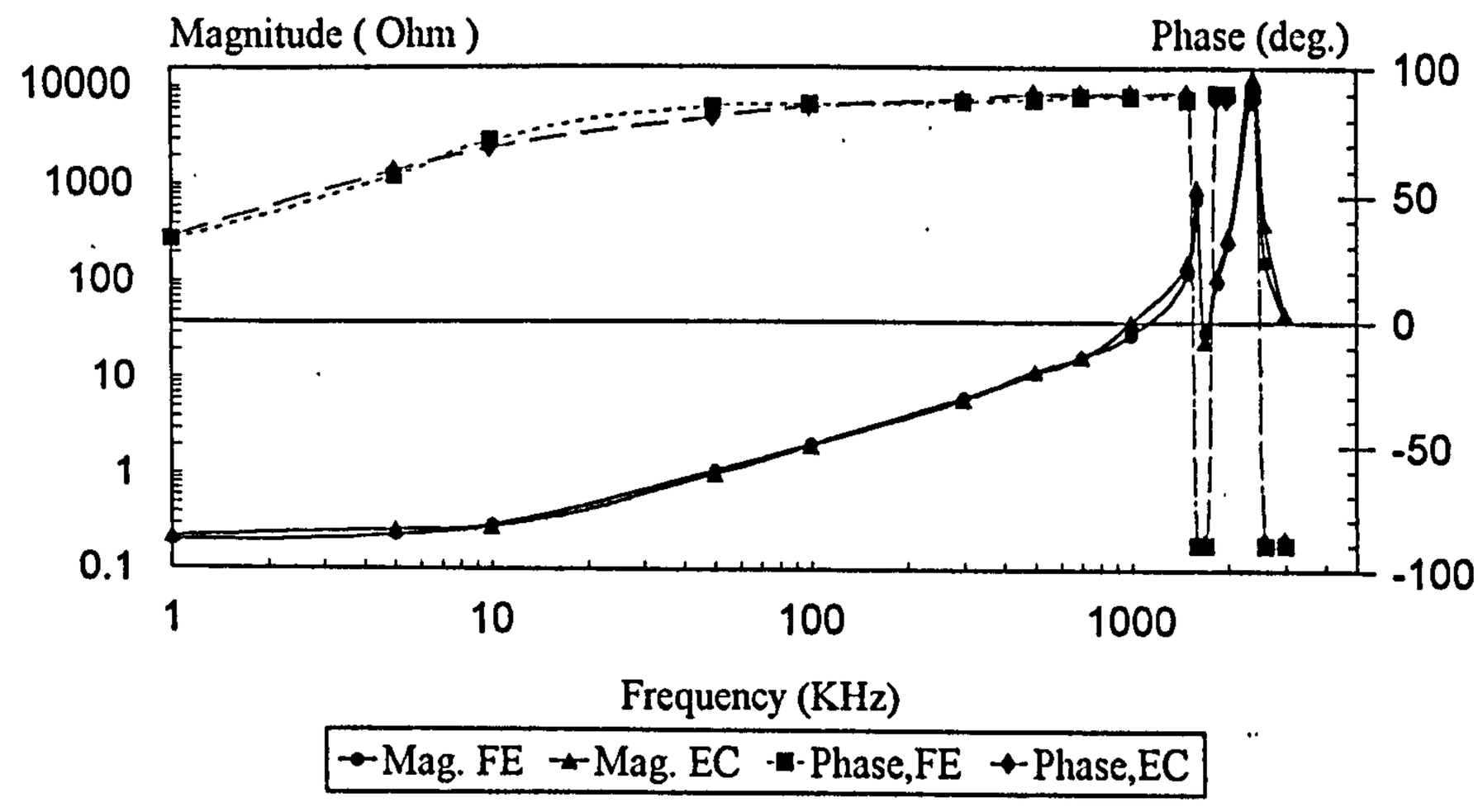

Fig.(7.5) : Calculated short circuit impedance

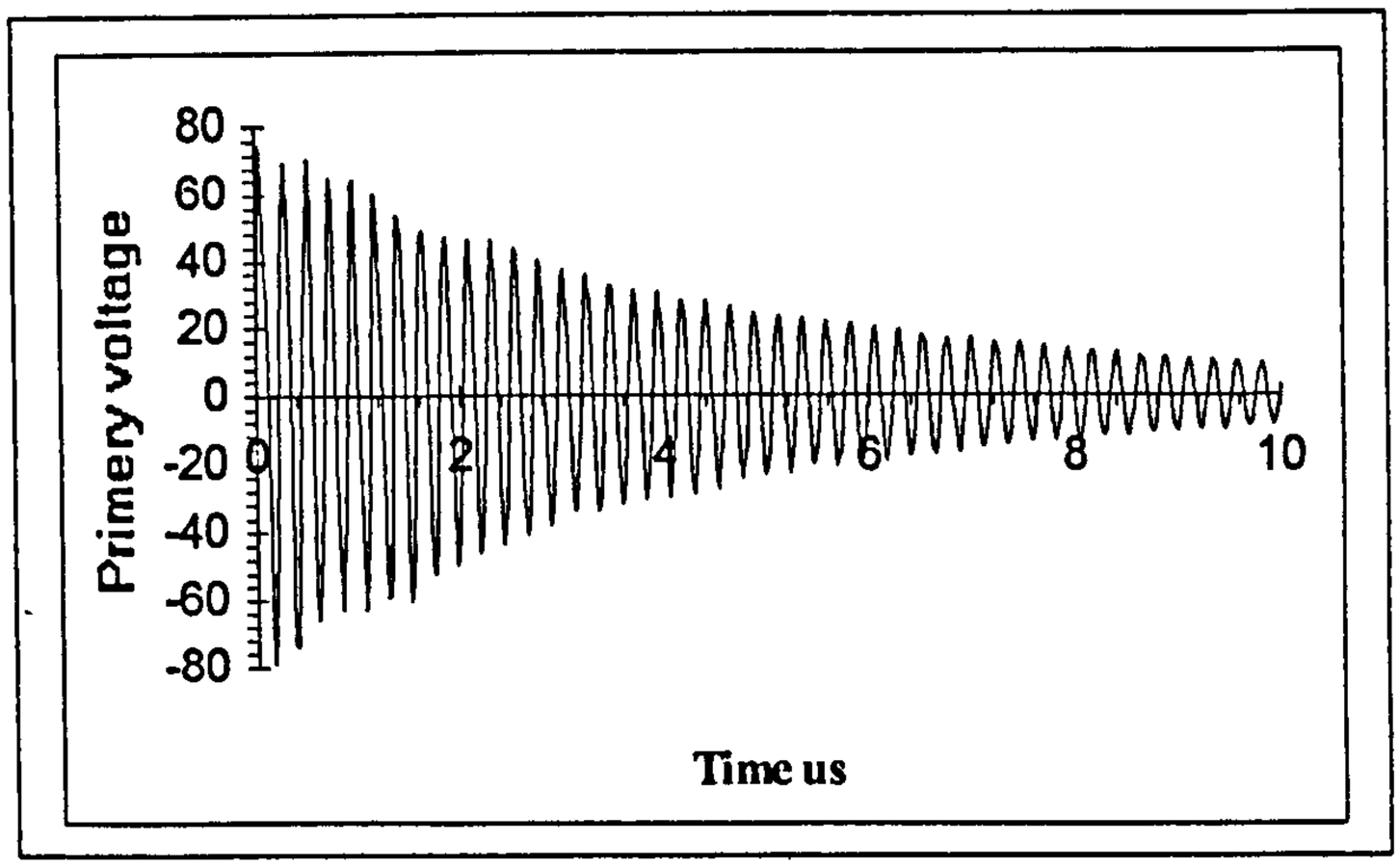

(a)

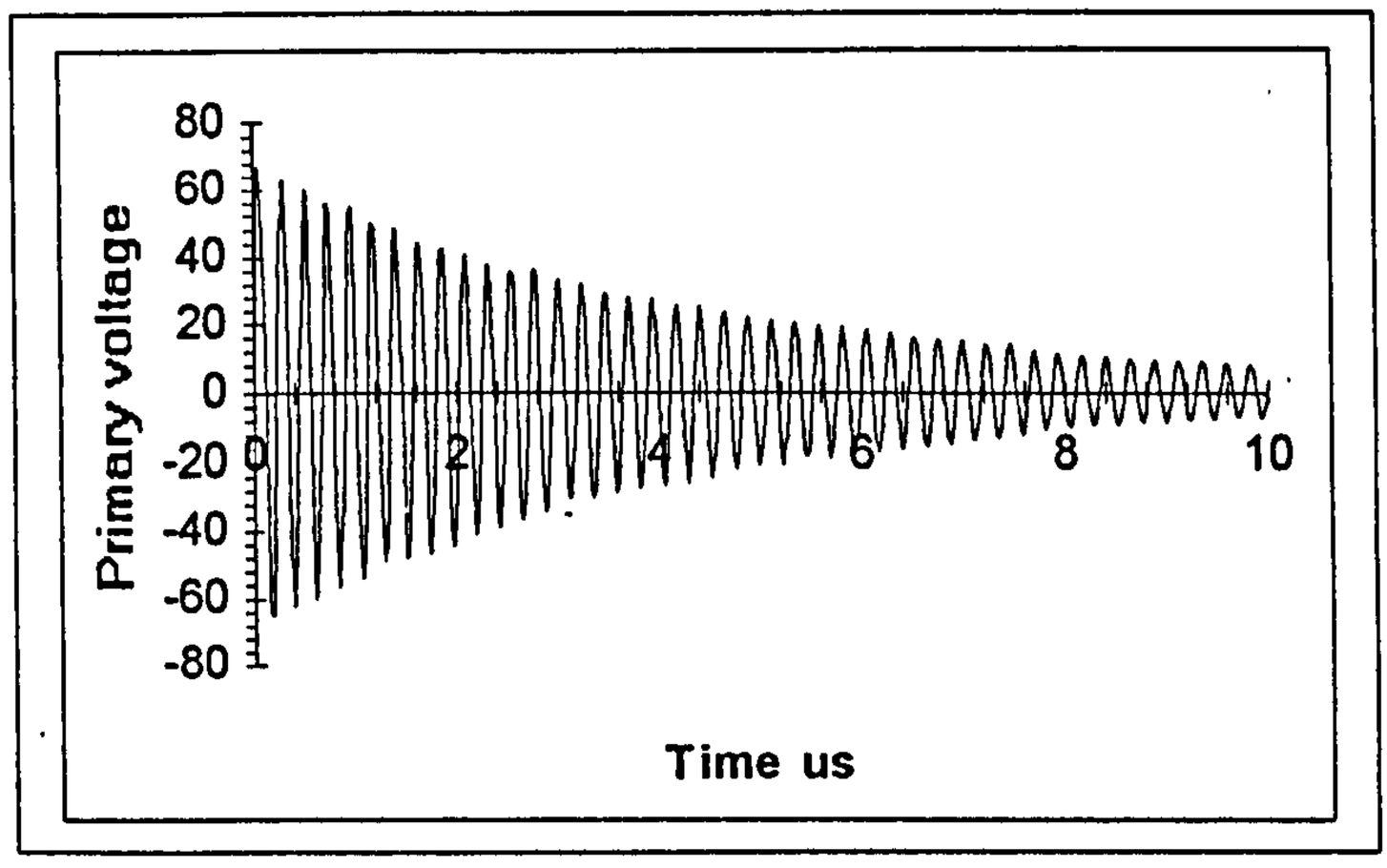

(b)

Fig. (7.6) : Primary voltage during the short circuit due to a unit step primary current
(a) : Calculated (b) : Measured

CHAPTER EIGHT
CONCLUSION

The transformer is a device that is present in all power supplies serving many purposes, such as isolation, step power up and down etc. The size of the power supply is reduced with an increase in the switching frequency. Increasing the switching frequency can lead to a large reduction in the magnetic components sizes and hence a smaller power supply unit. Nevertheless, high frequency operation means higher losses in the power supply both from device switching losses and in the transformer from eddy currents. The switching losses have been reduced by using a resonant type converter and other techniques such as zero voltage and / or zero current switching. As the power transformer size is reduced by increasing the frequency, eddy currents become one of the major limiting factors. Eddy currents in the transformer core can be reduced to an acceptable level by using high quality core materials. The windings eddy currents are the most complex to analyse.

The winding ac resistance and leakage inductance are strongly related to the eddy current effects. The term ac inductance is used to point to the fact that effective inductance (self and mutual) is reduced as the frequency rises. Practically, there will always be a frequency at which eddy currents become significant, and the conductor current is forced by its own magnetic field towards the surface. When the inductance falls because the area of the flux path is reduced, the resistance increases.

The two main effects that dominate winding eddy currents losses are skin and proximity effects. The self induced eddy currents in one conductor is called the skin effect eddy current. The proximity effect is due to the flux linking surrounding conductors which causes a circulating current in adjacent conductors. In addition, since the power supply topology at high frequency is resonant, the transformer parasitic elements form the second major design challenge. These elements are also resonant in nature and their minimisation is vital to reduce noise, EMI, and stress.

Attempts to obtain an accurate frequency response by detailed transformer modelling has attracted the attention of researchers. In parallel to experiment developments with various test methods, numerical computation is also attracting a high level of interest. One of the computing methods is electromagnetic field computation using the finite element method.

Returning to the main purpose of this work which is to study the winding eddy currents and transformer parasitic elements so as to minimise their effects. The practical implementation of a high frequency power supply and transformer testing was carried out in chapter two. A clamped mode series resonant converter was built to justify the simulation results. Full design of transformer and power supply was given in this chapter as well as a linear power amplifier which was used to test the high frequency transformer practically.

The magnetic field is the main source of eddy current generation and so two dimensional finite element analysis was used (chapter three). Two dimensional analysis can analyse the effects of eddy currents, but for a limited bands only, or more specifically until the appearance of the capacitive effect. The conductors in the model were considered as having a square cross sectional area equal to that of round wire so as to make the problem more manageable from a meshing view point. In this analysis care had be taken to model correctly the rapid decay in the field at the conductors boundaries. These boundaries have to be modelled with as many small elements as possible. Again, the depth of the modelled E-core viewed from the front is larger than that viewed from the sides. That means the area available for the magnetic path is different. Therefore, two models were used within the finite element computation. This has lead to the numerical results to be improved by 2% at 1KHz, and 8% at 1MHz in comparison with using one model only.

The transformer elements (resistance and inductance) can be computed both from short and open secondary winding computations. The finite element derived short circuit flux distribution (chapter three) shows that as the frequency is increased, the flux is concentrated in the space between the windings (primary and secondary).

This reflects losses due to the proximity effect and also changes in the leakage inductance. Two dimensional analysis can be used within the frequency range of dc-MHz. At higher frequencies, the capacitive effect cannot be neglected and so two dimensional analysis is no longer valid. The results also show that when the space between windings is half of a certain limit, the losses will be three times more (chapter three). When the space is doubled, the proximity effect is reduced but the leakage inductance is increased by almost one and half times its original value. The investigation continues to suggest that the best space between both windings so as to optimise the conditions and reduce to a minimum the losses and leakage, is when the space (between windings) is equal to or less than the thickness of the windings conductors. The investigation also includes the skin depth effect in the conductor (wire). The results show that when this depth is much greater than the depth of the wire, the magnetic field varies across the conductor. This field causes differential voltage in the wire and the resultant eddy currents are insufficient to redistribute the field. When the frequency increases to the level that the skin depth is much smaller than the wire thickness, the current inside the wire will be non uniformly distributed. Hence, the current density falls exponentially within the wire. In addition, as the frequency is increased, the actual area of the wire that carries current is reduced and then the ac resistance is far higher than dc. The finite element technique was used to estimate an optimum value of wire size that provides the best compromise between the number of wires and ac resistance. The investigation has lead to the point that the best ac to dc resistance ratio is achieved when the wire thickness is 1.2 times the skin depth. This result is supported analytically. It is vital to subdivide the wire into many fine wires so as to keep the eddy currents to a minimum, and then each of these wires is to occupy equally every position in the bundle.

The problem of keeping both the leakage inductance and ac resistance to reasonable limits at a certain frequency was also investigated. During the examination of this effect due to the increasing the number of layers, curves were computed to show the ratio of ac to dc components of leakage inductance and resistance. These values

were given against frequency, and presented in term of conductor size as a ratio to the skin depth. Using these curves is vital for the pre-design stage of the transformer. From these curves the required number of layers and how many fine wires at a certain frequency can found directly. The results show that an increase in the number of layers can give an increase in the ac resistance and a reduction in the ac inductance per turn as compared to dc values. It should be noticed that increasing the number of layers actually increases the copper content with respect to the air gap in the transformer window. When the field becomes skin limited there is less space available for the leakage flux and so it gives a reduction in the inductance. In the same way, the layers will lie close to each other and so the ac resistance will increase due to the proximity effects.

The core properties were also investigated with the secondary winding was open circuited. The results (not surprisingly) show that the self inductance is sensitive to the core permeability, while the resistance is sensitive to the core conductivity. As the permeability was reduced, the frequency at which the self inductance curve falls is reduced. This frequency represents the maximum frequency at which the core could realistically be used, and also shows that skin effect starts to dominate. For the best materials available, the megahertz zone represents the area where the skin effect eventually sets in.

At a certain operating frequency (say 1 MHz), two dimensional analysis is no longer useful. Because the transformer is a three dimensional device in nature where there is almost no axis of symmetry, both magnetic and electric fields are required to model the transformer, and they are working in a normal sense to each other. A three dimensional transformer model was built and solved using the full set of Maxwell's equation, this was described in chapter four. It is believed that this model is original. The transformer parasitic elements and their effects was the next concern of this work, where this three dimensional model was used to compute the frequency response characteristics of the transformer. These characteristics include the open and short circuit impedance computation. The computed results were compared with

the actual results and good agreement was achieved. This model proves that it is capable of handling any future investigation and promises to be a good tool in designing higher frequency transformers.

The modelling of the transformer transient characteristic was given as much attention as was given to the frequency response (chapter five). At high frequencies, frequency response computation is more effective than transient, due to the appearance of the capacitive effects. During the frequency response, the transformer was modelled across frequency range. This range cannot be specified during the transient where all the transformer natural frequencies are excited at once. Therefore a very high rate of sampling is required and this limits the analysis as well as the practical instruments available. As an example, the maximum time and frequency steps without introducing aliasing error was 2μsec and 3Hz at low frequency, and 0.008μsec and 150Hz at high frequency. If this figure is considered, the number of samples required for transient calculation is about 500000 (this figure is approximated where the number of samples should be a power of two), which is very high by any means. Nevertheless, the transient computation method used currently can easily handle a nanosecond time step computation. This method for the equivalent network solution uses the trapezoidal rule of integration. Each of the inductances or capacitances that exist in the network is transferred to an equivalent circuit of current source and resistance. The whole network looks like a resistive network that can be solved by well known methods. The winding is divided into a number of sections, each is represented by self and mutual inductances, distribution and ground capacitances, and resistances to take the losses into account. These elements were calculated using the finite element method. The transformer winding was transferred into an equivalent network. The first transient effect to be examined in this network was the over voltage stress. This stress is well known in industry and is subjected to an impulse signal to examining the winding insulation. The results showed that the voltage in the mid point of winding goes higher than the terminal voltage. It was believed that this resonant phenomena is related to the relative location of the

winding poles and zeros. Reducing the capacitance can allows over voltage stress to be reduced. The ground capacitance cannot be reduced much because it would involve using a bigger core, and so it is meaningless to increase the frequency for small size transformers. The frequency response computation of the terminal impedance confirms the need to reduce both ground and distribution capacitances. This response calculation also shows that the network response at which the resonance occurs is always different from the actual. Nevertheless, the accuracy of the calculation is believed to be limited by the way of representing the winding by an equivalent circuit and the number of elements involved. The disadvantage of this method is that it requires more computer capacity to include the huge admittance matrix. The method is expensive when used to model the whole transformer, but it can be used to study the transient phenomena in the winding.

The frequency response characteristics were used to derive an equivalent circuit of the transformer. The elements of this circuit were found from the poles and zeros that the impedance curves have shown. The simplified equivalent circuit was derived (chapter four) first and under the same principle, a wide frequency band transformer equivalent circuit was derived (chapter seven). The simplified equivalent circuit was used to examine the effect of transformer parasitic elements on the power supply performance (chapter six). The Spice program was used to simulate the converter model and to examine the transformer element's behaviour and their interaction with the resonant tank. Since the transformer elements are resonant elements, any reduction of any of them will be at the expense of the others, and so the elements need to be examined individually during the simulation. The transformer equivalent circuit was placed in series, and between the resonant tank elements of the converter. The normal operating waveforms of the converter during the simulation is justified as it corresponded with that actually obtained using the practical power supply. The converter was simulated above and below resonant frequency operation

When the magnetising inductance (Lm) was removed, the voltage across the resonant tank was reduced to 72% and increased to 120% of the normal operation at

below and above resonant respectively. When Lm is removed, the ground capacitance (Cg) becomes part of resonant tank capacitor (Cr) and so the resonant frequency is reduced due to the increase in the capacitance value. This frequency is then further away from the series resonant frequency for the below resonant case, and close to it for the above resonant case. This results in the voltage decreasing and increasing for the below and above cases respectively. Removing Lm also shows that an oscillation exists in the winding current, where the resonant frequency is near to dc, and so the operating frequency is much lower than resonant. The same and opposite situation happens when Cg is removed. The resonant tank voltage is increased to 110% and reduced to 70% below and above resonant frequency respectively. Removing Cg has shown a reduction in the winding current oscillation and it no longer exists above the resonant frequency.

The simulation waveforms of input/ output currents and voltages have shown less transformer elements effect on the power supply performance above resonance in comparison with below resonance. The ratio of switching to resonant frequency has also been considered, where the current research supports using a ratio of 0.8 below resonant and 1.2 above resonant. When the ratio is reduced further than 0.8, partial charge and discharge (which can be seen clearly in the resonant tank voltage waveform) will increase. In the same way, as the ratio goes higher than 1.2, the oscillation in the winding current will increase.

The effects of each of the elements on the output voltage have been investigated and given as graphs. These graphs have shown that any increases in Cg will result in a reduction in the output voltage. This reduction is greater as the frequency ratio goes lower than 0.8, but above resonance it is much lower than below resonance. When Lm is changing at a resonant ratio of 0.8 and 0.4, both cases have shown a point at which the output reaches a maximum. This point is different at the resonant ratio of 0.8 than it is at 0.4 and this means less air gap in the core is required as the ratio increases. This does not occur in the case where the converter is operating above resonant frequency. There is no significant effect on Lm if Cg is removed. The

simulation results confirm that for the best performance the reduction in the distribution capacitance has to be linked with a corresponding reduction in Cg.

The frequency response impedances can give all the information required to derive an equivalent circuit of the wide frequency band transformer (chapter seven). The equivalent circuit is used to reproduce the frequency response and good agreement was clearly obtained with the measured and finite element results.

APPENDIX A

A.1 : TWO DIMENSIONAL FINITE ELEMENT PROGRAM

The magnetic vector potential (A) which is the main tool in the finite element program can be expressed in two equations. One from the divergence of A which is always equal to zero everywhere, and second as the curl of another vector function which is the flux density.

$$\nabla \times A = B \qquad (1)$$

$$\nabla . A = 0 \qquad (2)$$

By taking the curl of equation (1) and considering the relation between flux density B and flux intensity H as $B = \mu H$ (neglect hystereses), the result is :

$$\nabla \times \nabla \times A = \nabla \times B = \mu \nabla \times H = \mu J \qquad (3)$$

The equation to be solved then is :

$$\nabla \times \left(\frac{1}{\mu} \nabla \times A \right) = J \qquad (4)$$

J is the current density and an important equation can be derived to represent its value. The differential form of Maxwell's equation describing the electric field is $\nabla \times E = -\frac{\partial B}{\partial t}$, which states that the curl of E is not zero, therefore $E = -\nabla V$ is not enough as the case of Electrostatic field. So this equation can be arranged to :

$$\nabla \times E = -\nabla \times \frac{\partial A}{\partial t} \Rightarrow \nabla \times \left(E + \frac{\partial A}{\partial t} \right) = 0 \qquad (5)$$

The curl of the terms in the parentheses equal to zero, therefore, it equals to the gradient of a scalar function.

$$E + \frac{\partial A}{\partial t} = -\nabla V \Rightarrow E = -\frac{\partial A}{\partial t} - \nabla V \qquad (6)$$

In the conductor, the relation between the electric field intensity and current density can be defined by ohm's law ($J = \sigma E$) . Equation 6 can be written as :

$$J = -\sigma \frac{\partial A}{\partial t} - \sigma \nabla V \qquad (7)$$

The final equation to be solved then is :

$$\nabla \times \left(\frac{1}{\mu} \nabla \times \mathrm{A} \right) = -\sigma \frac{\partial \mathrm{A}}{\partial \mathrm{t}} - \sigma \nabla \mathrm{V} \qquad (8)$$

In order to solve this equation, the method of Weighted residual was used in the program.

Together with the integration over the volume of the problem which is given as :

$$\iiint W \left(\nabla \times \frac{1}{\mu} \nabla \times \mathrm{A} - J \right) \mathrm{d\,V} = 0 \qquad (9)$$

In the two dimensions where A and J have only z-direction components, equation 9 equivalent per unit length to :

$$\iint W \left(\nabla \times \frac{1}{\mu} \nabla \times \mathrm{A}_z - J_z \right) \mathrm{d\,x\,d\,y} = 0 \qquad (10)$$

$$\nabla \times \nabla \times \mathrm{A} = -\frac{\partial}{\partial \mathrm{x}} \left(\frac{\partial \mathrm{A}_z}{\partial \mathrm{x}} \right) - \frac{\partial}{\partial \mathrm{y}} \left(\frac{\partial \mathrm{A}_z}{\partial \mathrm{y}} \right) \qquad (11)$$

By integrating the above equations (10 & 11) by parts (Green's Theorem), the result is :

$$\iint W \left(\nabla \times \frac{1}{\mu} \nabla \times \mathrm{A}_z - J_z \right) \mathrm{d\,x\,d\,y} + \int W \frac{1}{\mu} \frac{\partial \mathrm{A}_z}{\partial \mathrm{n}} \mathrm{d}\,\ell = 0 \qquad (12)$$

Where $\frac{\partial}{\partial \mathrm{n}}$ represent the normal component to the boundary surface of the xy plane, so :

$$\frac{1}{\mu} \frac{\partial \mathrm{A}_z}{\partial \mathrm{n}} = \frac{1}{\mu} \mathrm{B}_n = \mathrm{H}_t \qquad (13)$$

Within equation (12), the component of the current density can be simplified using the third equation of Maxwell, which is:

$$\nabla \times \mathrm{E} = -\frac{\partial \mathrm{B}}{\partial \mathrm{t}} = -\frac{\partial}{\partial \mathrm{t}} (\nabla \times \mathrm{A}) \qquad (14)$$

The integration of this equation for a single frequency variation is :

$$\mathrm{E} = -\mathrm{j}\,\omega \mathrm{A} + \nabla \mathrm{V} \qquad (15)$$

Where V is the integration constant. This equation shows that the electrical field comes from two components, one induced in a conductor by change in the magnetic field which is the first part of equation (15), and the second arise from immersion in the electrostatic field. The basic step of the finite element is to break up the area of interest into small elements, within each of which the vector potential is defined at the vertices (nodes). In the case where the shape of elements are triangular, the vector potential is:

$$\mathrm{A}_z = \sum_{k=1,3} N_k \mathrm{A}_k \qquad (16)$$

The Galerkin technique was used to simplify the problem by considering the weighted term W as the shape function (N) of the element considered. The formulation of whole the region that contains m number of elements is :

$$\sum_{\text{all element}} \left[\iint \frac{1}{\mu} \frac{\partial N_i}{\partial x} \sum_{k=1,3} \frac{\partial N_k A_k}{\partial x} + \frac{1}{\mu} \frac{\partial N_i}{\partial y} \sum_{k=1,3} \frac{\partial N_k A_k}{\partial y} \right] dx\, dy$$

$$\sum_{\text{all element}} \iint N_i \sigma j\omega \sum_{k=1,3} N_k A_k \, dx\, dy + \sum_{\text{all element}} \iint N_i \sigma \nabla V \, dx\, dy$$

$$+ \sum_{\text{all element}} \iint N_i \, J_z \, dx\, dy - \sum_{\text{all element}} \iint N_i \, H_t \, d\ell = 0$$

A.2 : THE USEFULNESS OF THE MAGNETIC VECTOR POTENTIAL.

As explained earlier in chapter three, the main parameter to be solved for by FE analysis is the magnetic vector potential (A), and all of the calculated quantities required can be found directly from it. The single value of A (in z direction) can be calculated at each node within the model. The flux and induced current resulting is then easily obtained from the definition of A. The magnetic flux can then be used to predict voltage and inductance. The relationship between the magnetic flux and A can be given as:

$$\Psi_m = \int B.ds = \int \nabla \times A \qquad \text{..... (1)}$$

This surface integral can be replaced by a line integral enclosing the surface (Stokes theorem),

$$\Psi_m = \oint A.d\ell \qquad \text{.....(2)}$$

In the case of steady state two-dimensional analysis with no capacitive effect, the complex value of the voltage can be calculated using Faraday's Law, which together with equation (2) gives:

$$V = -N\frac{\partial \Psi_m}{\partial t} = -N\frac{\partial}{\partial t}\oint \mathrm{A}.d\ell \qquad \ldots\ldots\ldots\ldots (3)$$

where N is the number of turns.

The inductance can be found from the definition of the flux linkage due to the current flowing in the conductor.

$$L = \lambda / I = N\Psi_m / I \qquad \ldots\ldots\ldots\ldots\ldots (4)$$

If both current and flux in equation (4) belong to the same coil, the inductance term is the self inductance. If the flux in the coil is due to the another coil current, it is the mutual inductance.

The resistance components of either dc or ac can be found from the value of A. The dc component does not need to be found by FEA, since it is given in the wire specification data. However, it can be calculated by considering the frequency to be zero (i.e. static) for a uniform conductor cross section area. In the case where the conductor area is not uniform, then a steady current solution is required.

The ac component due to frequency increases, can be found from the losses in the conductor, where the conductor current density (J) is:

$$J = \sigma \mathrm{E} = \sigma\left(-\frac{\partial \mathrm{A}}{\partial t} - \nabla V\right) \qquad \ldots\ldots\ldots\ldots\ldots (5)$$

The power loss per unit metre in the two dimensional analysis is then:

$$\mathrm{P} = \int \frac{J^2}{\sigma}\, ds \qquad \ldots\ldots\ldots\ldots\ldots (6)$$

APPENDIX B

The figure shows a simplified equivalent circuit suitable for transient analysis. The winding to winding capacitance is not included for simplicity. During the simulation of any circuit, each of the circuit elements is transferred into an equivalent current source and constant resistance. This technique was explained in detail in chapter five, and it is repeated here for completeness.

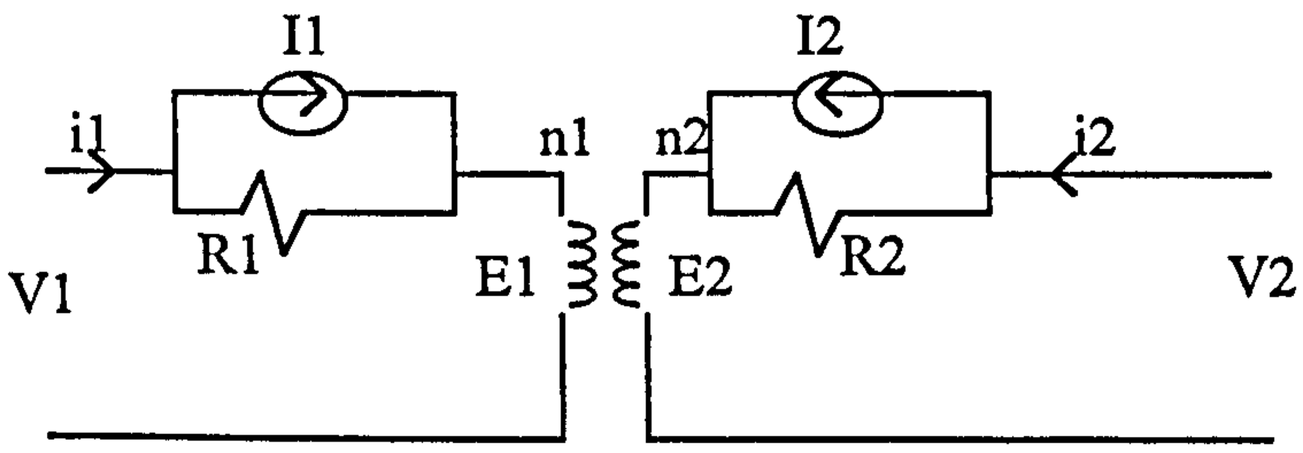

The circuit can be analysed using the input output relations as follow:

$$i_1R_1 + E_1 = V_1 + I_1R_1$$

$$i_2R_2 + E_2 = V_2 + I_2R_2$$

$$n_1i_1 + n_2 i_2 = 0$$

$$n_2E_1 - n_1 E_2 = 0$$

These relations can be arranged in a matrix form as follow :

$$\begin{bmatrix} \begin{bmatrix} R_1 & 0 \\ 0 & R_2 \end{bmatrix} & \begin{bmatrix} 1 & 1 \\ 1 & 1 \end{bmatrix} \\ \begin{bmatrix} n_1 & n_2 \\ 0 & 0 \end{bmatrix} & \begin{bmatrix} 0 & 0 \\ n_2 & -n_1 \end{bmatrix} \end{bmatrix} \begin{bmatrix} i(t) \\ E(t) \end{bmatrix} = \begin{bmatrix} \begin{bmatrix} 1 & 1 \\ 1 & 1 \end{bmatrix} & \begin{bmatrix} R_1 & 0 \\ 0 & R_2 \end{bmatrix} \\ \begin{bmatrix} 0 & 0 \\ 0 & 0 \end{bmatrix} & \begin{bmatrix} 0 & 0 \\ 0 & 0 \end{bmatrix} \end{bmatrix} \begin{bmatrix} V(t) \\ I(t-\Delta t) \end{bmatrix}$$

If the input voltage is given, the matrix can be used to solve for input and output current.

The matrix can be simplified in final form and given as :

$$[i(t)] = [Y][V(t)] + [I(t-\Delta t)]$$

Where Y is a matrix contain the known resistances and turn ratios. Further details of this method can be found in many publications as for instance Chimklai, et al [12].

REFERENCES

1- P.L.Dowell, " Effect of eddy currents in transformer winding.", IEE Proc., Vol.113, No.8, Aug.1966, PP. 1387-1394.

2- P.Silvester, " Network analog solution of skin and proximity effect problem.", IEEE Trans. on PAS, Vol.86, No.2, Feb.1967, PP.241-247.

3- P.Silvester, " Ac resistance and reactance of isolated rectangular conductor.", IEEE Trans. on PAS, Vol.86, No.6, June 1967, PP. 770-775.

4- P.I.Fergested, and T.Henriksen," Transient Oscillation in mutiwinding transformers.", IEEE Trans. on PAS, Vol.93, March 1974, PP. 500-509.

5- R.Kasturi, G.R.K.Murty," Computation of impulse voltage stresses in transformer windings.", IEE Proc. Vol.126, No.5, May 1979, PP. 397-400.

6- C.E.Lin, C.L.Cheng, et al." Investigation of magnetizing inrush current in transformers.", IEEE Trans on PD, Vol.8, No.1, Jan.1993, PP. 246-253.

7- W.J.McNutt, T.J.Blalock, et al.," Response of transformer winding to system transient voltage.", IEEE Trans. on PAS, Vol. 93, March 1993, PP. 457-467.

8- Adielson T., Carlson A., et al, " Resonant over-voltage in EHV transformers, modelling and application",IEEE Trans., Vol. PAS-100, 1981, PP. 3563-3572.

9- R.C.Degeneff," A general method for determining resonances in transformer windings.", IEEE Trans. on PAS, Vol.96, No.2, April 1977, PP. 423-430.

10- P.T.M.Vaessen, " Transformer model for high frequencies.", IEEE Trans. on PD, Vol.3, No.4, Oct.1988, PP. 1761-1768.

11- Keyhani,A., Chua S.W., et al, " Maximum likelihood estimation of transformer high frequency parameters from test data ", IEEE Trans. on PD, Vol. 6, No.2, April 1991, PP. 858-865.

12- Chimklai S., Marti J.R., " Simplified three phase transformer model for electromagnetic transient studies ", IEEE Trans. on PD., Vol. 10, No. 3, July 1995, PP 1316-1325.

13- O.C.Zienkiewicz, " The finite element method.",3rd edition, McGraw-Hill, New-york, 1977.

14- R.L.Stoll," The analysis of eddy currents.", Oxford, 1974

15- O.W.Anderson," Transformer leakage flux programn based on the FEM.", IEEE Trans. on PAS, Vol.92, July.1973, PP.682-689.

16- M.V.K.Chari," FE solution of eddy current problem in magnetic structures.", IEEE Trans. on PAS, Vol.93, 1974, PP. 62-72.

17- A.Konrad," Eddy currents and modelling.", IEEE Trans. on Mag., Vol.21, No.5, Sep.1985, PP. 1805-1810.

18- S.Yamada, and E.Otsuki," Analysis of eddy current loss in Mn-Zn Ferrites for power supplies.", IEEE Trans. on Mag., Vol.31, No.6, Nov.1995, PP. 4062-4064.

19- A.W.Lotfi, F.C.Lee, et al." Two dimensional skin effect in power foils for high frequency application.", IEEE Trans. on Mag., Vol.31, No.2, March1995, PP. 1003-1006.

20- J.H.McWhirter," Computation of three dimensional eddy currents in thin conductors.", IEEE Trans. on Mag., Vol.18, No.2, March 1982, PP. 456-460.

21- M.J.Balchin, J.A.M. Davidson," Numerical method for calculating magnetic flux and eddy current distribution in three dimensions.", IEE Proc., Vol.127, Part-A, No.1, Jan. 1980, PP. 46-53.

22- Y.Ohdachi, Y.Kawase, et al.," Load characteristics analysis of coupling transformer using 3D finite element method with edge elements.", IEEE Trans. on Mag., Vol.30, No.5, Sep.1994, PP.3721-3724.
23- Tutorial by Kriezis, Tsiboukis, et al.," Eddy currents, theory and applications.", IEEE Proc., Vol.80, No.10,Oct.1992, PP. 1556-1588.
24- Y.Tanizume, H.Yamashita, et al.," Tetrahedral elements generation using topological mapping and space dividing for 3D magnetic field FEM.", IEEE Trans. on Mag., Vol26, No.2, March 1990, PP. 775-778.
25- O.Biro, K.Pries," Finite element analysis of 3D eddy currents.", IEEE Trans. on Mag., Vol.26, 1990, PP.418-423.
26- M.P.Perry," Multiple layer series connected winding design for minimum losses. ", IEEE Trans. on PAS, Vol.98, No.1, Jan.1979, PP. 116-123.
27- B.Beland," Eddy current in circular, square and rectangular rods.", IEE Proc., Vol. 130, No.3, Part-A, may1983, PP. 112-121.
28- J.Wiess, V.K.Garge,et al." Eddy current loss calculation in multiconductor system.", IEEE Trans on Mag., Vol. 19,.No.5, Sep.1983, PP. 2207-2209.
29- P.Chowdhuri," Calculation of series capacitance for transient analysis of windings.", IEEE Trans. on PD, Vol.PWRD2, No.1, Jan.1987, PP. 133-138.
30- J.Vandelac, and P.D.Ziogas," A novel approach for minimizing high frequency transformer copper losses.", IEEE Trans. on PE, Vol.3, No.3, July 1988, PP. 266-277.
31- I.R.Ciric," Proximity effect between a wire carrying current and a rotating cylinderical conductor.", IEE Proc., Vol.130, Part-A, No.3, may 1983, PP. 122-128.
32- S.Isaka, T.Tokumasu, et al.," Finite element analysis of eddy currents in transformer parallel conductors.", IEEE Trans. On PAS, Vol.104, No. 10, Oct. 1985, PP. 2731-2737.
33- A.F.Goldberg, T.G. Kassakian, et al., " Issues related to 1-10MHz transformer design.",IEEE Trans. on PE, Vol.4, No.1, jan.1989, PP. 113-124.
34- D.J.Wilcox, W.G.Hurley, et al.," Calculation of self and mutual impedance between sections of transformer windings.", IEE Proc. Part-C, Vol.136, No.5, Sep.1989, PP. 308-314.
35- D.J.Wilcox, " Theory of transformer modelling using modal analysis.", IEE Proc. Part-C, Vol.138, No.2, march 1991, 121-128.
36- K.van der Wint," Interaction between a series resonant converter and a transformer.", EPE Conference, Firenze 1991, PP. 2.1-2.7.
37- V.Woivre, J.P.Arthaud, et al." Transient over voltage study and model for shell type power transformer.", IEEE Trans. on PD, Vol.8, No.1, Jan.1993, PP. 212-219.
38- A.Morched, L.Marti, et al." A high frequency transformer model for the EMTP.", IEEE Trans. on PD, Vol.8, No.3, July 1993, PP. 1615-1624.
39- F.De leon, and A.Semlyen," Detailed modelling of eddy current effects for transformer transient.", IEEE Trans. on PD, Vol.9, No.2, April 1994, PP. 1140-1150.
40- A.Ahmad,P.H.Auriol, et al.," Shell form power transformer modelling at high frequency.", IEEE Trans. on Mag., Vol.30, No.5, Sep.1994, PP.3729-3732.
41- B.Ahmed, J.Ahmad,et al.," Computing Ferrite core losses at high frequency by finite elements method including temprature influence.", IEEE Trans. on Mag., Vol.30, No.5, Sep.1994, PP. 3733-3736.
42- A.Basak, Y.U.Chi-Hang, et al." Effecient transformer design by computing core loss using a novel approach.", IEEE Trans. on Mag., Vol.30, No.5, Sep.1994, PP. 3725-3728.

43- F.De leon, and A.Semlyen," Asimple representation of dynamic hysteresis losses in power transformers.", IEEE Trans. on PD, Vol.10, No.1, Jan. 1995, PP. 315-321.
44- B.Tala-Lghil, X.Tian, et al.," A new method to eliminate the effects of the high voltage transformer parasitic elements in a static resonant supply.", EPE Conference, Firenze 1991, PP. 2.468-2.473.
45- J.A.Sabate, and F.C.Lee," Off-line application of the fixed frequency clamped mode series resonant converter.", IEEE Trans. on PE, Vol.6, No.1, Jan. 1991, PP. 39-46.
46- D.T.Khai, t al. " Modelling of magnetizing inductance and leakage inductance in a matrix transformer.", IEEE Trans.on PE, Vol.8, No.2, April 1993, PP. 200-207.
47- R.Farrington, M.M.Jovanovic, et al." A new family of isolated converters that uses the magnetizing inductance of the transformer to achieve zero voltage switching ", IEEE Trans. on PE, Vol.8, No.4, Oct.1993, PP. 535-545.
48- M.M.Jovanovic, A.Wojciech, et al." High frequency off line power conversion using zero voltage switching quasiresonant, and multiresonant techniques.", IEEE Trans. on PE, Vol.4, No.4, Oct.1989, PP. 459-469.
49- K.Chen, and T.A Stuart, " A 1.6KW, 110KHz, dc-dc converter optimized for IGBT's.", IEEE Trans. on PE, Vol.8, No.1, 1993, PP. 18-25.
50- Abraham I. Pressman"Switching Power Supply Design",McGraw-Hill, 1991.
51- " Soft Ferrites, data handbook", Philips component, MA01, 1991.
52- " Unitrod switching regulated power supply design ",Seminar manual, USA, 1993.
53- S.M.Miri, T.U.Feng, et al., " Design of low leakage power supply transformer for high precision electronic instruments.", IEEE Trans. on IM., Vol.42, No.4, Aug.1993, PP. 854-859.
54- IR, " Product selector guide, power MOSFET ", HEXFET data book, 1985.
55- Y.Chin, and F.C.Lee," Constant frequency parallel resonant converter.",IEEE Trans. on IA, Vol.25, No.1, Jan. 1989, PP. 133-142.
56- Bhat,A.K., " Analysis and design of series-parallel resonant converter", IEEE Trans. on PE, Vol.8,No.1,Jan. 1993, PP 1-7.
57- P.H.Swanepoel, J.D.Vanwyk,et al.," transformer coupled direct base drive technology for high power-high voltage bipolar transistor PWM converter.", IEEE Trans. on IA, Vol.25, No.6, Nov.1989, PP.1158-1166.
58- F.U.Cheng-Tsai, " Small signal and transient analysis of a zero voltage switched, phase-controlled PWM converter using averaged switched model.", IEEE Trans. on IA, Vol.29, No.3, May 1993, PP. 493-499.
59- K.W.Cheng, and P.D.Evans," Calculation of winding losses in high frequency toroidal inductors using multi-strand conductors.", Birmingham University, EPA1771, Sep.1993.
60- A.Hund, " High Frequency measurements. ", 2-nd edition, McGraw-Hill, London, 1951.
61- V.J.Thottuvelil,T.G.Wilson, et al., " High frequency measurment techniques for magnetic cores.", IEEE Trans. on PE, Vol.5, No.1, Jan.1990, PP. 41-48.
62- Hurtley W.G., et al, " Calculation of leakage inductance in transformer windings ", IEEE Trans. on PE, Vol.9, No.1, Jan. 1994, PP 121-126.
63- Q.Su, R.E.James, et al. " A Z-transform model of transformer for the study of electromagnetic transients in power systems.", IEEE Trans on PS, Vol.5, No.1, Feb.1990, PP. 27-33.

64- E.Arri, A. carta, et al.," Diagnosis of the state of power transformer windings by on-line measurement of stray reactance.", IEEE Trans. on IM, Vol.42, No.2, April 1993, PP. 372-378.
65- Kraus, J.D. " Electromagnetics ", Fourth edition, McGraw-Hill International edition, 1991.
66- D.S.Kershaw," The Incomplete Cholesky Conjugate Gradient Method for iterative solution of system of linear equations.", Journal comp. Phys., Vol.26, 1978, PP.43-65.
67- O.H.Zinke and W.F.Schmidt," Linear ac magnetic circuit theory.", IEEE Trans. on Mag., Vol.29, No.5, Sep.1993, PP. 2207-2212.
68- A.Konarad, M.V.K.Chari,et al.," New finite element techniques for skin effect problems.", IEEE Trans. on Mag., Vol.18, No.2, March1982, PP. 450-455.
69- A.F.Goldberg, T.G.Kassakian, et al." Finite element analysis of copper loss in 1-10MHz transformers.", IEEE Trans.on PE, Vol.4, No.2, April 1989,PP. 157-167.
70- C.F.Bryant, B.Dillon,et al.," Solving high frequency problems using the magnetic vector potential with Lorentz gauge.", IEEE Trans. on Mag., Vol. 28, No.2, March 1992, PP. 1182-1185.
71- W.G.Hurley, and M.C.Duffy," Calculation of self and mutual impedance in planar magnetic structures.", IEEE Trans. on Mag., Vol.31, No.4, July 1995, PP. 2416-2423.
72- Masoum M.A.S., et al, " Transformer magnetising current and iron core losses in harmonic power flow", IEEE Trans. on PD, Vol.9, No.1, Jan.1994, PP 10-20.
73- P.Fernandes, P. Girdinio, et al., " Local error estimates for adaptive mesh refinement.", IEEE Trans. on Mag. vol.24, No.1, 1988, PP. 299-302.
74- C.F.Bryant, C.R.I. Emson, et al.," A comparision of Lorentz gauge formulations in eddy current computations.", IEEE Trans. on Mag., Vol. 26, No.2 March1990,PP. 430-433.
75- M.Ehsani, O.H.Stielau, et al.," Integrated reactive components in power electronic circuits.", IEEE Trans on PE, Vol.8, No.2, April 1993, PP. 208-215.
76- T. fawzi, P.E.Burke," The accurate computation of self and mutual inductance of circular coil.", IEEE Trans. on PAS, Vol.97, No.2, 1978.
77- D.A.Calahan," Computer aided network design.", Revised edition, McGraw-Hill, 1972.
78- L.O.Chua, and P.M.Lin," Computer aided analysis of electronic circuits.",Pren-Hall, 1975.
79- F.H.Branin," Computer methods of network analysis.", IEEE Proc., Vol. 55, No.11, Nov.1967, PP.1787-1800.
80- W.F.Tinney, and J.W.Walker," Direct solution of sparse network equations by optimally ordered triangular factorization.", IEEE Proc., Vol.55, No.11, Nov.1967, PP. 1802-1807.
81- W.D.Hermann," Digital computer solution of electromagnetic transient in single and multiphase network.", IEE Trans. on PAS, Vol.88, 1969, PP.388-393.
82- Hosseinian S.H.," Improvements in simulation methods for power system harmonic and transient studies", Ph.D. Thesis, 1996, Newcastle University,UK.
83- Muhammed A.H.," Calculation of transient fields in turbogenerators using finite elements and Fourier transform", M.Phil Thesis, 1993, Newcastle University, UK.
84- R.Kelkar, R.Wunderlich, et al.," Software breadboards for power electronic circuits.", IEEE Trans. on PE, Vol.6, No.2, April 1991, PP. 170-177.
85- "Mospower application.", Siliconix Incorporated, data book, USA 1985.
86- K.Shenai," A circuit simulation model for high frequency power mosfets.", IEEE Trans. on PE, Vol.6, No.3, July 1991, PP.539-547.

87- B.Cogitore, J.P.Keradec,et al.," The two winding transformer, an experimental method to obtain a wide frequency range equivalent circuit.", IEEE Trans. On IM, Vol.43, No.2, April 1994, PP. 364-371.
88- S.Chimklai, and J.R.Marti," Simplified three phase transformer model for electromagnetic transient studies.", IEEE Trans. on PD, Vol.10, No.3, July 1995, PP. 1316-1325.
89- de Leon,F.,and Semlyen A.," Reduced order model for transformer transients", IEEE on PD,Vol.7, No.1, PP. 361-369, Jan. 1992.
90- A.Keyhani, S.W.Chua, et al.," Maximum liklihood estimation of transformer high frequency parameters from test data.", IEEE Trans.on PD, Vol.6, No.2, April 1991, PP. 858-865.
91- Gupta S.C.," Delta function ", Math. of Comput., Vol.24, 1964, PP 16.

92- I.Marinova, Y.Midorikawa, et al. " Thin film transformer and its analysis by integral equation method.", Trans. on Mag., Vol.31, No.4, July1995, PP. 2432-2437.